

POLITECNICO DI TORINO

Department of Structural, Geotechnical and Building Engineering

Master of Science in Civil Engineering



DEVELOPMENT OF A RATIONAL METHODOLOGY FOR THE DESIGN OF LINKED COMPOUND SHEARWALLS IN TALL BUILDINGS IN HIGH-SEISMIC REGIONS

Skidmore, Owings & Merrill LLP

Supervisors:

Prof. Giuseppe Andrea Ferro

Dott. Fabio Bazzucchi

Company Supervisors:

Eng. Mark Sarkisian

Eng. Neville Mathias

Eng. David Shook

Dissertation of:

Giulio Vannini 229995

Academic Year 2017/2018

ACKNOWLEDGEMENTS

First and foremost, I would like to thank Professor Giuseppe Andrea Ferro who gave me the chance and the responsibility to work together on this particular and innovative area of interest. Cooperate with him on the present work has been for me a great source of growth and a strong incentive to increase my knowledge. I will always be grateful to him for giving me the opportunity to have this remarkable work experience abroad and to collaborate with some of the most qualified engineers of the world.

I would like to thank Doctor Fabio Bazzucchi who started investigating on this branch of structural engineering and helped me in overcoming the obstacles we encountered in developing this work, with his courtesy and willingness.

I am deeply indebted to Engineer Mark Sarkisian, Partner of seismic and structural engineering of Skidmore, Owings & Merrill, who accepted to collaborate with Professor Ferro on this thesis topic and host me in the San Francisco office.

I would also like to extend my thanks to Engineer Neville Mathias and Engineer David Shook, Associate Directors of SOM, able to help me to find brilliant solutions to the problems we had to face, with insightful explanations that remarked their passion for structural engineering and their widespread knowledge on this field.

A huge thank you goes to the whole structural team of SOM in San Francisco Office for the wonderful time spent together: I have always felt part of the team, inside and outside the office. Moreover, I was honored to work alongside them, an experience that turned out to be a great chance of learning for me.

All my gratitude goes to my parents, Monica and Enrico, for having given me the precious opportunity to study at the Politecnico di Torino and for having made all this possible with their tireless sustain.

A special thanks to Lavinia, for having been always present and an amazing partner for celebrations in moments of joy and fundamental support in difficulties.

I would also like to extend my thanks to my all fantastic friends, to have been close to me despite the distance.

I wish even to thank my Smartroom flatmates, who have accompanied me throughout this journey making it much more electrifying.

Thank you also to Alessandro, Stefano and Mattia, incredible and supportive flatmates in these last months.

ABSTRACT

The increasing advancement of the structural field of civil engineering has led Engineers from all over the world to challenge themselves in the construction of ever taller buildings, a trend that has undergone a strong acceleration especially recently. Alongside this fast race towards the sky, however, there has been no improvement in the updating and development of the codes that rule this type of buildings or in the adjustment of the guidelines that provide the design methodologies and requirements. The adoption of current codes, specifically developed for stand-alone shear walls of structures with a low number of stories, to linked compound shear walls of multi-story buildings, consequently produces overly conservative and rigid design solutions with no dissipative behavior when subjected to seismic loads.

To address this lack of appropriate design criteria, the modern procedure followed to design the above mentioned reinforced concrete structural elements of tall buildings and to check their performance in the event of an earthquake is the Performance Based Seismic Design (PBSD). It is based on Nonlinear Response History Analysis (NLRHA) with Ground Motions on buildings dimensioned using Response Spectrum Analysis (RSA) traditional design methodologies, in order to validate the latter and verify that they predict with good reliability the nonlinear behavior of the structure.

The present study investigates the traditional design methodologies of the central cores of tall buildings and evaluates their performance through the PBSD. After a deep evaluation of the results, a new methodology linked compound shear walls is proposed in order to provide solutions not overly conservative and effectively ductile, and also able to predict with the best possible accuracy the nonlinear behavior of these particular high-rise structures.

SINTESI

Il continuo progresso del settore dell'ingegneria civile strutturale ha spinto gli ingegneri di tutto il mondo a sfidarsi nella costruzione di edifici sempre più alti, trend che ha subito una forte accelerazione specialmente in epoca moderna. Tuttavia, a fronte di questa veloce corsa verso il cielo, non si è verificato un altrettanto rapido aggiornamento e ampliamento delle norme che regolano questo tipo di edifici né l'adeguamento delle linee guida che ne forniscono le metodologie e i requisiti di progettazione.

Le norme vigenti sono state concepite ad hoc per setti isolati di sezione rettangolare di strutture con un numero limitato di piani. La loro applicazione a pareti a sezione variabile di edifici multipiano restituisce di conseguenza soluzioni progettuali esageratamente conservative, rigide ed aventi un comportamento dissipativo nullo al comparire di una sollecitazione sismica.

Per sopperire alla carenza di criteri di progettazione adeguati, è stata approntata la procedura moderna detta Performance Based Seismic Design (PBSD) usata sia per il dimensionamento che per la verifica delle prestazioni dei nuclei negli edifici alti in cemento armato. Il metodo menzionato consiste nel compiere Analisi Dinamiche Non Lineari (NLRHA) con Accelerogrammi su edifici dimensionati tramite le metodologie tradizionali di progettazione, ovvero con Analisi Dinamiche con Spettro di Risposta Elastico (RSA), al fine di validarne i risultati e appurare che riproducano con sufficiente accuratezza il comportamento non lineare della struttura.

Questo lavoro di tesi analizza le tradizionali metodologie di progettazione dei nuclei centrali degli edifici alti e ne verifica le prestazioni tramite la PBSD. A valle di un'approfondita valutazione dei risultati, sono proposte nuove metodologie di progettazione degli elementi in studio al fine di fornire soluzioni non esageratamente conservative ed efficacemente duttili, e soprattutto tali da riprodurre con la massima accuratezza possibile il comportamento non lineare degli edifici alti.

TABLE OF CONTENTS

List of Figures	V
List of Tables	XIII
Chapter 1 Introduction	1
1.1 Analysis Methodologies	3
1.2 Layout of the Thesis	6
Chapter 2 Analysis Model and Seismic Loads	9
2.1 Prototype Model Description	9
2.2 Seismic Load Combinations	12
2.2.1 Response Spectra	13
2.2.2 Ground Motions	15
Chapter 3 Design Methodologies	21
3.1 Linear Analysis Model Description	21
3.1.1 Modal Participation Mass Ratios	24
3.2 Traditional Response Spectrum Design Methodologies	25
3.2.1 Code Response Spectrum Design Methodology	25
3.2.2 Axial Force – Biaxial Bending Design (MCE R=7.5).....	31
3.2.3 Axial Force – Biaxial Bending Design (MCE R=3).....	35
3.3 Proposed Design Methodologies.....	39
3.3.1 Response Spectrum Design	41
3.3.2 Response Spectrum Analysis Story Drift	42

3.3.3	Response Spectrum Analysis Story Shear	43
3.3.4	Wall Reinforcement Option A (MCE R=7.5)	44
3.3.5	Wall Reinforcement Option B (MCE R=3).....	48
3.3.6	Linear Response History Design	52
3.3.7	Wall Reinforcement Option C (MCE R=7.5).....	53
3.3.8	Wall Reinforcement Option D (MCE R=3)	54
3.3.9	Linear Response History Analysis Story Drift	59
3.3.10	Linear Response History Analysis Story Shear.....	61
Chapter 4 Nonlinear Verification Analysis		63
4.1	Nonlinear Analysis Model Description	63
4.1.1	Nonlinear Fiber Shear Walls Description.....	70
4.1.2	Nonlinear Coupling Beams Description.....	73
4.2	Response Spectrum Analysis Prediction of Nonlinear Behavior	77
4.2.1	Option A (MCE R=7.5) Nonlinear Analysis Results	77
4.2.2	Option B (MCE R=3) Nonlinear Analysis Results	91
4.3	Linear Response History Analysis Prediction of Nonlinear Behavior	105
4.3.1	Option D (MCE R=3) Nonlinear Analysis Results	105
Chapter 5 Results Comparison		119
5.1	Prediction of Nonlinear Behavior: Story Drift	119
5.1.1	Story Drift - X Direction	119
5.1.2	Story Drift - Y Direction	123
5.2	Prediction of Nonlinear Behavior: Story Shear	126
5.2.1	Story Shear - X Direction	126
5.2.2	Story Shear - Y Direction	130
5.3	Coupling Beams Plastic Rotation Comparison.....	133

5.3.1	Coupling Beams Plastic Rotation - X Direction.....	133
5.3.2	Coupling Beams Plastic Rotation - Y Direction.....	134
5.4	Shear Walls Fibers Strain Comparison	136
5.4.1	Shear Walls Fibers Strain – X Direction	136
5.4.2	Shear Walls Fibers Strain – Y Direction	139
5.5	Prediction of Nonlinear Behavior: Flexure Demands.....	142
5.5.1	Stand-Alone Shear Wall (I Shape).....	142
5.5.2	Composite Shear Wall (L Shape)	147
5.6	Total Reinforcements Amounts and Costs Comparison	151
5.6.1	MCE (R=7.5)	152
5.6.2	MCE (R=3)	153
	Conclusions.....	155
	References.....	159

LIST OF FIGURES

Figure 1.1 (a) Building Central Core; (b) Analysis Model Lateral View; (c) Analysis Model Plan View	1
Figure 1.2 (a) Stand-Alone Shear Wall; (b) 3D Core composed of Linked L Shapes; (c) 3D Core composed of Linked T Shapes.....	2
Figure 1.3 Transbay District, Block 9, San Francisco, California.....	4
Figure 1.4 500 Folsom Project, Skidmore, Owings & Merrill LLP	4
Figure 1.5 Prototype Model Structural Plan View on ETABS 2016.....	5
Figure 2.1 3-D Finite Element Computer Linear Model, CSI Software ETABS 2016	10
Figure 2.2 Prototype Model Structural Plan on ETABS 2016	11
Figure 2.3 Prototype Model Structural Elevation on ETABS 2016	11
Figure 2.4 Ramp Function	13
Figure 2.5 MCE and DBE Response Spectrum.....	14
Figure 2.6 Design Basis Earthquake (DBE) in ETABS 2016	14
Figure 2.7 Maximum Considered Earthquake (MCE) in ETABS 2016.....	15
Figure 2.8 11 Ground Motions	16
Figure 2.9 Scale Factors (500 Folsom Calculation Book).....	16
Figure 2.10 Kocaeli (Yarimca) Ground Motion	17
Figure 2.11 Kocaeli (Yarimca) Ground Motion in ETABS 2016 – X Direction	17
Figure 2.12 Kocaeli (Yarimca) Ground Motion in ETABS 2016 – Y Direction	18
Figure 2.13 Response Spectrum Ground Motion Kocaeli (Yarimca)Related	19
Figure 2.14 Rayleigh Damping Modeling	19
Figure 3.1 8ksi Unconfined Concrete Stress-Strain Plot	21
Figure 3.2 Shear Walls Stiffness Modifiers.....	22

Figure 3.3 Link Beams Stiffness Modifiers	23
Figure 3.4 3-D Finite Element Computer Code Linear Model, CSI Software ETABS 2016	26
Figure 3.5 Code Linear Model Structural Plan on ETABS 2016.....	27
Figure 3.6 Code Linear Model Structural Elevation on ETABS 2016.....	27
Figure 3.7 Code R=7.5 Stand-Alone Shear Wall Flexure Demands	28
Figure 3.8 Code R=7.5 Stand-Alone Shear Wall Rebar Distribution	28
Figure 3.9 Code R=7.5 Compound Shear Wall Rebar Distribution.....	29
Figure 3.10 Code R=3 Stand-Alone Shear Wall Flexure Demands	30
Figure 3.11 Code R=3 Stand-Alone Shear Wall Rebar Distribution	30
Figure 3.12 Compound Shear Wall Plan	31
Figure 3.13 Compound R=7.5 Shear Wall Flexure Demands	32
Figure 3.14 Compound R=7.5 Shear Wall Rebar Distribution	33
Figure 3.15 Compound Shear Wall Total Longitudinal Reinforcement Areas – MCE (R=7.5).....	34
Figure 3.16 Compound Shear Wall Plan	35
Figure 3.17 Compound R=3 Shear Wall Flexure Demands	36
Figure 3.18 Compound R=3 Shear Wall Rebar Distribution	37
Figure 3.19 Compound Shear Wall Total Longitudinal Reinforcement Areas – MCE (R=3).....	38
Figure 3.20 L-Shape Piers	39
Figure 3.21 L-Shape Section Stress Distribution	40
Figure 3.22 I-Shape Piers	40
Figure 3.23 I-Shape Walls Flexure Demands.....	41
Figure 3.24 Maximum Story Drift, MCE (R=7.5) and MCE (R=3)	42
Figure 3.25 Story Shear, MCE (R=7.5) and MCE (R=3).....	43
Figure 3.26 Option A_RSA MCE (R=7.5) Stand-Alone Shear Wall Rebar Distribution.....	44
Figure 3.27 Option A_RSA MCE (R=7.5) Stand-Alone Shear Wall Flexure Demands Plot.....	44
Figure 3.28 Option A_RSA MCE (R=7.5) Rebar Amounts	45

Figure 3.29 Option A_RSA MCE (R=7.5) Compound Shear Wall Rebar Distribution	46
Figure 3.30 Option A_RSA MCE (R=7.5) Compound Shear Wall Flexure Demands Plot.....	47
Figure 3.31 Option B_RSA MCE (R=3) Stand-Alone Shear Wall Rebar Distribution	48
Figure 3.32 Option B_RSA MCE (R=3) Stand-Alone Shear Wall Flexure Demands Plot.....	48
Figure 3.33 Option B_RSA MCE (R=3) Rebar Amounts	49
Figure 3.34 Option B_RSA MCE (R=3) Compound Shear Wall Rebar Distribution.....	50
Figure 3.35 Option B_RSA MCE (R=3) Compound Shear Wall Flexure Demands Plot.....	51
Figure 3.36 Option C_LRHA MCE (R=7.5) Stand-Alone Shear Wall Flexure Demands Plot.....	53
Figure 3.37 Option C_LRHA MCE (R=7.5) Compound Shear Wall Flexure Demands Plot.....	54
Figure 3.38 Option D_LRHA MCE (R=3) Stand-Alone Shear Wall Rebar Distribution	54
Figure 3.39 Option D_LRHA MCE (R=3) Compound Shear Wall Flexure Demands Plot.....	55
Figure 3.40 Option D_LRHA MCE (R=3) Rebar Amounts.....	56
Figure 3.41 Option D_LRHA MCE (R=3) Compound Shear Wall Rebar Distribution	57
Figure 3.42 Option D_LRHA MCE (R=3) Compound Shear Wall Flexure Demands Plot.....	58
Figure 3.43 X Direction Maximum Story Drift MCE (R=3).....	59
Figure 3.44 Y Direction Maximum Story Drift MCE (R=3).....	60
Figure 3.45 LRHA X Direction Story Shear MCE (R=3)	61
Figure 3.46 LRHA X Direction Story Shear MCE (R=3)	62
Figure 4.1 3-D Finite Element Computer Fiber Model, CSI Software ETABS 2016.....	64
Figure 4.2 Nonlinear Prototype Model Structural Plan on ETABS 2016	65

Figure 4.3 Nonlinear Prototype Model Structural Elevation on ETABS 2016	65
Figure 4.4 8ksi Unconfined and Confined Concrete Stress-Strain Plot	66
Figure 4.5 A706Gr60 Rebar Steel Stress-Strain Plot	67
Figure 4.6 Shear Walls Stiffness Modifiers	68
Figure 4.7 Coupling Beams Stiffness modifiers.....	68
Figure 4.8 Link Beams in Wall Stiffness Modifiers.....	69
Figure 4.9 Example of Shear Walls Reinforcement	70
Figure 4.10 (a) Boundary Zone Fibers Distribution; (b) Panel Zone Fibers Distribution.....	71
Figure 4.11 Sample Boundary Zone Fiber Hinge Specification in ETABS.....	71
Figure 4.12 Sample Panel Zone Fiber Hinge Specification in ETABS	72
Figure 4.13 Example of Diagonally Reinforced Coupling Beams	73
Figure 4.14 Shear Hinge.....	74
Figure 4.15 Rotational Hinges.....	74
Figure 4.16 Parametric Force-Deformation Curve of Plastic Hinges	75
Figure 4.17 Full Confinement of Diagonally Reinforced Link Beams (ACI 318-11)	76
Figure 4.18 Option A_RSA MCE (R=7.5) Rebar Amounts	77
Figure 4.19 Option A_MCE (R=7.5) – NLRHA X Direction Story Drift	79
Figure 4.20 Option A_MCE (R=7.5) – NLRHA Y Direction Story Drift	80
Figure 4.21 X Direction Shear Resistant Core	80
Figure 4.22 Option A_MCE (R=7.5) – NLRHA X Direction Story Shear	81
Figure 4.23 Y Direction Shear Resistant Core	81
Figure 4.24 Option A_MCE (R=7.5) – NLRHA Y Direction Story Shear	82
Figure 4.25 Coupling Beam 4 Plastic Hinges Position	82
Figure 4.26 Option A_MCE (R=7.5) – NLRHA X Direction Link Beam 4 Plastic Hinge Rotation.....	83
Figure 4.27 Coupling Beam 3 Plastic Hinges Position	83
Figure 4.28 Option A_MCE (R=7.5) – NLRHA Y Direction Link Beam 3 Plastic Hinge Rotation.....	84
Figure 4.29 Pier 1 Fibers Position	84

Figure 4.30 Option A_MCE (R=7.5) – NLRHA X Direction Pier 1 Corner Side Fiber Strain.....	85
Figure 4.31 Option A_MCE (R=7.5) – NLRHA X Direction Pier 1 Coupling Beam Side Fiber Strain	86
Figure 4.32 Pier 7 Fibers Position	86
Figure 4.33 Option A_MCE (R=7.5) – NLRHA Y Direction Pier 7 Corner Side Fiber Strain.....	87
Figure 4.34 Option A_MCE (R=7.5) – NLRHA Y Direction Pier 7 Coupling Beam Side Fiber Strain	88
Figure 4.35 Option A_MCE (R=7.5) – NLRHA Stand-Alone Shear Wall Flexure Demands	89
Figure 4.36 Option A_MCE (R=7.5) – NLRHA Compound Shear Wall Flexure Demands	90
Figure 4.37 Option B_RSA MCE (R=3) Rebar Amounts	91
Figure 4.38 Option B_MCE (R=3) – NLRHA X Direction Story Drift.....	93
Figure 4.39 Option B_MCE (R=3) – NLRHA Y Direction Story Drift.....	94
Figure 4.40 X Direction Shear Resistant Core	94
Figure 4.41 Option B_MCE (R=3) – NLRHA X Direction Story Shear	95
Figure 4.42 Y Direction Shear Resistant Core	95
Figure 4.43 Option B_MCE (R=3) – NLRHA Y Direction Story Shear	96
Figure 4.44 Coupling Beam 4 Plastic Hinges Position.....	96
Figure 4.45 Option B_MCE (R=3) – NLRHA X Direction Link Beam 4 Plastic Hinge Rotation.....	97
Figure 4.46 Coupling Beam 3 Plastic Hinges Position.....	97
Figure 4.47 Option B_MCE (R=3) – NLRHA Y Direction Link Beam 3 Plastic Hinge Rotation.....	98
Figure 4.48 Pier 1 Fibers Position	98
Figure 4.49 Option B_MCE (R=3) – NLRHA X Direction Pier 1 Corner Side Fiber Strain.....	99
Figure 4.50 Option B_MCE (R=3) – NLRHA X Direction Pier 1 Coupling Beam Side Fiber Strain	100

Figure 4.51 Pier 7 Fibers Position	100
Figure 4.52 Option B_MCE (R=3) – NLRHA Y Direction Pier 7 Corner Side Fiber Strain.....	101
Figure 4.53 Option B_MCE (R=3) – NLRHA Y Direction Pier 7 Coupling Beam Side Fiber Strain	102
Figure 4.54 Option B_MCE (R=3) – NLRHA Stand-Alone Shear Wall Flexure Demands	103
Figure 4.55 Option B_MCE (R=3) – NLRHA Compound Shear Wall Flexure Demands	104
Figure 4.56 Option D_LRHA MCE (R=3) Rebar Amounts	105
Figure 4.57 Option B_MCE (R=3) – NLRHA X Direction Story Drift	107
Figure 4.58 Option D_MCE (R=3) – NLRHA Y Direction Story Drift	108
Figure 4.59 X Direction Shear Resistant Core	108
Figure 4.60 Option D_MCE (R=3) – NLRHA X Direction Story Shear.....	109
Figure 4.61 Y Direction Shear Resistant Core	109
Figure 4.62 Option D_MCE (R=3) – NLRHA Y Direction Story Shear.....	110
Figure 4.63 Coupling Beam 4 Plastic Hinges Position	110
Figure 4.64 Option D_MCE (R=3) – NLRHA X Direction Link Beam 4 Plastic Hinge Rotation.....	111
Figure 4.65 Coupling Beam 3 Plastic Hinges Position	111
Figure 4.66 Option D_MCE (R=3) – NLRHA Y Direction Link Beam 3 Plastic Hinge Rotation.....	112
Figure 4.67 Pier 1 Fibers Position	112
Figure 4.68 Option D_MCE (R=3) – NLRHA X Direction Pier 1 Corner Side Fiber Strain.....	113
Figure 4.69 Option D_MCE (R=3) – NLRHA X Direction Pier 1 Coupling Beam Side Fiber Strain	114
Figure 4.70 Pier 7 Fibers Position	114
Figure 4.71 Option D_MCE (R=3) – NLRHA Y Direction Pier 7 Corner Side Fiber Strain.....	115

Figure 4.72 Option D_MCE (R=3) – NLRHA Y Direction Pier 7 Coupling Beam Side Fiber Strain	116
Figure 4.73 Option D_MCE (R=3) – NLRHA Stand-Alone Shear Wall Flexure Demands 1	117
Figure 4.74 Option D_MCE (R=3) – NLRHA Stand-Alone Shear Wall Flexure Demands 2	118
Figure 4.75 Option D_MCE (R=3) – NLRHA Compound Shear Wall Flexure Demands	118
Figure 5.1 Option A_MCE (R=7.5) – X Direction Story Drift Comparison.....	120
Figure 5.2 Option B_MCE (R=3) - X Direction Story Drift Comparison.....	121
Figure 5.3 Option D_MCE (R=3) - X Direction Story Drift Comparison	122
Figure 5.4 Option A_MCE (R=7.5) - Y Direction Story Drift Comparison	123
Figure 5.5 Option B_MCE (R=3) - Y Direction Story Drift Comparison.....	124
Figure 5.6 Option D_MCE (R=3) - Y Direction Story Drift Comparison	125
Figure 5.7 X Direction Shear Resistant Core	126
Figure 5.8 Option A_MCE (R=7.5) – X Direction Story Shear Comparison	127
Figure 5.9 Option B_MCE (R=3) - X Direction Story Shear Comparison	128
Figure 5.10 Option D_MCE (R=3) - X Direction Story Shear Comparison	129
Figure 5.11 Y Direction Shear Resistant Core	130
Figure 5.12 Option A_MCE (R=7.5) - Y Direction Story Shear Comparison	130
Figure 5.13 Option B_MCE (R=3) - Y Direction Story Shear Comparison	131
Figure 5.14 Option D_MCE (R=3) - Y Direction Story Shear Comparison	132
Figure 5.15 Coupling Beam 4 Plastic Hinges Position.....	133
Figure 5.16 X Direction Link Beam 4 Plastic Hinge Rotation Comparison	134
Figure 5.17 Coupling Beam 3 Plastic Hinges Position.....	135
Figure 5.18 Y Direction Link Beam 3 Plastic Hinge Rotation Comparison	135
Figure 5.19 Pier 1 Fibers Position	136
Figure 5.20 X Direction Pier 1 Corner Side Fiber Strain Comparison.....	137
Figure 5.21 X Direction Pier 1 Coupling Beam Side Fiber Strain Comparison.....	138
Figure 5.22 Pier 7 Fibers Position	139
Figure 5.23 Y Direction Pier 7 Corner Side Fiber Strain Comparison.....	140

Figure 5.24 Y Direction Pier 7 Coupling Beam Fiber Strain Comparison	141
Figure 5.25 Stand-Alone Shear Wall Flexure Demands Plot - MCE (R=7.5)	143
Figure 5.26 Stand-Alone Shear Wall Flexure Demands Plot - MCE (R=3)	145
Figure 5.27 Compound Shear Wall Flexure Demands Plot - MCE (R=7.5).....	147
Figure 5.28 Compound Shear Wall Flexure Demands Plot - MCE (R=3).....	149
Figure 5.29 L-Shape Shear Wall Total Longitudinal Reinforcement Areas – MCE (R=7.5).....	152
Figure 5.30 L-Shape Shear Wall Total Longitudinal Reinforcement Areas – MCE (R=3).....	153

LIST OF TABLES

Table 3.1 Stiffness/Property Modifiers.....	22
Table 3.2 Linear Model Modal Participation Mass Ratios	24
Table 4.1 A706Gr60 Fibers Rebar Steel Properties	66
Table 4.2 Stiffness/Property Modifiers.....	67
Table 4.3 Stiffness/Property Modifiers.....	67
Table 4.4 Link Beams Force-Deformation Input Parameters.....	75
Table 4.5 Option A_RSA MCE (R=7.5) Modal Participation Mass Ratios.....	78
Table 4.6 Option B_RSA MCE (R=3) Modal Participation Mass Ratios	92
Table 4.7 Option D_LRHA MCE (R=3) Modal Participation Mass Ratios.....	106

CHAPTER 1

INTRODUCTION

Due to their slenderness, tall buildings have distinct and complex responses to lateral loads imposed by wind or earthquakes. The prediction of tall buildings response to lateral loads is a critical challenge for structural engineers. While a number of analysis procedures exist, not all are appropriate for each type of Lateral Force Resisting System (LFRS). One of the most common lateral resisting systems for tall buildings is the reinforced concrete central “core”. A central core is common in tall buildings and contains all vertical services including elevators, stairs, mechanical shafts, plumbing risers and electrical risers. Depending on code requirements or building height, the core may or may not be combined with a perimeter frame and/or outriggers. The lateral force-resisting system is typically composed of shear walls distributed around the perimeter of the central core connected together by link beams.

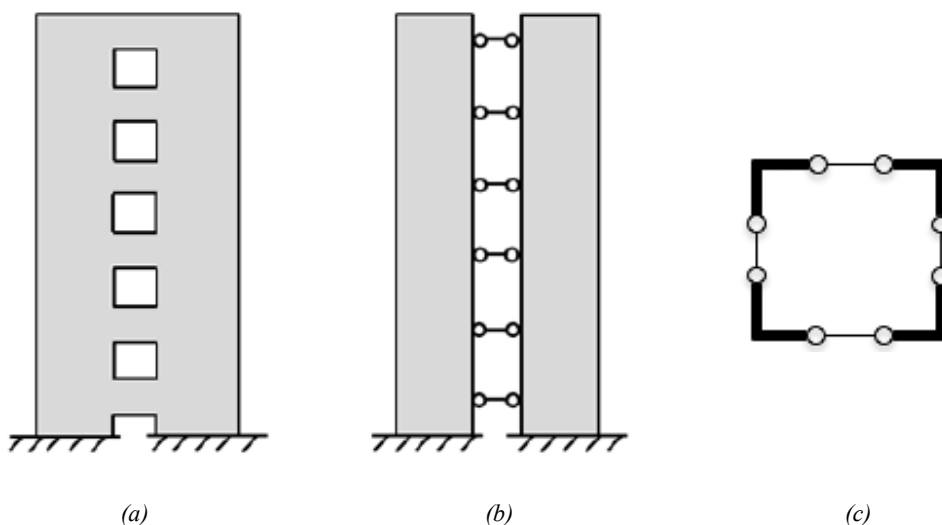


Figure 1.1 (a) Building Central Core; (b) Analysis Model Lateral View; (c) Analysis Model Plan View

The composite resistance of shear walls and link beams in multiple directions surrounding vertical services compose a core which has substantially more stiffness and strength than they would have individually.

Cast-in-place reinforced concrete shear walls are also very cost-efficient to construct, therefore making their use common world-wide. They are especially common in earthquake-prone countries and regions such as Japan, New Zealand and South-East Asia, Mexico and Peru, Middle East, South Europe and California.

Unfortunately, building codes and most design recommendations are most appropriate for smaller buildings with stand-alone shear walls and fail to adequately address slender three dimensionally linked cores composed of “I”, “L” or “T” shapes.

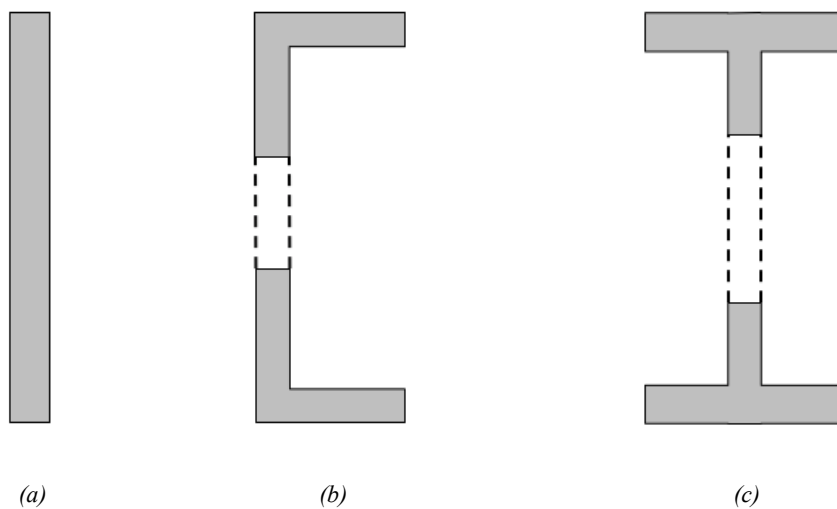


Figure 1.2 (a) Stand-Alone Shear Wall; (b) 3D Core composed of Linked L Shapes; (c) 3D Core composed of Linked T Shapes

Where building codes or design guides do address these shear wall configurations they are often overly conservative in some regards and potentially non-conservative in others. There is therefore a need for the development of a practical and rational methodology for engineers to use when designing these systems.

The purpose of this thesis is explore and evaluate procedures used to design the cores in tall buildings in high-seismic regions.

1.1 Analysis Methodologies

Response Spectrum Analysis (RSA) is commonly used for seismic design of tall buildings. While modern methods such as Performance Based Seismic Design (PBSD) utilize Nonlinear Response History Analysis (NLRHA) for verification of building performance, the design is typically based on RSA. Using RSA for design and NLRHA for verification of design has produced reliable designs. Unfortunately NLRHA often reveals highly conservative boundary zone design, sometimes non conservative shear design, and undesirably low ductility in shear walls.

RSA is the easiest and fastest way to obtain force demands such as axial force, shear and bending moment of wall piers. Unfortunately, RSA does give appropriate combinations of axial force and shear resulting in very high reinforcement quantities. In multistory high-rise buildings being too conservative in wall vertical reinforcement can lead to higher shear demands than predicted by RSA and increase potential for brittle shear failure. In addition, overly conservative quantities of rebar results in inefficient use of materials, money and time.

The topic of this thesis fits into this landscape trying to find a rational methodology to extract force demands for the design of lateral force resisting systems composed of ductile reinforced concrete compound shear walls and ductile link beams. For this purpose, various linear and nonlinear analysis will be performed on a prototype model, in order to identify strengths and weakness of each analysis method when compared to NLRHA results. A key goal of this research is find a new methodology of design which is able to accurately predict behaviors observed in NLRHA results. Building response including story drift, story shear, link beams rotations, shear walls fiber strains and pier axial-moment demands will be evaluated when comparing design analysis procedures to NLRHA results.

L-shaped compound shear walls will be evaluated as two planar piers and as combined.



Figure 1.3 Transbay District, Block 9, San Francisco, California.

As mentioned above, the analysis will be performed on a prototype model built as a simplification of the 500 Folsom Project of Skidmore, Owings & Merrill LLP. This project is a new residential 42-story tower located in the Transbay District, Block 9, of San Francisco, California.



Figure 1.4 500 Folsom Project, Skidmore, Owings & Merrill LLP

The geometry and the sizes of the Prototype Model structural elements are based on the aforementioned building and the lateral forces resisting system is modeled as a doubly symmetric core made by four corner L-shape compound shear walls linked by coupling beams.

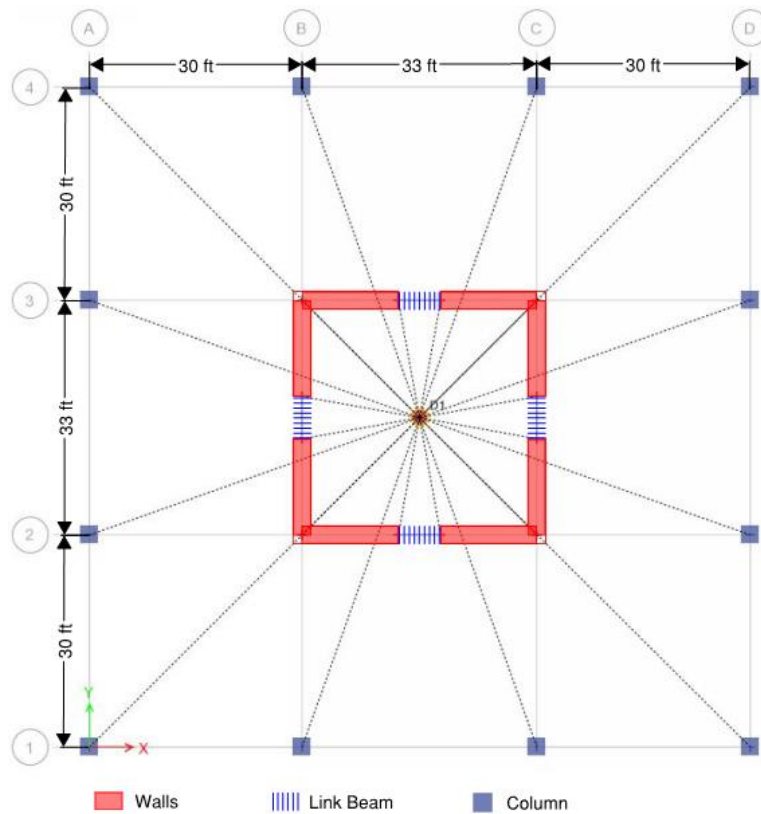


Figure 1.5 Prototype Model Structural Plan View on ETABS 2016

The project site-specific response spectrum and ground motions are used for the analysis.

Analysis will be performed with the CSI Software ETABS 2016, both linear analysis and nonlinear direct integration (DI) analysis. Reinforced concrete walls will be designed and optimized with S-Concrete, a software developed by S-Frame Software Inc.

1.2 Layout of the Thesis

The present work is divided into five chapters, described below:

- *Chapter 2* gives the background of the prototype model, including design criteria, geometry and dimensions. Response spectra and ground motions used for the analysis are shown and described too in this chapter.
- *Chapter 3* presents two common design procedures based on RSA, the traditional code one and the pure Axial Force - Biaxial Bending one. Afterwards, other two additional design procedures are proposed, both based on a whole linear model performed first with a RSA and secondly with a linear response history analysis (LRHA).

Regarding RSA, the prototype model is whole modeled with linear structural elements and it is analyzed under two types of response spectra in order to have two different design choices to evaluate. First of all, a Design Basis Earthquake (DBE) RSA scaled by an R factor equal to 5 will be performed. It is useful to specify that this response spectrum is the same as the Maximum Considered Earthquake (MCE) scaled by an R factor equal to 7.5. Secondly, a RSA based on a MCE response spectrum scaled by an R factor equal to 3 will be performed. Based on these two analysis, two related fiber nonlinear models will be built and analyzed in the following chapter. The MCE R=7.5 reinforcement option is chosen because it is the typical standard design procedure; the MCE R=3 reinforcement option is a common design choice in PBSB and it is quite stiffer than the previous soft one. These two design options will represent two different and extreme cases in order to have a good picture of the study.

Moreover, two LRHA based on the respective R values of 7.5 and 3 ground motions will be performed on the same linear model to show the correlations and differences with the previous ones. Based on these two proposed design procedures other two reinforcement options will be considered. In LRHA instance, only the R=3 MCE design procedure will be considered useful and the

related fiber nonlinear model will be built and analyzed in order to have NLRHA comparison.

- *Chapter 4* evaluates the RSA and LRHA design methodologies proposed in the previous chapter through NLRHA. The three evaluation procedures will be performed on three nonlinear fiber models, having the same nonlinear coupling beams but different nonlinear shear walls. The fiber walls are modeled taking in account the quantity of rebar based on the three proposed design methodologies developed in the Chapter 3.
- *Chapter 5* summarizes all the traditional and proposed design methodologies results with their relative nonlinear analysis. It aims to find a rational design methodology to provide a not over reinforced design able to predict in the best way the real behavior of the building comparing story drift, story shear, coupling beams rotations, shear walls fiber strains and wall piers axial-moment demands. Results are summarized and compared to present a high-level review of the research.
- *Conclusions* at the end resume what has been done in the present work, running through the main features. This chapter will show the rational methodology to follow in the design procedure to have reliable results in a short while and without so complex analysis. Engineers will be able to have a new method of design which is able to accurately predict behaviors observed in NLRHA without being overly conservative and to have a ductile building able to dissipate the right quantity of energy when earthquakes occur.

CHAPTER 2

ANALYSIS MODEL AND SEISMIC LOADS

This chapter describes in detail the 3D model of the present thesis, based on the 500 Folsom Project of Skidmore, Owings and Merrill. The project background and design criteria will be referred to the related Structural Seismic Design Calculation Book.

2.1 Prototype Model Description

A 3-D finite element computer model using the CSI Software ETABS 2016, *Figure 2.1*, is used to perform all the analysis conducted in the present work.

The Prototype Model is a 40-stories building, pinned restrained at all the basement joints. Each floor is 10 feet high and the square plan has 93 feet x 93 dimensions.

The core is 33 feet x 33 feet, with 30 inches thickness walls all the way up the building defined with 8ksi unconfined concrete. On each side there is a 6 feet wide central opening and a link beam 24 inches deep at the level of each floor. Coupling beams material is 8ksi concrete. This configuration runs along the total height of the core. At each floor level there are 8 inches thickness flat slabs, modelled as rigid diaphragms. Columns are 30 inches x 30 inches and defined with 8ksi unconfined concrete. All reinforcing steel is A706Gr60.

As it easy to guess, there are no perimeter beams, to not increase the construction cost and to realize an esthetically better building. The resisting system is then a single lateral force resisting system and not a dual lateral force resisting system (shear walls + moment frame) as the code requires.

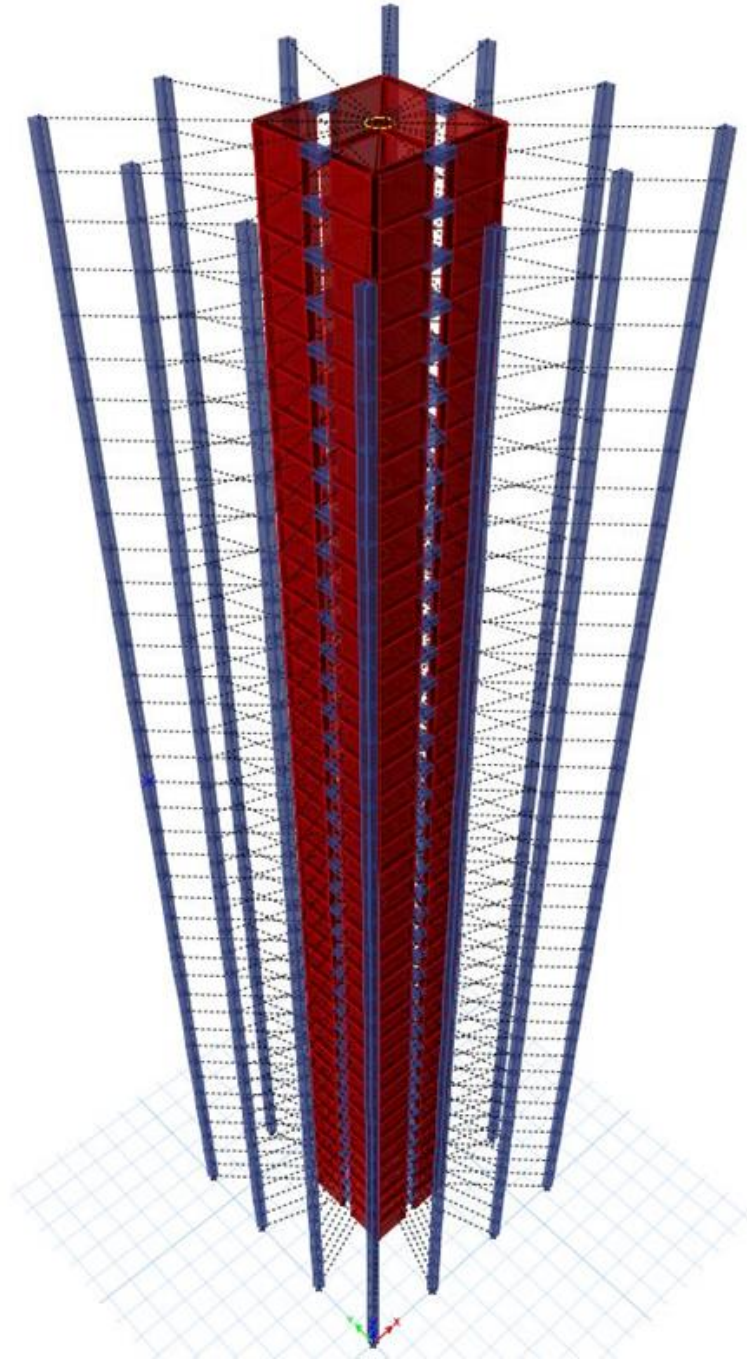


Figure 2.1 3-D Finite Element Computer Linear Model, CSI Software ETABS 2016

The plan and elevation of the Prototype Model are shown in *Figure 2.2* and *Figure 2.3*:

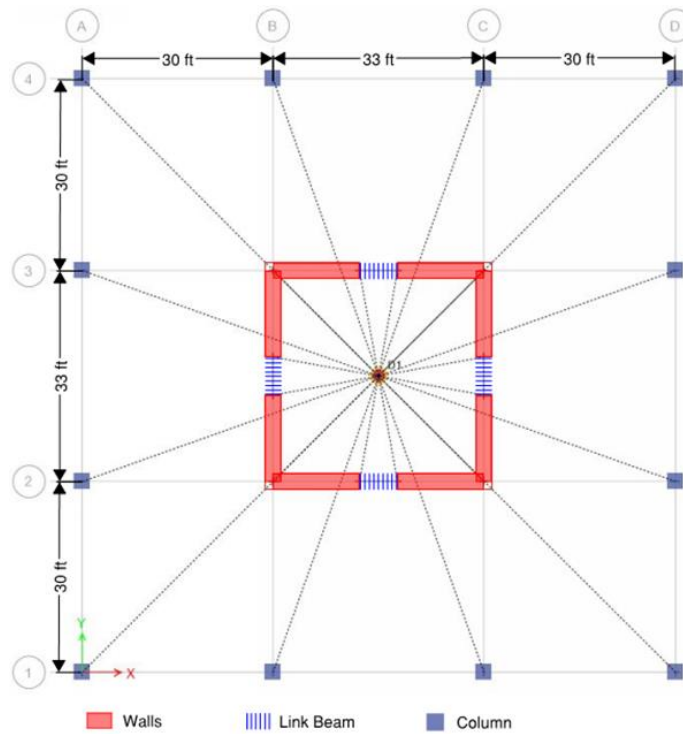


Figure 2.2 Prototype Model Structural Plan on ETABS 2016

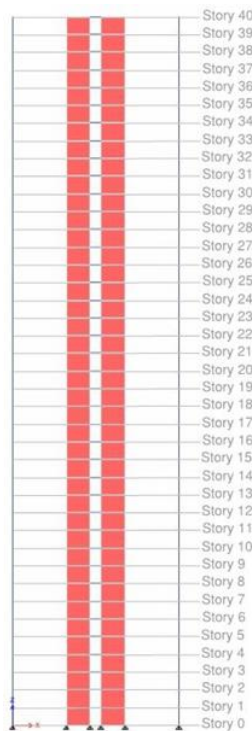


Figure 2.3 Prototype Model Structural Elevation on ETABS 2016

2.2 Seismic Load Combinations

The load combinations used are:

- $1.0D + 0.5L + L_{exp} \pm 1.0E_X \pm 0.3E_Y$
- $1.0(D+SDL) + 0.5L + L_{exp} \pm 0.3E_X \pm 1.0E_Y$

where L_{exp} is the expected live load.

The applied loads are as follows:

Dead load:

- Self-Weight 150 pcf
- Superimposed Dead Load 20 psf
- Partition Load 20 psf
- Façade Line Load 150 plf, applied along the perimeter of structure

Live load:

- Live Load 40 psf
- No expected live load is considered

For seismic mass, the self-weight, SDL, partition load and façade load are considered.

Gravity loads, in NLRHA, are applied using a Ramp Function as shown in *Figure 2.4*, such that the structure is in the correct state of stress prior to ground motion application. Additionally, the constant portion of the ramp function allows the structure to stop oscillating vertically before the ground motion is applied. Damping of 99% is applied.

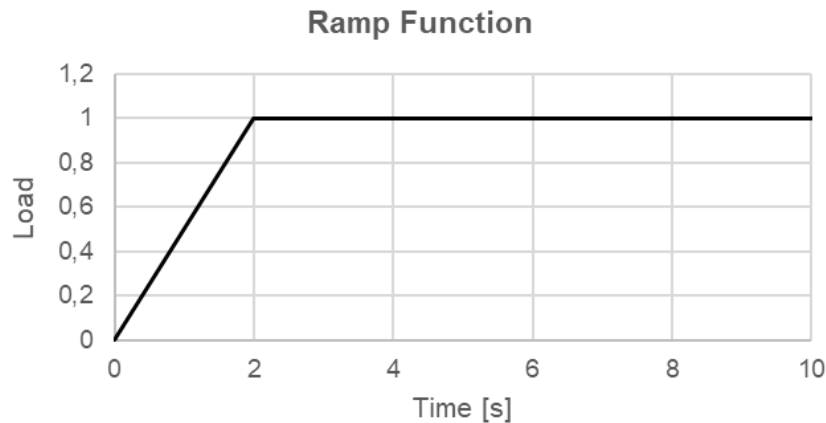


Figure 2.4 Ramp Function

2.2.1 Response Spectra

To estimate anticipated ground shaking at the site, a site specific response spectra for two levels of shaking corresponding to the Maximum Calculated Earthquake (MCE) and Design Basis Earthquake (DBE), consistent with the ASCE 7-10, are utilized, *Figure 2.5*. The MCE is defined as the lesser of the probabilistic spectrum in the maximum direction having 2% probability of exceedance in 50 years or the 84th percentile in the maximum direction of the deterministic event on the governing fault(s). The Design Basis Earthquake (DBE) is defined as 2/3 of the MCE, and in order to this it can be considered as the same of the Maximum Considered Earthquake scaled by an R factor equal to 7.5, *Figure 2.6* and *Figure 2.7*.

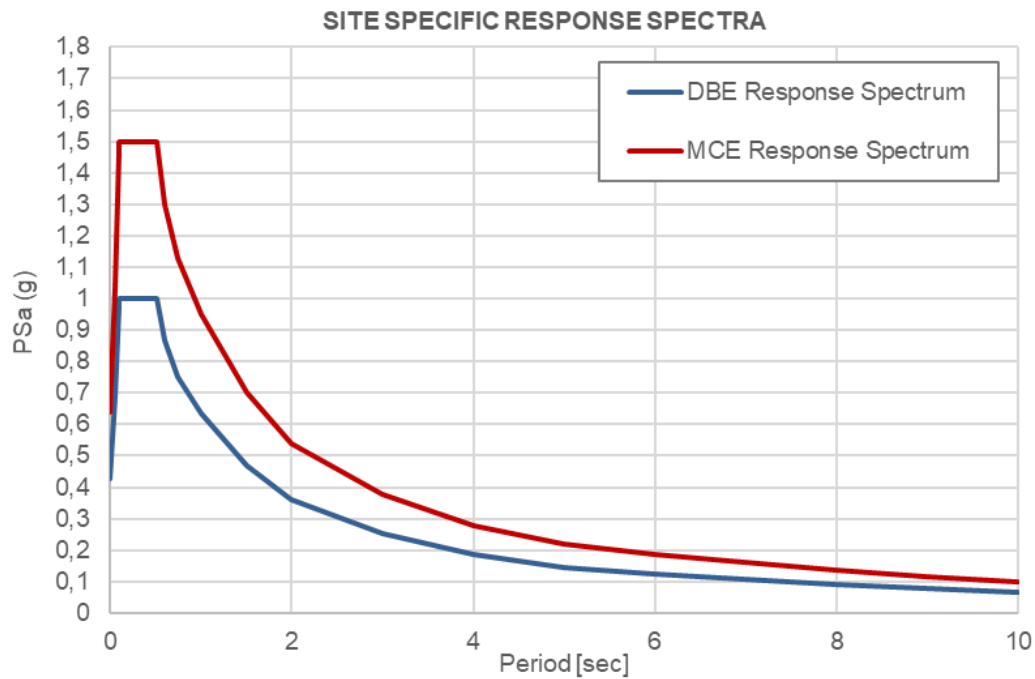


Figure 2.5 MCE and DBE Response Spectrum

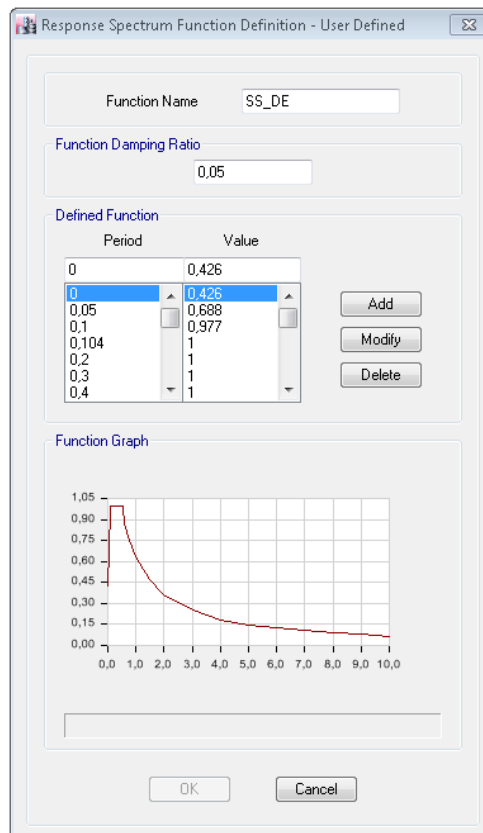


Figure 2.6 Design Basis Earthquake (DBE) in ETABS 2016

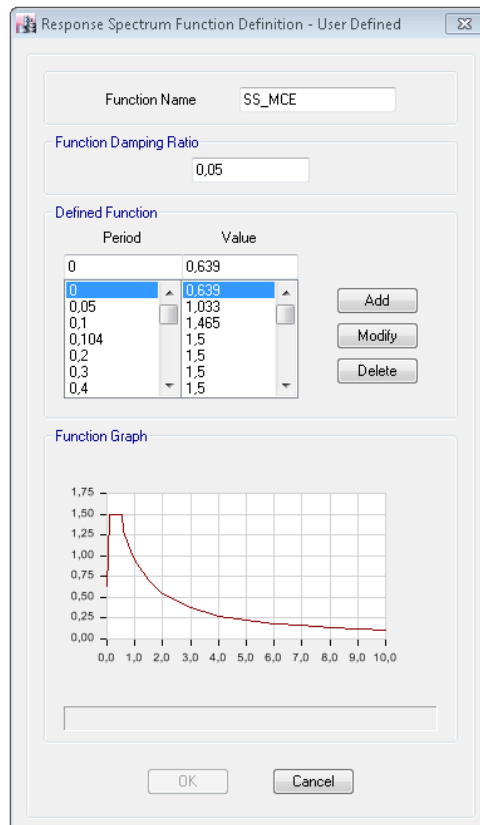


Figure 2.7 Maximum Considered Earthquake (MCE) in ETABS 2016

2.2.2 Ground Motions

The site-specific Long Period Ground Motions consist of 11 time histories scaled to two different conditional mean spectrums (*Baker, Journal of Structural Engineering 137(3), 2011*). The ground motions will be randomly rotated. The Maximum Considered Earthquake Level Evaluation of the primary structural system is required to demonstrate adequate safety against collapse. In fact, PBSO analysis often requires 7 or more pairs of earthquakes. They are provided by geotechnical engineers as pairs made, displaying the X direction component and the Y direction component of the ground motion. To validate a PBSO project and its results, codes require that all the analysis have been performed with a minimum number of 11 Ground Motions, *Figure 2.7*.

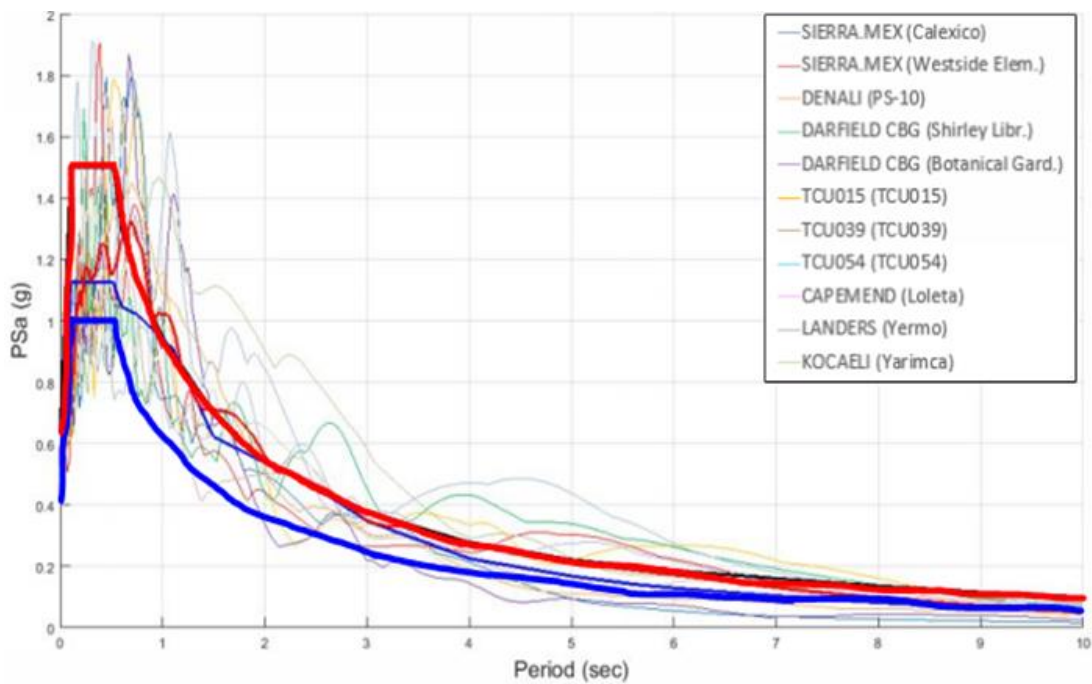


Figure 2.8 11 Ground Motions

The scaled factors are the following, *Table 2.1*:

Long Period Ground Motion	Scale Factor [No units]	Scale Factor [in/s ²]	Scale Factor [ft/s ²]
A - CAPEMEND (Loleta FS-Long)	1.93	745.75	62.15
B - KOCAELI (Yarimca)	1.05	405.72	33.81
C - TCU054	1.80	695.52	57.96
D - LANDERS (Yermo)	1.73	668.47	55.71
E - TCU015	2.49	962.14	80.18
F - TCU039	1.42	548.69	45.72
G - DENALI (PS-10 Long)	0.84	324.58	27.05
H - DARFIELD CBG (Botanical Gardens)	1.76	680.06	56.67
I - DARFIELD SHLC (Shirley Library)	1.59	614.38	51.20
J - SIERRA.MEX CIW (Westside Elem.)	0.91	351.62	29.30
K - SIERRA.MEX CXO (Calexico)	1.54	595.06	49.59

Figure 2.9 Scale Factors (500 Folsom Calculation Book)

As a sample, the Kocaeli (Yarimca) long period ground motion is shown below, *Figure 2.9*, *Figure 2.10* and *Figure 2.11*:

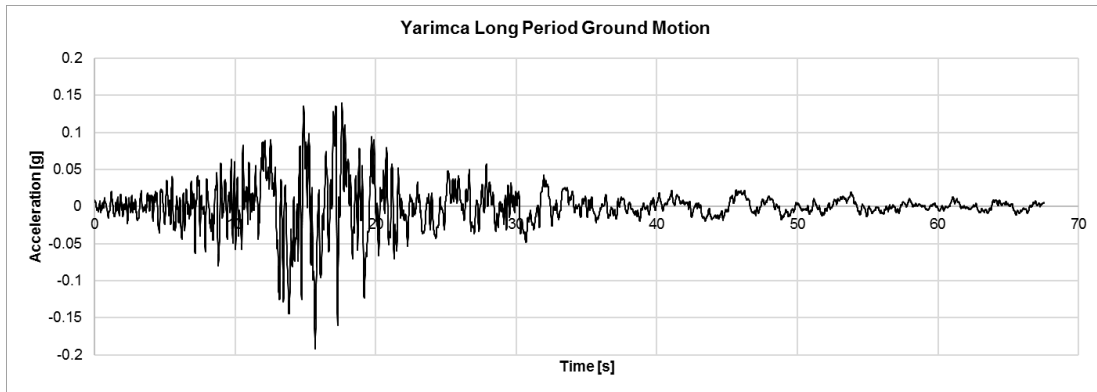


Figure 2.10 Kocaeli (Yarimca) Ground Motion

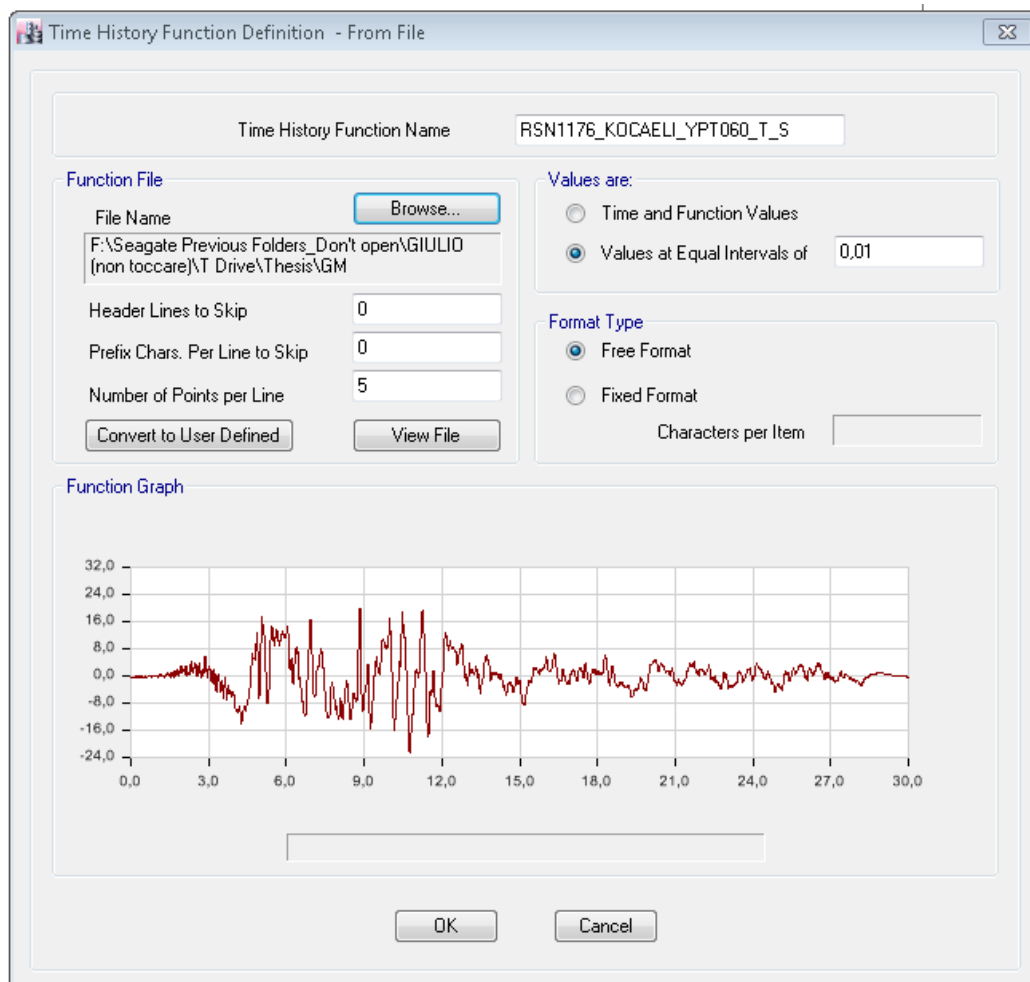


Figure 2.11 Kocaeli (Yarimca) Ground Motion in ETABS 2016 – X Direction

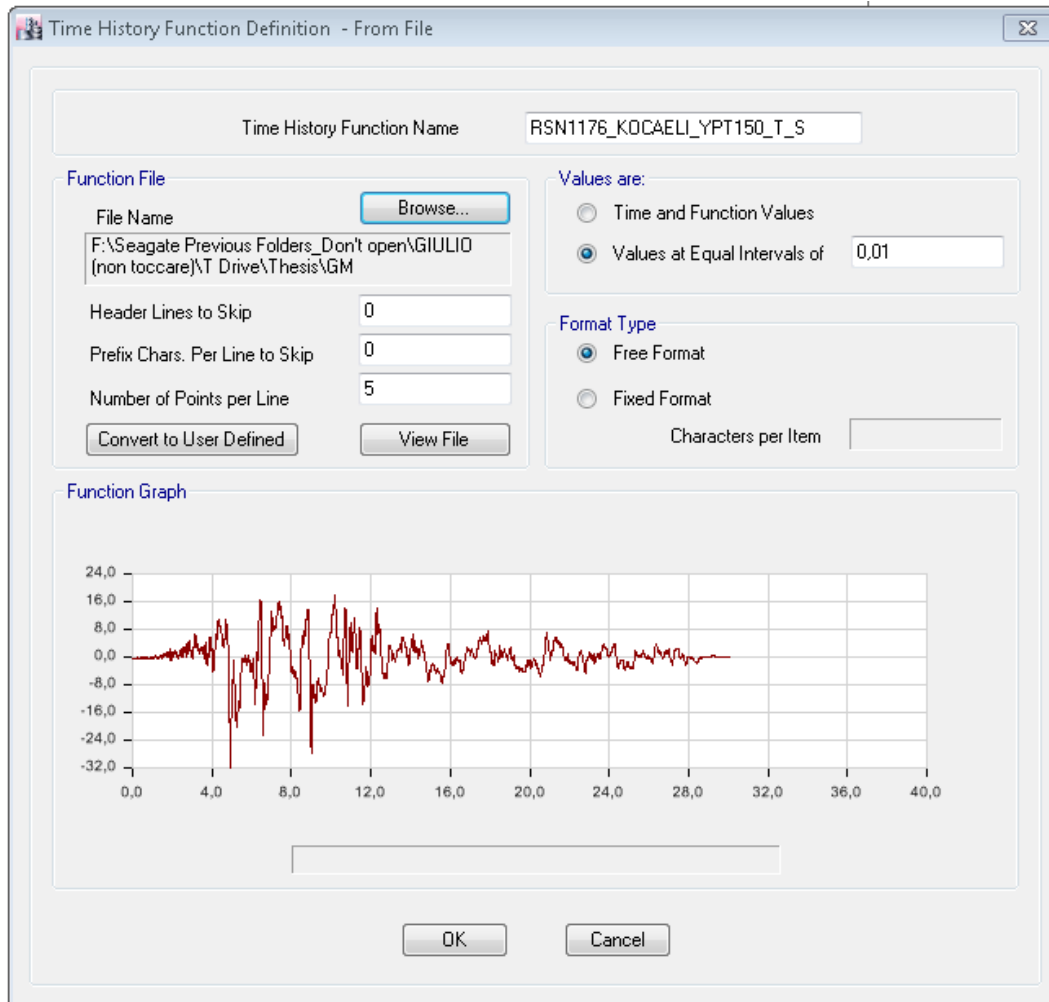


Figure 2.12 Kocaeli (Yarimca) Ground Motion in ETABS 2016 – Y Direction

The response spectrum (from Chapter 9 of 500 Folsom Calculation Book) is shown in Figure 2.12, where it is compared to the site-specific MCE level spectrum with $S_{MS} = 1.5g$. The ground motion was scaled by 1.05 times to match the spectrum, and then by 386 to converted from g to in/s².

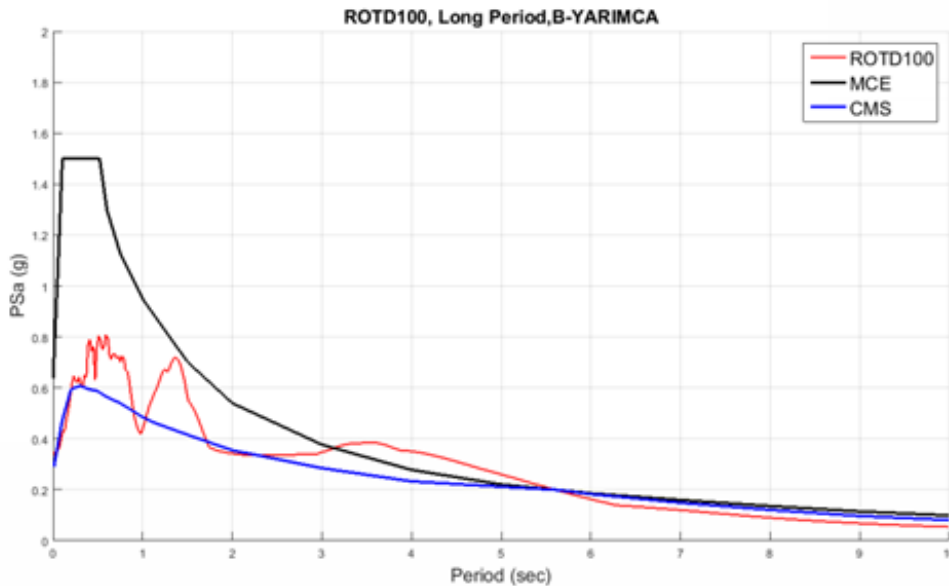


Figure 2.13 Response Spectrum Ground Motion Kocaeli (Yarimca) Related

Modal damping of 2.4% and Rayleigh damping of 0.1% is applied for the ground motion time history analysis. The Rayleigh damping is defined at two periods, the first is a period corresponding to 0.25 of the fundamental period and the second corresponds to 1.5 of the fundamental period. This is shown in Figure 2.13, referred to 500 Folsom chapter 10.3.1.

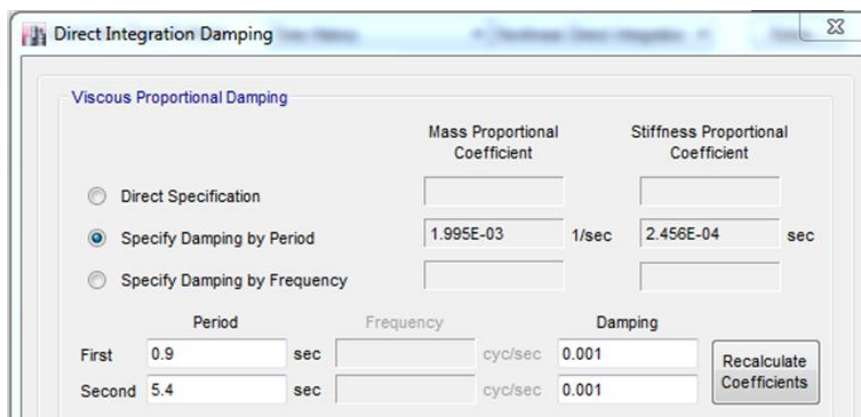


Figure 2.14 Rayleigh Damping Modeling

CHAPTER 3

DESIGN METHODOLOGIES

3.1 Linear Analysis Model Description

A 3-D finite element computer model using the ETABS CSI software, already described in Chapter 2.1, is used to perform linear elastic modal response spectrum analysis that conform to ASCE 7-10.

Material and component modelling are based on Chapter 11 of the 500 Folsom Calculation Book. For 8ksi confined concrete, the ETABS default Mander curve is used, plotted in *Figure 3.1*:

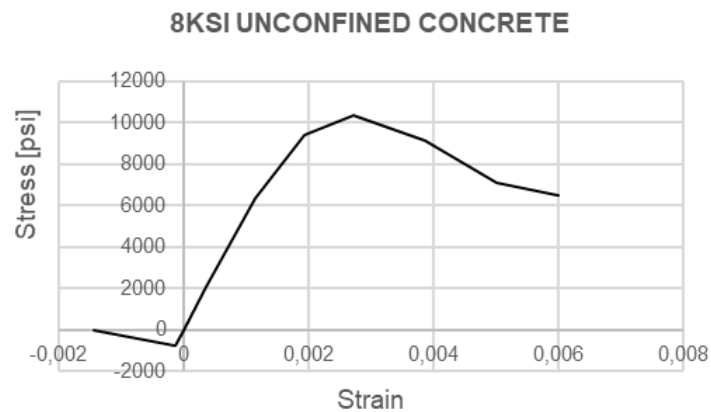


Figure 3.1 8ksi Unconfined Concrete Stress-Strain Plot

Young's Modulus is calculated with:

$$E_c = w_c^{1.5} \sqrt{f'_c}$$

Per ACI318-11 Section 8.5.1. Overstrength factor was included in this property.

Shear walls are modelled as shell elements. Coupling beams and Columns are modelled as frame elements.

The following property modifiers are adopted per 500 Folsom calculation book section 2.3.3.3.2:

	Flexure	Shear	Axial
Shear Walls	N/A	0.5 A_{vg}	1.0 A_g
Link Beams	0.07 (l/h) $I_g = 0.21 I_g$	-	1.0 A_g
Columns	0.5 I_g	1.0 A_{vg}	1.0 A_g

Table 3.1 Stiffness/Property Modifiers

Accordingly to *Table 3.1*, the following modifiers are applied to shear walls, *Figure 3.2*, and to link beams, *Figure 3.3*:

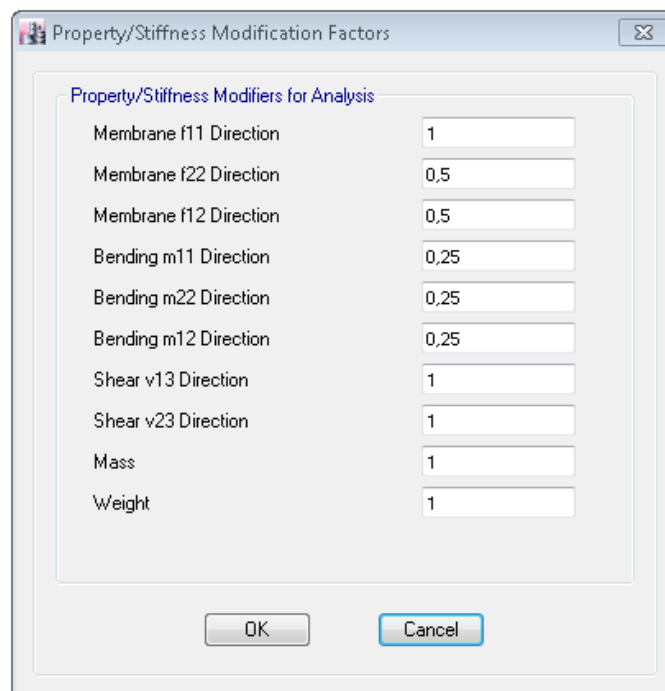


Figure 3.2 Shear Walls Stiffness Modifiers

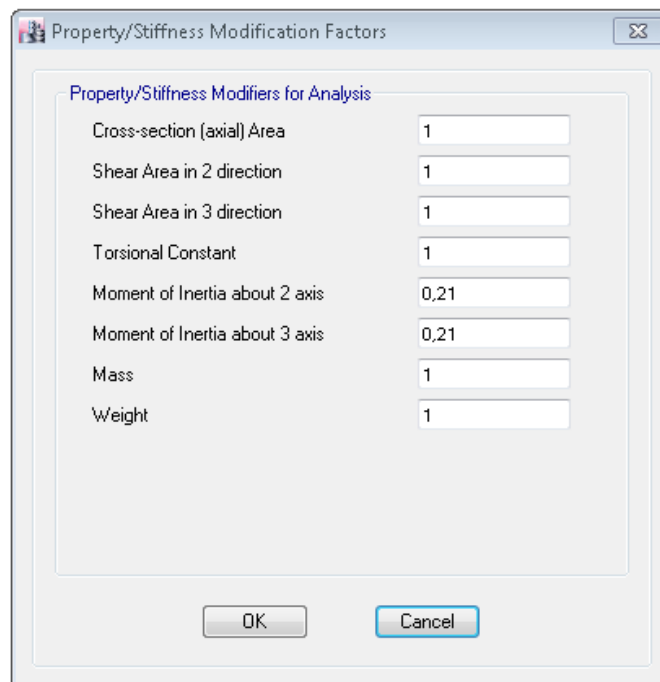


Figure 3.3 Link Beams Stiffness Modifiers

3.1.1 Modal Participation Mass Ratios

The Modal results of the Linea Prototype Model are shown just for the first 30 Modes, avoiding the negligible other ones, *Table 3.2*:

Mode	Period [sec]	UX	UY	RZ	Sum UX	Sum UY	Sum RZ
1	5.706	0.6551	8.61E-07	0	0.6551	8.61E-07	0
2	5.706	8.617E-07	0.6551	0	0.6551	0.6551	0
3	3.48	0	0	0.775	0.6551	0.6551	0.775
4	1.218	0.1916	0.0001	0	0.8468	0.6552	0.775
5	1.218	0.0001	0.1916	0	0.8469	0.8469	0.775
6	1.095	0	0	0.0949	0.8469	0.8469	0.8699
7	0.611	0	0	0.0396	0.8469	0.8469	0.9095
8	0.545	0.0532	5.436E-07	0	0.9001	0.8469	0.9095
9	0.545	5.436E-07	0.0532	0	0.9001	0.9001	0.9095
10	0.4	0	0	0.0231	0.9001	0.9001	0.9326
11	0.334	0.0272	0.0001	0	0.9273	0.9001	0.9326
12	0.334	0.0001	0.0272	0	0.9273	0.9273	0.9326
13	0.285	0	0	0.0155	0.9273	0.9273	0.9481
14	0.23	0.0003	0.0165	0	0.9276	0.9438	0.9481
15	0.23	0.0165	0.0003	0	0.9441	0.9441	0.9481
16	0.215	0	0	0.0112	0.9441	0.9441	0.9593
17	0.17	0.00001598	0.0117	0	0.9441	0.9558	0.9593
18	0.17	0.0117	0.00001598	0	0.9558	0.9558	0.9593
19	0.169	0	0	0.0084	0.9558	0.9558	0.9677
20	0.137	0	0	0.0064	0.9558	0.9558	0.9741
21	0.132	0.0084	0.0001	0	0.9642	0.9559	0.9741
22	0.132	0.0001	0.0084	0	0.9643	0.9643	0.9741
23	0.115	0	0	0.005	0.9643	0.9643	0.9791
24	0.107	0.0047	0.0018	0	0.9691	0.9661	0.9791
25	0.107	0.0018	0.0047	0	0.9709	0.9709	0.9791
26	0.098	0	0	0.0039	0.9709	0.9709	0.983
27	0.089	0.001	0.0041	0	0.9719	0.975	0.983
28	0.089	0.0041	0.001	0	0.976	0.976	0.983
29	0.086	0	0	0.0031	0.976	0.976	0.9861
30	0.076	0	0	0.0025	0.976	0.976	0.9886

Table 3.2 Linear Model Modal Participation Mass Ratios

3.2 Traditional Response Spectrum Design Methodologies

The first step of the present research is evaluating the Traditional Design Methodology in structural analysis of tall buildings, whose the design is typically based on RSA. This is the easiest and fastest way to obtain force demands such as axial force, shear and bending moment of wall piers. Unfortunately, RSA does give appropriate combinations of axial force and bending moment resulting in very high reinforcement quantities.

3.2.1 Code Response Spectrum Design Methodology

The common design methodology of the worldwide codes consists in thinking of any type of section as a set of rectangular section walls, each able to counteract only the loads coplanar to their own plane and not offer any stiffness out of the plane. This solution may also be justified for buildings with a limited number of floors but not suitable for the design of tall buildings reinforced concrete piers, as it leads to overly reinforced solutions.

Considering the combination of load with seismic solicitation mainly acting in the x-direction, codes require that only walls with a plane direction parallel to the x-direction be considered as resistant, *Figure 3.4*:

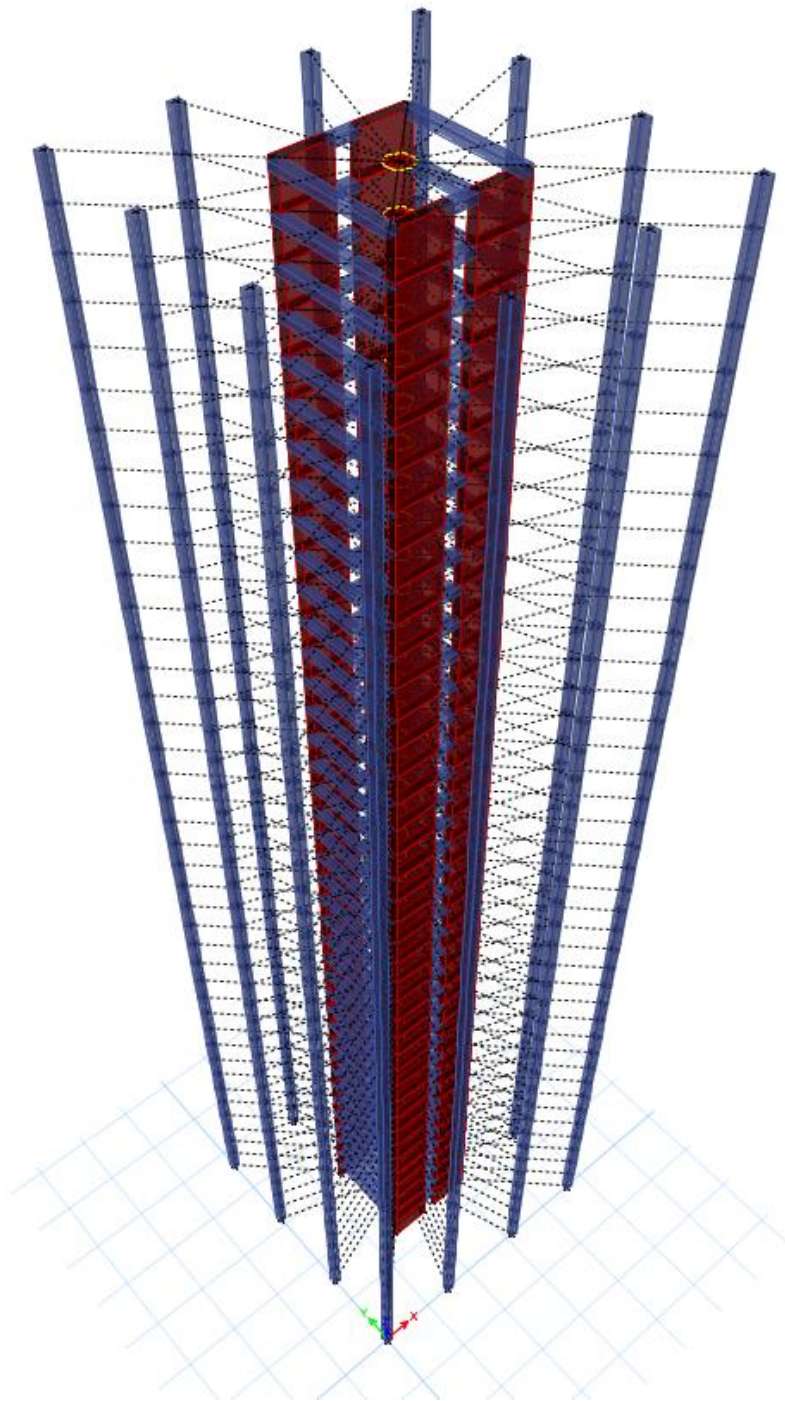


Figure 3.4 3-D Finite Element Computer Code Linear Model, CSI Software ETABS 2016

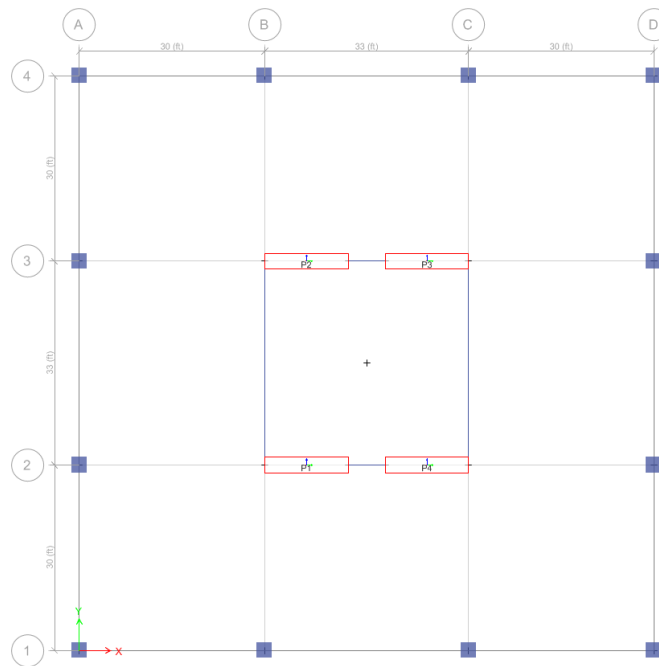


Figure 3.5 Code Linear Model Structural Plan on ETABS 2016

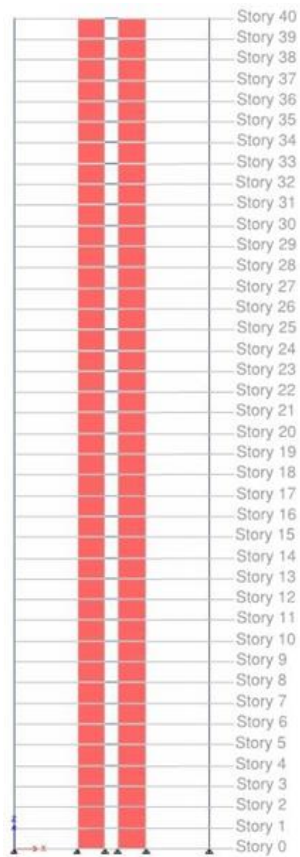


Figure 3.6 Code Linear Model Structural Elevation on ETABS 2016

The Axial Force - Bending Moment couples, resulting by a RSA based on the MCE Response Spectrum, will be scaled by an R factor equal to 7.5 and by another R factor equal to 3.

3.2.1.1 MCE (R=7.5)

RSA with an R factor equal to 7.5 results in the following M-N couples, *Figure 3.7*:

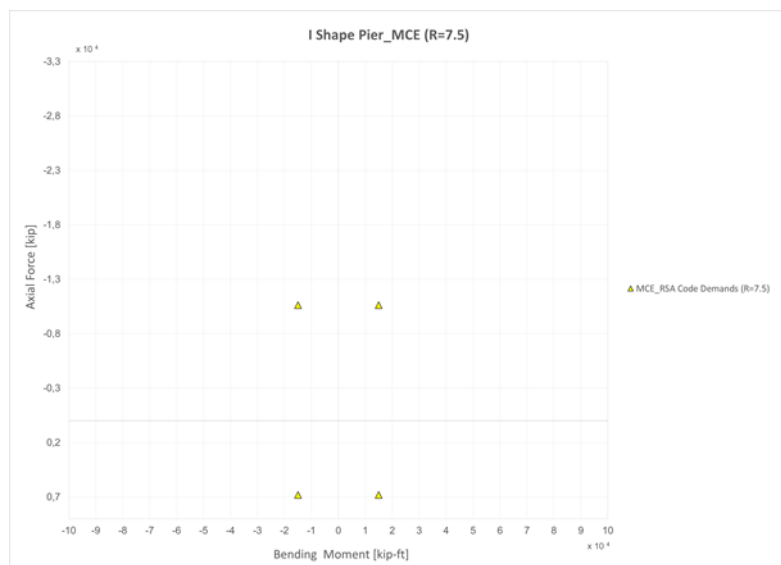


Figure 3.7 Code R=7.5 Stand-Alone Shear Wall Flexure Demands

Designing with these Flexure Demands, the I-Shape pier result is the following rebar configuration, *Figure 3.8*:

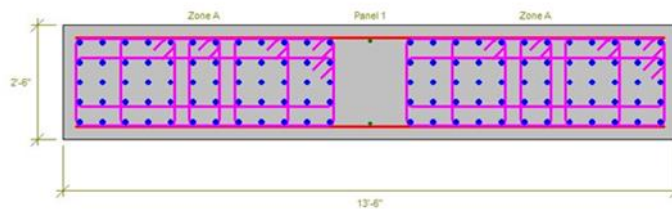


Figure 3.8 Code R=7.5 Stand-Alone Shear Wall Rebar Distribution

By joining the two I-Shaped rectangular sections reinforced in the same way, the following reinforcement distribution is obtained for the L-Shape pier, *Figure 3.9*:

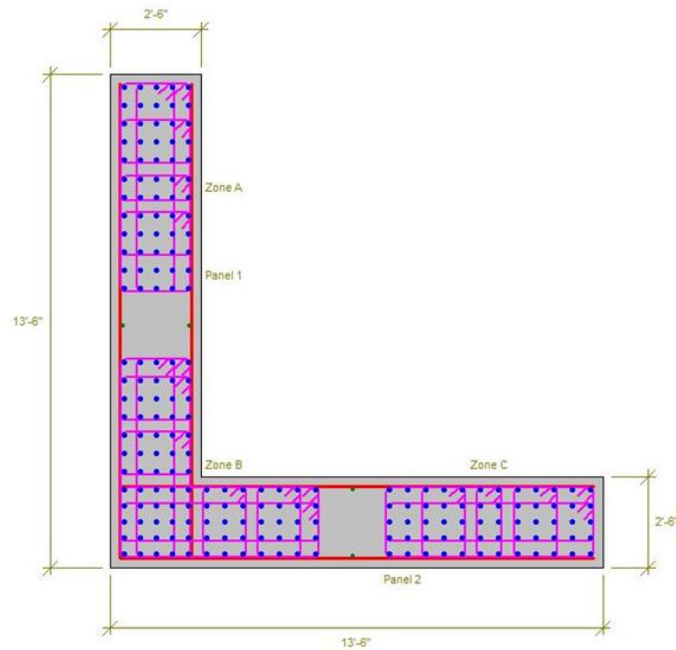


Figure 3.9 Code R=7.5 Compound Shear Wall Rebar Distribution

The *Figure 3.9* section is clearly too conservative.

3.2.1.2 MCE (R=3)

RSA with an R factor equal to 3 results in the following M-N couples, *Figur3.10*:

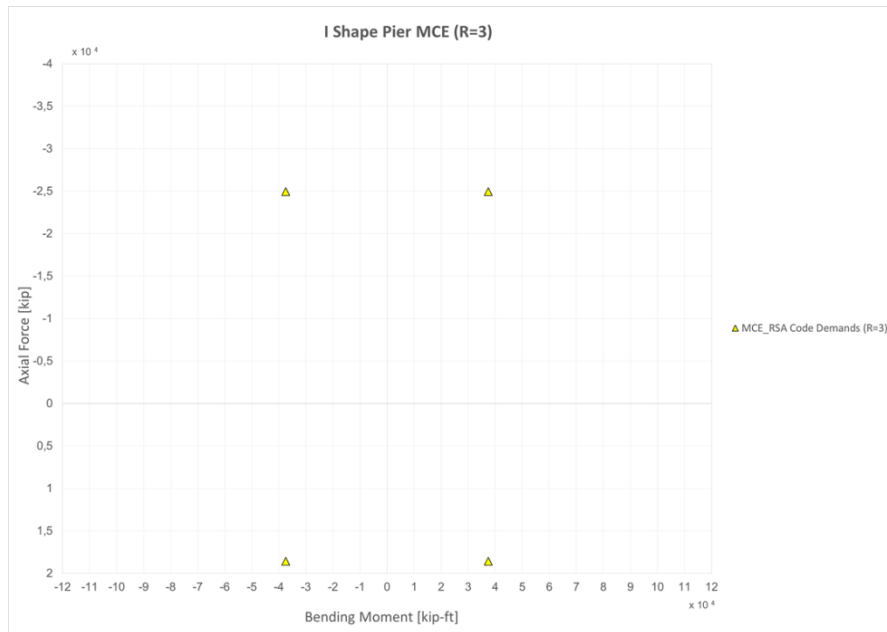


Figure 3.10 Code R=3 Stand-Alone Shear Wall Flexure Demands

Designing with these Flexure Demands, the I-Shape pier result is the following rebar configuration, *Figure 3.11*:

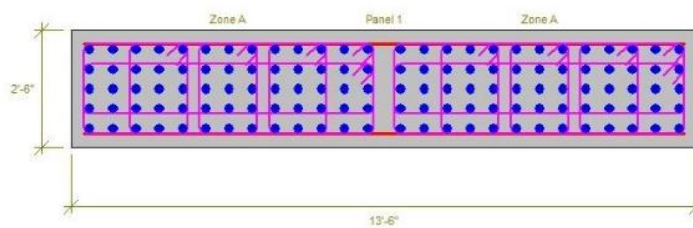


Figure 3.11 Code R=3 Stand-Alone Shear Wall Rebar Distribution

As it is easy to guess, this solution is again overly reinforced.

3.2.2 Axial Force – Biaxial Bending Design (MCE R=7.5)

The piers are now considered as L-Shape sections, *Figure 3.12*..

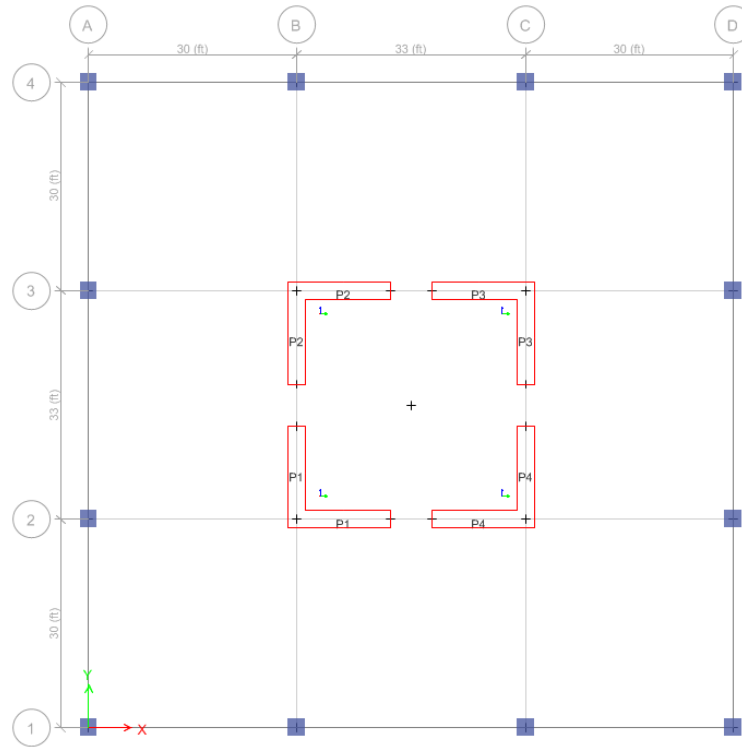


Figure 3.12 Compound Shear Wall Plan

RSA returns axial forces acting on the whole L and coupled with the bending moment applied in the gravity centre of the L-Shape pier. These Flexure Demands in case of R factor equal to 7.5 are shown in the following *Figure 3.13*:

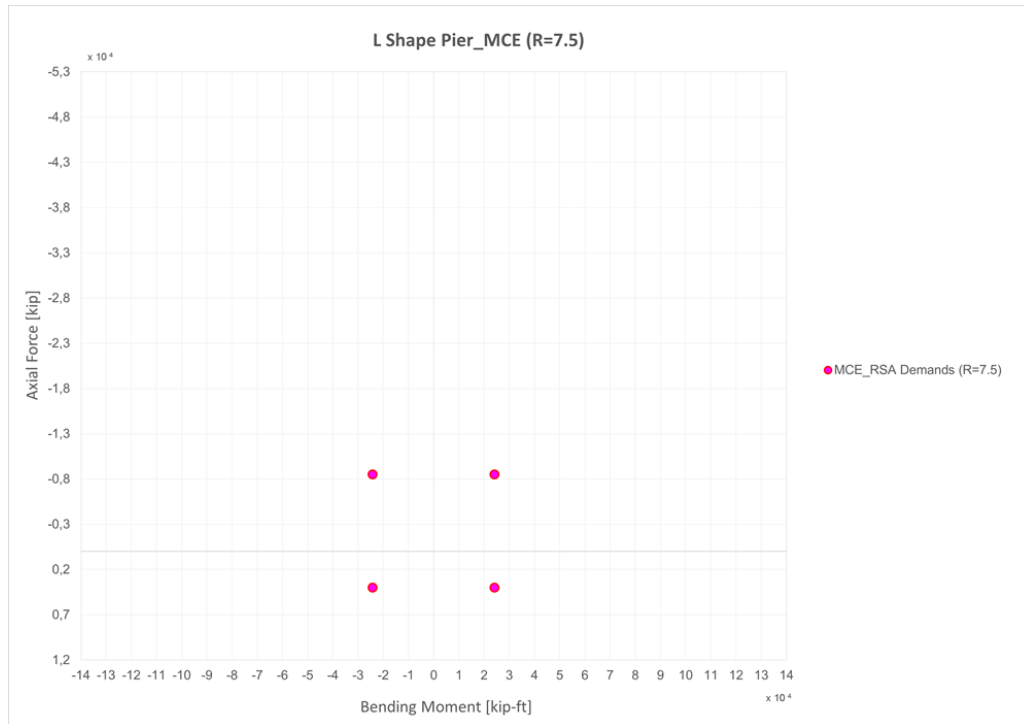


Figure 3.13 Compound R=7.5 Shear Wall Flexure Demands

Designing the L-Shape wall with the widely known Axial Force – Biaxial Bending Moment procedure, the following reinforcement distribution is obtained, *Figure 3.14*:

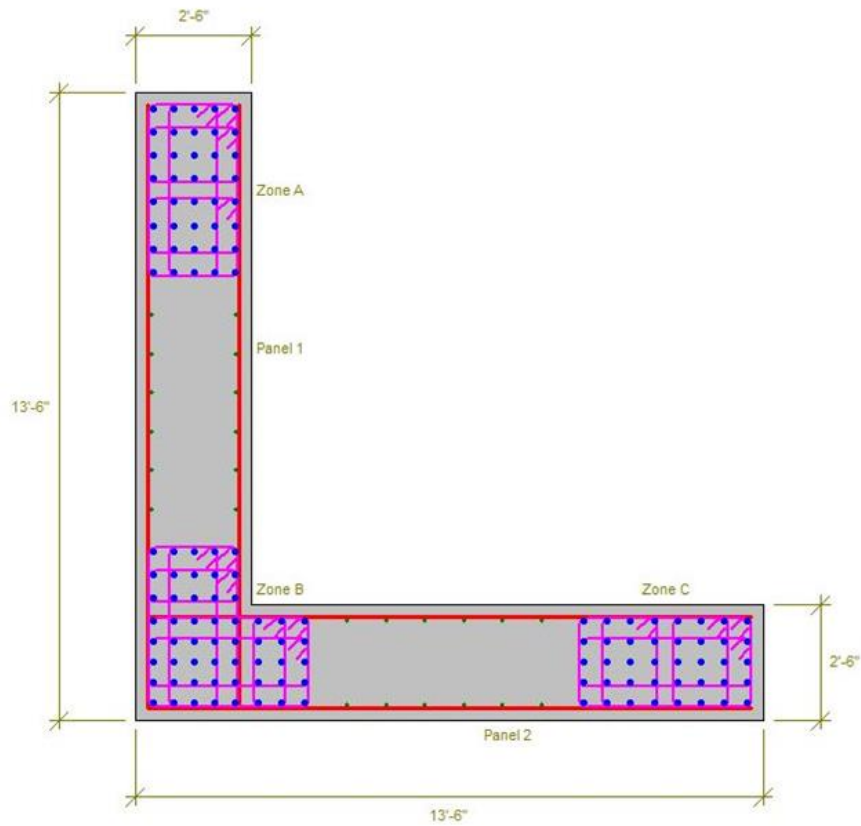


Figure 3.14 Compound R=7.5 Shear Wall Rebar Distribution

Calculating the total core longitudinal reinforcement amounts for all the 8 groups of 5 stories each and summarizing it over the total height of the building, it is possible to have the Total Rebar Area profile, *Figure 3.15*:

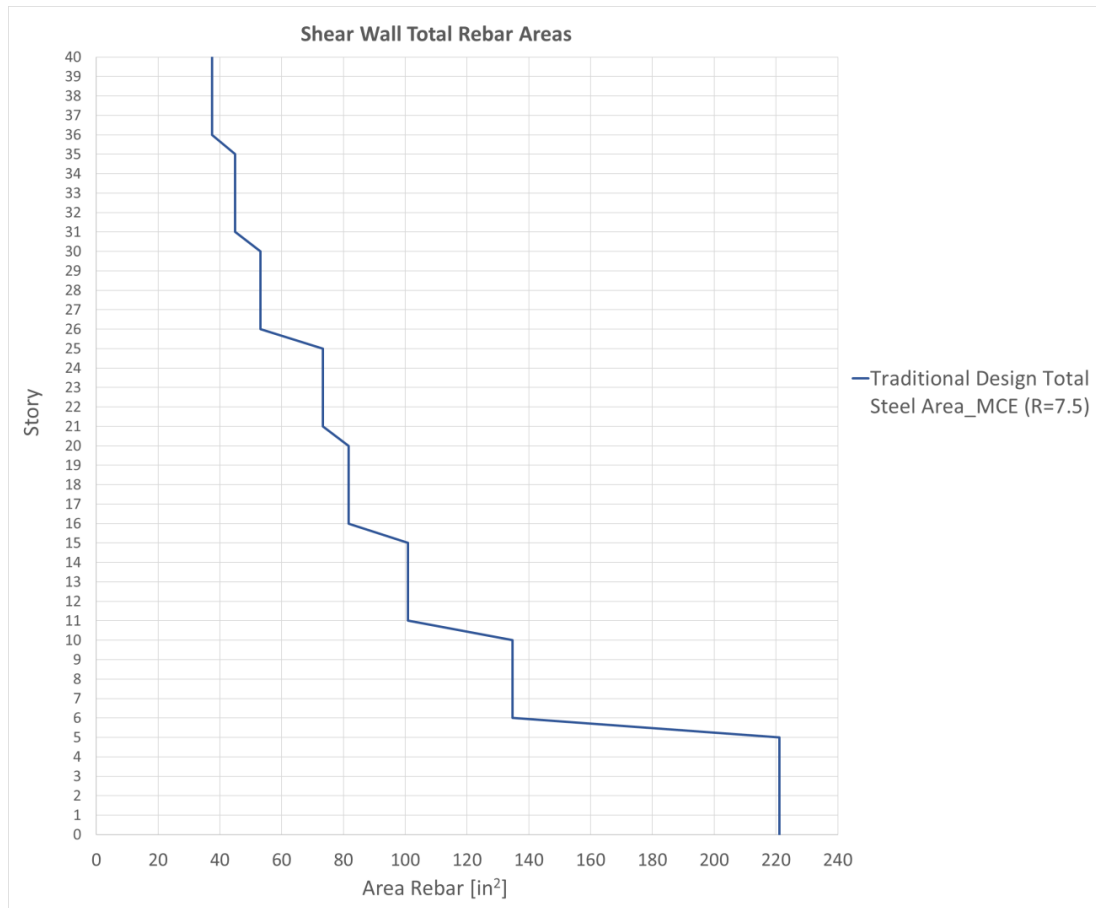


Figure 3.15 Compound Shear Wall Total Longitudinal Reinforcement Areas – MCE (R=7.5)

The total amount of longitudinal steel rebar needed for the whole core is a Volume of 448'344.00 in³.

3.2.3 Axial Force – Biaxial Bending Design (MCE R=3)

The piers are now considered as L-Shape sections, as already done in the previous Chapter, *Figure 3.16*:

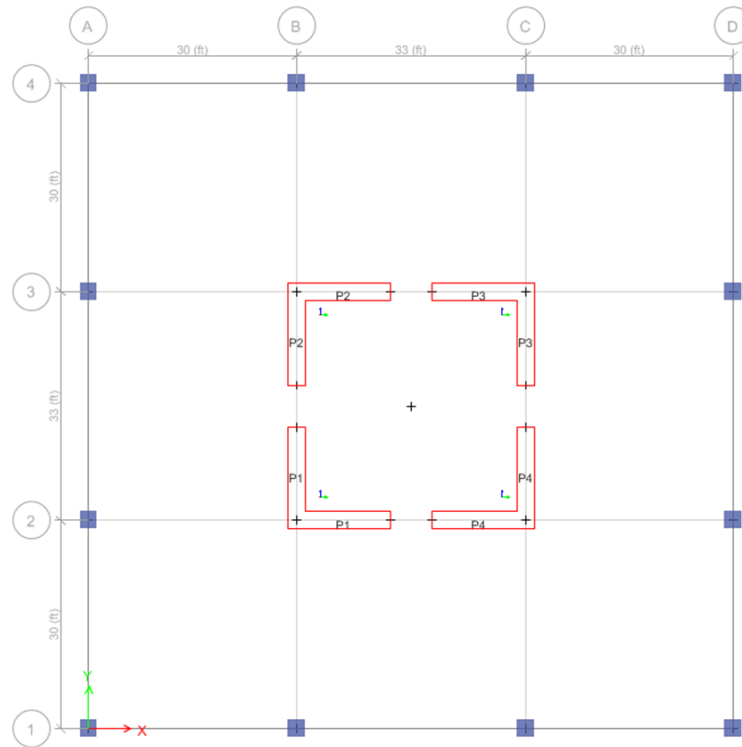


Figure 3.16 Compound Shear Wall Plan

RSA returns axial forces acting on the whole L and coupled with the bending moment applied in the gravity centre of the L-Shape pier. These Flexure Demands in case of R factor equal to 3 are shown in the following *Figure 3.17*:

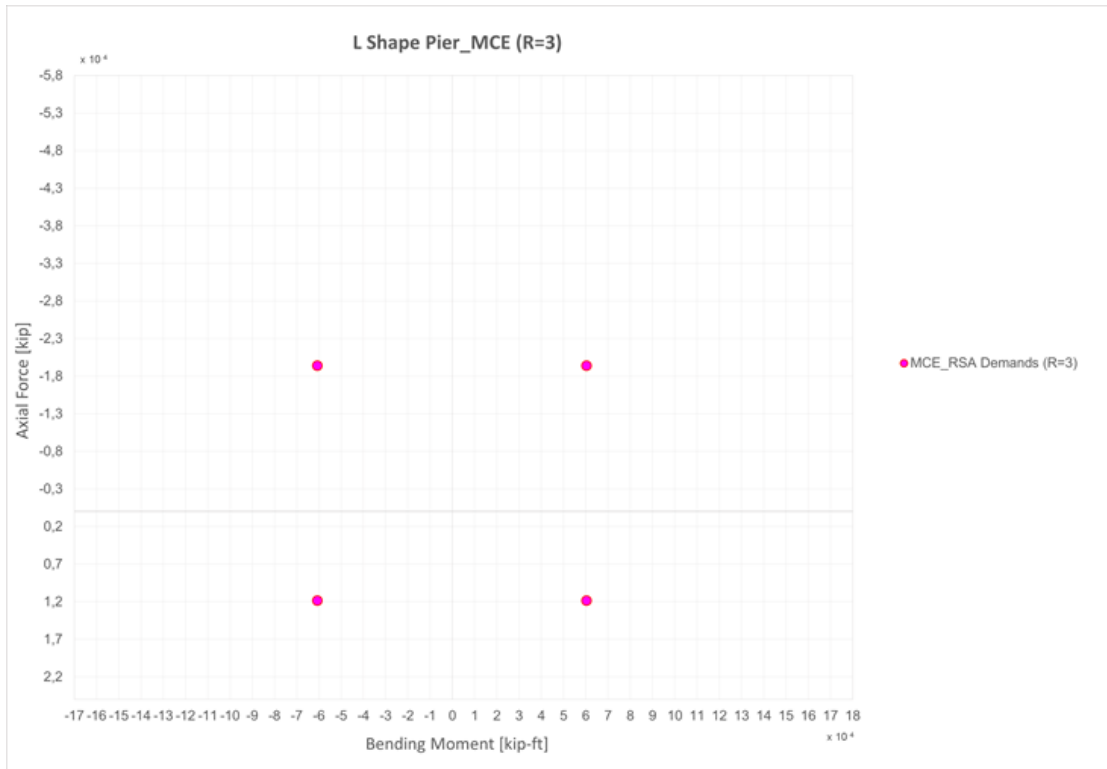


Figure 3.17 Compound R=3 Shear Wall Flexure Demands

Designing the L-Shape wall with the widely known Axial Force – Biaxial Bending Moment procedure, the following reinforcement distribution is obtained, *Figure 3.18*:

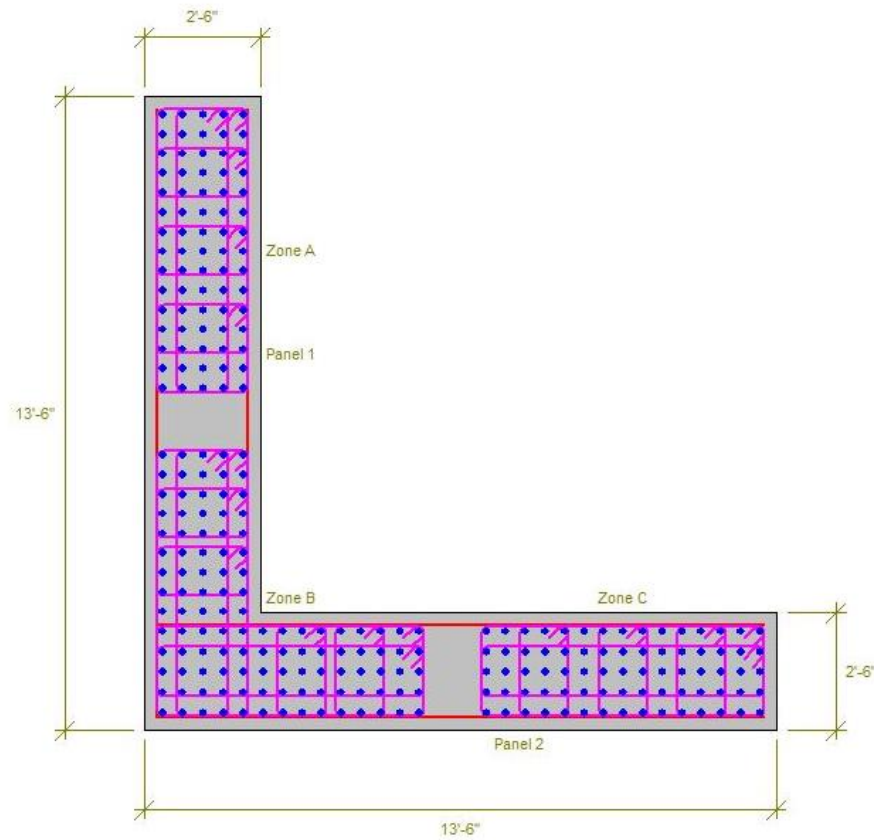


Figure 3.18 Compound R=3 Shear Wall Rebar Distribution

Calculating the total core longitudinal reinforcement amounts for all the 8 groups of 5 stories each and summarizing it over the total height of the building, it is possible to have the Total Rebar Area profile, *Figure 3.19*:

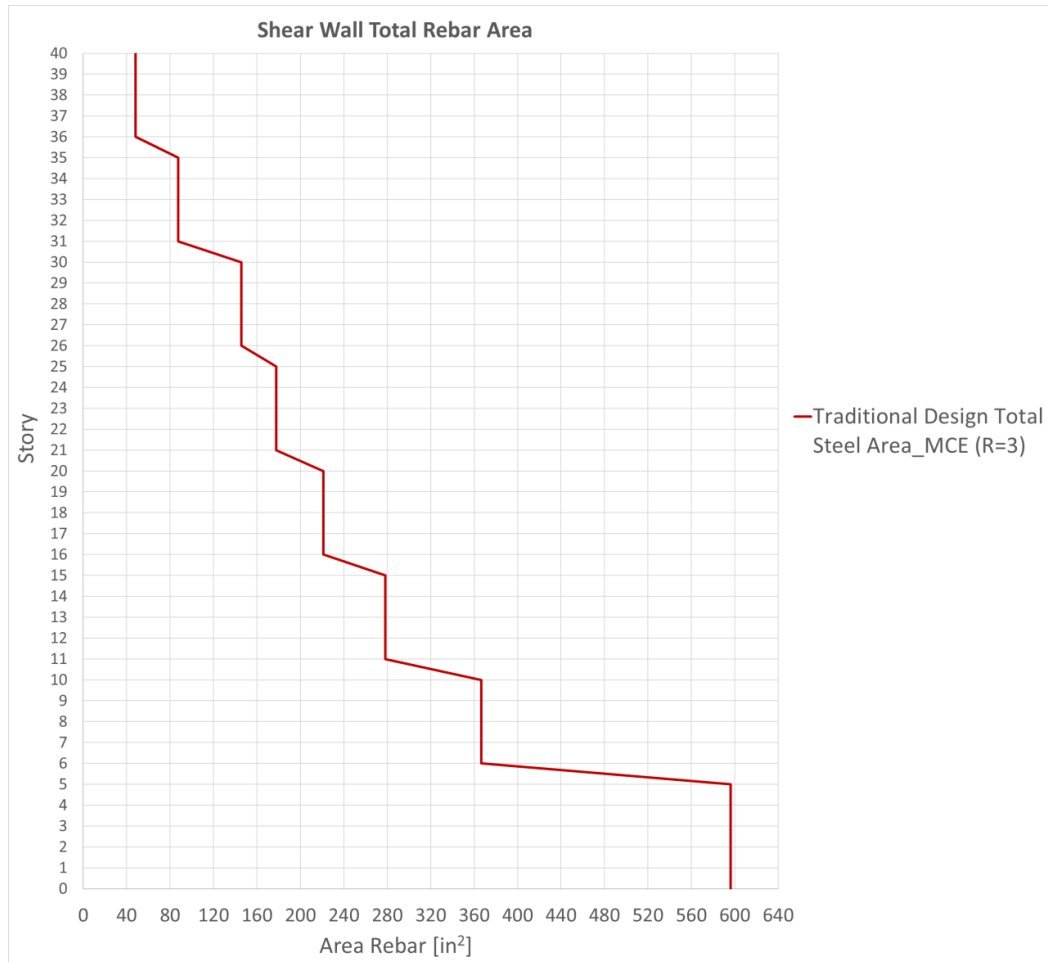


Figure 3.19 Compound Shear Wall Total Longitudinal Reinforcement Areas – MCE (R=3)

The total amount of longitudinal steel rebar needed for the whole core is a Volume of 1'152'750.00 in³.

3.3 Proposed Design Methodologies

This chapter proposes a new design methodology based on RSA. After having carried out this linear dynamic analysis on the prototype model, the L-Shape wall pier shows a stress distribution all over its section. This stress diagram is obtained considering the pier as a simple cantilever beam with L-Shape cross section. The compound wall is thus evaluated as it really is, *Figure 3.20*:

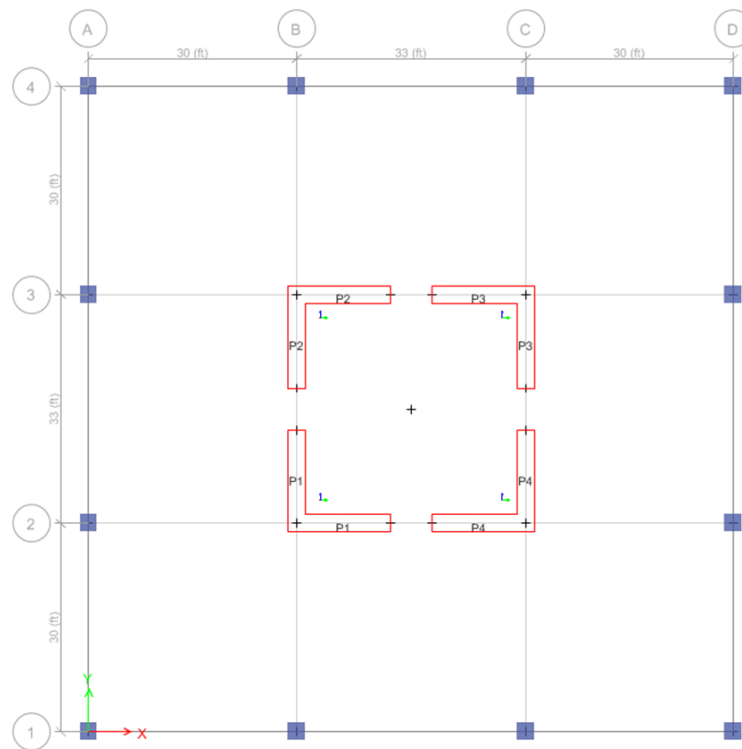


Figure 3.20 L-Shape Piers

Once deduced the global stress distribution, *Figure 3.21*, it is now possible to divide the L-Shape pier into two stand-alone I-Shape piers, *Figure 3.22*, and design them as separate planar walls.

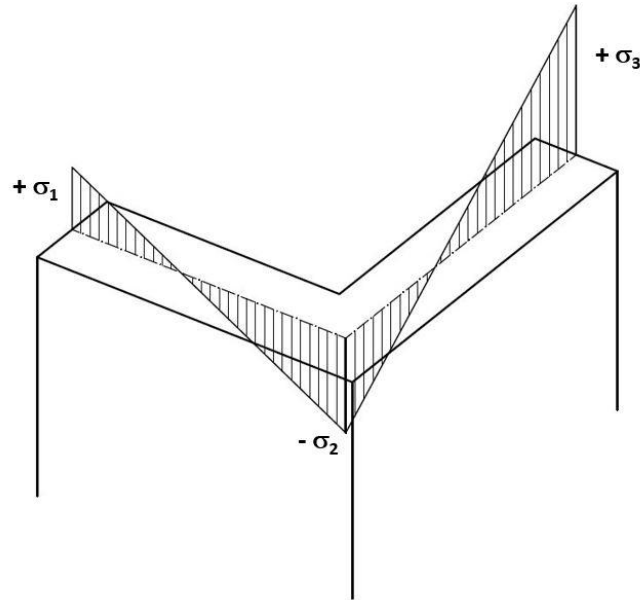


Figure 3.21 L-Shape Section Stress Distribution

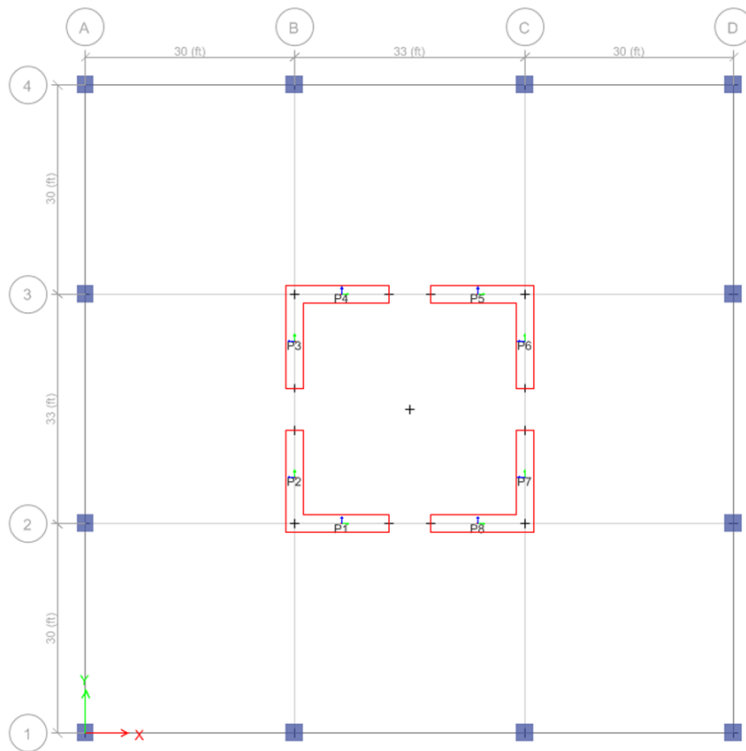


Figure 3.22 I-Shape Piers

By integration of the stress diagrams on each flange, the Flexure Demands for the design of all the I-Shape walls are extracted, *Figure 3.23*.

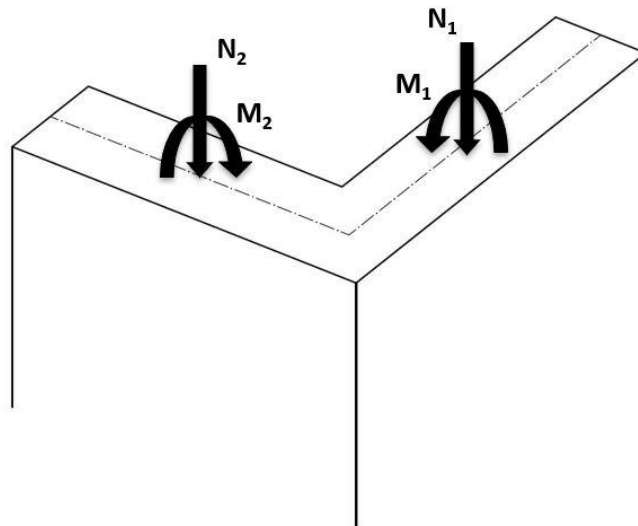


Figure 3.23 I-Shape Walls Flexure Demands

The L-Shaped walls are then modelled as two separate I-Shape rectangular section walls but initially perceived as a single L pier, from which derives the stress distribution which gives the M-N couples for each flange.

As it is easy to guess, once known the stress distribution on any shape section, it would be possible to optimize the reinforcement configuration in order to maximize the energy dissipation with the minimum amount of rebar.

3.3.1 Response Spectrum Design

Following the Proposed Design Procedure explained in the previous chapter, the RSA provides the Flexure Demands extracted by the whole L-Shape pier and then calculated also for the Stand-Alone Flanges. It should be underlined that for all the sections design, the maximum values of each type of solicitation were not simply coupled together, but the used flexure demand couples were obtained by taking the maximum value for each type of solicitation coupled with its corresponding value for the other solicitation, that is not in fact the maximum value.

The Axial Force - Bending Moment couples, resulting by a RSA based on the MCE Response Spectrum, will be scaled by an R factor equal to 7.5 and by another R factor equal to 3. The obtained couples of values will represent two different proposed design methodologies: Option A_RSA MCE (R=7.5) and Option B_RSA MCE (R=3).

3.3.2 Response Spectrum Analysis Story Drift

The following plot shows the maximum story drift in X and Y direction of the Response Spectrum Analysis, MCE (R=7.5) and MCE (R=3).

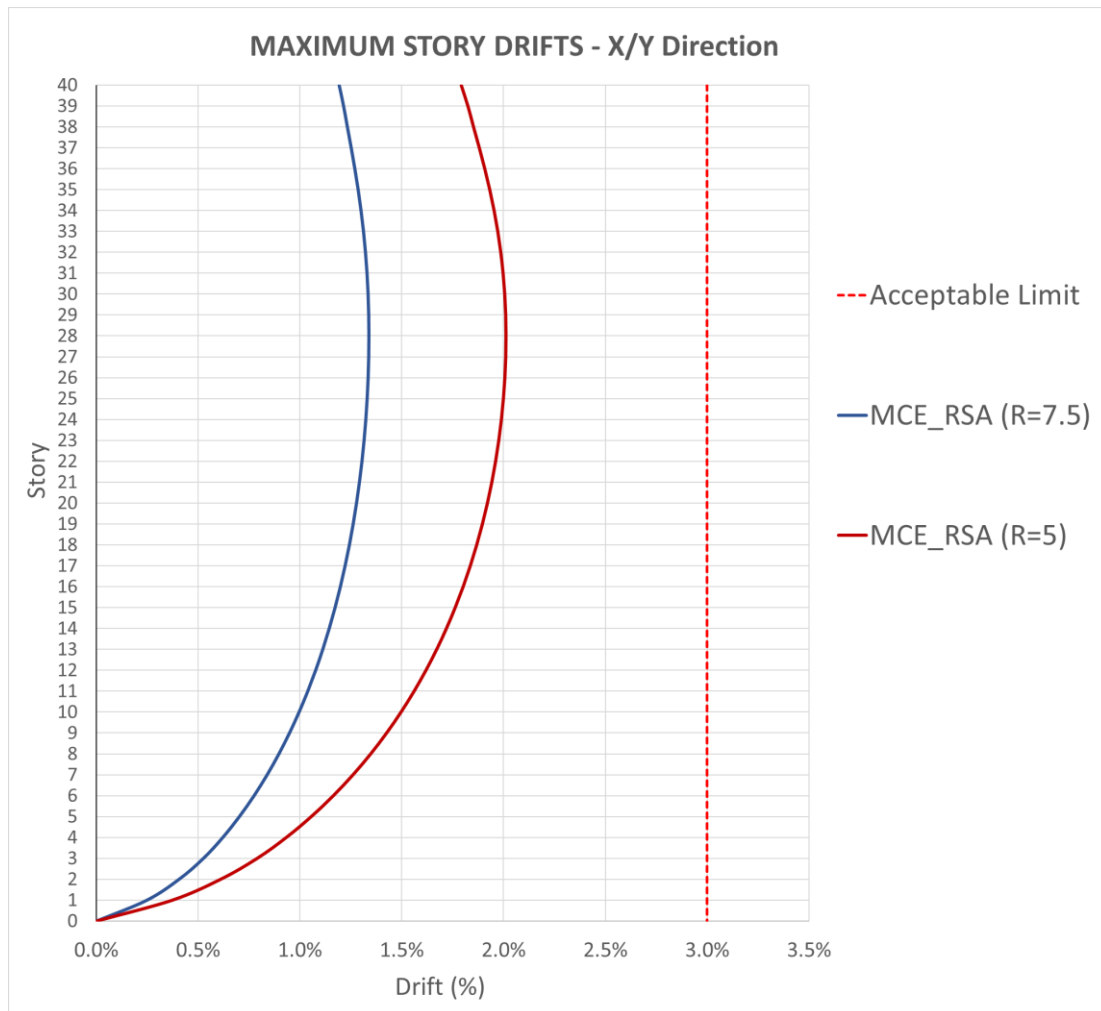


Figure 3.24 Maximum Story Drift, MCE (R=7.5) and MCE (R=3)

3.3.3 Response Spectrum Analysis Story Shear

The following plot shows the story shear in X and Y direction of the Response Spectrum Analysis, MCE (R=7.5) and MCE (R=3).

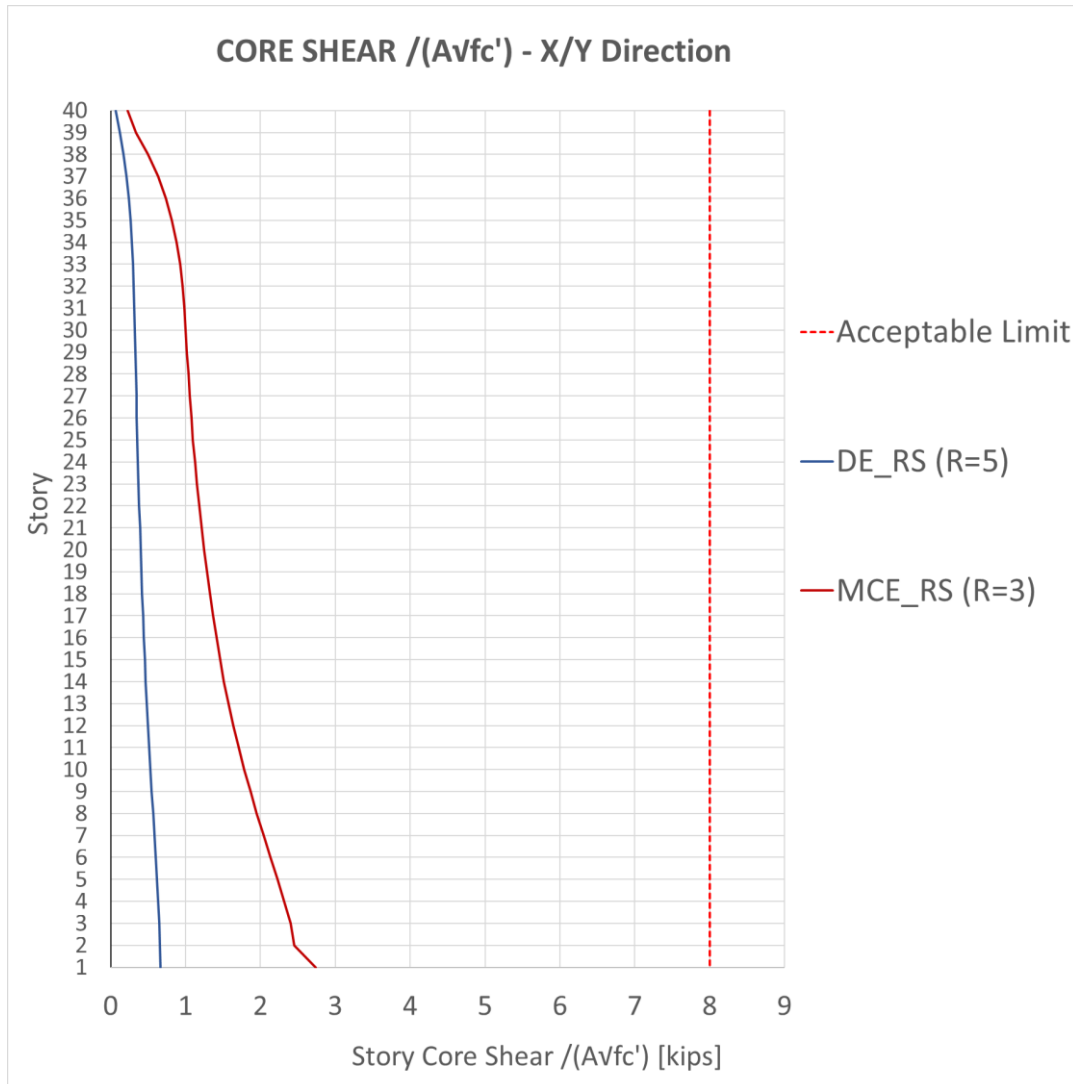


Figure 3.25 Story Shear, MCE (R=7.5) and MCE (R=3)

3.3.4 Wall Reinforcement Option A (MCE R=7.5)

Option A_RSA MCE (R=7.5) Flexure Demands are given.

Designing with these M-N couples, the I-Shape pier result is the following rebar configuration, *Figure 3.24*:

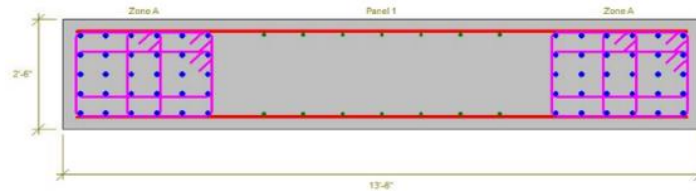


Figure 3.26 Option A_RSA MCE (R=7.5) Stand-Alone Shear Wall Rebar Distribution

The Option A Flexure Demands are much smaller than the Traditional Code Design ones and they lead to a reinforcement distribution which gives a Capacity Curve of the I-Shape wall not including those latter, *Figure 3.25*. This means that Option A both leads to a less rebar amount and consequently provides more ductility.

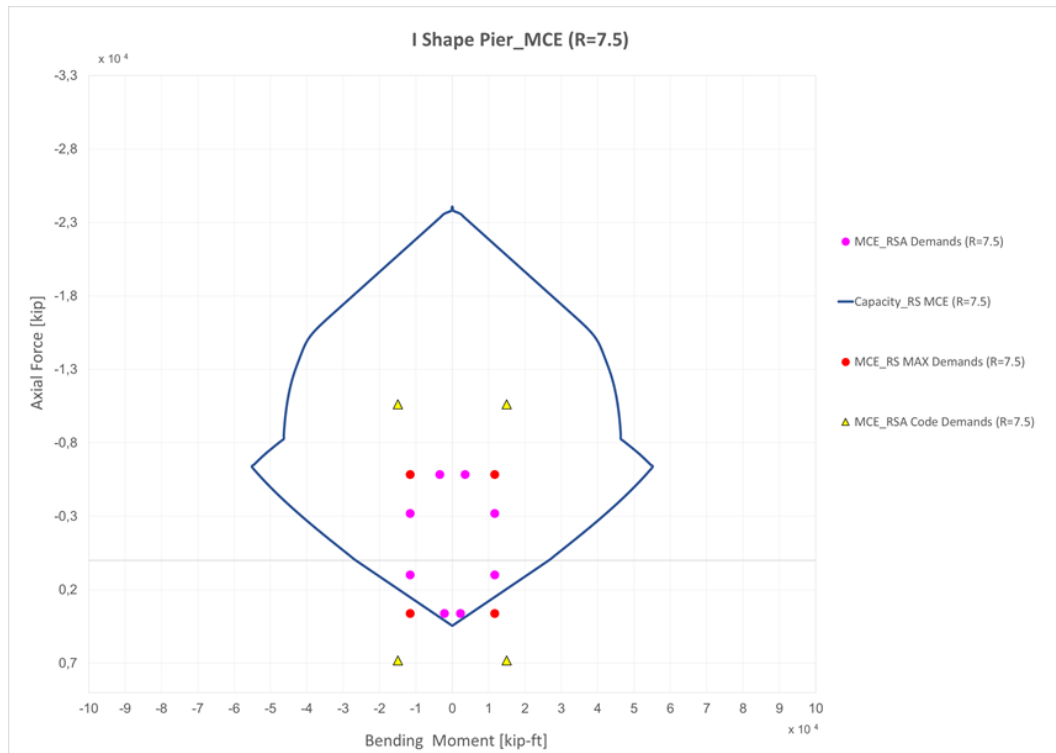


Figure 3.27 Option A_RSA MCE (R=7.5) Stand-Alone Shear Wall Flexure Demands Plot

Doing the same proposed design methodology for all the 8 groups of 5 stories each, the Rebar Area Ratio (ρ) profile is given, *Figure 3.26*:

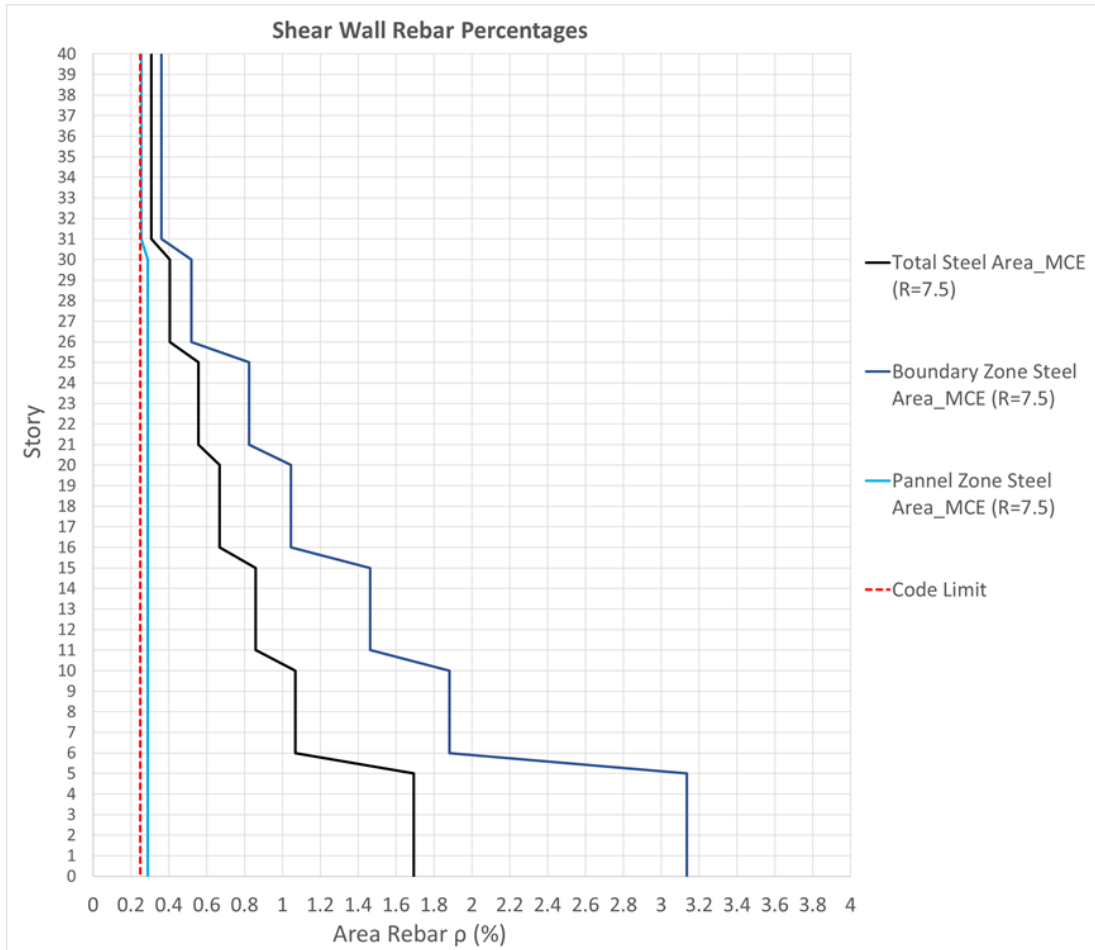


Figure 3.28 Option A_RSA MCE (R=7.5) Rebar Amounts

By joining the two I-Shaped rectangular sections reinforced in the same way, the following reinforcement distribution is obtained for the L-Shape pier:

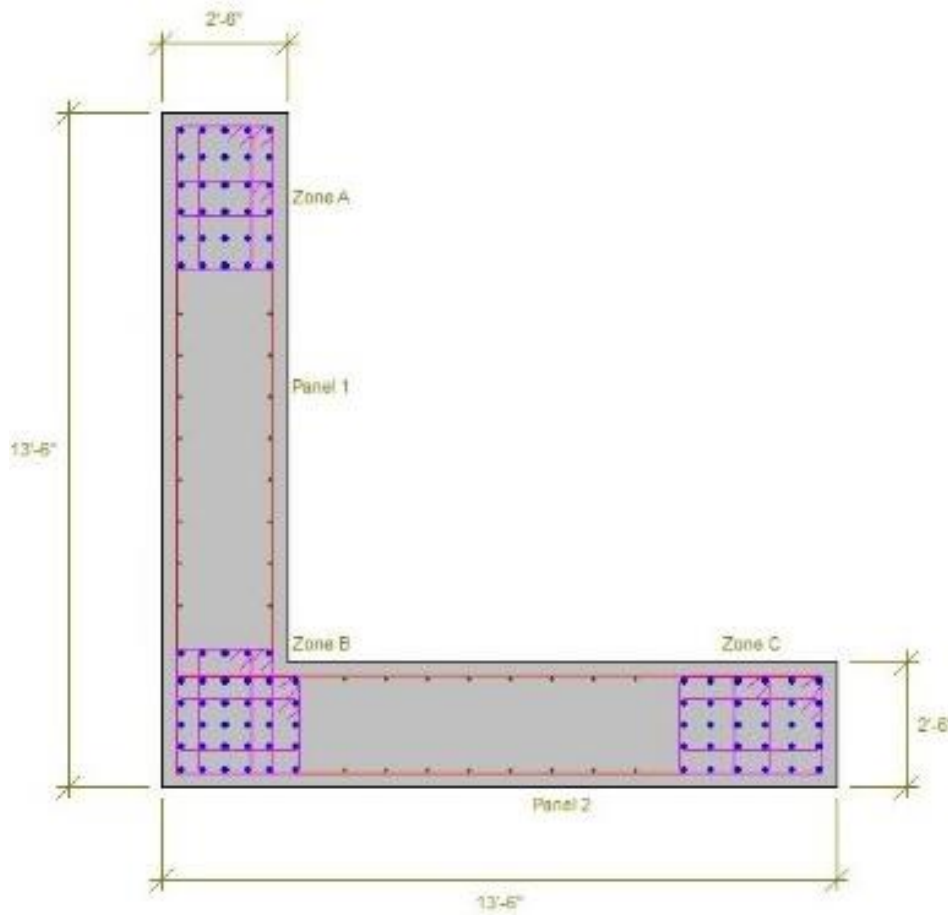


Figure 3.29 Option A_RSA MCE (R=7.5) Compound Shear Wall Rebar Distribution

This L-Shape rebar configuration displays a Capacity Curve, *Figure 3.28*, which is smaller than the hypothetical one obtained if the L section was designed as a global pier with the Flexure Demands given directly by the RSA for the L-Shape wall, as done in Chapter 3.3.1:

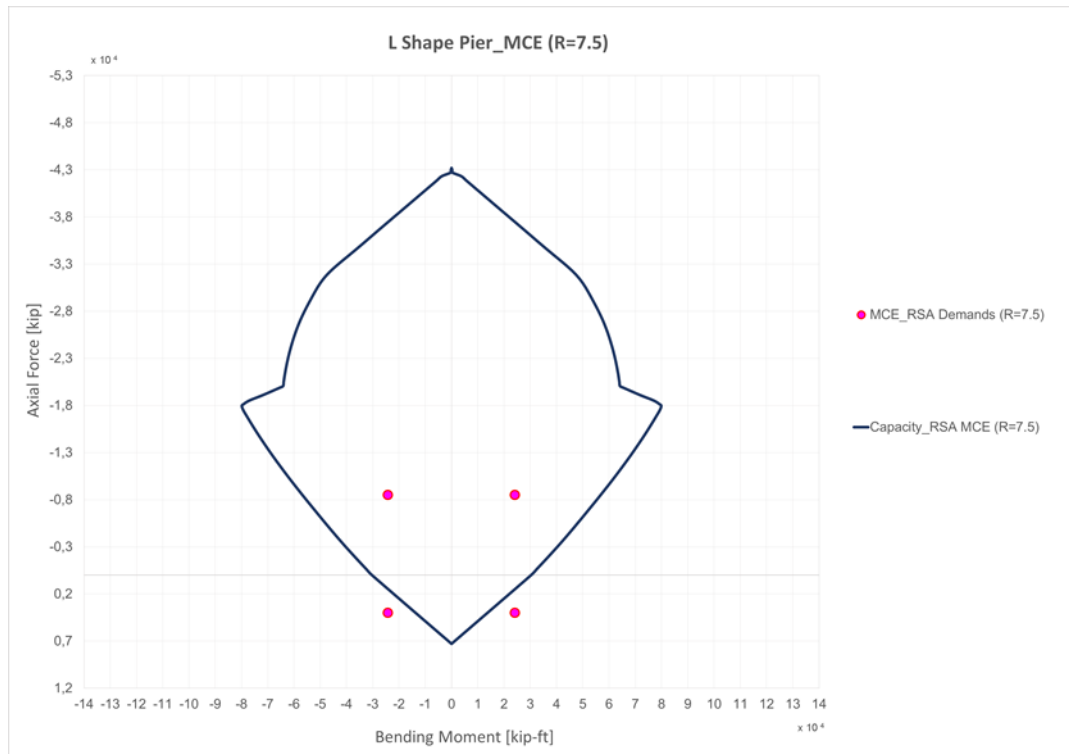


Figure 3.30 Option A_RSA MCE (R=7.5) Compound Shear Wall Flexure Demands Plot

3.3.5 Wall Reinforcement Option B (MCE R=3)

As done for Option A, Option B_RSA MCE (R=3) Flexure Demands are given with an R factor equal to 3.

Designing with these M-N couples, the I-Shape pier result is the following rebar configuration, *Figure 3.31*:

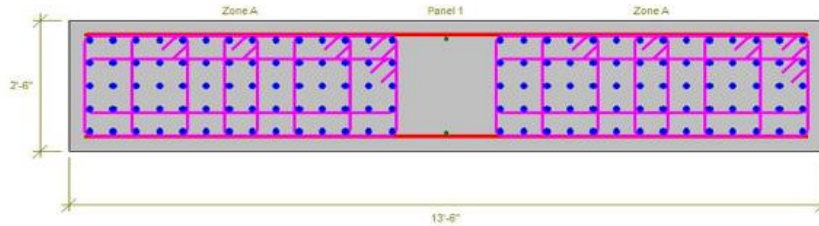


Figure 3.31 Option B_RSA MCE (R=3) Stand-Alone Shear Wall Rebar Distribution

The Option B Flexure Demands are much smaller than the Traditional Code Design ones, and this gap is more marked compared to Option A, and they lead to a reinforcement distribution which gives also here a Capacity Curve of the I-Shape wall not including those latter, *Figure 3.32*. This means that Option B both leads to a less rebar amount and consequently provides more ductility, with better results than Option A:

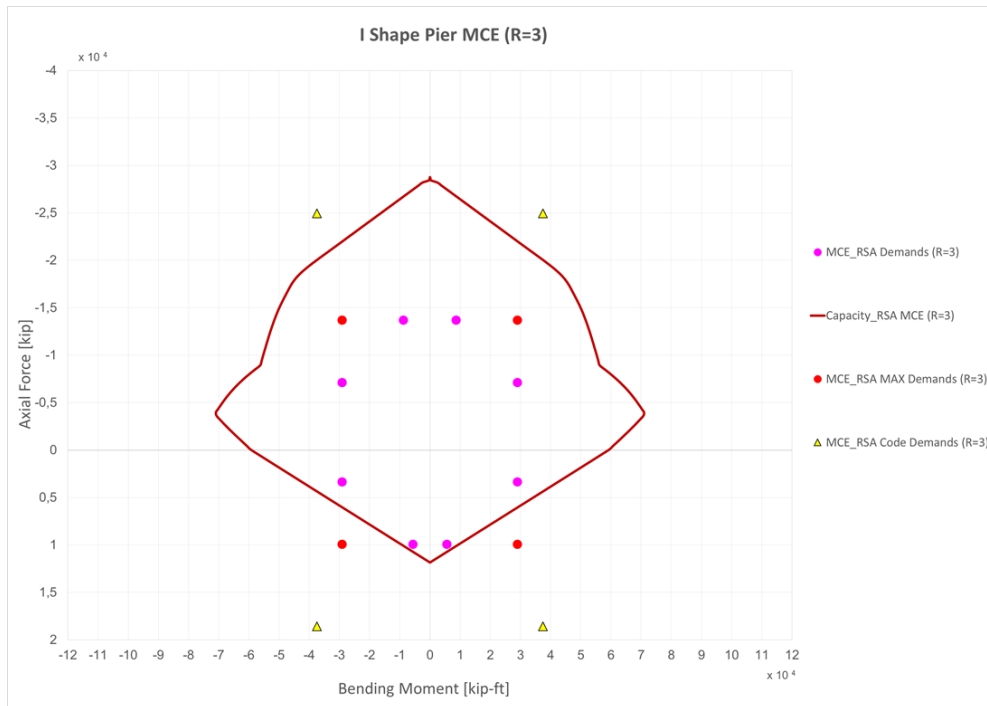


Figure 3.32 Option B_RSA MCE (R=3) Stand-Alone Shear Wall Flexure Demands Plot

As already done in Option A, the same proposed design methodology is applied for all the 8 groups of 5 stories each and the Rebar Area Ratio (ρ) profile results, Figure 3.33:

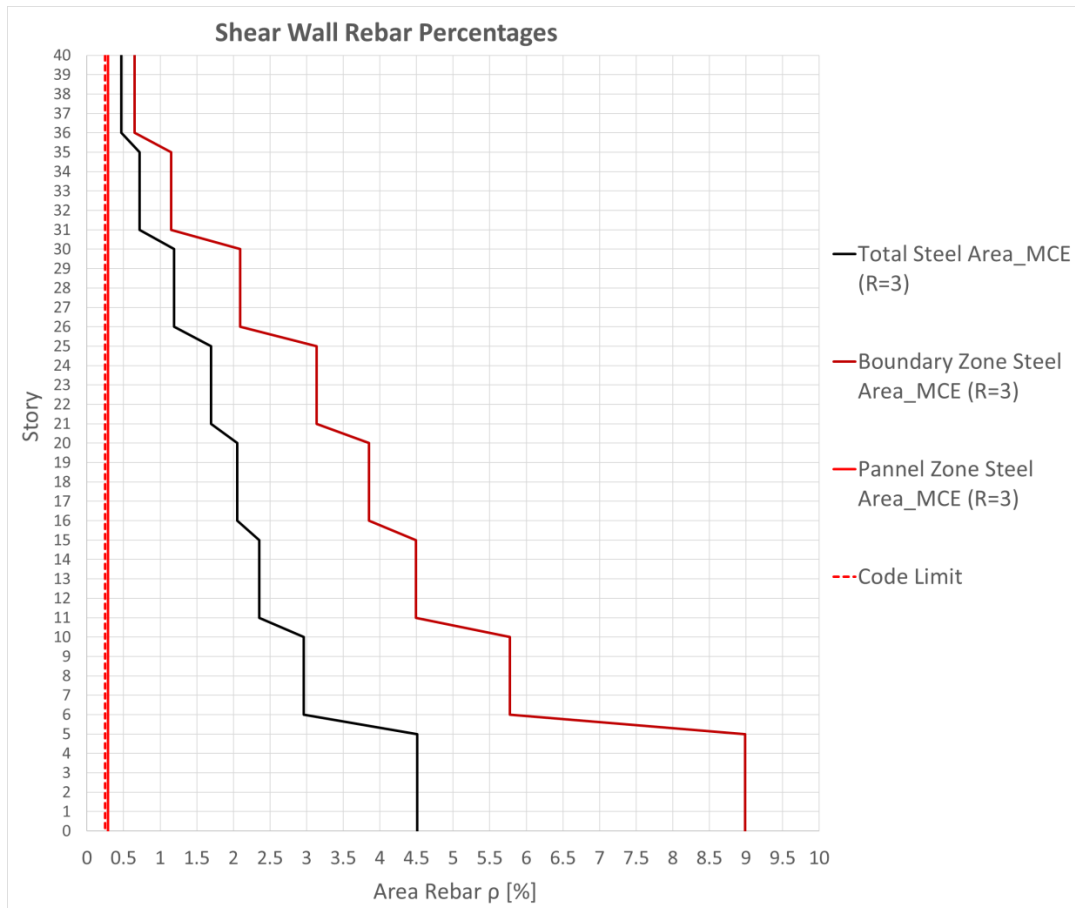


Figure 3.33 Option B_RSA MCE (R=3) Rebar Amounts

By joining the two I-Shaped rectangular sections reinforced in the same way, the following reinforcement distribution is obtained for the L-Shape pier:

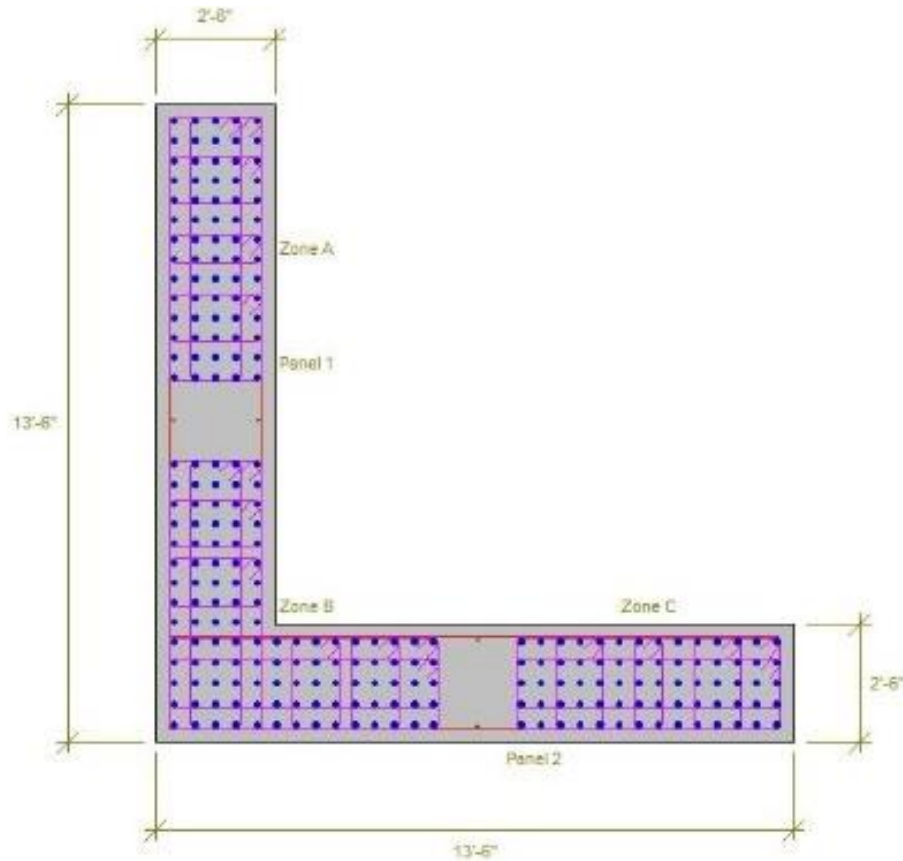


Figure 3.34 Option B_RSA MCE (R=3) Compound Shear Wall Rebar Distribution

This L-Shape rebar configuration displays a Capacity Curve, *Figure 3.35*, which is smaller than the hypothetical one obtained if the L section was designed as a global pier with the Flexure Demands given directly by the RSA for the L-Shape wall, as done in chapter 3.2.3:

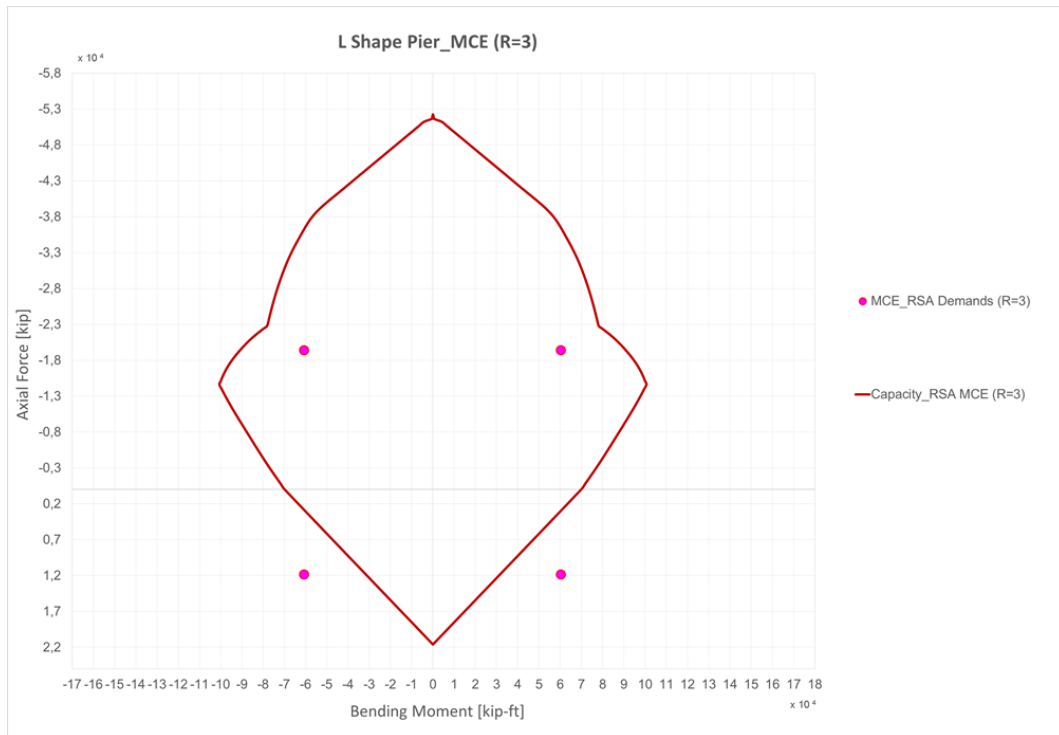


Figure 3.35 Option B_RSA MCE (R=3) Compound Shear Wall Flexure Demands Plot

3.3.6 Linear Response History Design

This chapter explains another proposed design methodology based on LRHA. After having performed this linear dynamic analysis on the prototype model, the L-Shape wall pier shows a stress distribution all over its section. This stress diagram is obtained considering the pier as a simple cantilever beam with L-Shape cross section. The compound wall is thus evaluated as it really is.

In this case, differently by the RSA case, Flexure Demands couples acting on the L-Shape pier section are extracted by calculating the average of the maximum and of the minimum values resulting by the 11 performed ground motions on each pier. The average is made collecting the maximum and minimum demands with same sign from the spaghetti, and not between all. These average values of each type of solicitation are, also in this case, coupled with the average of the corresponding values for the other solicitation, that is not in fact the maximum value. For each Pier the following M-N couples are then extracted:

$$\text{avg}_{11GM} \left(\min_M(V, M) \right)$$

$$\text{avg}_{11GM} \left(\min_V(V, M) \right)$$

$$\text{avg}_{11GM} \left(\max_M(V, M) \right)$$

$$\text{avg}_{11GM} \left(\max_V(V, M) \right)$$

Once known the Flexure Demands on the L-Shape pier, it is easy calculate the stand-alone I-Shape walls N-M couples with the same proposed procedure explained at the beginning of this Chapter 3.3.

The Axial Force - Bending Moment couples, resulting by a LRHA based on the MCE Response Spectrum, will be again scaled by an R factor equal to 7.5 and by another R factor equal to 3. The obtained couples of values will represent two

different proposed design methodologies: Option C_LRHA MCE (R=7.5) and Option D_LRHA MCE (R=3).

3.3.7 Wall Reinforcement Option C (MCE R=7.5)

Option C_LRHA MCE (R=7.5) Flexure Demands are given by the procedure above explained.

As it is possible to notice, designing with these M-N couples will turn out in a section reinforcement configuration which is almost the minimum indicated by the code. This is easy guessed cause the Option C spaghetti barely reach positive values able to give tensile axial forces, *Figure 3.36*.

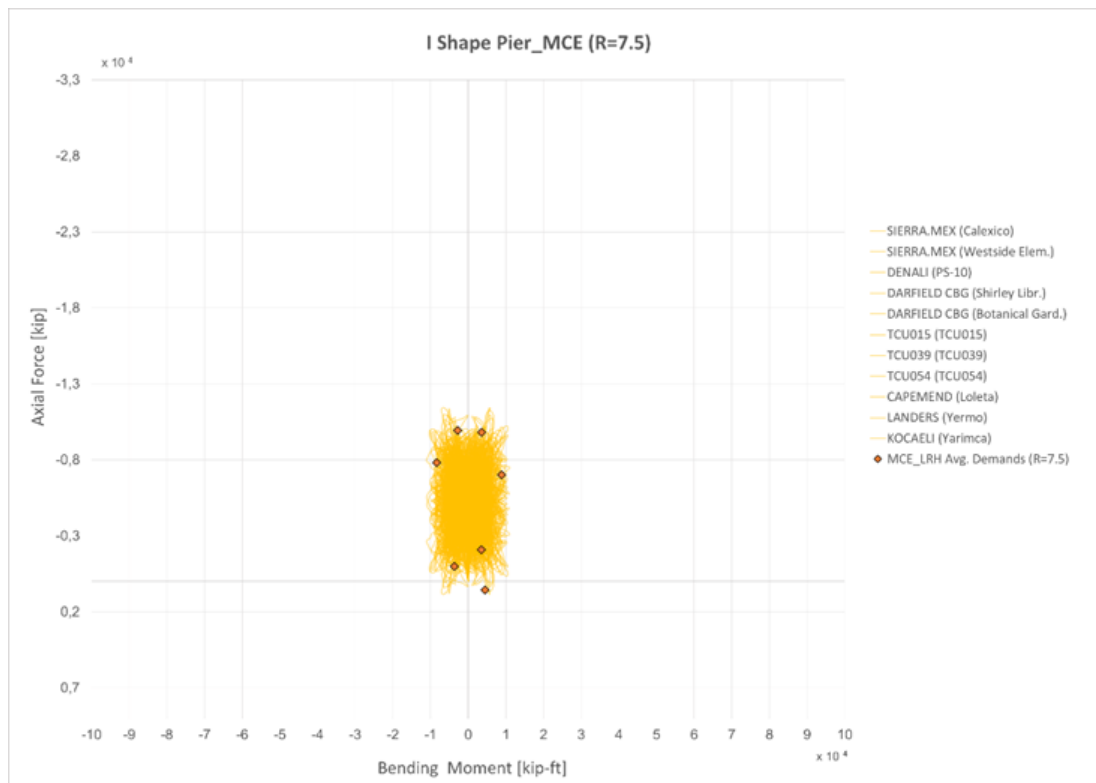


Figure 3.36 Option C_LRHA MCE (R=7.5) Stand-Alone Shear Wall Flexure Demands Plot

Moreover, this design provides the minimum reinforcement quantities in all the levels above the first 5 stories group. This means the absence of boundary zones and the pier will act as a totally panel zone. In order to this, Option C will be avoided as a proposed design methodology.

In case of L-Shape pier, the same situation is observed. Option C will be then totally neglected in the present research.

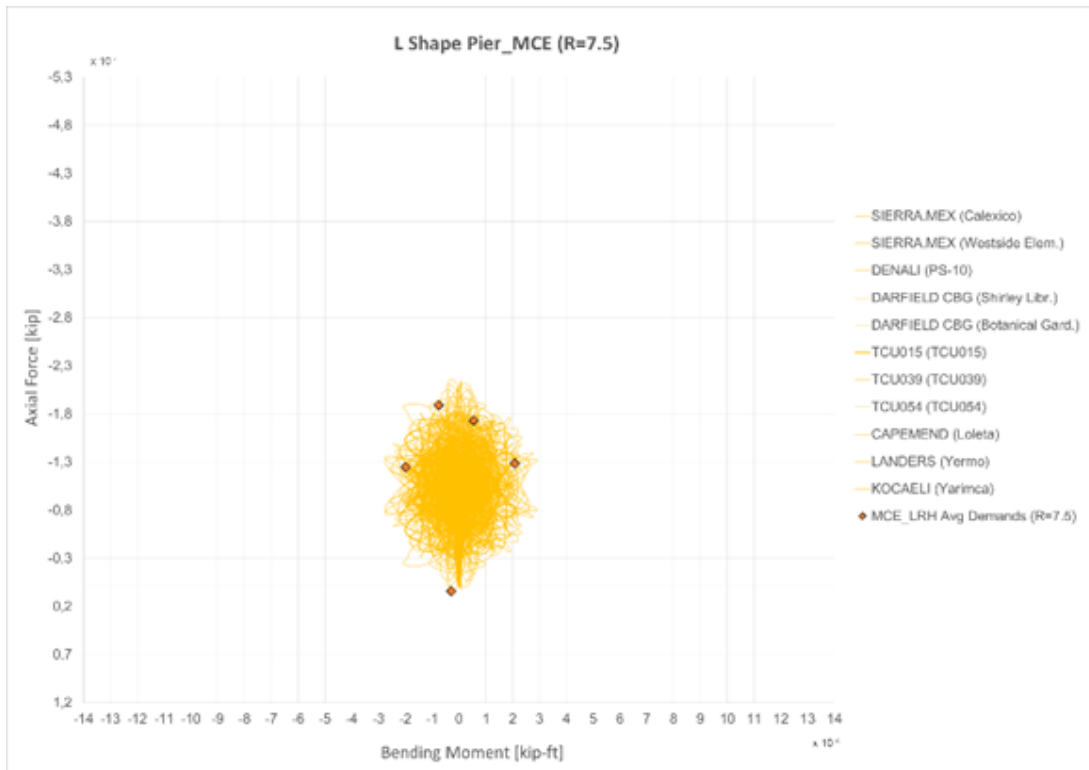


Figure 3.37 Option C_LRHA MCE (R=7.5) Compound Shear Wall Flexure Demands Plot

3.3.8 Wall Reinforcement Option D (MCE R=3)

Option D_LRHA MCE (R=3) Flexure Demands are given by scaling by an R factor equal to 3.

Designing with these M-N couples, the I-Shape pier result is the following rebar configuration, *Figure 3.38*:

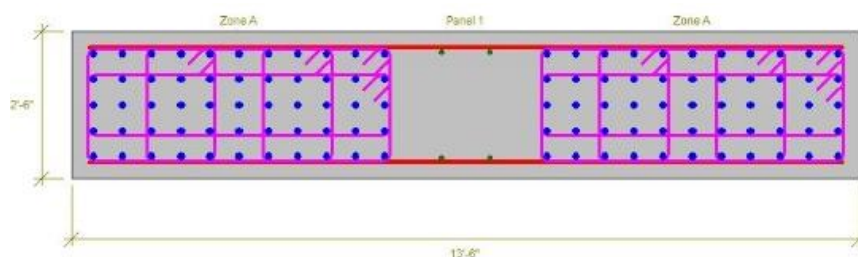


Figure 3.38 Option D_LRHA MCE (R=3) Stand-Alone Shear Wall Rebar Distribution

This Option D reinforcement distribution leads to the following Capacity Curve of the I-Shape wall, *Figure 3.39* :

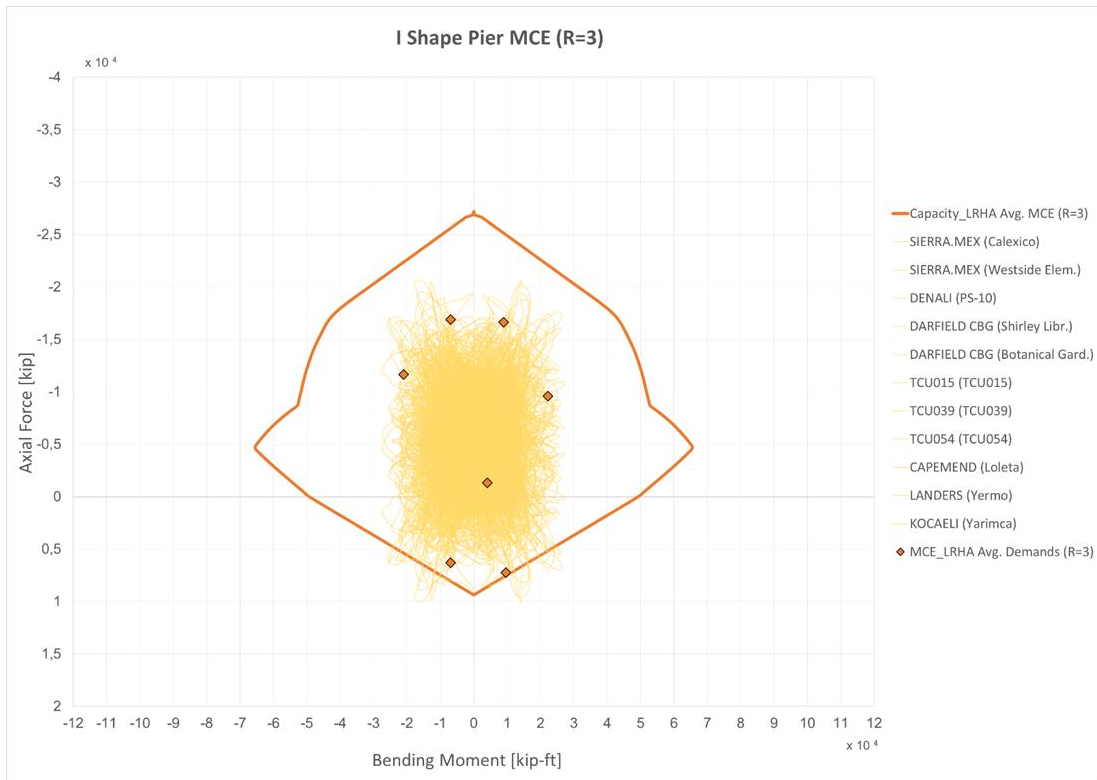


Figure 3.39 Option D_LRHA MCE (R=3) Compound Shear Wall Flexure Demands Plot

Doing the same proposed design methodology for all the 8 groups of 5 stories each, the Rebar Area Ratio (ρ) profile is given, *Figure 40*:

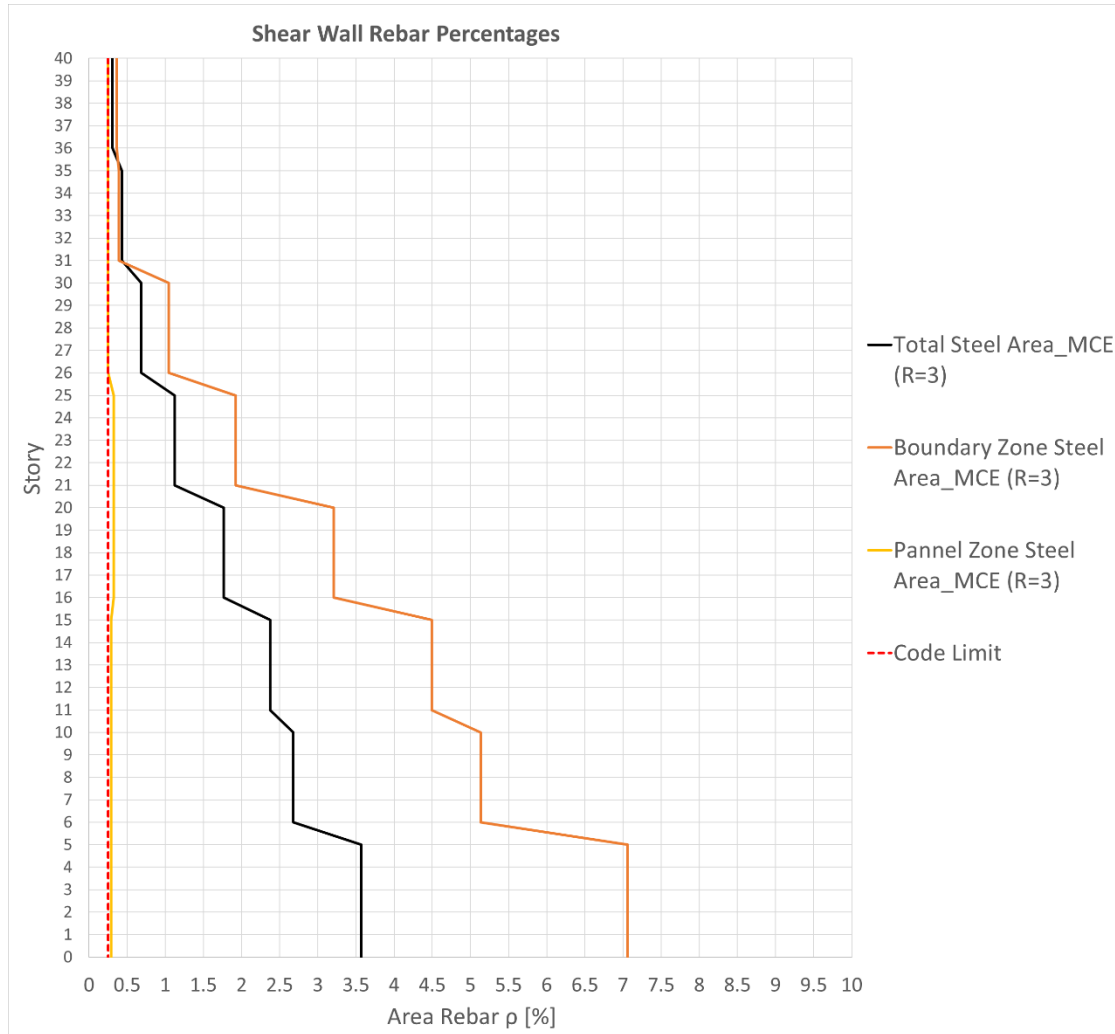


Figure 3.40 Option D_LRHA MCE (R=3) Rebar Amounts

By joining the two I-Shaped rectangular sections reinforced in the same way, the following reinforcement distribution is obtained for the L-Shape pier:

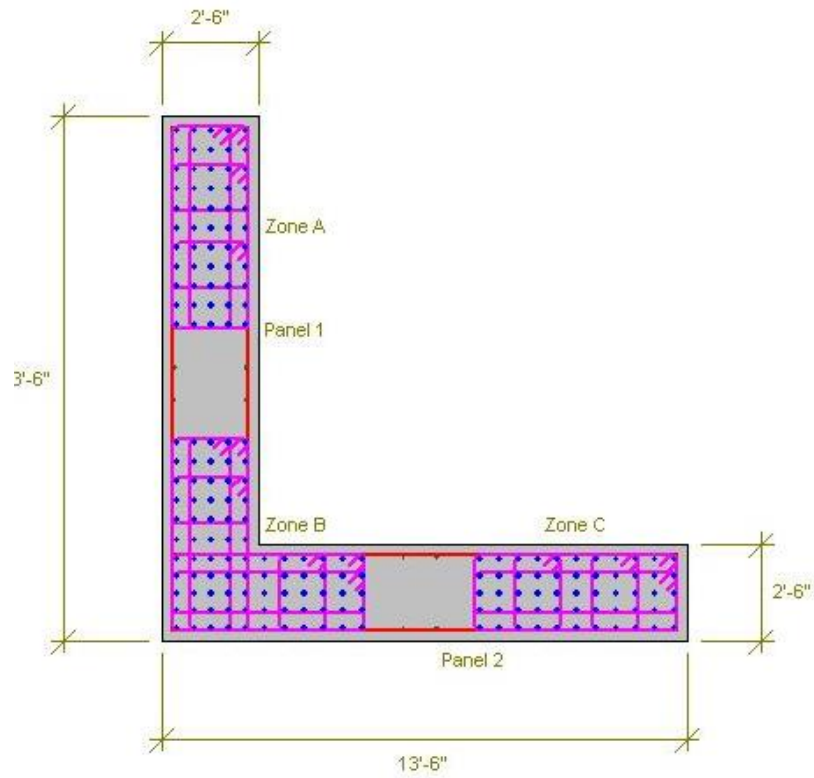


Figure 3.41 Option D_LRHA MCE (R=3) Compound Shear Wall Rebar Distribution

This L-Shape rebar configuration displays a Capacity Curve, *Figure 3.41*:

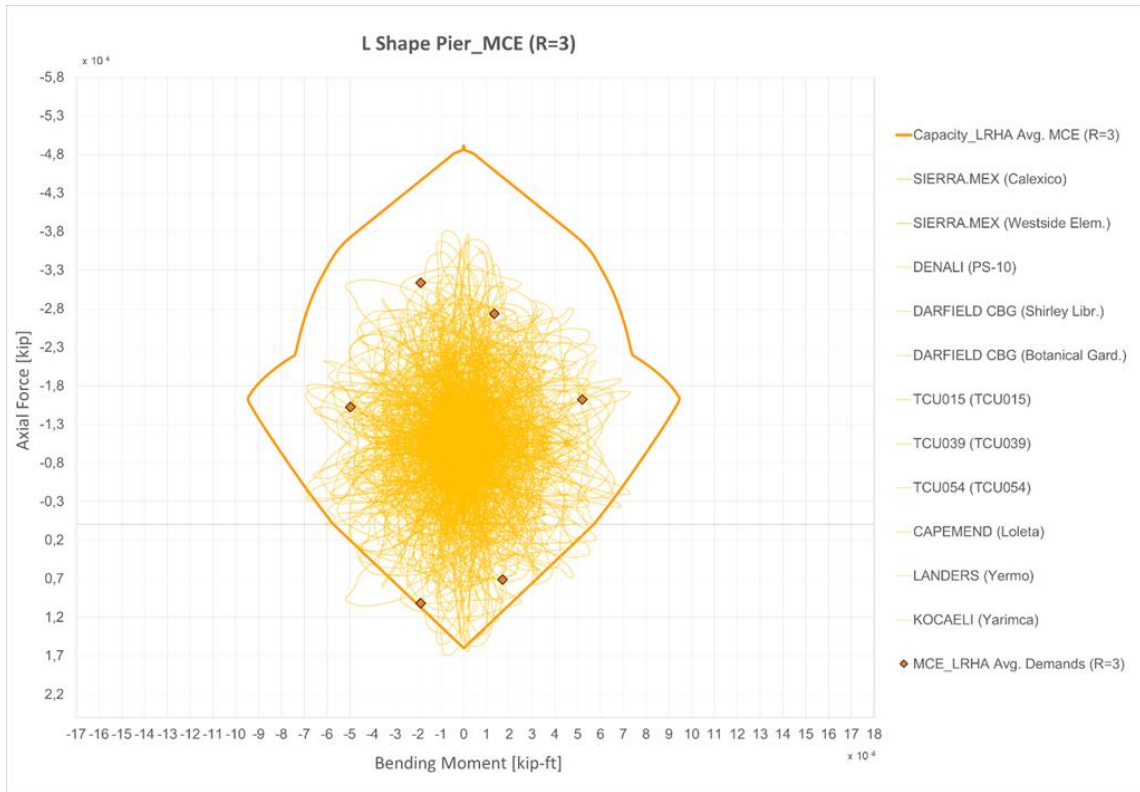


Figure 3.42 Option D_LRHA MCE (R=3) Compound Shear Wall Flexure Demands Plot

3.3.9 Linear Response History Analysis Story Drift

The following plots show the maximum story drift in X and Y direction of the Linear Response History Analysis MCE (R=3).

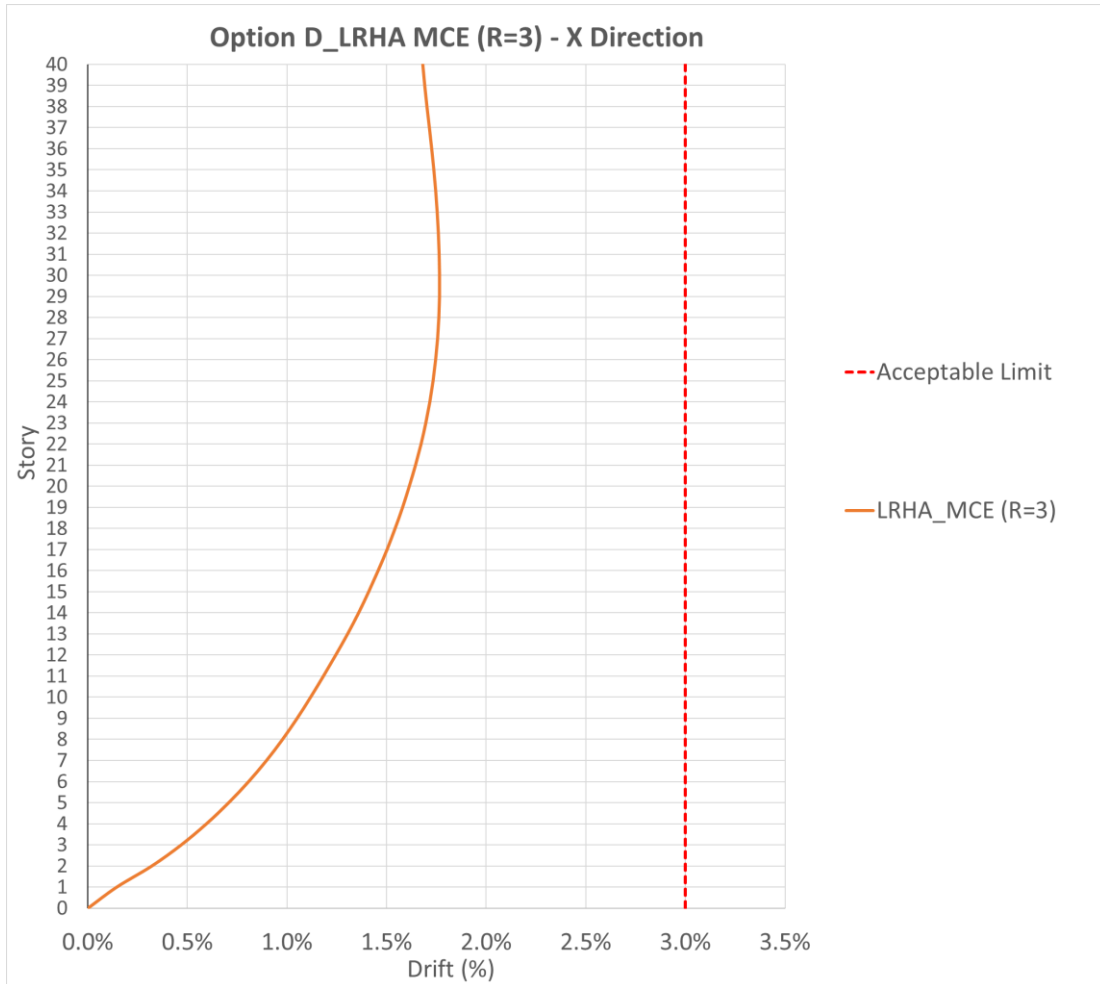


Figure 3.43 X Direction Maximum Story Drift MCE (R=3)

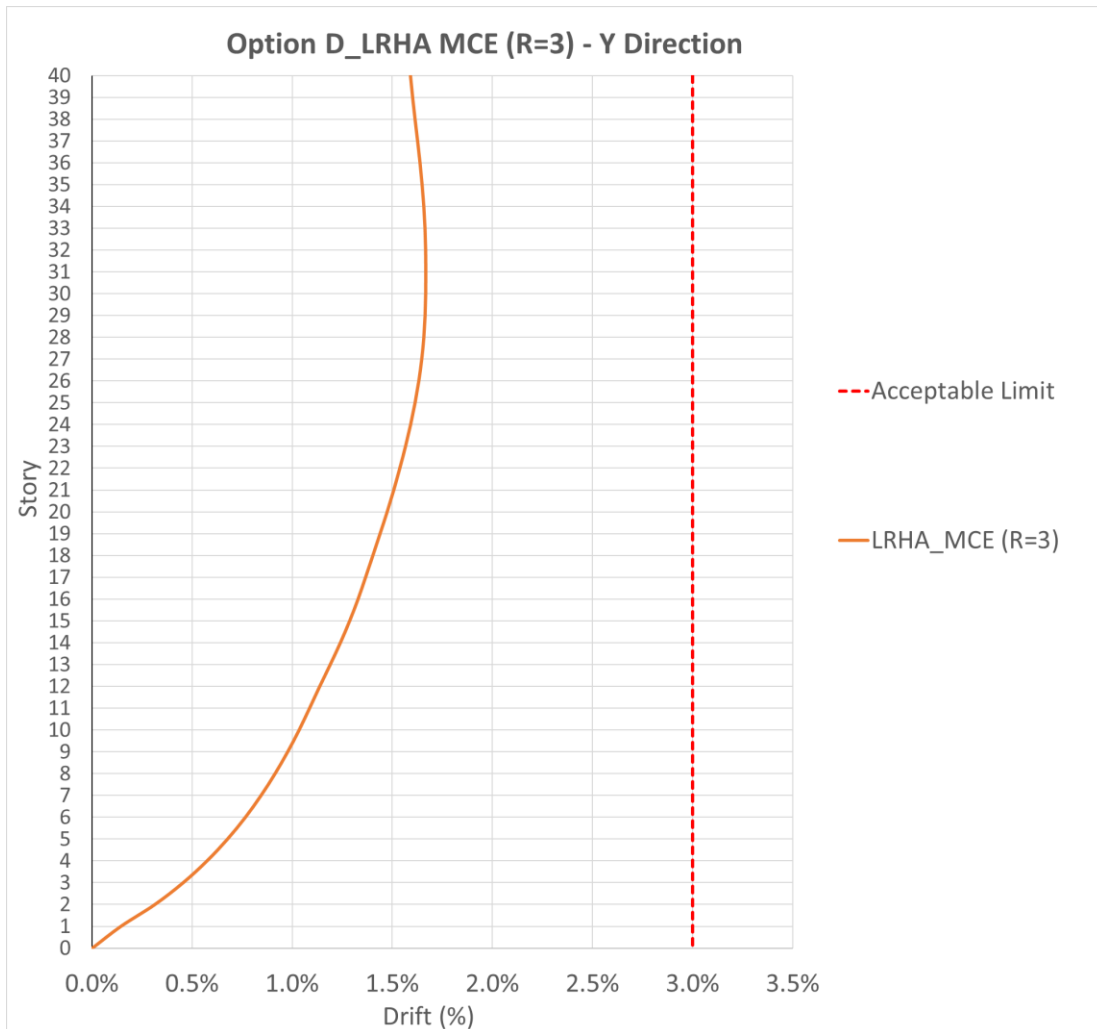


Figure 3.44 Y Direction Maximum Story Drift MCE (R=3)

3.3.10 Linear Response History Analysis Story Shear

The following plots show the story shear in X and Y direction of the Linear Response History Analysis MCE (R=3).

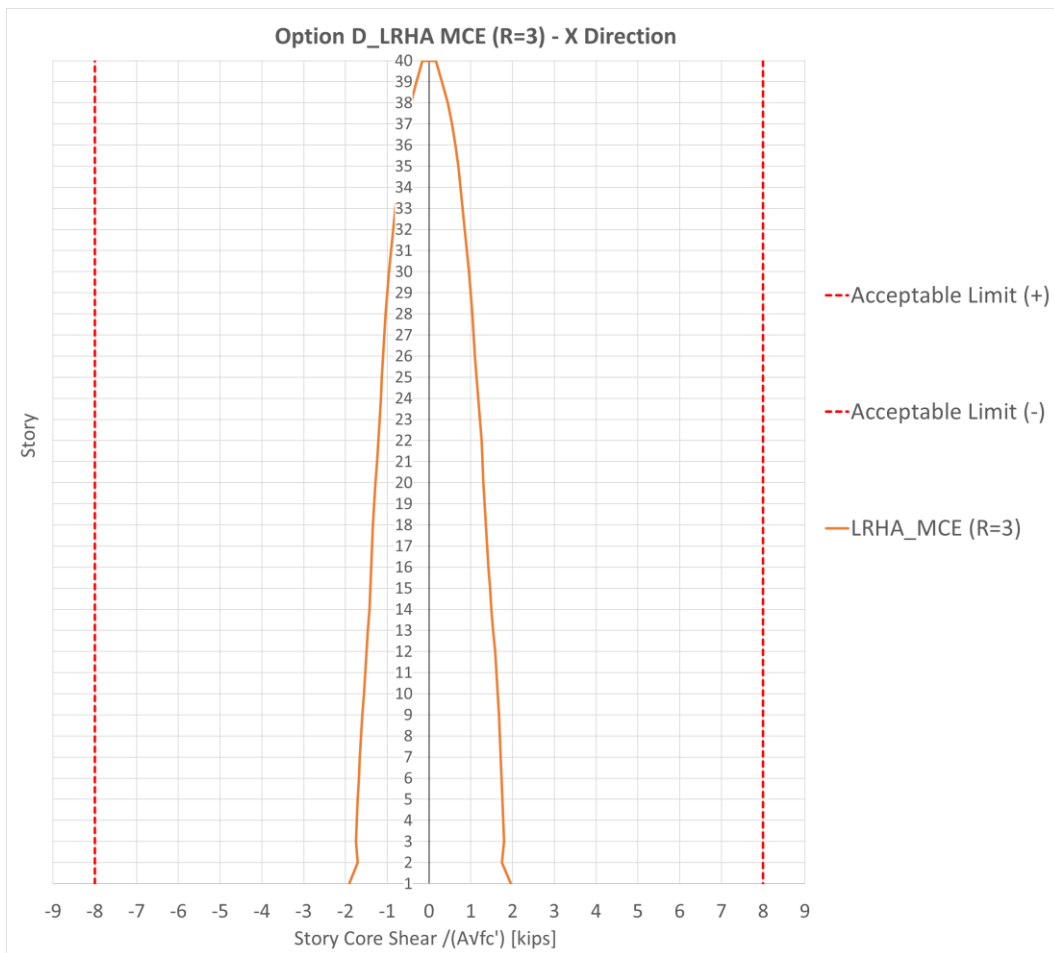


Figure 3.45 LRHA X Direction Story Shear MCE (R=3)

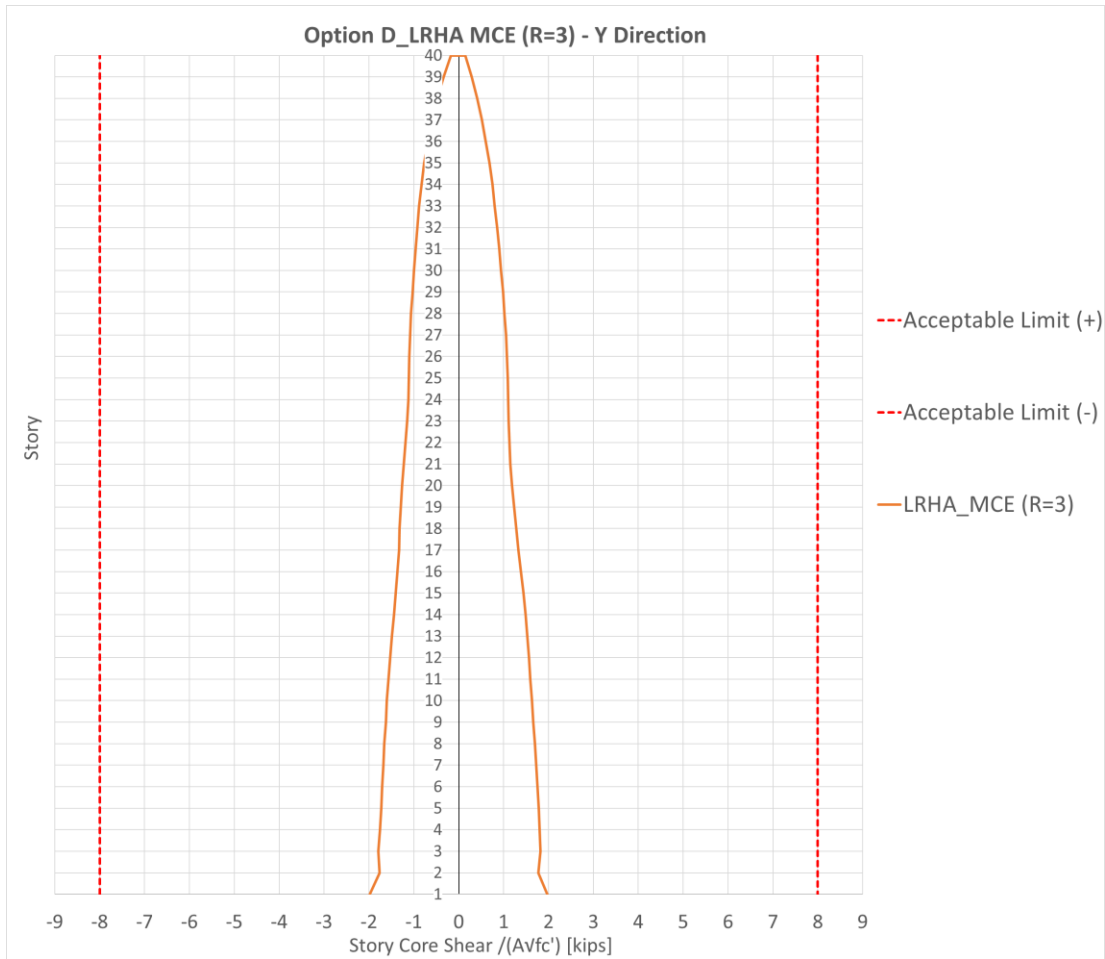


Figure 3.46 LRHA X Direction Story Shear MCE (R=3)

CHAPTER 4

NONLINEAR VERIFICATION ANALYSIS

4.1 Nonlinear Analysis Model Description

A 3-D finite element computer model using the CSI Software ETABS 2016, *Figure 4.1*, is used to perform all the nonlinear analysis conducted in the present work.

The geometry and the elevation of the nonlinear prototype model are the same of the linear one already described in Chapter 2.1.

The Nonlinear Response History Analysis are conducted on three Fiber Model Options, based on the three above mentioned proposed designs, able to provide energy dissipation through the plastic rotation of the plastic hinges modelled in the coupling beams and through the shear walls fibers yielding.

Accordingly with this, the core walls are divided in Boundary Zones and Panel Zones. Boundary Zones are 25% the length of the core flange and so equal to 40.5 inches. All boundary zones are modelled with 8ksi confined concrete and all the panel zones are modelled with 8ksi unconfined concrete. All fibers steel is A706Gr60.

Slabs are modelled as rigid diaphragms to decrease analysis time. Instead of modelling the slabs and applying loads onto the slabs, these loads are translated into point loads that are applied at the top of column and wall elements at each level, determined by vertical reactions in a one-story model in ETABS. This allows to decrease the analysis running time too.

For each Option, Nonlinear Direct Integration (DI) are run.

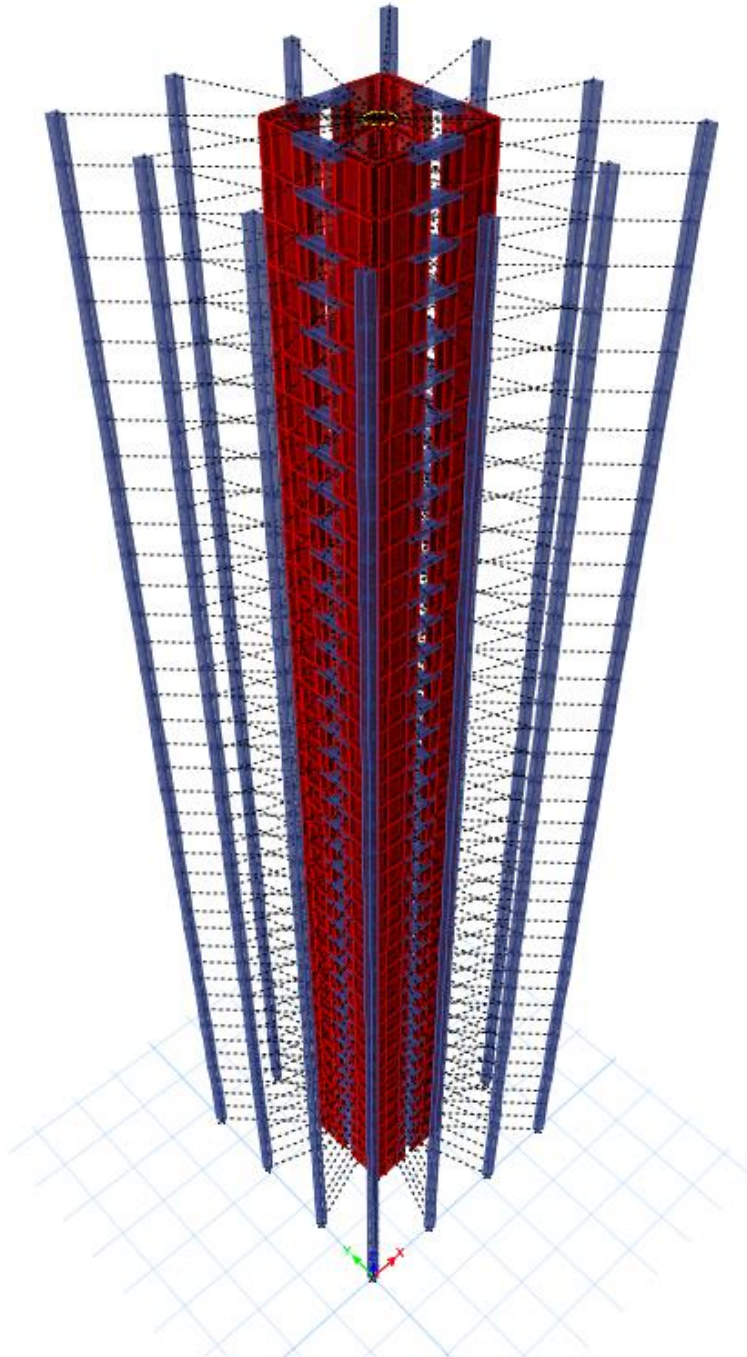


Figure 4.1 3-D Finite Element Computer Fiber Model, CSI Software ETABS 2016

The plan and elevation of the Nonlinear Prototype Model are shown in *Figure 4.2* and *Figure 4.3*:

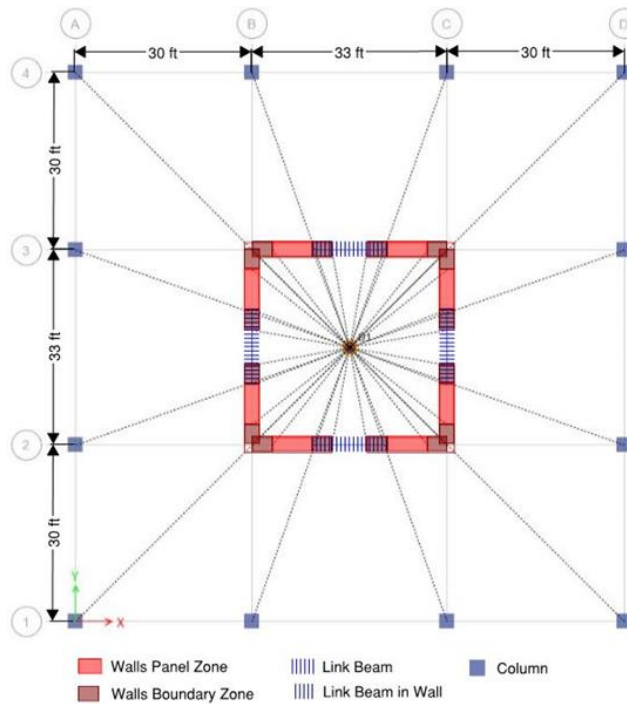


Figure 4.2 Nonlinear Prototype Model Structural Plan on ETABS 2016

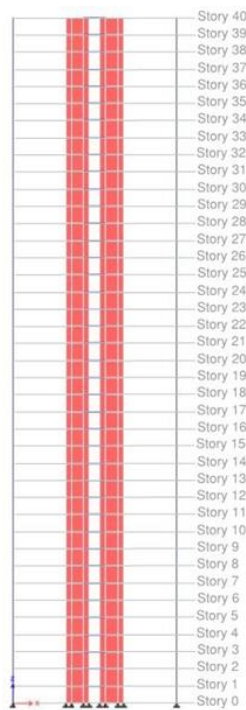


Figure 4.3 Nonlinear Prototype Model Structural Elevation on ETABS 2016

As already said in Chapter 3.1, material and component modelling are based on Chapter 11 of the 500 Folsom Calculation Book. For 8ksi unconfined and confined concrete, the ETABS default Mander curves are used, plotted in *Figure 4.4*:

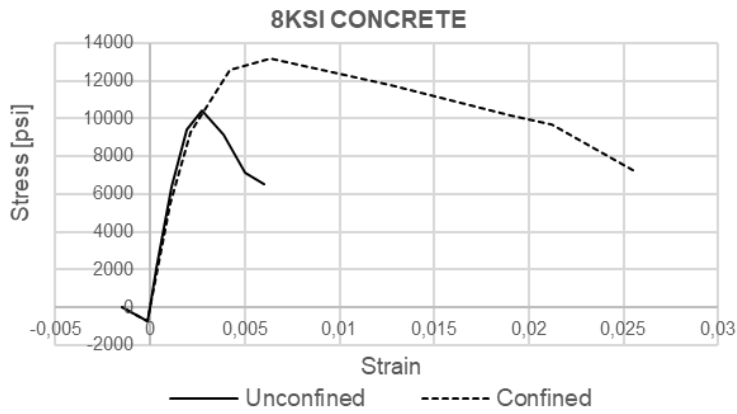


Figure 4.4 8ksi Unconfined and Confined Concrete Stress-Strain Plot

Young’s modulus calculated with:

$$E_c = w_c^{1.5} \sqrt{f'_c}$$

Per ACI318-11 Section 8.5.1. Overstrength factor was included in this property.

The reinforcing steel used is A706 Grade 60 rebar with the following properties,

Table 4.1:

Properties	E [ksi]	Weight [pcf]	Fy [ksi]	Fu [ksi]	Fye [ksi]	Fue [ksi]
A706Gr60	29000	490	60	80	66	88

Table 4.1 A706Gr60 Fibers Rebar Steel Properties

The stress-strain plot is shown in *Figure 4.5*:

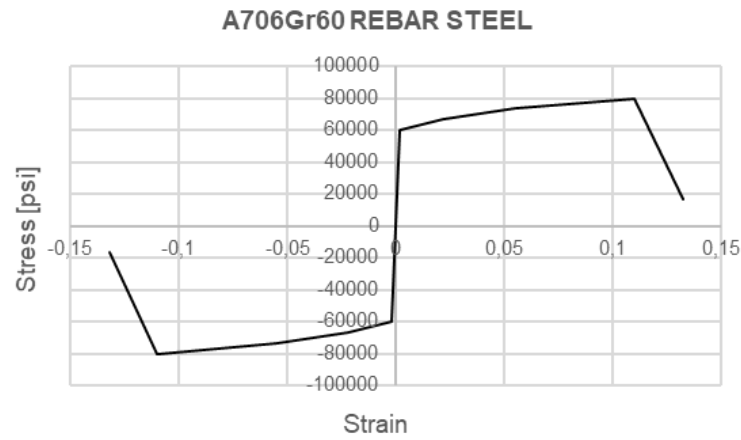


Figure 4.5 A706Gr60 Rebar Steel Stress-Strain Plot

The following property modifiers are adopted per 500 Folsom calculation book section 2.3.3.3.2:

	Flexure	Shear	Axial
Shear Walls	N/A	0.5 A_{vg}	1.0 A_g
Link Beams	0.07 (l/h) $I_g = 0.21 I_g$	-	1.0 A_g
Columns	0.5 I_g	1.0 A_{vg}	1.0 A_g

Table 4.2 Stiffness/Property Modifiers

Link beams in walls have a nil axial force stiffness modifier to not transfer shear to the wall, and a big moment of inertia about 3 axes to not allowed rotation inside the wall and transfer the moment by the beams to the wall.

	Cross Section Area	Moment of Inertia about horizontal axis	Mass
Link Beam (in Wall)	0.0000001	10000000	0.01

Table 4.3 Stiffness/Property Modifiers

Accordingly to *Table 4.2*, the following modifiers are applied to shear walls, *Figure 4.3*, to link beams, *Figure 4.4*, and to link beams in the wall, *Figure 4.5*:

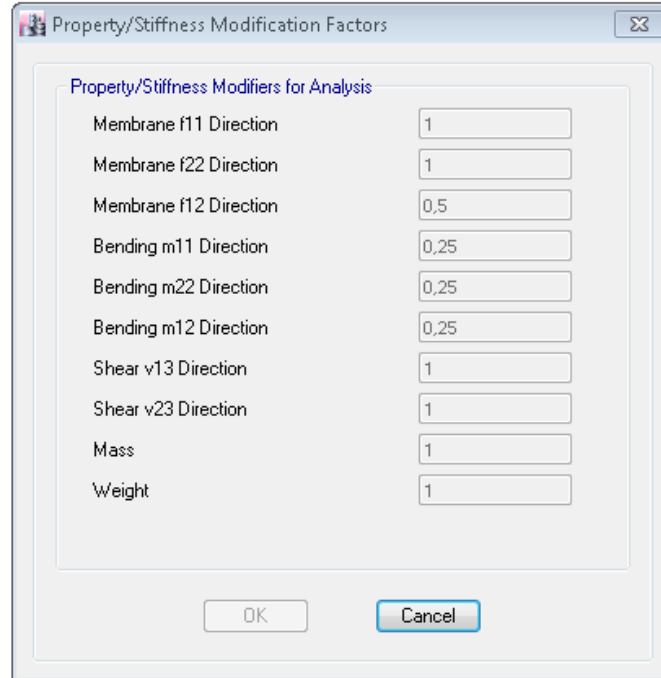


Figure 4.6 Shear Walls Stiffness Modifiers

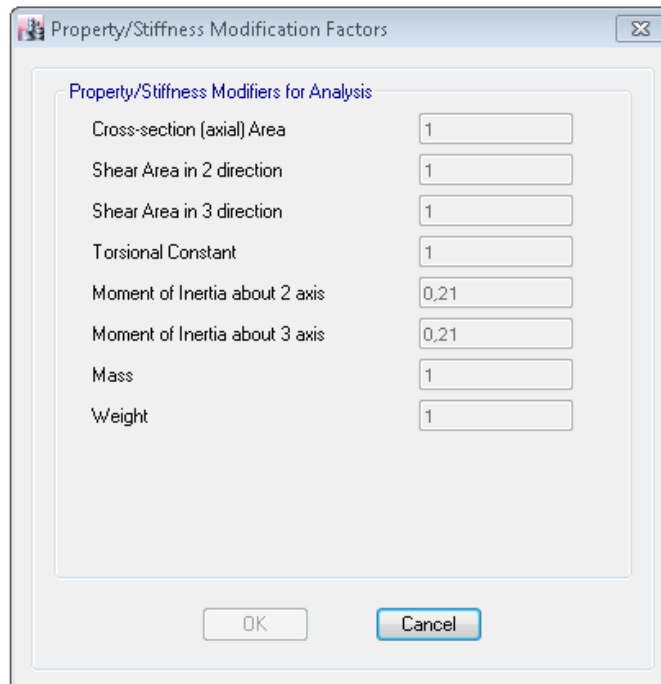


Figure 4.7 Coupling Beams Stiffness modifiers

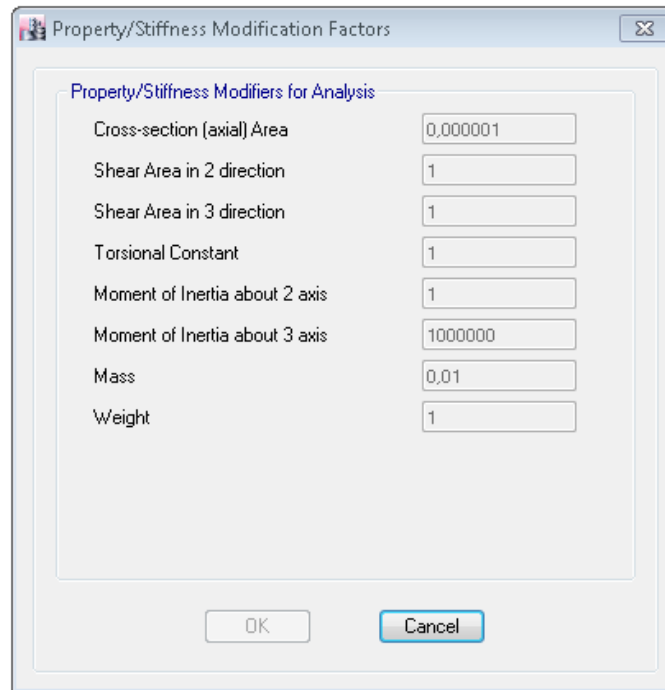


Figure 4.8 Link Beams in Wall Stiffness Modifiers

The expected material properties are assumed to be the following to account for overstrength, per PEER 2010 Section 7.5.2 Table 7.1:

- Reinforcing Steel 1.17 f_y
- Concrete 1.3 f'_c

The acceptance criteria are adopted from 500 Folsom and illustrated as follows.

- Shear walls:

The maximum compressive strain is limited to 0.012 in confined concrete and 0.0015 in unconfined concrete. The maximum longitudinal reinforcement strain is limited to 0.05 in tension and 0.012 in compression. Yield strain is 0.0024 (or 0.24%) in tension.

- Link Beams:

The plastic rotation limit is 0.05 radians (or 5%) for diagonally reinforced link beams. The total rotation limit is 0.06 radians. The yield rotation is 0.01 radians.

- Global Level:

The mean of the absolute peak story drift ratio is limited to 0.03 (or 3% drift). The maximum story drift ratio is limited at 0.045.

4.1.1 Nonlinear Fiber Shear Walls Description

Shear walls are modelled as shell elements with wall properties and with assigned Fiber P-M3 hinges. Explicit wall fiber hinge models are constructed for the Boundary Zones and the Panel Zones, accordingly with the real rebar distribution, *Figure 4.9*. The axial/bending behavior of the wall and wall segments is then modeled using inelastic fiber sections.



Figure 4.9 Example of Shear Walls Reinforcement

The finite shear wall elements mesh for the walls is designed so that it corresponds to the boundary zone widths and locations in the wall. In other words, each wall segment is divided horizontally into three shear wall elements: two separate elements represented the Boundary Zones, separated by one element that covers the Panel Zone. In each of these shear wall elements, at two or four concrete fibers and steel fibers are distributed uniformly over the width and the length of the element as indicated in the wall cross sections shown below, *Figure 4.10*.

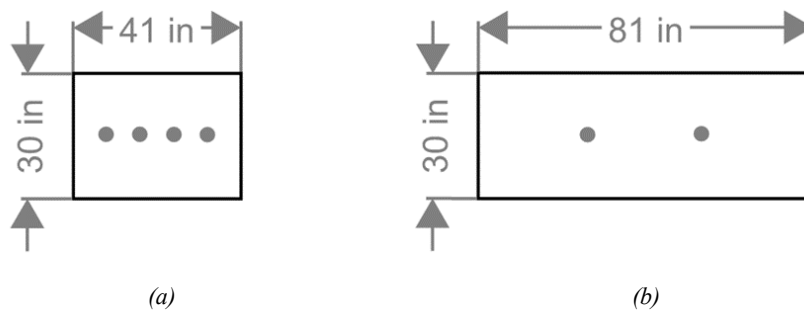


Figure 4.10 (a) Boundary Zone Fibers Distribution; (b) Panel Zone Fibers Distribution

Samples of shear walls fiber hinges specifications in ETABS are displayed below, *Figure 4.11* and *Figure 4.12*:

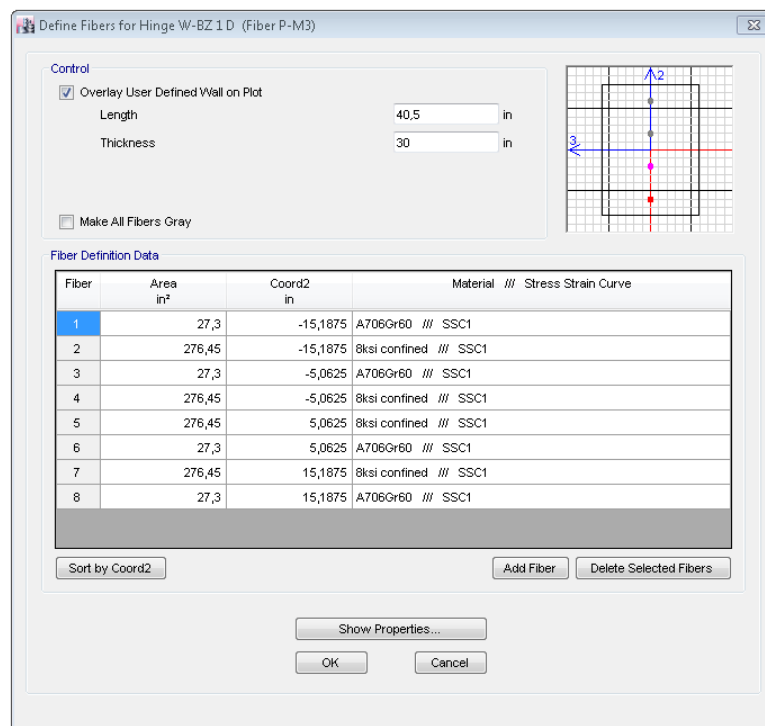


Figure 4.11 Sample Boundary Zone Fiber Hinge Specification in ETABS

Chapter 4 Nonlinear Verification Analysis

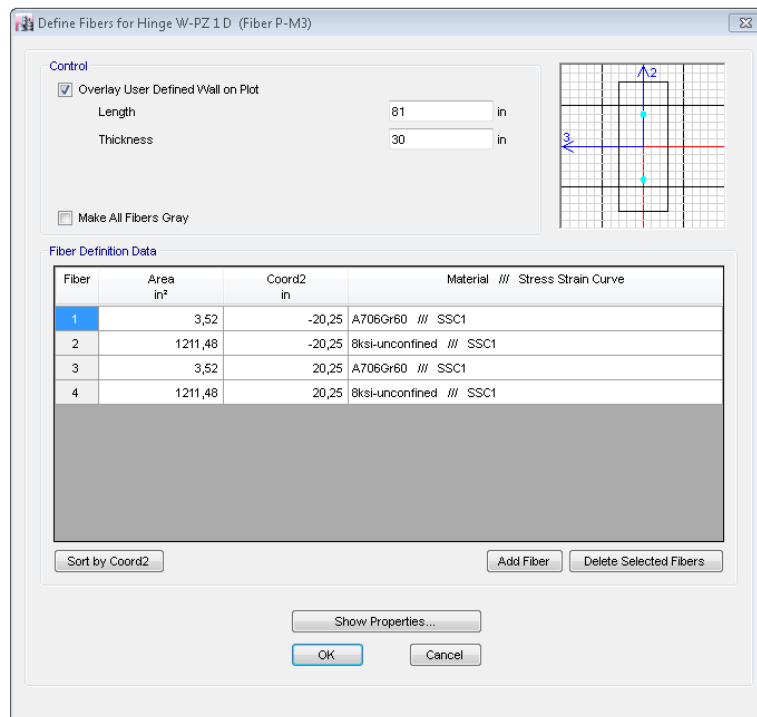


Figure 4.12 Sample Panel Zone Fiber Hinge Specification in ETABS

4.1.2 Nonlinear Coupling Beams Description

Link beams can be conventionally or diagonally reinforced. In the current study, Coupling Beams are assumed to be diagonally reinforced, as shown below, *Figure 4.13*.



Figure 4.13 Example of Diagonally Reinforced Coupling Beams

Nonlinear behavior of these horizontal linking elements of the core is usually modelled with either shear hinges or rotational hinges, shown in *Figure 4.13* and *Figure 4.14*.

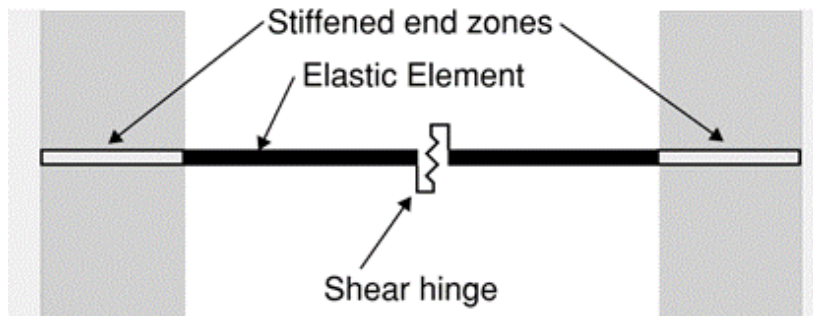


Figure 4.14 Shear Hinge

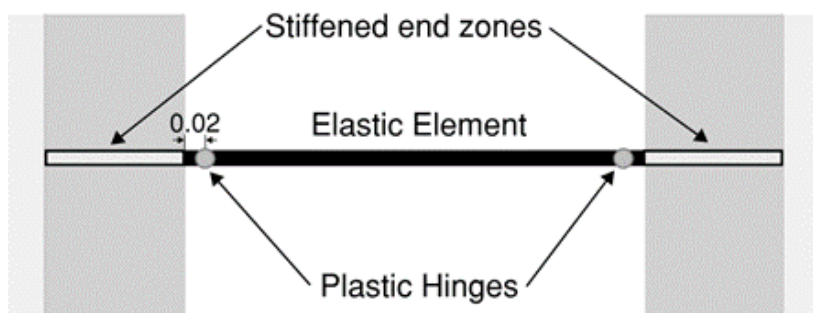


Figure 4.15 Rotational Hinges

In the Prototype Model of the present work, Coupling Beams are assumed to be diagonally reinforced and they are modelled with two Rotational Hinges. As shown above, *Figure 4.15*, inelastic behavior elements are lumped at the ends of the beam. Plastic Hinges are in fact modelled at relative distance of 0.02 from either end of the beam element.

As already described in Chapter 4.1, Link Beam elements are extended into the wall by the length of the first boundary zone in order to transfer moments. The beam elements in the wall are modelled with high rotation stiffness (using about 20 times EI of link beam), but low axial stiffness (small EA) in order to not transfer shear to the wall.

The Force-Deformation Curve is shown below, *Figure 4.16*.

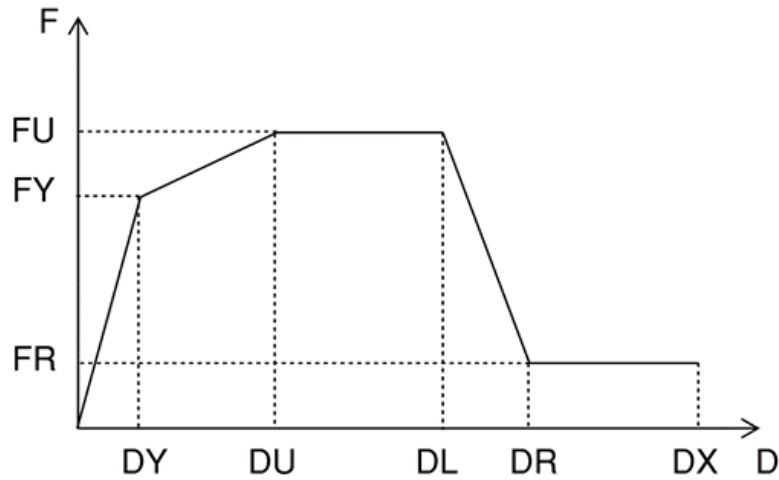


Figure 4.16 Parametric Force-Deformation Curve of Plastic Hinges

Force-deformation Parameters are shown generally below, *Table 4.4*, where D can be replaced with Rotation “ θ ”.

Beam type	Beam Group	θ_U	θ_L	θ_R	θ_X	FY/FU	FR/FU
Diagonally Reinforced	$2.0 \leq L_n/h \leq 4.0$	-	0.05	0.085	0.120	0.75	0.001

Table 4.4 Link Beams Force-Deformation Input Parameters

Figure 4.16 and *Table 4.4* summarize the selected modeling parameters for each link beam defined as follows: θ_U is plastic link beam deformation at the ultimate stress, θ_L is the plastic link beam rotation at the onset of strength degradation, θ_R is the plastic link beam rotation at the residual strength, θ_X is the plastic link beam chord rotation at analysis termination, FY is the yield strength, FU is the ultimate strength and FR is the residual capacity. It is noteworthy to specify that the aforementioned rotations are plastic rotations.

The ultimate strength is found with ACI318-11 equation 21-9:

$$V_n = 2A_{vd}f_y \sin \alpha \leq 10\sqrt{f'_c}A_{cw}$$

Depending on the link beams reinforcement configuration.

Typical details for diagonally reinforced link beams are shown below, *Figure 4.17*, accordingly with ACI 318-11.

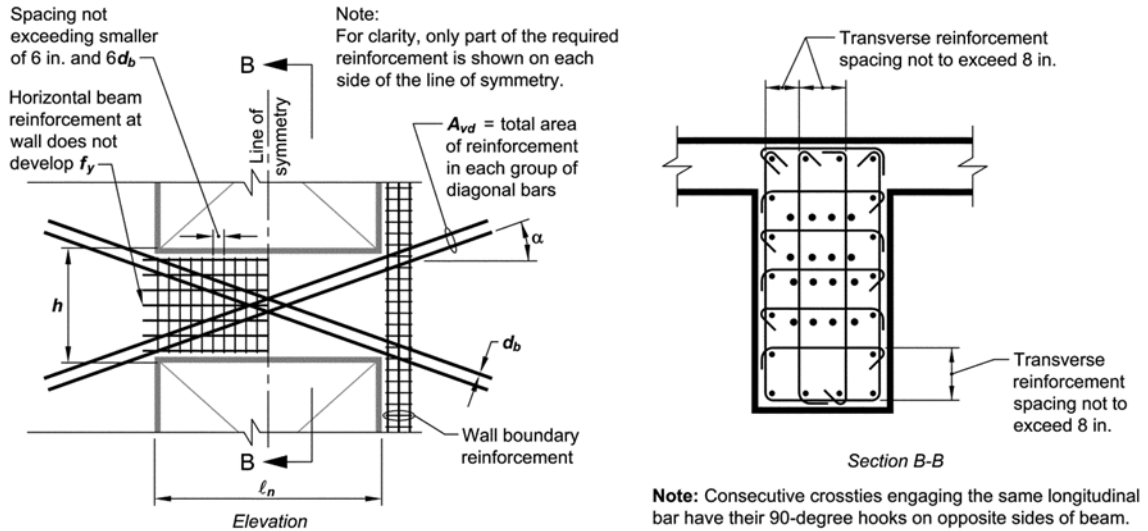


Figure 4.17 Full Confinement of Diagonally Reinforced Link Beams (ACI 318-11)

Assuming in the Prototype Model 12 #11 diagonal bars for the link beams, the ultimate strength of our 30"x24" link beams can be calculated as:

$$V_n = 2A_{vd}f_y \sin \alpha = 2(12 \times 1.56in^2)(60ksi) \sin 0.23 = 513 \text{ kips}$$

$$V_n < 10\sqrt{f'_c}A_{cw} = 10\sqrt{8000psi}(24in \times 30in)/1000 = 644 \text{ kips}$$

$$M_y = 0.75 V_n L_{LK \text{ effective}} = 1629 \text{ kip} - ft$$

4.2 Response Spectrum Analysis Prediction of Nonlinear Behavior

In the present chapter are presented the NLRHA results, conducted by Nonlinear Direct Integration (DI). The two Options based on the RSA Proposed Design Methodologies explained in Chapter 3.3.1 are: Option A_RSA MCE (R=7.5) and Option B_MCE (R=3).

On each plot, the NLRHA results are displayed as all the Ground Motion runs (pair of motions) and the mean of all these runs.

4.2.1 Option A (MCE R=7.5) Nonlinear Analysis Results

Based on the Option A design proposed in Chapter 3.3.2, the rebar distribution is known along all the building height, *Figure 4.18*. Accordingly with this, it is possible to build the Option A Nonlinear Fiber Model.

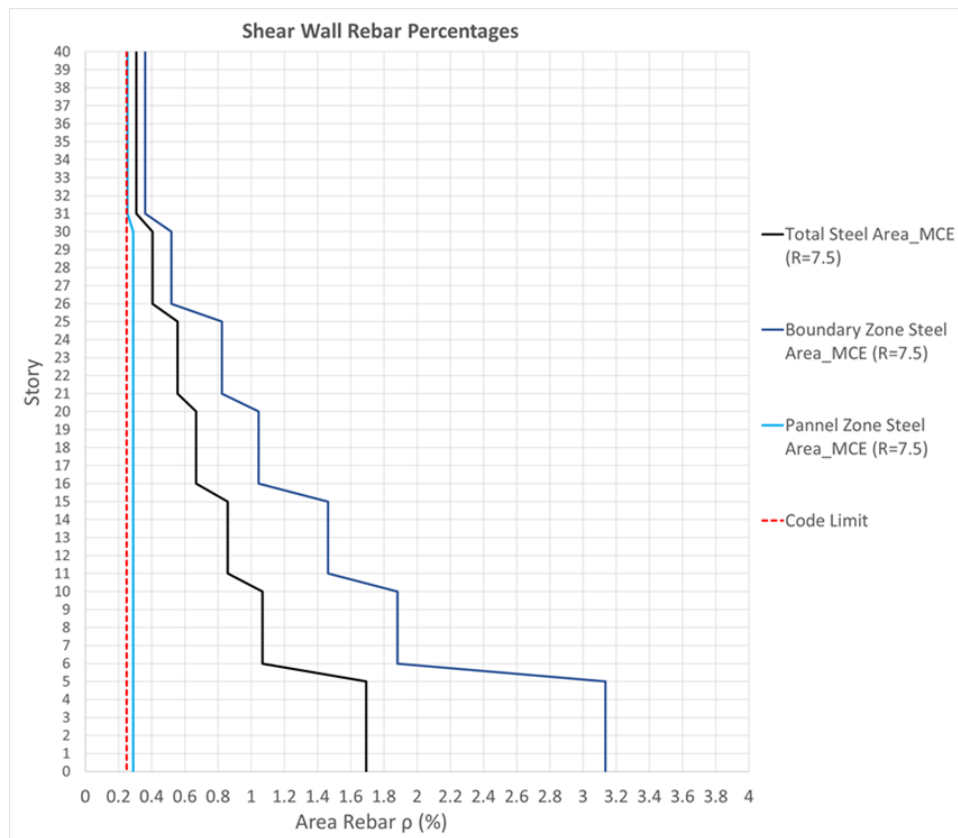


Figure 4.18 Option A_RSA MCE (R=7.5) Rebar Amounts

4.2.1.1 Modal Participation Mass Ratios

The Modal results of Option A_RSA MCE (R=7.5) Model are shown just for the first 30 Modes, avoiding the negligible other ones, *Table 4.5*:

Mode	Period [sec]	UX	UY	RZ	Sum UX	Sum UY	Sum RZ
1	3.793	0	0.6631	0	0	0.6631	0
2	3.793	0.6631	0	0	0.6631	0.6631	0
3	2.726	0	0	0.7569	0.6631	0.6631	0.7569
4	0.891	0	0.1793	0	0.6631	0.8424	0.7569
5	0.891	0.1793	0	0	0.8424	0.8424	0.7569
6	0.843	0	0	0.0998	0.8424	0.8424	0.8566
7	0.451	0	0	0.0439	0.8424	0.8424	0.9006
8	0.401	0	0.052	0	0.8424	0.8944	0.9006
9	0.401	0.052	0	0	0.8944	0.8944	0.9006
10	0.284	0	0	0.0261	0.8944	0.8944	0.9266
11	0.242	0.000001288	0.0284	0	0.8944	0.9229	0.9266
12	0.242	0.0284	0.000001288	0	0.9229	0.9229	0.9266
13	0.196	0	0	0.0174	0.9229	0.9229	0.944
14	0.163	0.000001394	0.0179	0	0.9229	0.9407	0.944
15	0.163	0.0179	0.000001394	0	0.9407	0.9407	0.944
16	0.144	0	0	0.0123	0.9407	0.9407	0.9563
17	0.118	0.00000246	0.0125	0	0.9407	0.9532	0.9563
18	0.118	0.0125	0.00000246	0	0.9532	0.9532	0.9563
19	0.111	0	0	0.0091	0.9532	0.9532	0.9654
20	0.09	0.000002312	0.0091	0	0.9532	0.9623	0.9654
21	0.09	0.0091	0.000002312	0	0.9623	0.9623	0.9654
22	0.089	0	0	0.0069	0.9623	0.9623	0.9723
23	0.074	0	0	0.0054	0.9623	0.9623	0.9776
24	0.072	0.0067	0.0002	0	0.969	0.9625	0.9776
25	0.072	0.0002	0.0067	0	0.9692	0.9692	0.9776
26	0.063	0	0	0.0042	0.9692	0.9692	0.9818
27	0.059	0.000001766	0.0054	0	0.9692	0.9746	0.9818
28	0.059	0.0054	0.000001766	0	0.9746	0.9746	0.9818
29	0.054	0	0	0.0033	0.9746	0.9746	0.9851
30	0.05	0.000001731	0.0043	0	0.9746	0.9789	0.9851

Table 4.5 Option A_RSA MCE (R=7.5) Modal Participation Mass Ratios

4.2.1.2 Option A - Drift

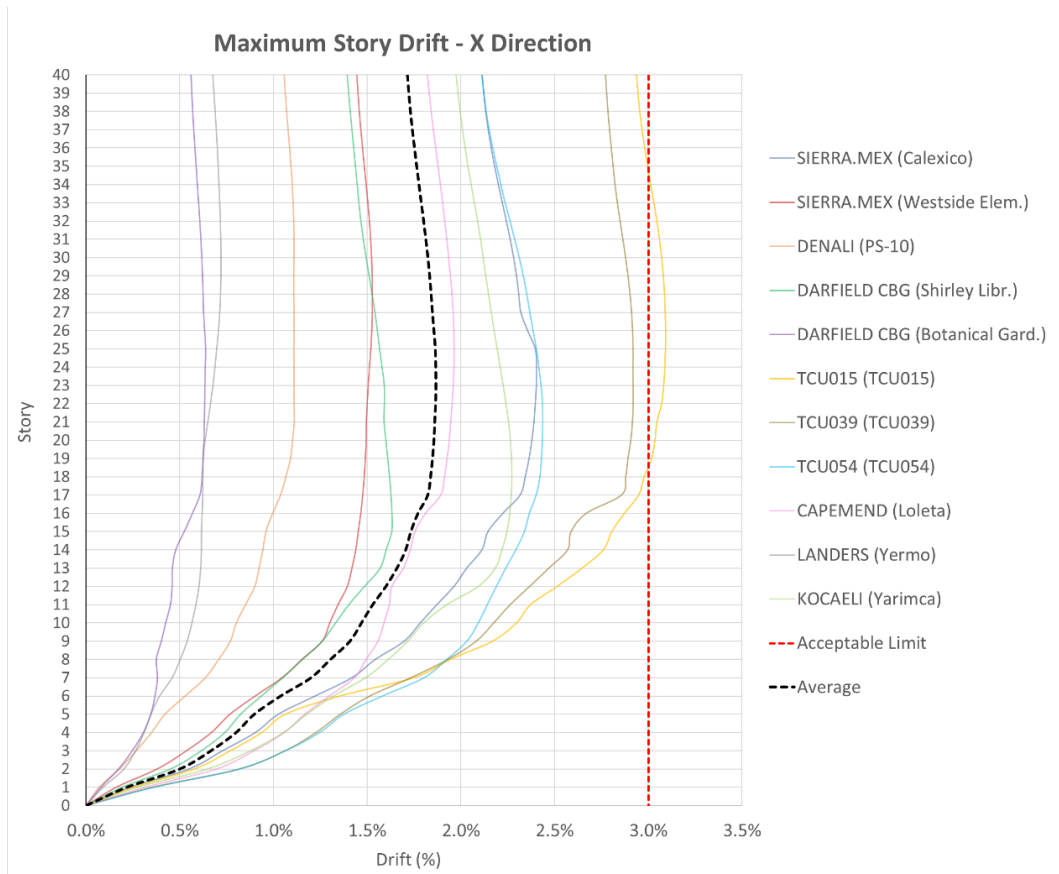


Figure 4.19 Option A_MCE (R=7.5) – NLRHA X Direction Story Drift

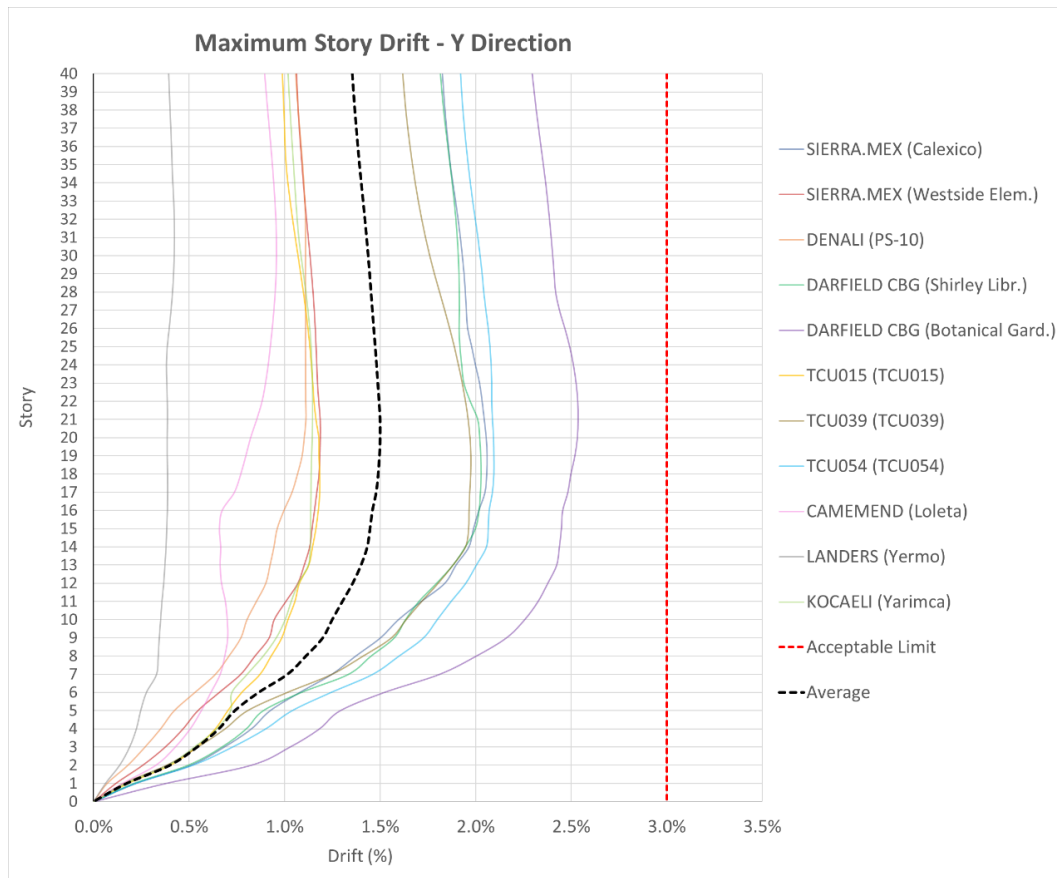


Figure 4.20 Option A_MCE (R=7.5) – NLRHA Y Direction Story Drift

4.2.1.3 Option A - Core Shear

As already mentioned, along X direction the walls able to be resistant are shown in the following *Figure 4.21*:

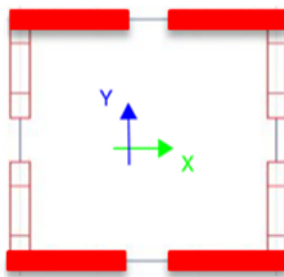


Figure 4.21 X Direction Shear Resistant Core

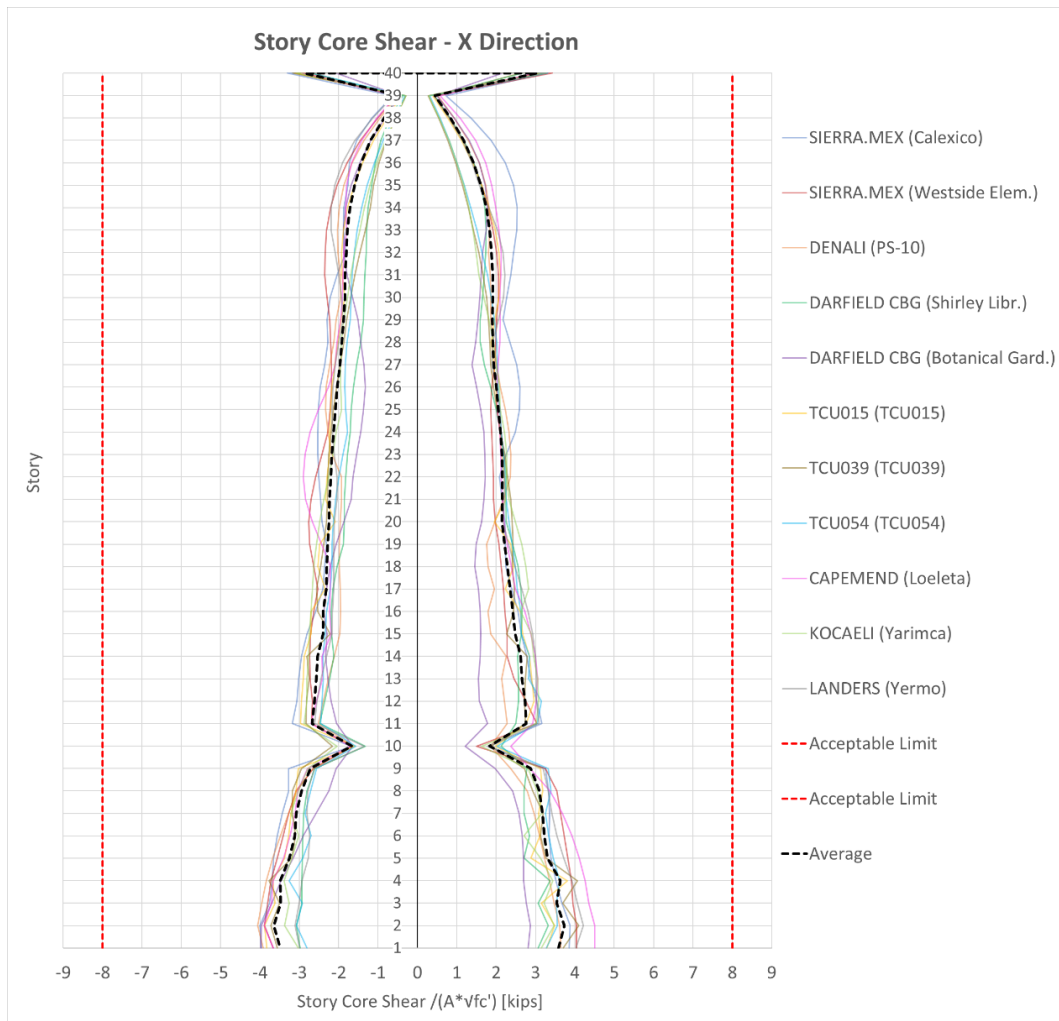


Figure 4.22 Option A_MCE (R=7.5) – NLRHA X Direction Story Shear

As done for the X direction, even for the Y direction the walls able to be resistant are shown in the following Figure 4.23:

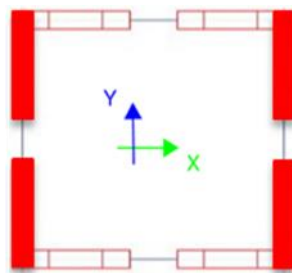


Figure 4.23 Y Direction Shear Resistant Core

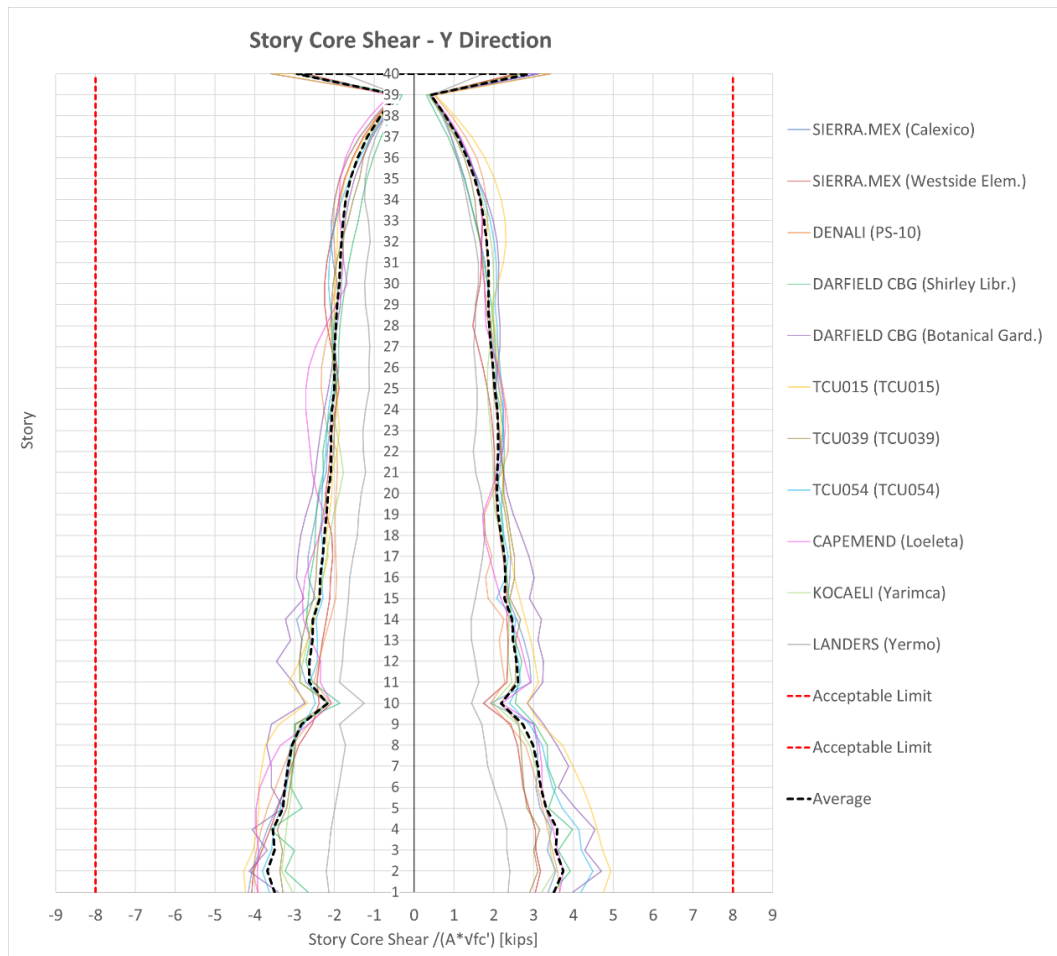


Figure 4.24 Option A_MCE (R=7.5) – NLRHA Y Direction Story Shear

4.2.1.4 Option A – Coupling Beam Plastic Rotation

Along X direction the results of only one plastic hinge of the Link Beam 4 are shown cause the most significant. The location of the mentioned plastic hinge is shown in blue in the following Figure 4.25:

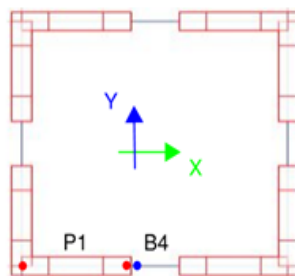


Figure 4.25 Coupling Beam 4 Plastic Hinges Position

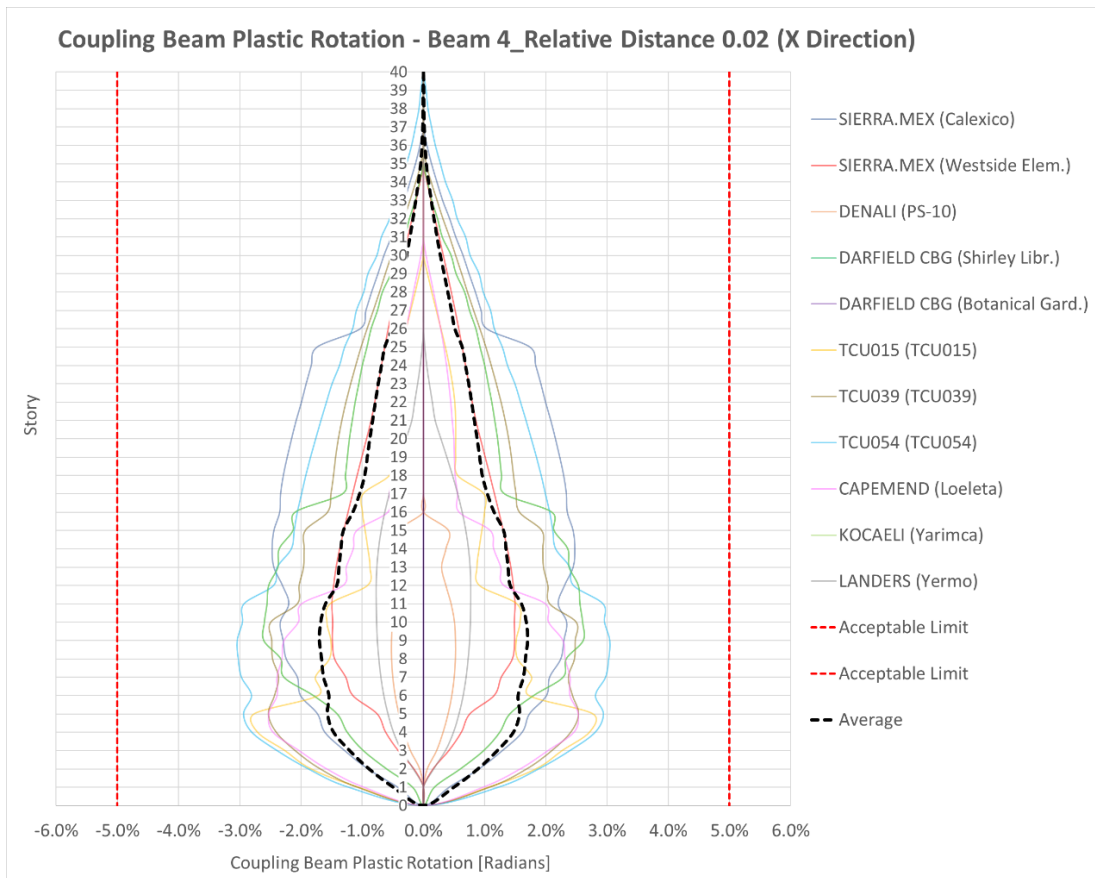


Figure 4.26 Option A_MCE (R=7.5) – NLRHA X Direction Link Beam 4 Plastic Hinge Rotation

As done for the X direction, along the Y direction the results of only one plastic hinge of the Link Beam 3 are shown cause the most significant. The location of the mentioned plastic hinge is shown in blue in the following Figure 4.27:

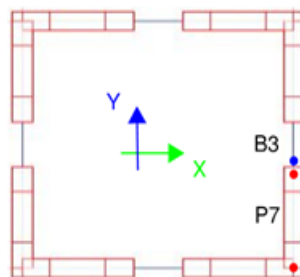


Figure 4.27 Coupling Beam 3 Plastic Hinges Position

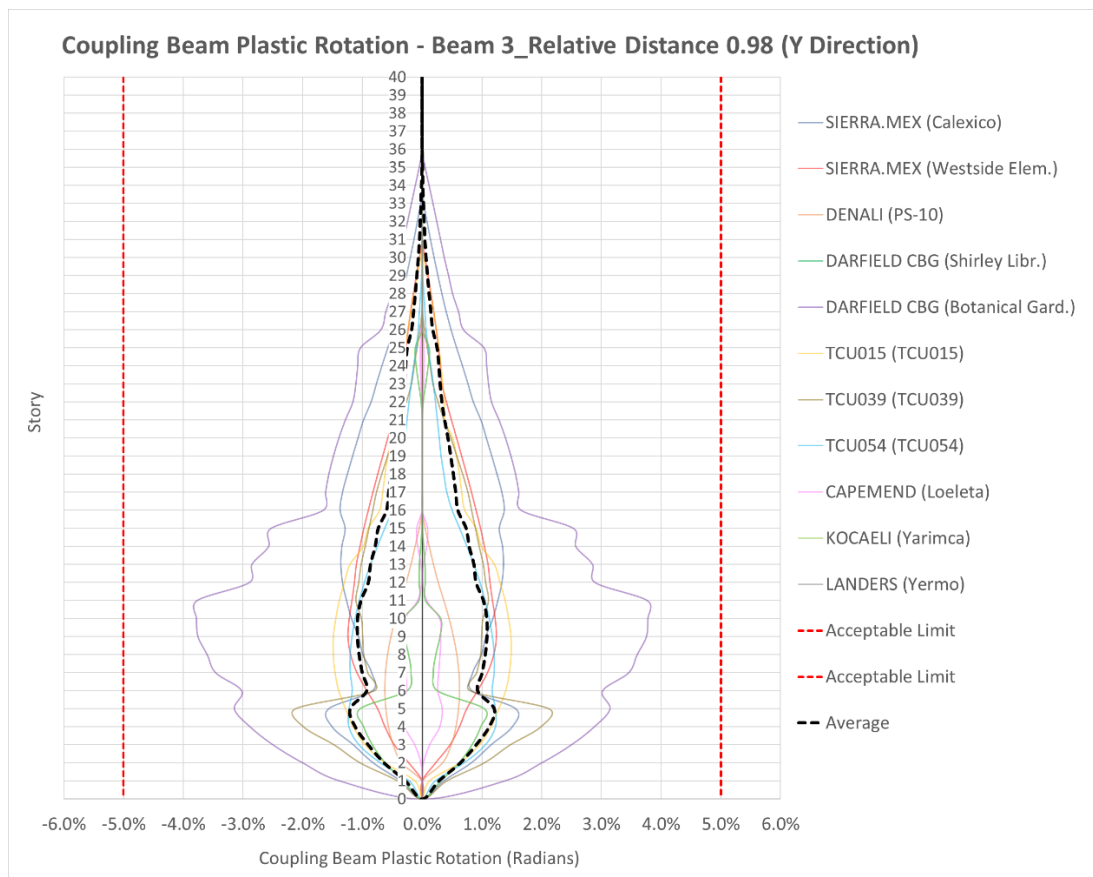


Figure 4.28 Option A_MCE (R=7.5) – NLRHA Y Direction Link Beam 3 Plastic Hinge Rotation

4.2.1.5 Option A – Shear Wall Fiber Strain

Along X direction the results of only two fibers are shown, particularly the two outermost edge fibers of the analyzed pier, cause the most significant. In X direction are displayed the plots of Pier 1 Boundary Zones. The location of the two mentioned fibers are shown in red in the following Figure 4.29:

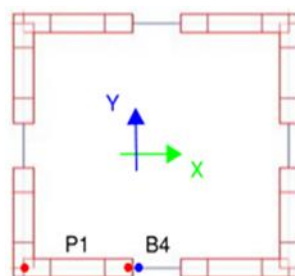


Figure 4.29 Pier 1 Fibers Position

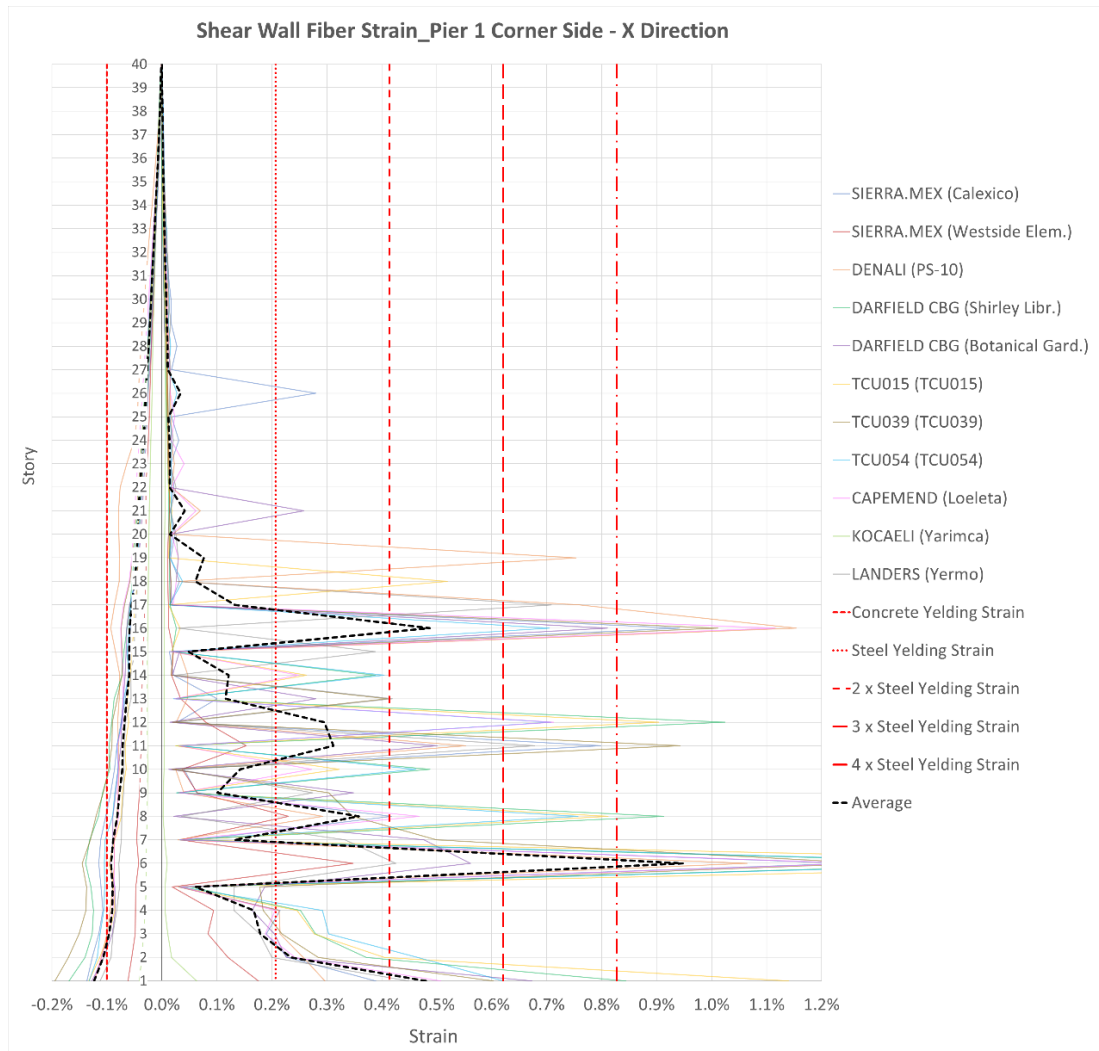


Figure 4.30 Option A_MCE (R=7.5) – NLRHA X Direction Pier 1 Corner Side Fiber Strain

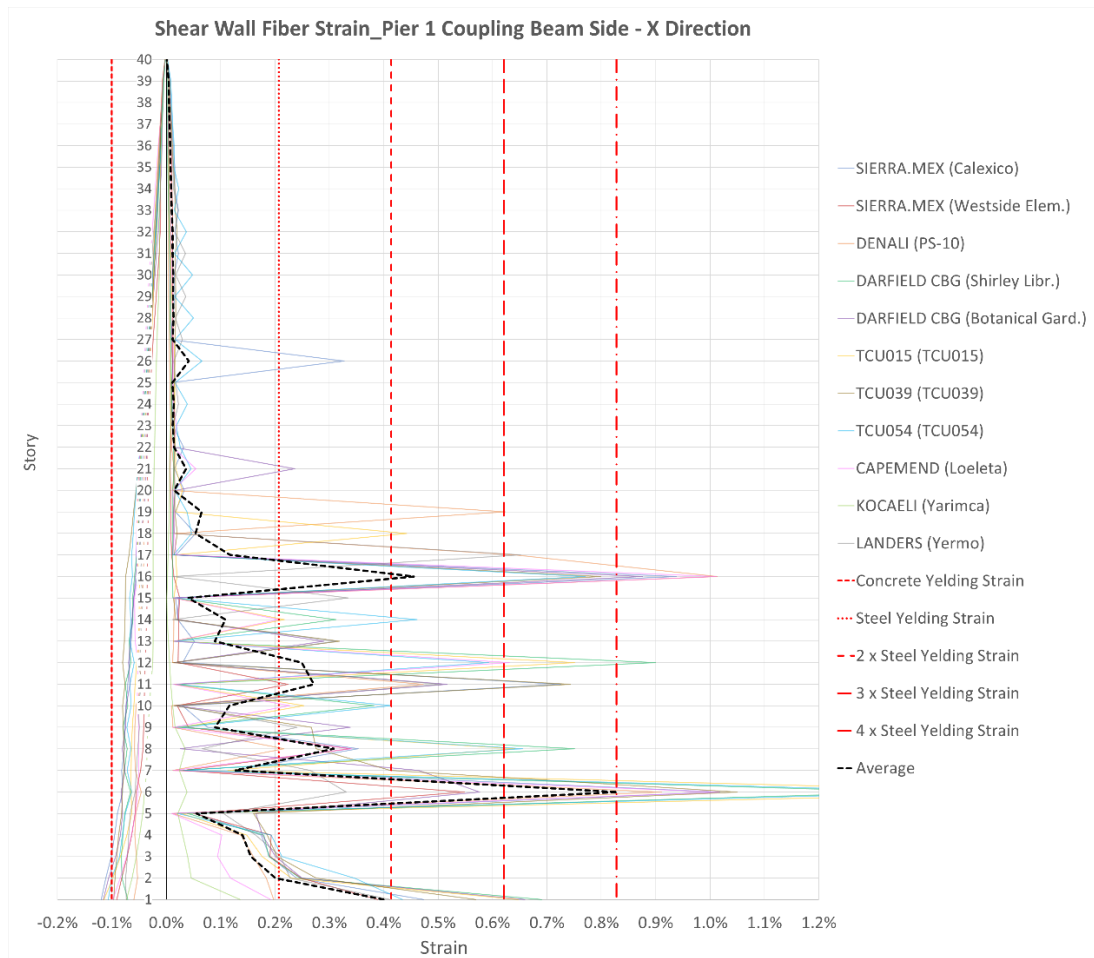


Figure 4.31 Option A_MCE (R=7.5) – NLRHA X Direction Pier 1 Coupling Beam Side Fiber Strain

Along Y direction the results of only two fibers are shown, particularly the two outermost edge fibers of the analyzed pier, cause the most significant. In Y direction are displayed the plots of Pier 7 Boundary Zones. The location of the two mentioned fibers are shown in red in the following Figure 4.32:

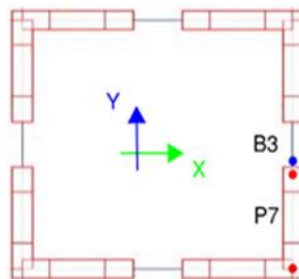


Figure 4.32 Pier 7 Fibers Position

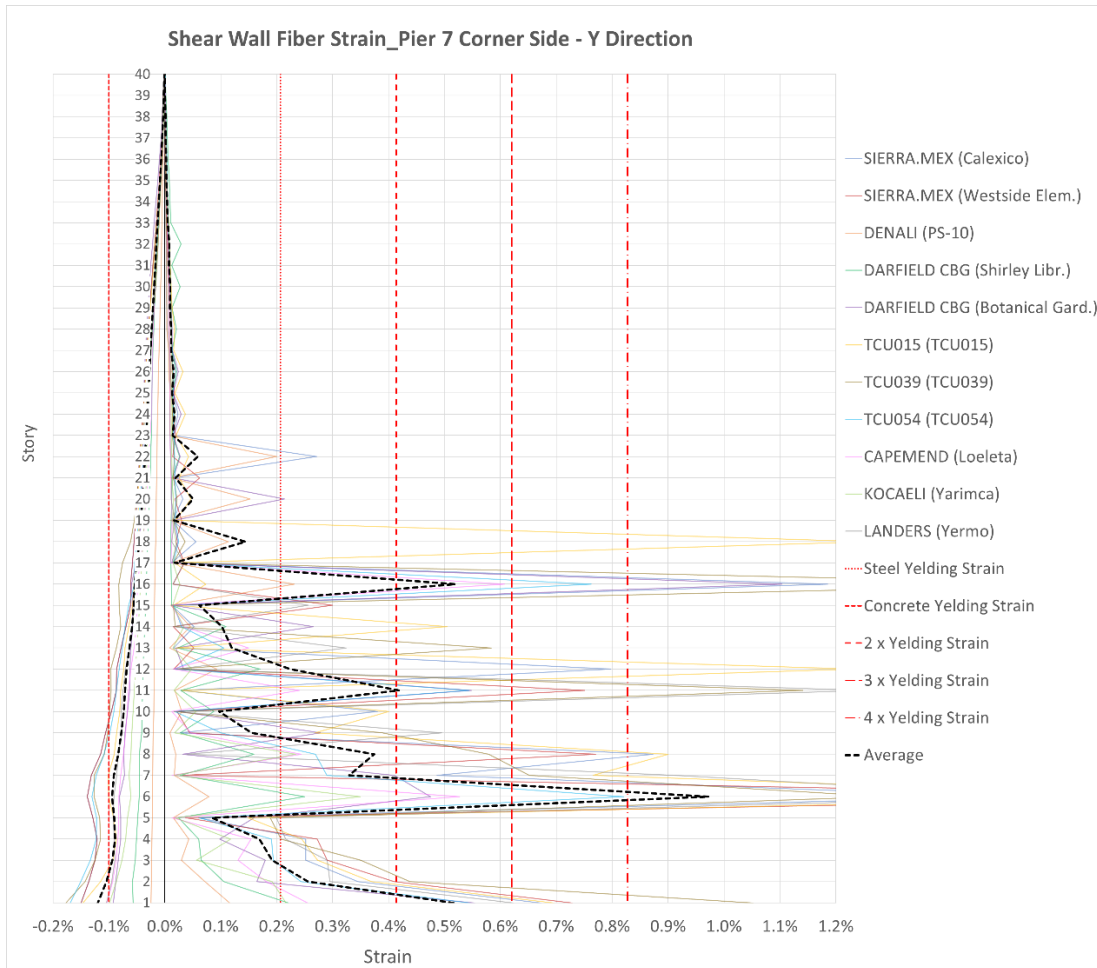


Figure 4.33 Option A_MCE (R=7.5) – NLRHA Y Direction Pier 7 Corner Side Fiber Strain

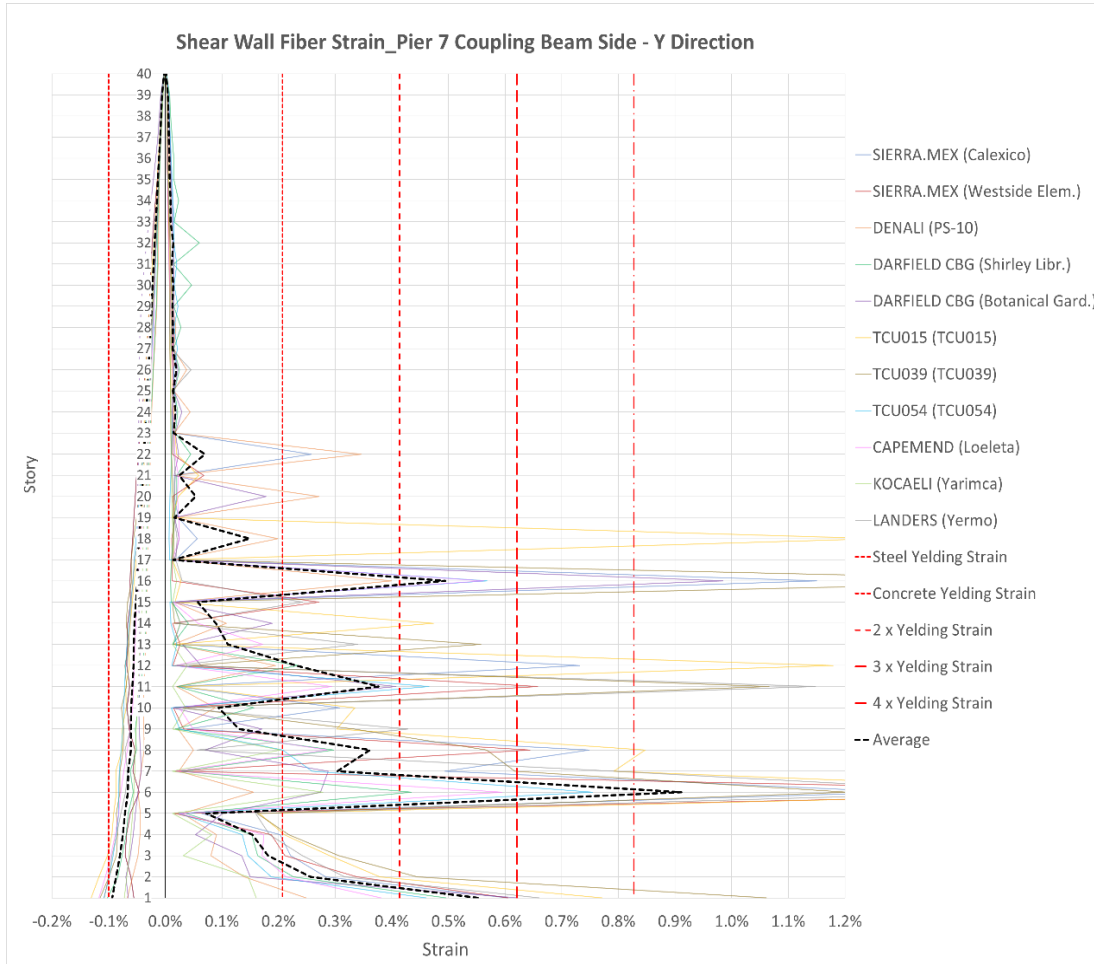


Figure 4.34 Option A_MCE (R=7.5) – NLRHA Y Direction Pier 7 Coupling Beam Side Fiber Strain

4.2.1.6 Option A – Flexure Demands

The NLRHA spaghetti and their corresponding Flexure Demands couples are shown below. The M-N plots are built following the same procedure proposed in Chapter 3.3.4.

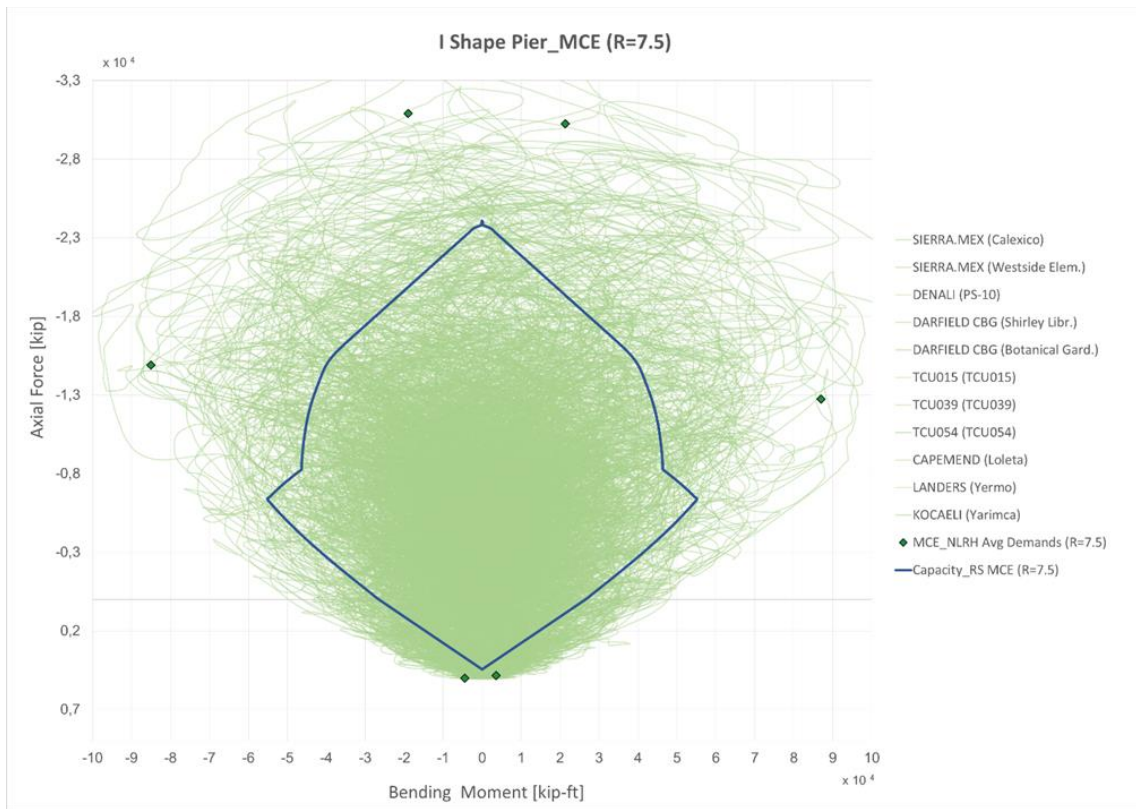


Figure 4.35 Option A_MCE (R=7.5) – NLRHA Stand-Alone Shear Wall Flexure Demands

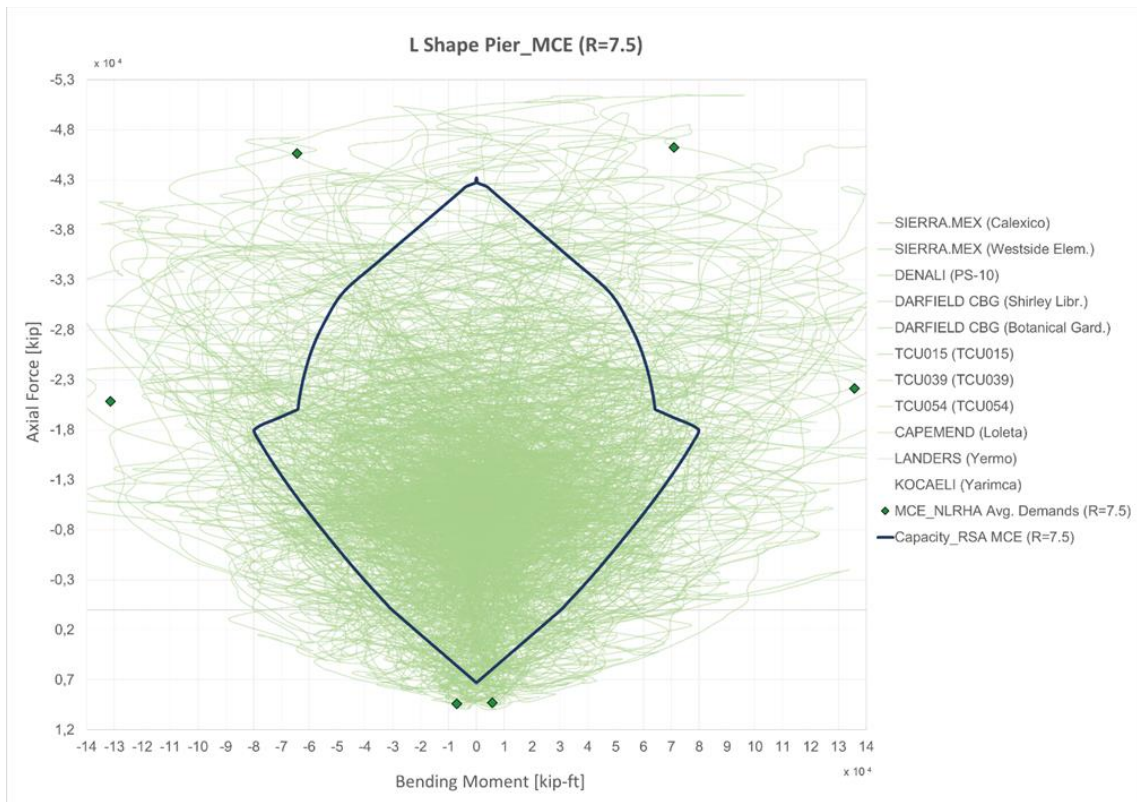


Figure 4.36 Option A_MCE (R=7.5) – NLRHA Compound Shear Wall Flexure Demands

4.2.2 Option B (MCE R=3) Nonlinear Analysis Results

Based on the Option B design proposed in Chapter 3.3.3, the rebar distribution is known along all the building height, *Figure 4.37*. Accordingly with this, it is possible to build the Option B Nonlinear Fiber Model.

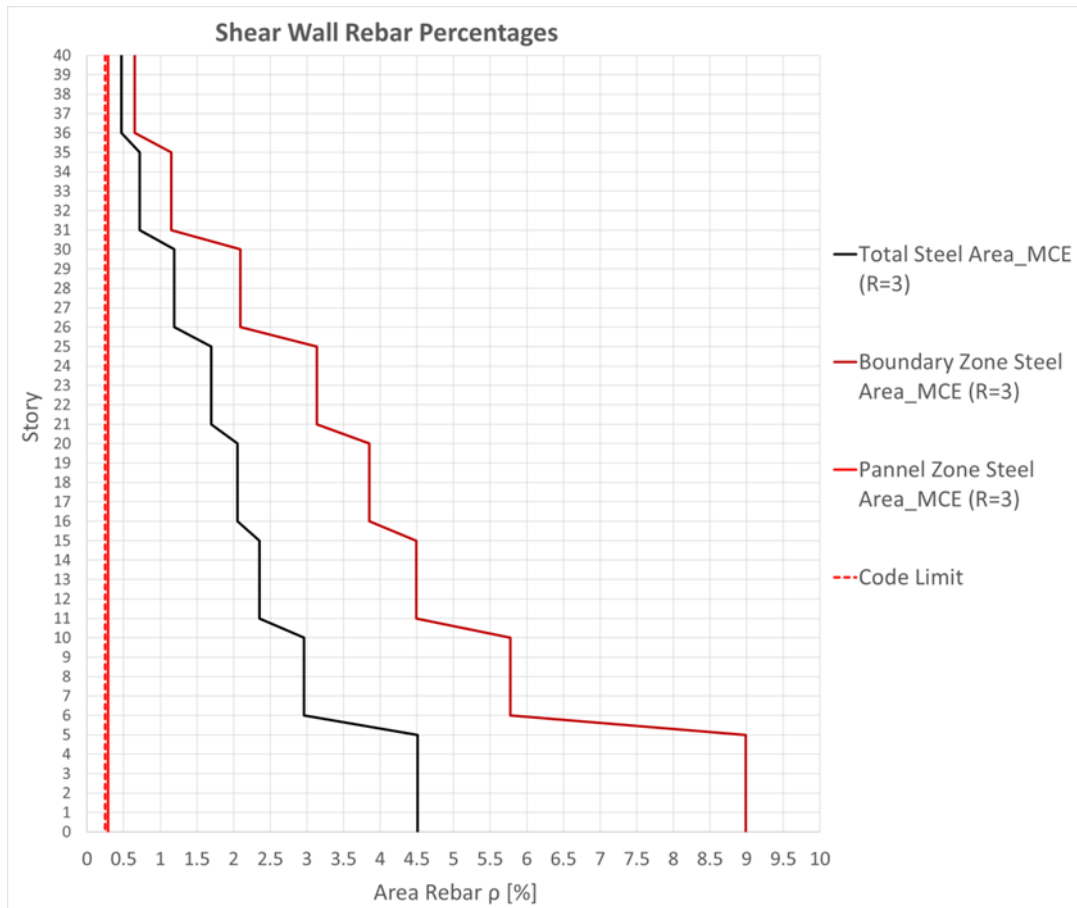


Figure 4.37 Option B_RSA MCE (R=3) Rebar Amounts

4.2.2.1 Modal Participation Mass Ratios

The Modal results of Option B_RSA MCE (R=3) Model are shown just for the first 30 Modes, avoiding the negligible other ones, *Table 4.6*:

Mode	Period [Sec]	UX	UY	RZ	Sum UX	Sum UY	Sum RZ
1	3.663	0	0.6621	0	0	0.6621	0
2	3.663	0.6621	0	0	0.6621	0.6621	0
3	2.705	0	0	0.7536	0.6621	0.6621	0.7536
4	0.873	0.178	0.000001282	0	0.8401	0.6621	0.7536
5	0.873	0.000001282	0.178	0	0.8401	0.8401	0.7536
6	0.835	0	0	0.1008	0.8401	0.8401	0.8544
7	0.445	0	0	0.0447	0.8401	0.8401	0.8991
8	0.394	0.0001	0.0524	0	0.8403	0.8926	0.8991
9	0.394	0.0524	0.0001	0	0.8927	0.8927	0.8991
10	0.279	0	0	0.0266	0.8927	0.8927	0.9257
11	0.237	0.0281	0.0008	0	0.9208	0.8936	0.9257
12	0.237	0.0008	0.0281	0	0.9216	0.9216	0.9257
13	0.192	0	0	0.0177	0.9216	0.9216	0.9434
14	0.159	0.0182	0.0000373	0	0.9398	0.9217	0.9434
15	0.159	0.0000373	0.0182	0	0.9398	0.9398	0.9434
16	0.141	0	0	0.0125	0.9398	0.9398	0.956
17	0.116	0.0127	0.000008547	0	0.9525	0.9399	0.956
18	0.116	0.000008547	0.0127	0	0.9525	0.9525	0.956
19	0.109	0	0	0.0092	0.9525	0.9525	0.9652
20	0.089	0.0092	0.0001	0	0.9617	0.9526	0.9652
21	0.089	0.0001	0.0092	0	0.9618	0.9618	0.9652
22	0.088	0	0	0.007	0.9618	0.9618	0.9722
23	0.073	0	0	0.0055	0.9618	0.9618	0.9777
24	0.071	0.007	0.0001	0	0.9688	0.9619	0.9777
25	0.071	0.0001	0.007	0	0.9688	0.9688	0.9777
26	0.062	0	0	0.0042	0.9688	0.9688	0.9819
27	0.058	0.0056	0.000006447	0	0.9744	0.9688	0.9819
28	0.058	0.000006447	0.0056	0	0.9744	0.9744	0.9819
29	0.054	0	0	0.0033	0.9744	0.9744	0.9852
30	0.049	0.0038	0.0006	0	0.9783	0.975	0.9852

Table 4.6 Option B_RSA MCE (R=3) Modal Participation Mass Ratios

4.2.2.2 Option B – Drift

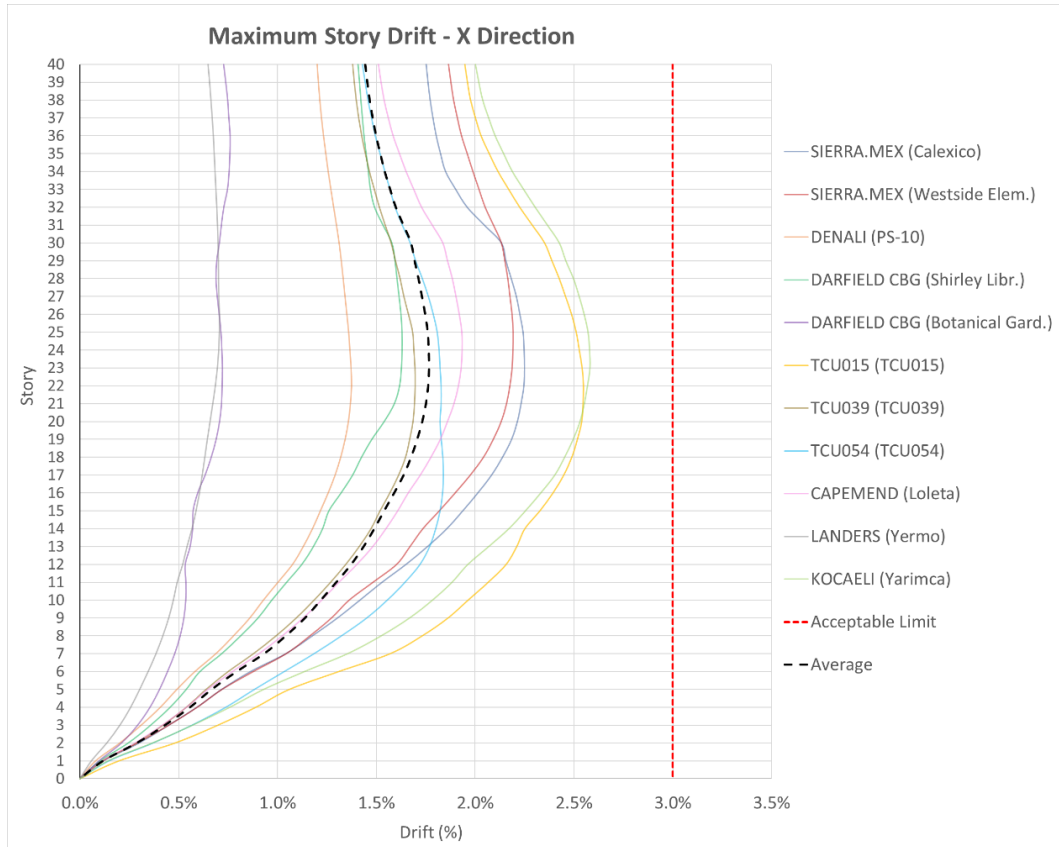


Figure 4.38 Option B_MCE (R=3) – NLRHA X Direction Story Drift

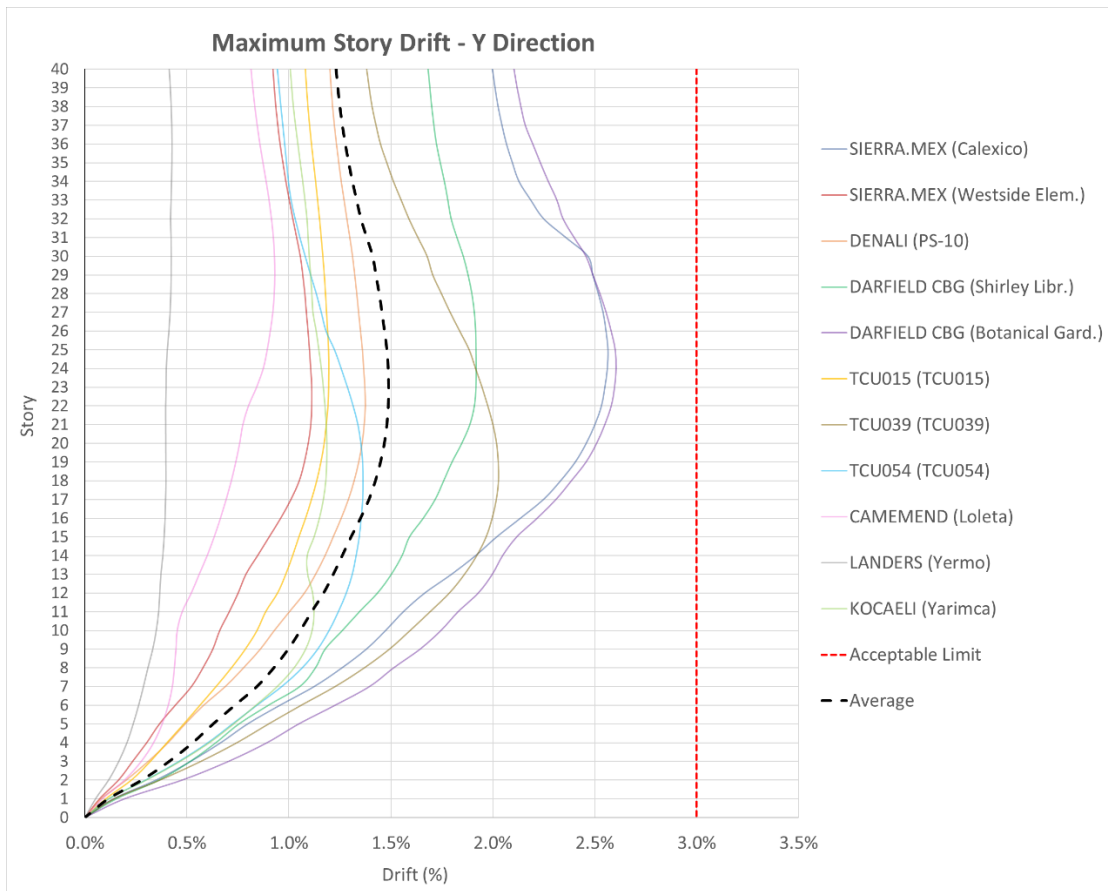


Figure 4.39 Option B_MCE (R=3) – NLRHA Y Direction Story Drift

4.2.2.3 Option B – Core Shear

As already mentioned, along X direction the walls able to be resistant are shown in the following Figure 4.40:

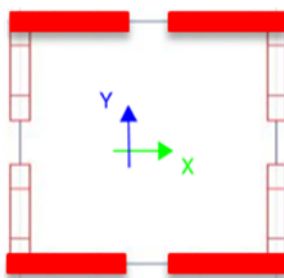


Figure 4.40 X Direction Shear Resistant Core

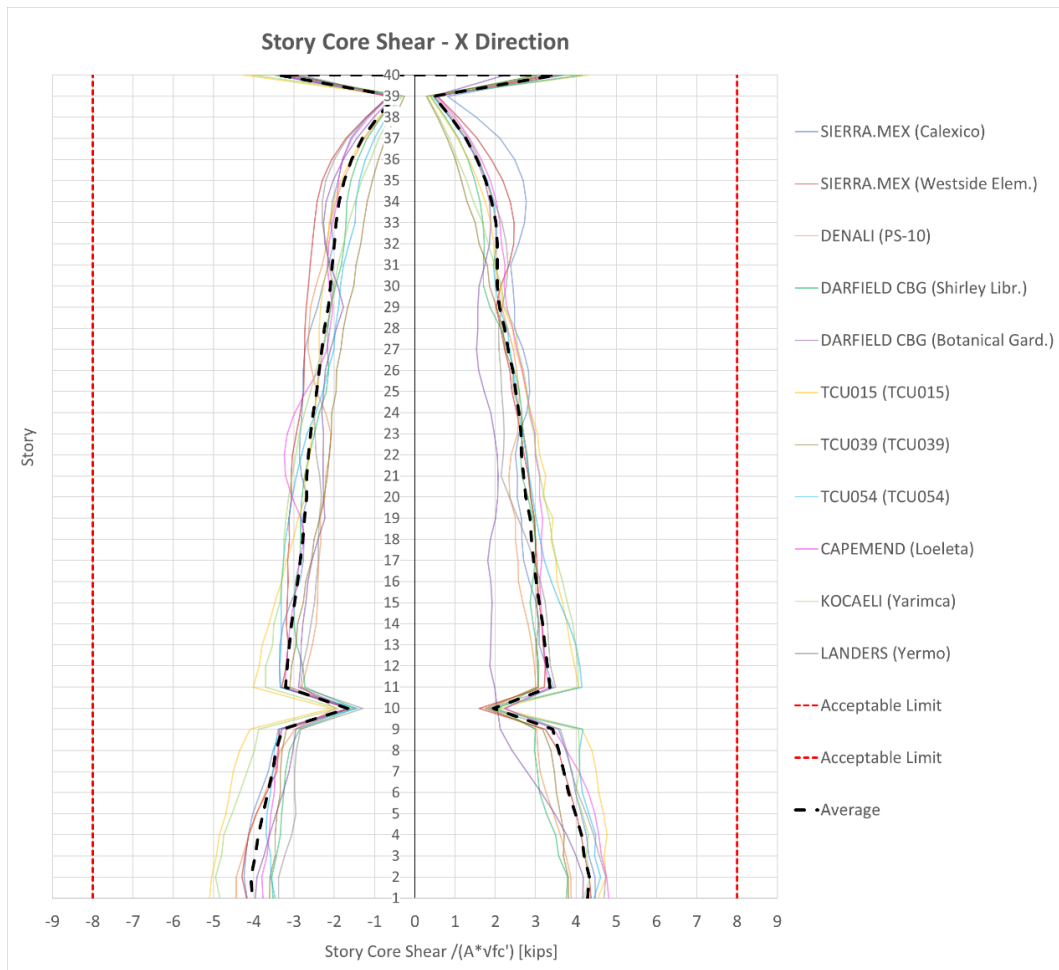


Figure 4.41 Option B_MCE (R=3) – NLRHA X Direction Story Shear

As done for the X direction, even for the Y direction the walls able to be resistant are shown in the following Figure 4.42:

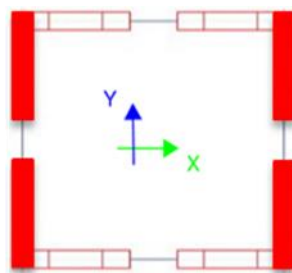


Figure 4.42 Y Direction Shear Resistant Core

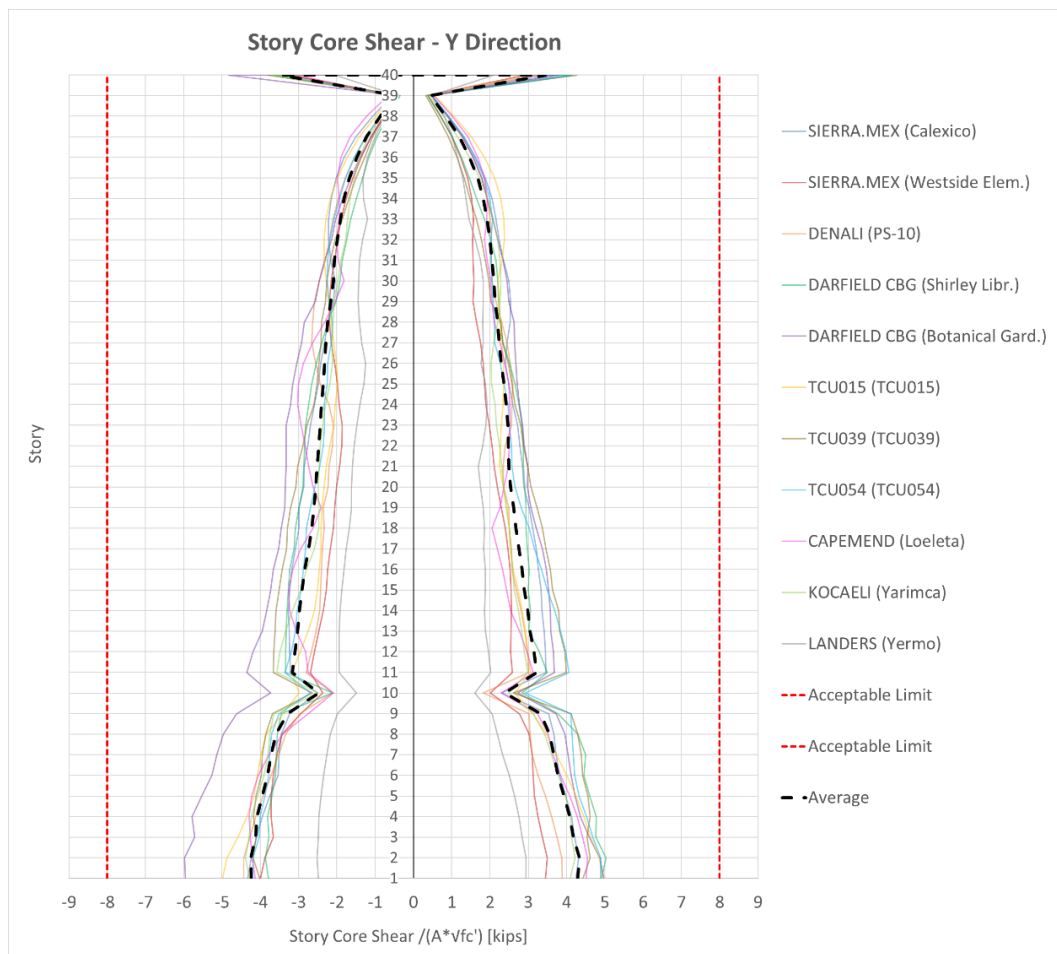


Figure 4.43 Option B_MCE (R=3) – NLRHA Y Direction Story Shear

4.2.2.4 Option B – Coupling Beam Plastic Rotation

Along X direction the results of only one plastic hinge of the Link Beam 4 are shown cause the most significant. The location of the mentioned plastic hinge is shown in blue in the following Figure 4.44:

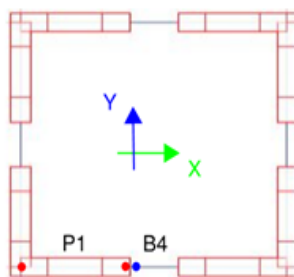


Figure 4.44 Coupling Beam 4 Plastic Hinges Position

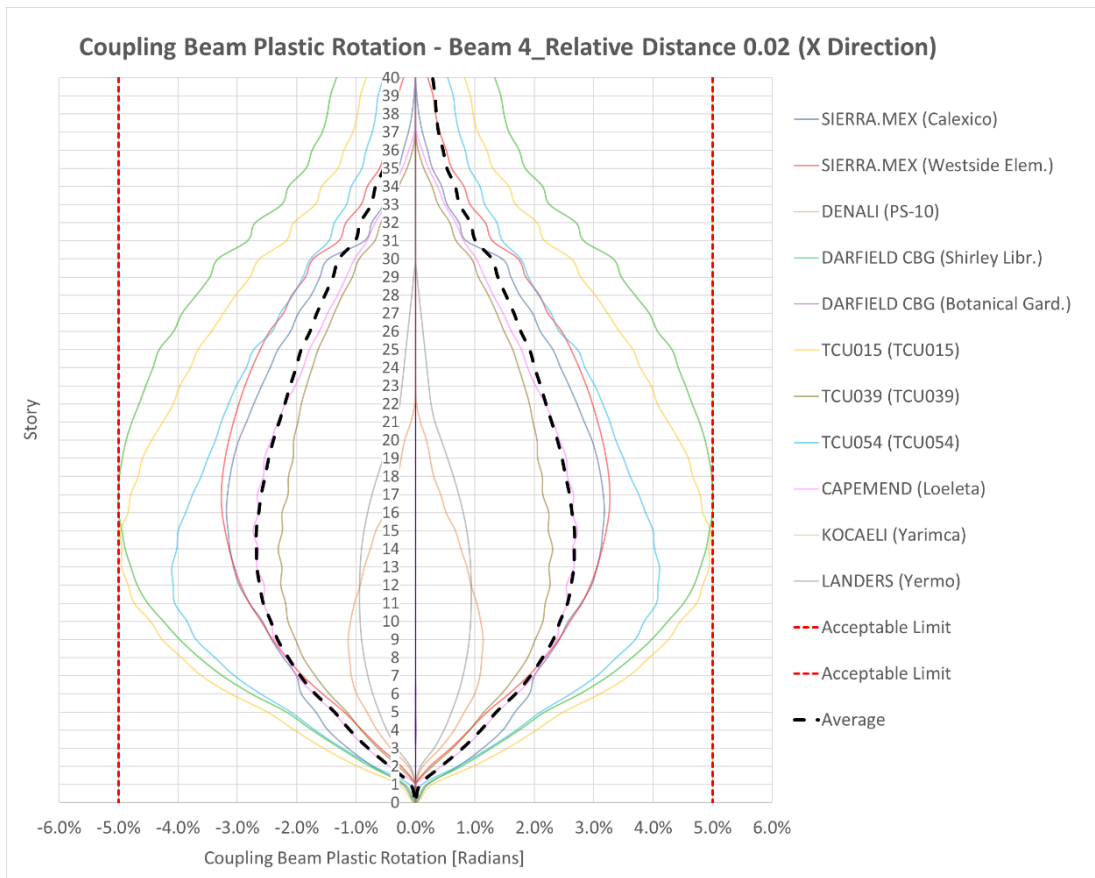


Figure 4.45 Option B_MCE (R=3) – NLRHA X Direction Link Beam 4 Plastic Hinge Rotation

As done for the X direction, along the Y direction the results of only one plastic hinge of the Link Beam 3 are shown cause the most significant. The location of the mentioned plastic hinge is shown in blue in the following Figure 4.46:

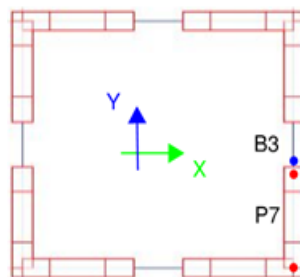


Figure 4.46 Coupling Beam 3 Plastic Hinges Position

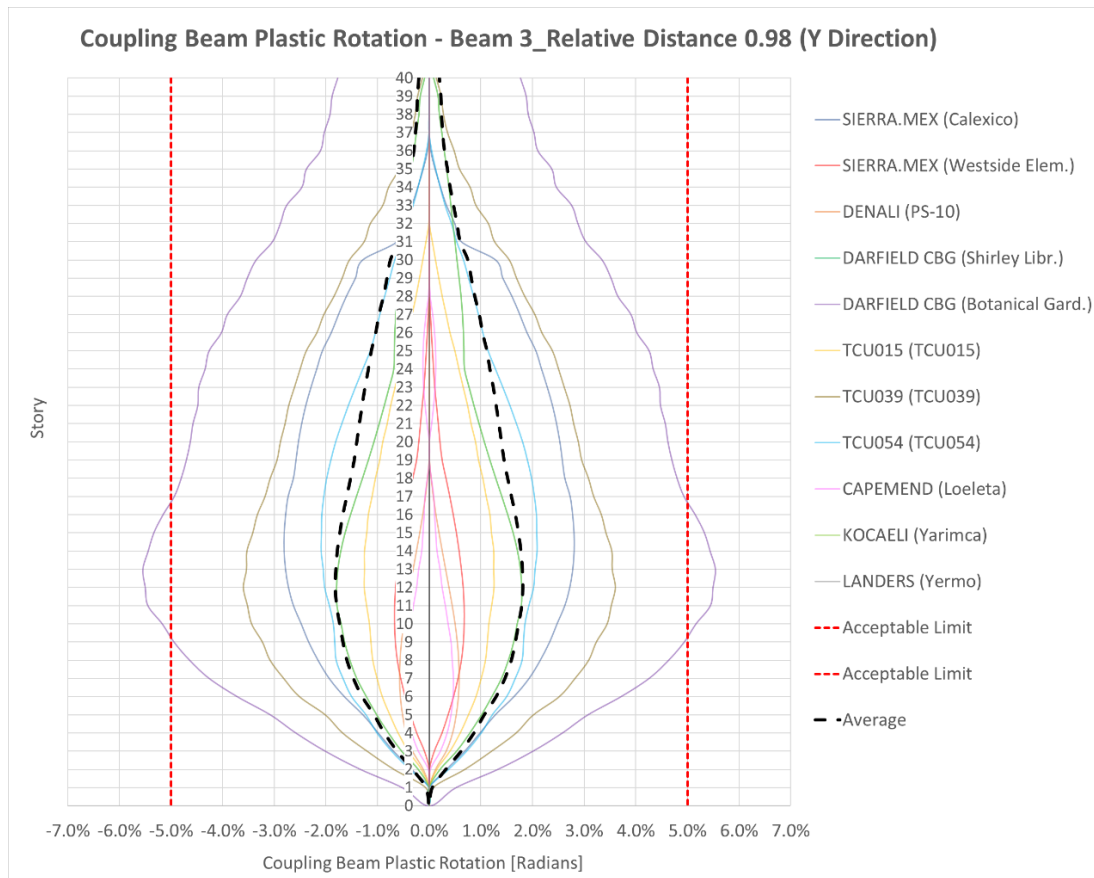


Figure 4.47 Option B_MCE (R=3) – NLRHA Y Direction Link Beam 3 Plastic Hinge Rotation

4.2.2.5 Option B – Shear Wall Fiber Strain

Along X direction the results of only two fibers are shown, particularly the two outermost edge fibers of the analyzed pier, cause the most significant. In X direction are displayed the plots of Pier 1 Boundary Zones. The location of the two mentioned fibers are shown in red in the following Figure 4.48:

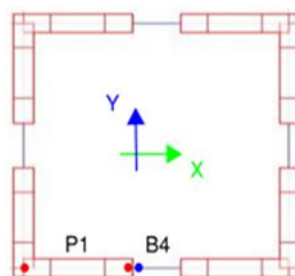


Figure 4.48 Pier 1 Fibers Position

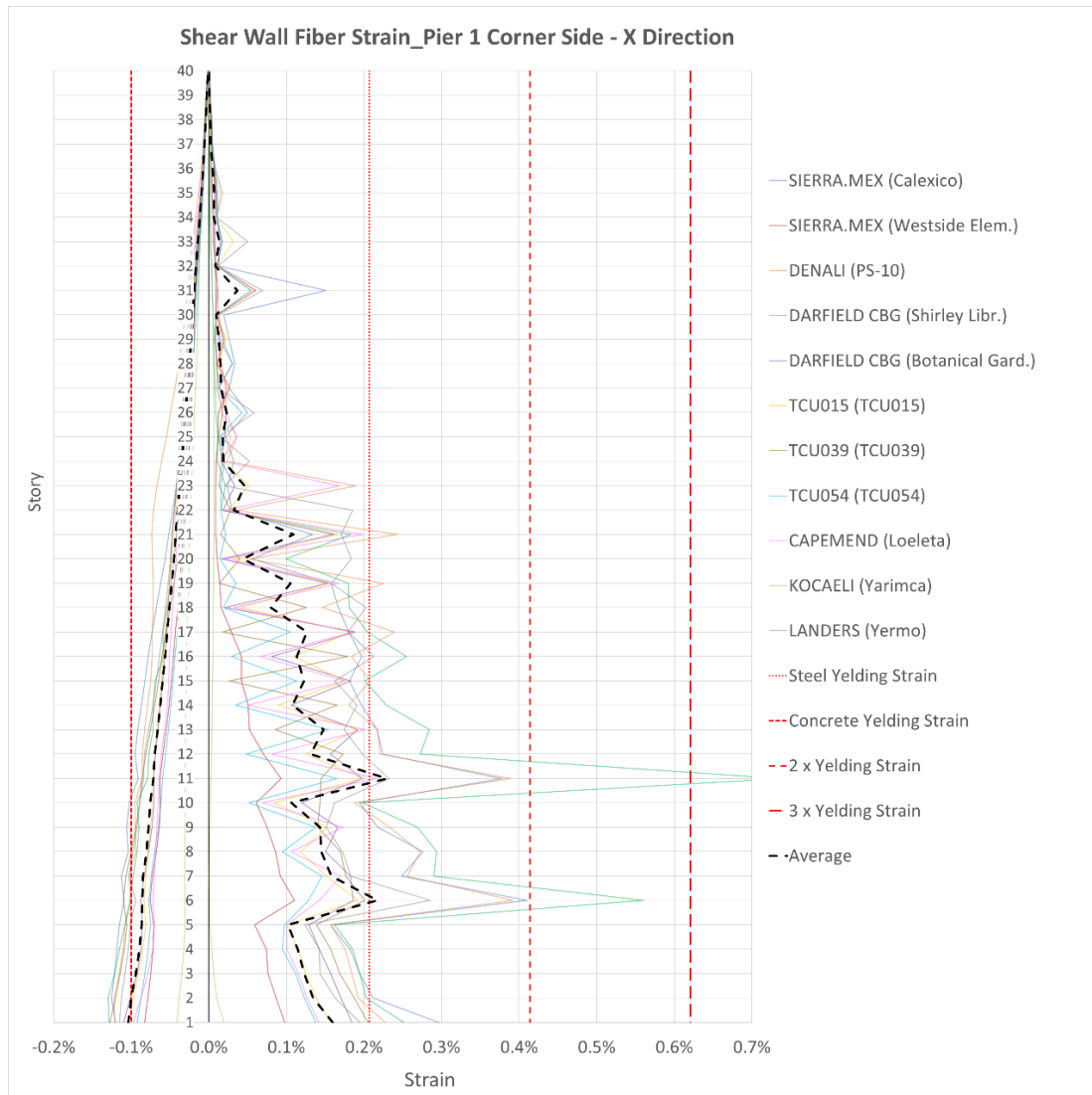


Figure 4.49 Option B_MCE (R=3) – NLRHA X Direction Pier 1 Corner Side Fiber Strain

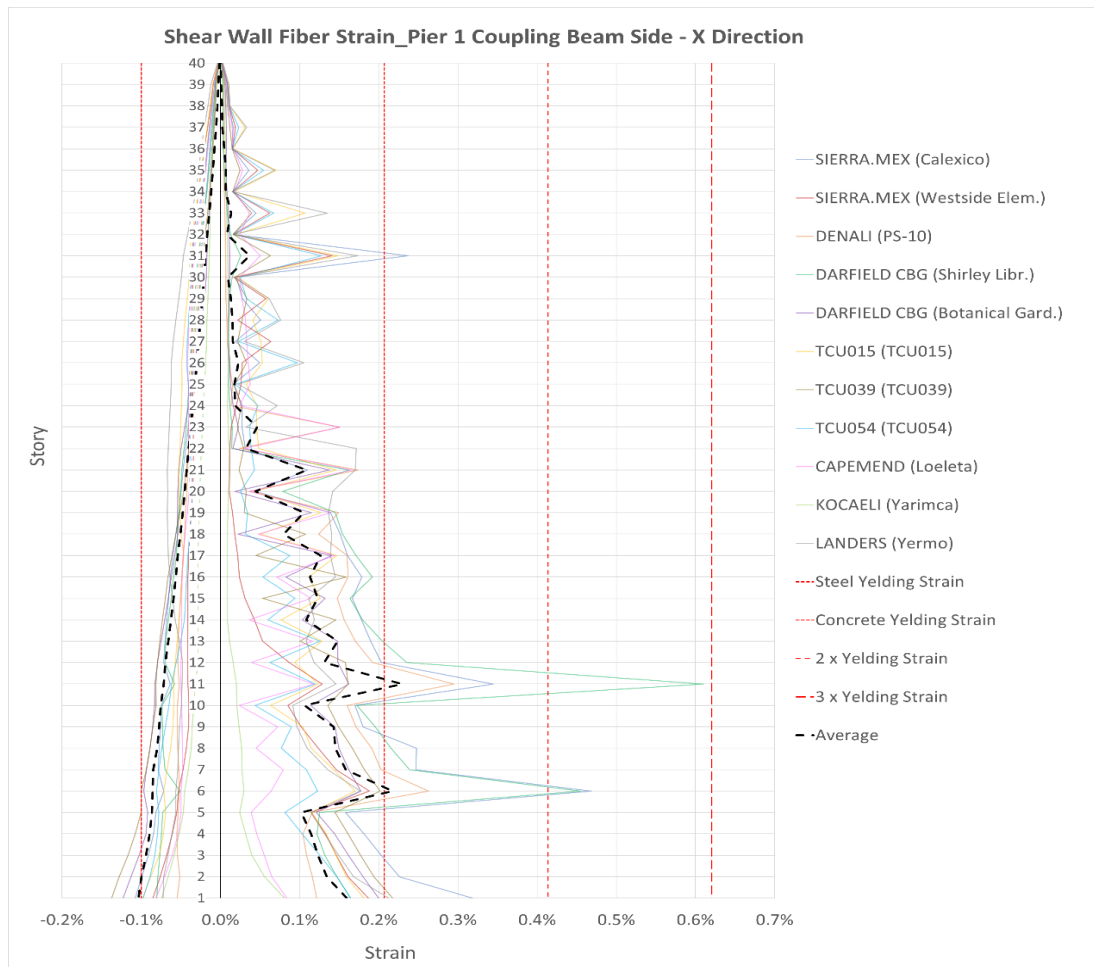


Figure 4.50 Option B_MCE (R=3) – NLRHA X Direction Pier 1 Coupling Beam Side Fiber Strain

Along Y direction the results of only two fibers are shown, particularly the two outermost edge fibers of the analyzed pier, cause the most significant. In Y direction are displayed the plots of Pier 7 Boundary Zones. The location of the two mentioned fibers are shown in red in the following Figure 4.51:

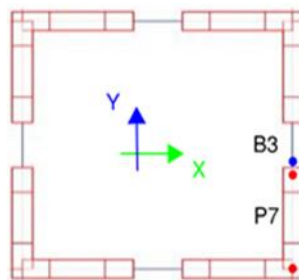


Figure 4.51 Pier 7 Fibers Position

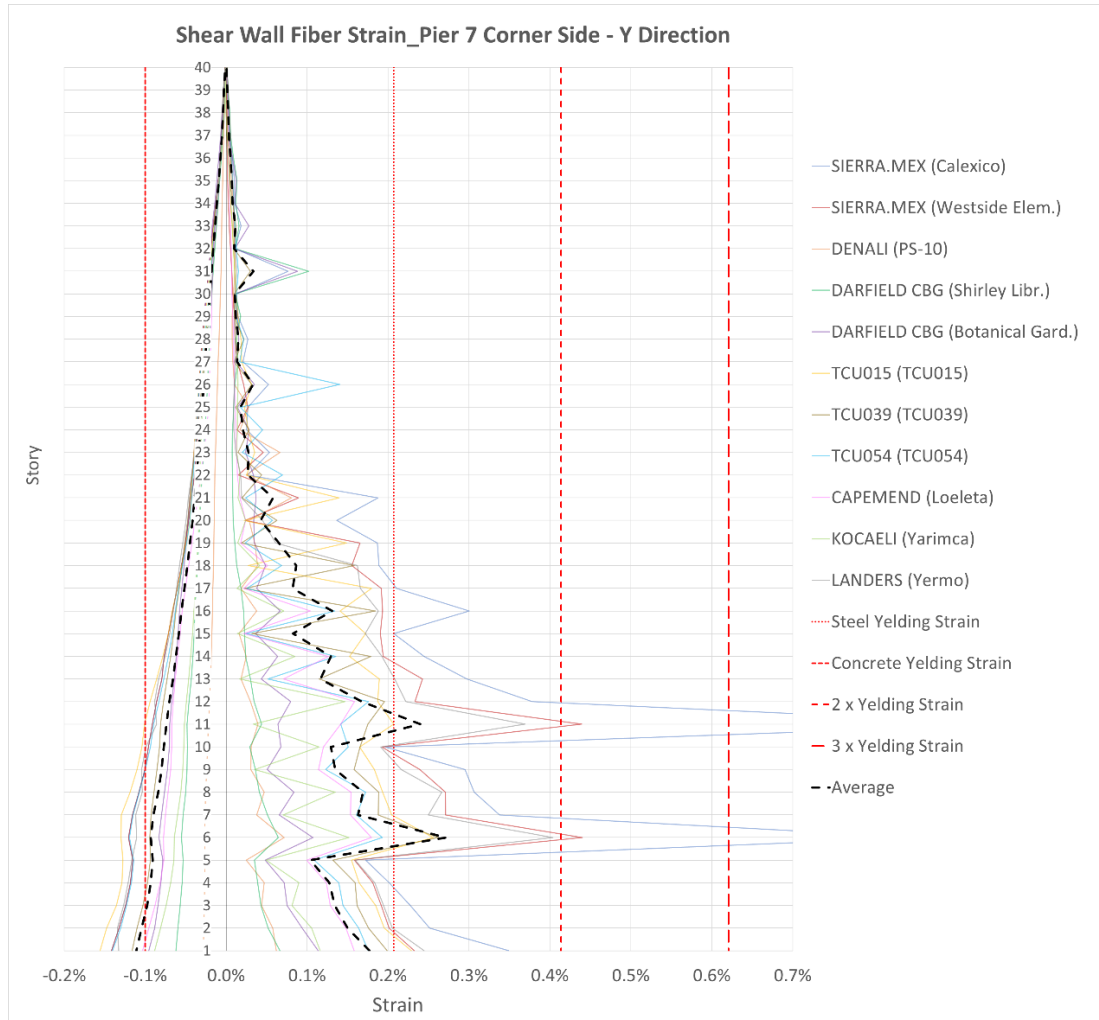


Figure 4.52 Option B_MCE (R=3) – NLRHA Y Direction Pier 7 Corner Side Fiber Strain

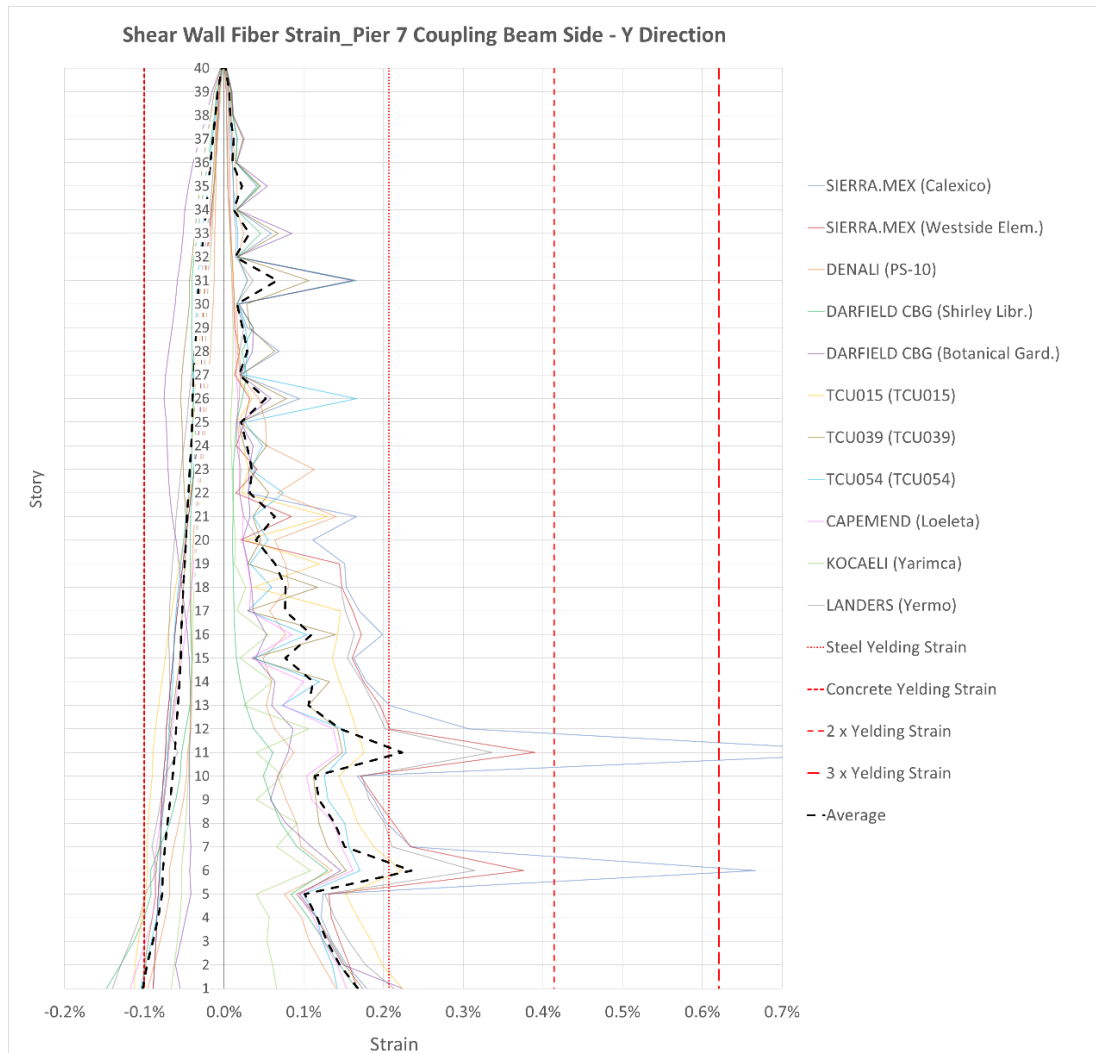


Figure 4.53 Option B_MCE (R=3) – NLRHA Y Direction Pier 7 Coupling Beam Side Fiber Strain

4.2.2.6 Option B – Flexure Demands

The NLRHA spaghetti and their corresponding Flexure Demands couples are shown below. The M-N plots are built following the same procedure proposed in Chapter 3.3.4.

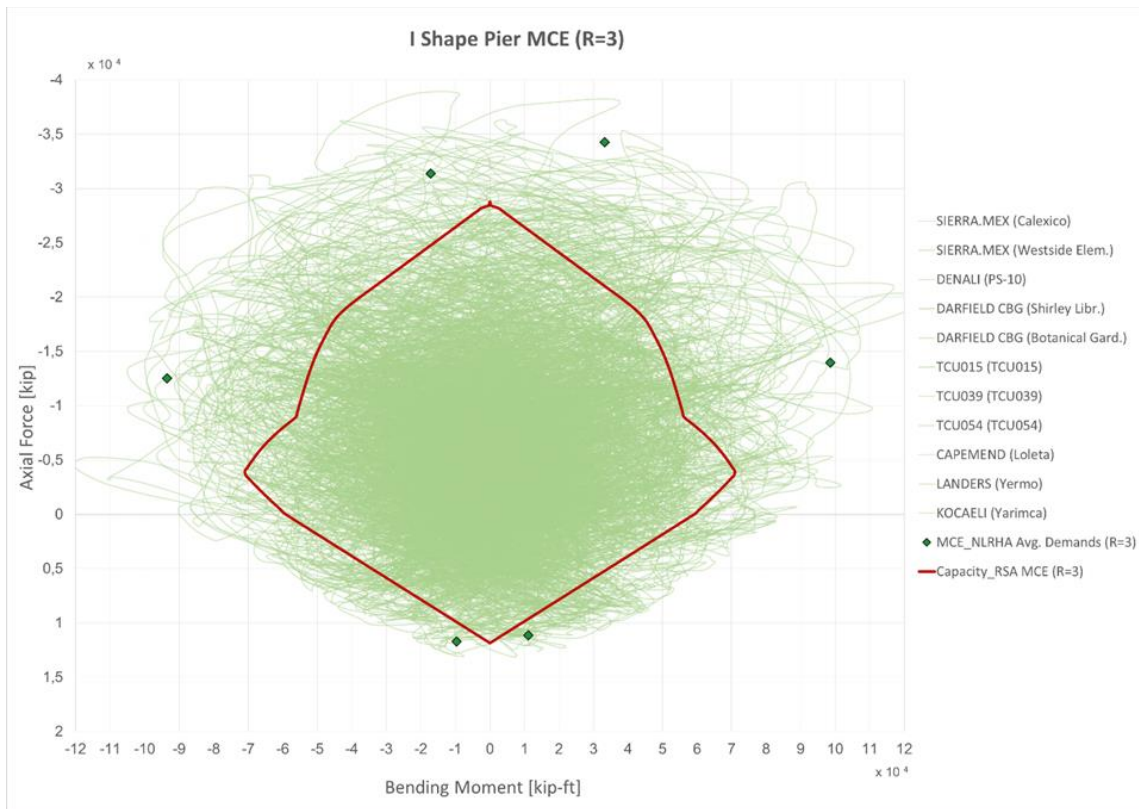


Figure 4.54 Option B_MCE (R=3) – NLRHA Stand-Alone Shear Wall Flexure Demands

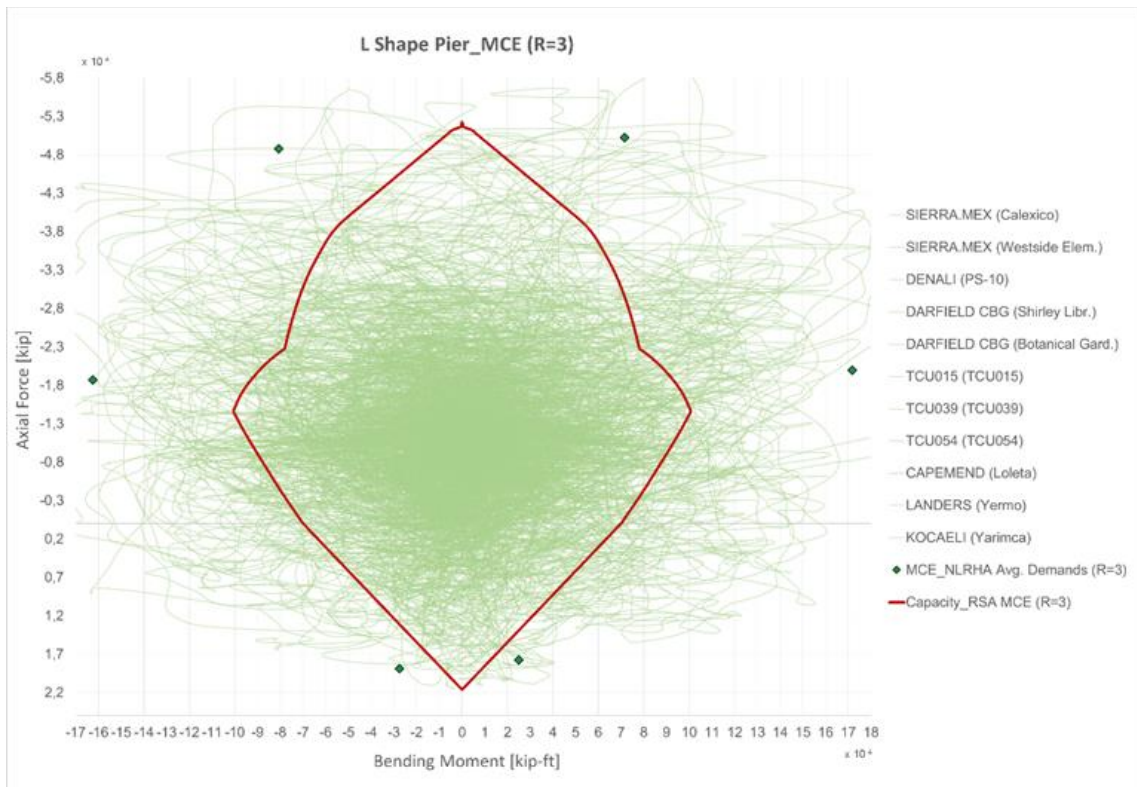


Figure 4.55 Option B_MCE (R=3) – NLRHA Compound Shear Wall Flexure Demands

4.3 Linear Response History Analysis Prediction of Nonlinear Behavior

In the present chapter are presented the NLRHA results, conducted by Nonlinear Direct Integration (DI). The Option D_MCE (R=3), based on the LRHA Proposed Design Methodologies explained in Chapter 3.3.4 is the only one evaluated.

On each plot, the NLRHA results are displayed as all the Ground Motion runs (pair of motions) and the mean of all these runs.

4.3.1 Option D (MCE R=3) Nonlinear Analysis Results

Based on the Option D design proposed in Chapter 3.3.6, the rebar distribution is known along all the building height, *Figure 4.56*. Accordingly with this, it is possible to build the Option D Nonlinear Fiber Model.

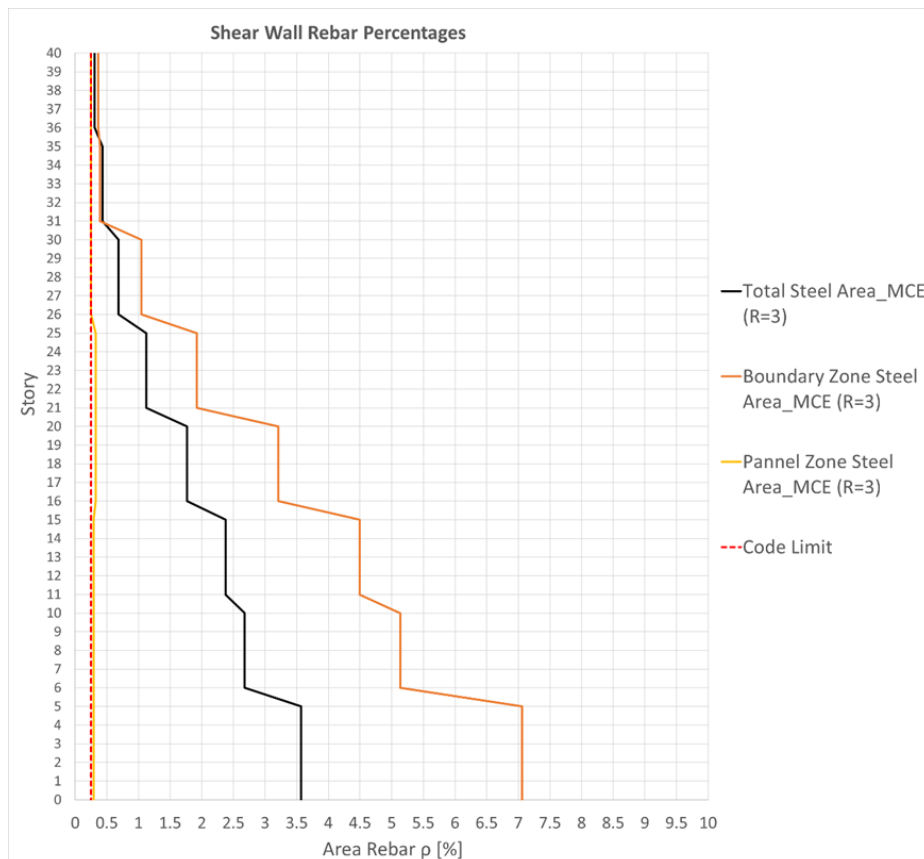


Figure 4.56 Option D_LRHA MCE (R=3) Rebar Amounts

4.3.1.1 Modal Participation Mass Ratios

The Modal results of Option D_LRHA MCE (R=3) Model are shown just for the first 30 Modes, avoiding the negligible other ones, *Table 4.6:*

Mode	Period [sec]	UX	UY	RZ	Sum UX	Sum UY	Sum RZ
1	3.784	0	0.6634	0	0	0.6634	0
2	3.784	0.6634	0	0	0.6634	0.6634	0
3	2.726	0	0	0.7568	0.6634	0.6634	0.7568
4	0.89	0	0.179	0	0.6634	0.8423	0.7568
5	0.89	0.179	0	0	0.8423	0.8423	0.7568
6	0.843	0	0	0.0997	0.8423	0.8423	0.8566
7	0.451	0	0	0.0439	0.8423	0.8423	0.9005
8	0.401	0.052	5.793E-07	0	0.8943	0.8423	0.9005
9	0.401	5.793E-07	0.052	0	0.8943	0.8943	0.9005
10	0.283	0	0	0.0261	0.8943	0.8943	0.9266
11	0.241	0.0084	0.02	0	0.9028	0.9144	0.9266
12	0.241	0.02	0.0084	0	0.9228	0.9228	0.9266
13	0.195	0	0	0.0174	0.9228	0.9228	0.944
14	0.163	0.0179	0.000001149	0	0.9407	0.9228	0.944
15	0.163	0.000001149	0.0179	0	0.9407	0.9407	0.944
16	0.144	0	0	0.0123	0.9407	0.9407	0.9563
17	0.118	0.0125	0.00001	0	0.9532	0.9407	0.9563
18	0.118	0.00001	0.0125	0	0.9532	0.9532	0.9563
19	0.111	0	0	0.0091	0.9532	0.9532	0.9654
20	0.09	0.0091	0.000005367	0	0.9623	0.9532	0.9654
21	0.09	0.000005367	0.0091	0	0.9623	0.9623	0.9654
22	0.089	0	0	0.0069	0.9623	0.9623	0.9723
23	0.074	0	0	0.0054	0.9623	0.9623	0.9776
24	0.072	0.0069	0.000002778	0	0.9692	0.9623	0.9776
25	0.072	0.000002778	0.0069	0	0.9692	0.9692	0.9776
26	0.063	0	0	0.0042	0.9692	0.9692	0.9818
27	0.059	0.0054	9.322E-07	0	0.9747	0.9692	0.9818
28	0.059	9.322E-07	0.0054	0	0.9747	0.9747	0.9818
29	0.054	0	0	0.0033	0.9747	0.9747	0.9851
30	0.05	0.0043	6.074E-07	0	0.9789	0.9747	0.9851

Table 4.7 Option D_LRHA MCE (R=3) Modal Participation Mass Ratios

4.3.1.2 Option D – Drift

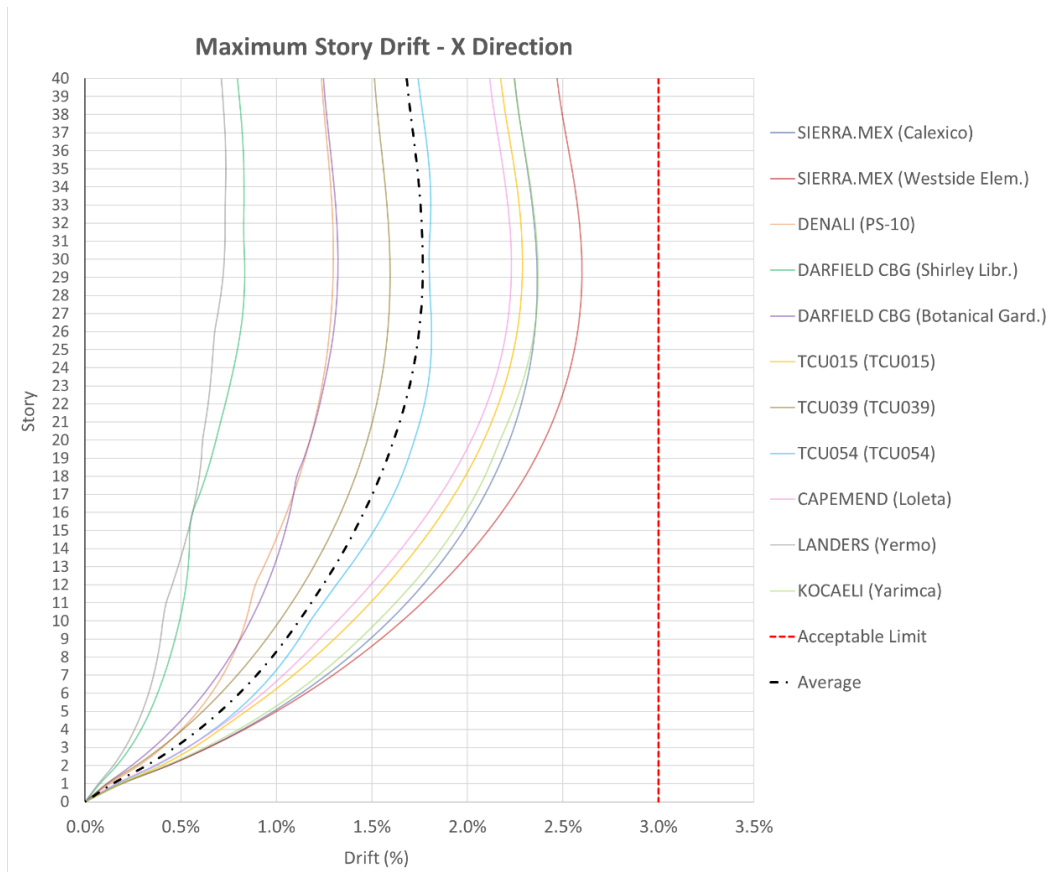


Figure 4.57 Option B_MCE (R=3) – NLRHA X Direction Story Drift

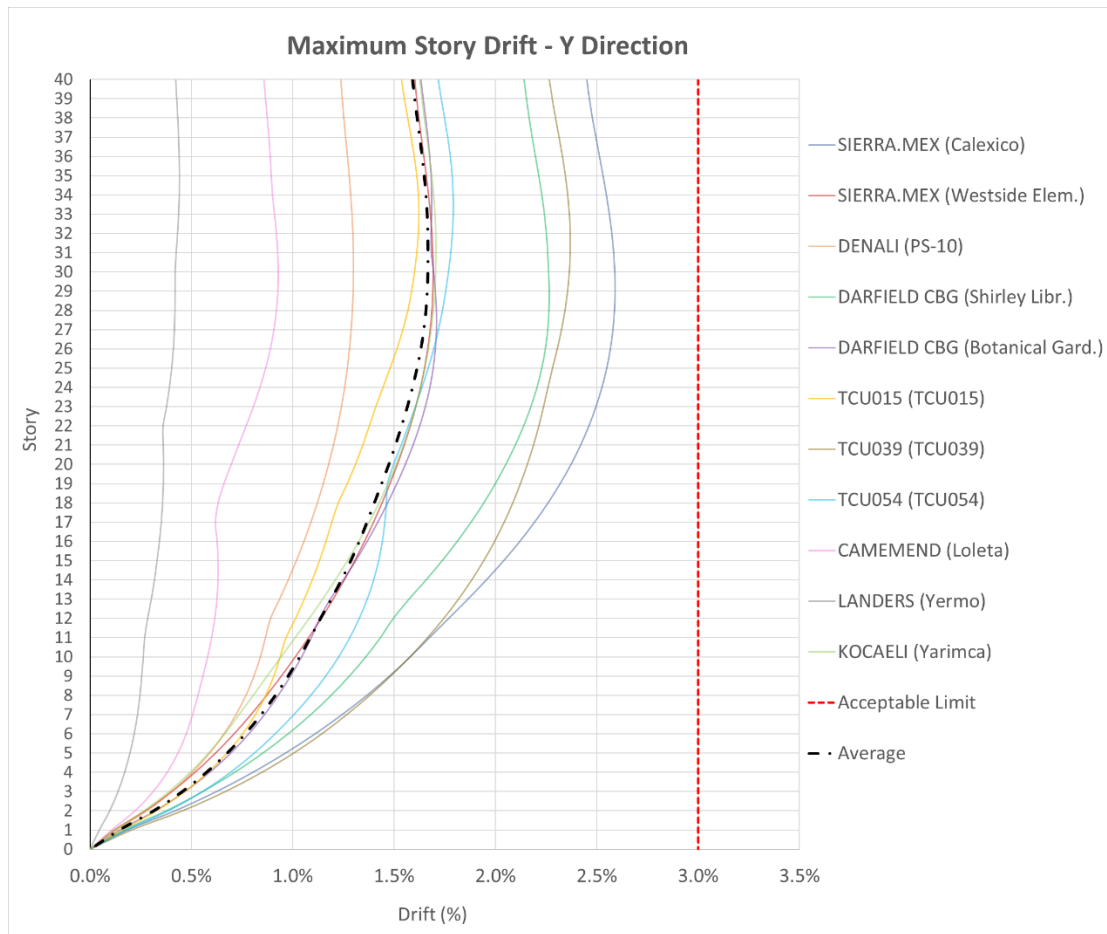


Figure 4.58 Option D_MCE (R=3) – NLRHA Y Direction Story Drift

4.3.1.3 Option D – Core Shear

As already mentioned, along X direction the walls able to be resistant are shown in the following Figure 4.59:

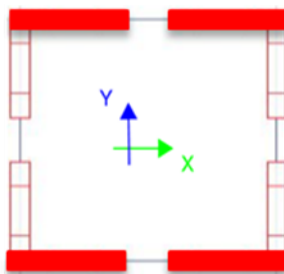


Figure 4.59 X Direction Shear Resistant Core

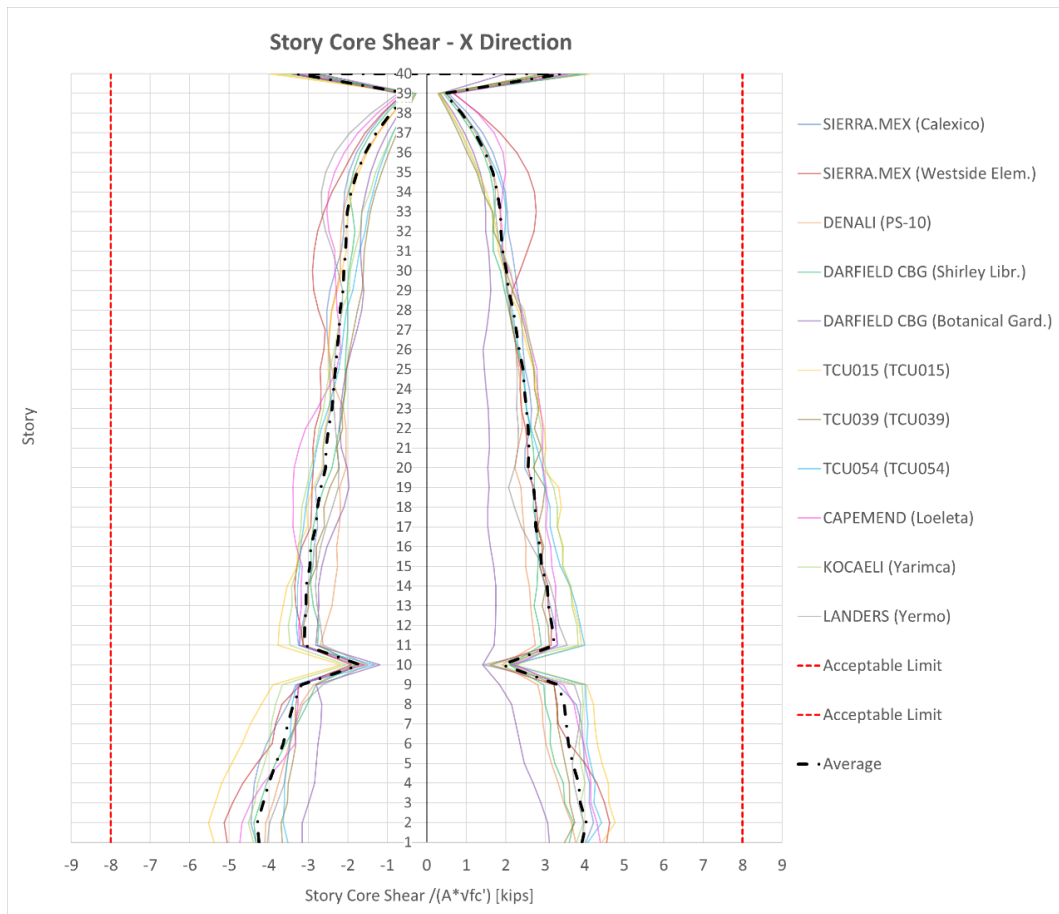


Figure 4.60 Option D_MCE (R=3) – NLRHA X Direction Story Shear

As done for the X direction, even for the Y direction the walls able to be resistant are shown in the following Figure 4.61:

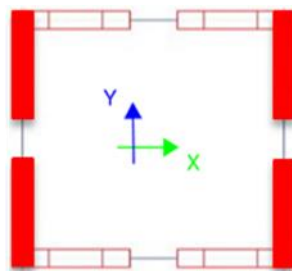


Figure 4.61 Y Direction Shear Resistant Core

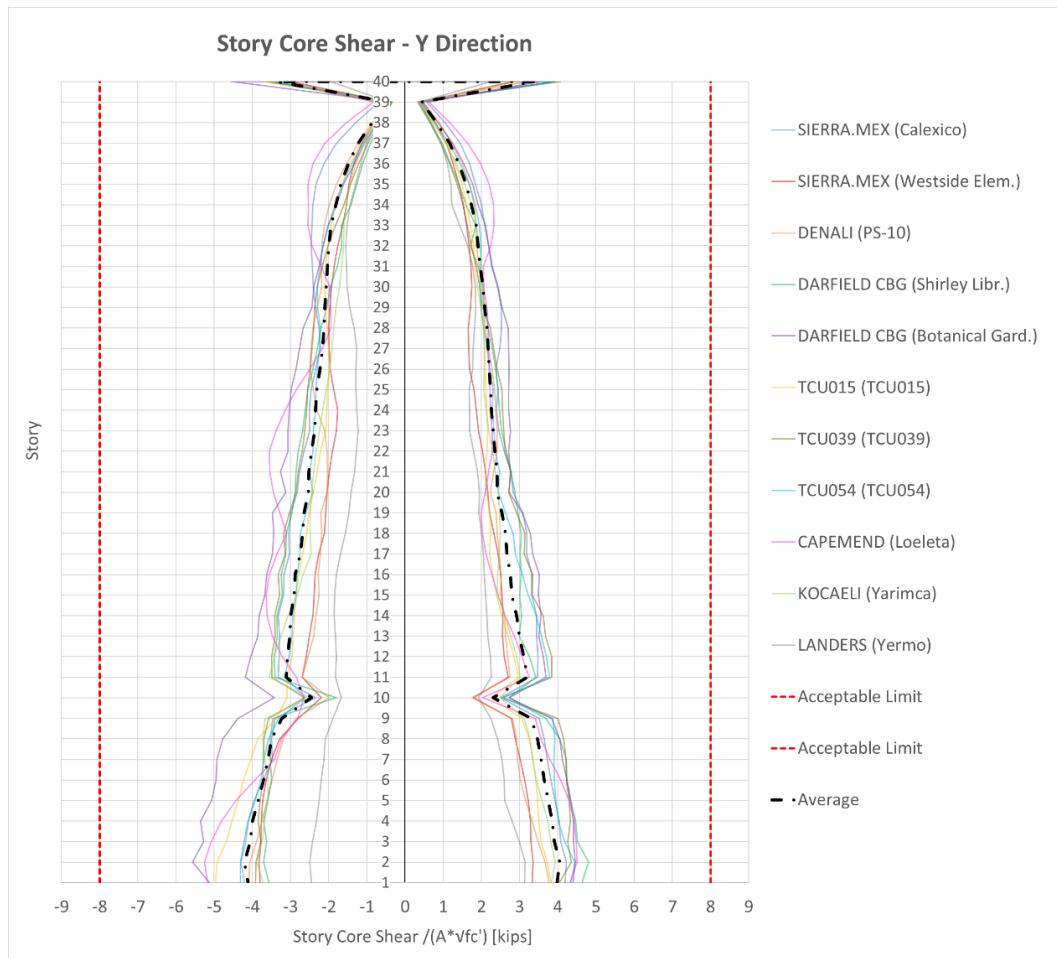


Figure 4.62 Option D_MCE (R=3) – NLRHA Y Direction Story Shear

4.3.1.4 Option D – Coupling Beam Plastic Rotation

Along X direction the results of only one plastic hinge of the Link Beam 4 are shown cause the most significant. The location of the mentioned plastic hinge is shown in blue in the following Figure 4.63:

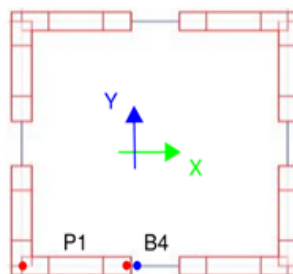


Figure 4.63 Coupling Beam 4 Plastic Hinges Position

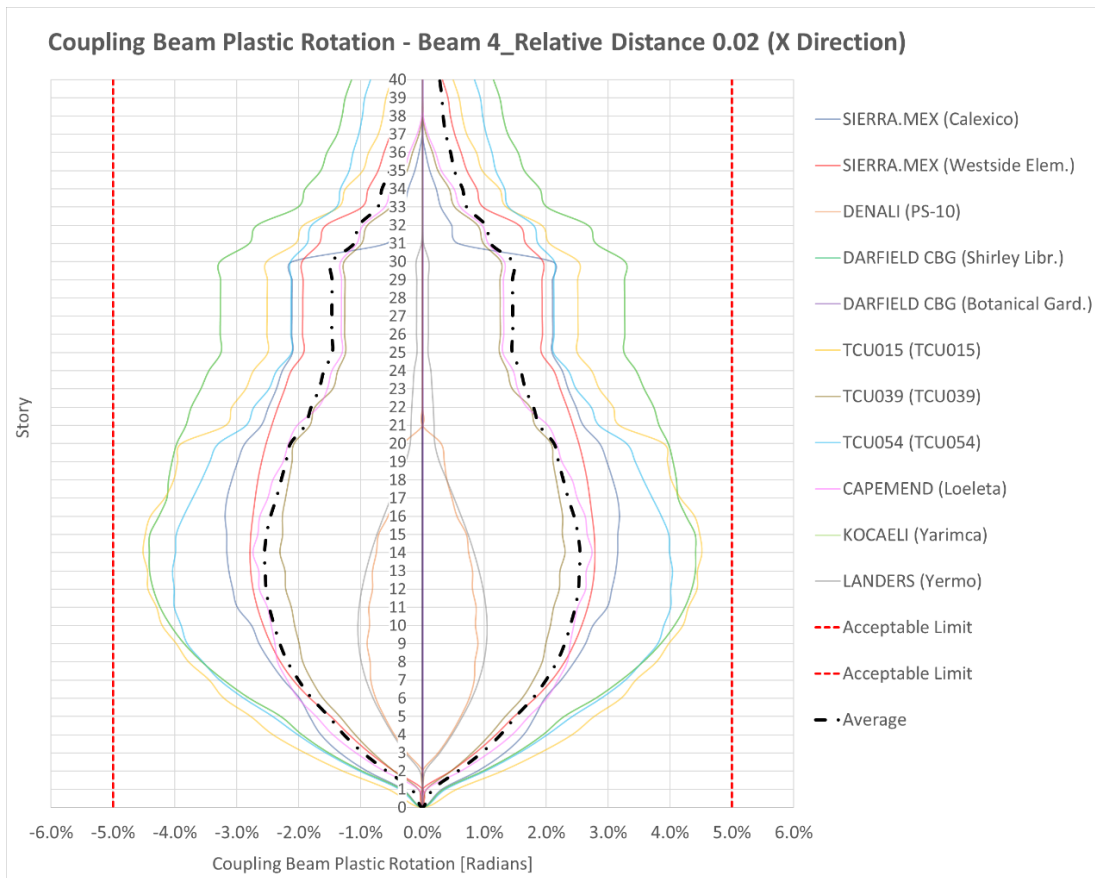


Figure 4.64 Option D_MCE (R=3) – NLRHA X Direction Link Beam 4 Plastic Hinge Rotation

As done for the X direction, along the Y direction the results of only one plastic hinge of the Link Beam 3 are shown cause the most significant. The location of the mentioned plastic hinge is shown in blue in the following Figure 4.65:

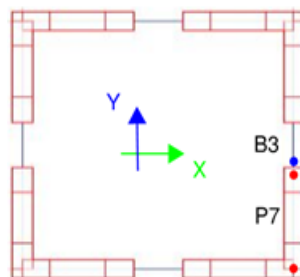


Figure 4.65 Coupling Beam 3 Plastic Hinges Position

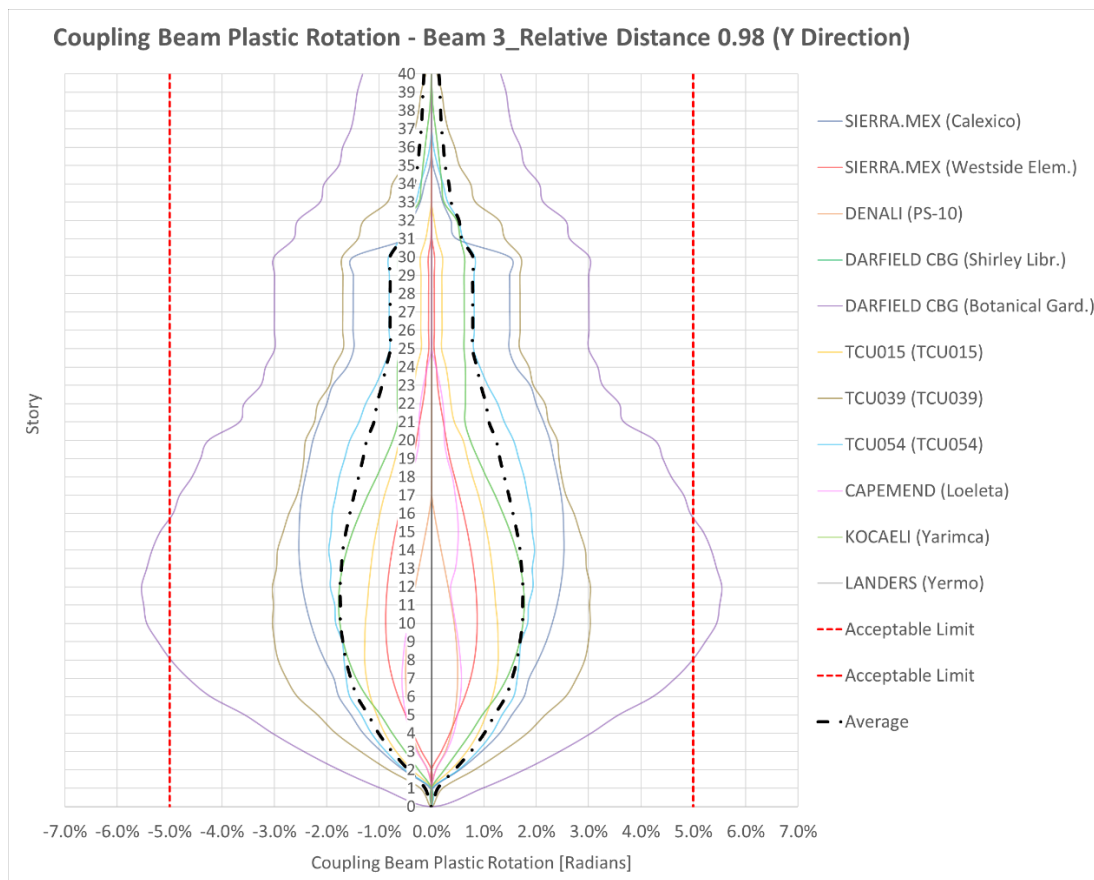


Figure 4.66 Option D_MCE (R=3) – NLRHA Y Direction Link Beam 3 Plastic Hinge Rotation

4.3.1.5 Option D – Shear Wall Fiber Strain

Along X direction the results of only two fibers are shown, particularly the two outermost edge fibers of the analyzed pier, cause the most significant. In X direction are displayed the plots of Pier 1 Boundary Zones. The location of the two mentioned fibers are shown in red in the following Figure 4.67:

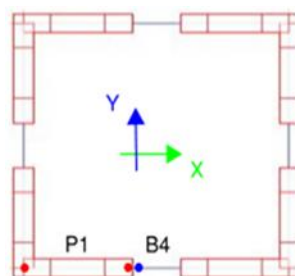


Figure 4.67 Pier 1 Fibers Position

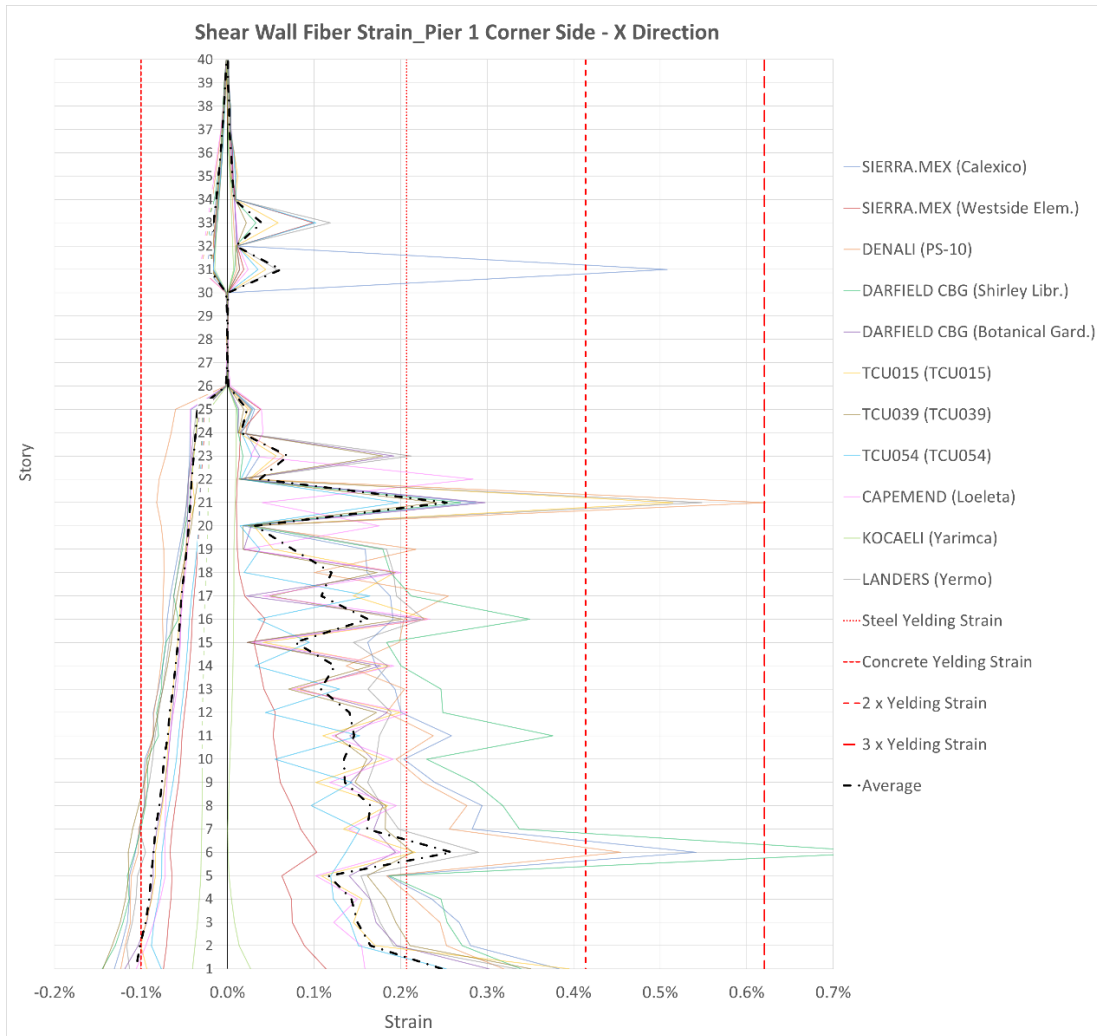


Figure 4.68 Option D_MCE (R=3) – NLRHA X Direction Pier 1 Corner Side Fiber Strain

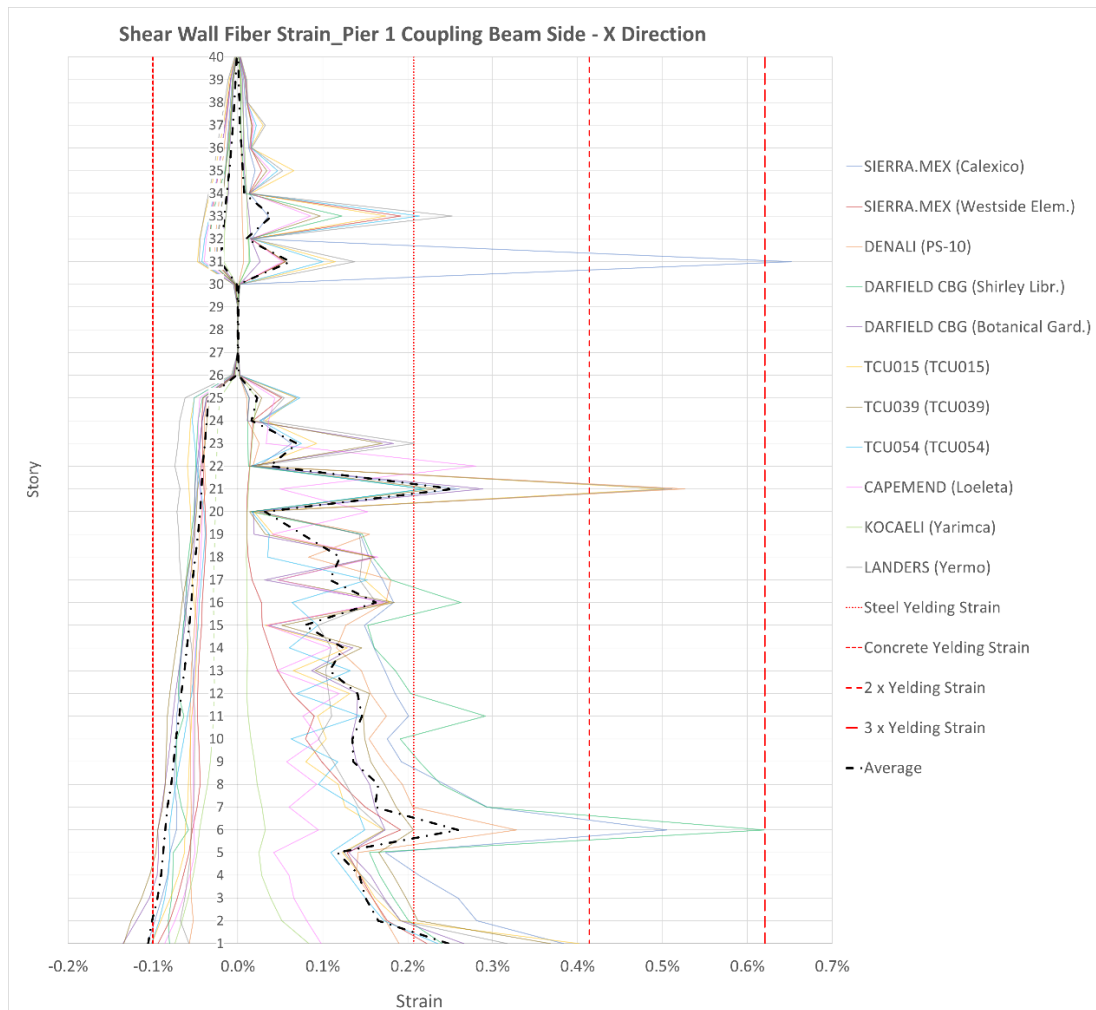


Figure 4.69 Option D_MCE (R=3) – NLRHA X Direction Pier 1 Coupling Beam Side Fiber Strain

Along Y direction the results of only two fibers are shown, particularly the two outermost edge fibers of the analyzed pier, cause the most significant. In Y direction are displayed the plots of Pier 7 Boundary Zones. The location of the two mentioned fibers are shown in red in the following Figure 4.70

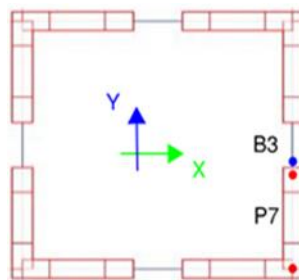


Figure 4.70 Pier 7 Fibers Position

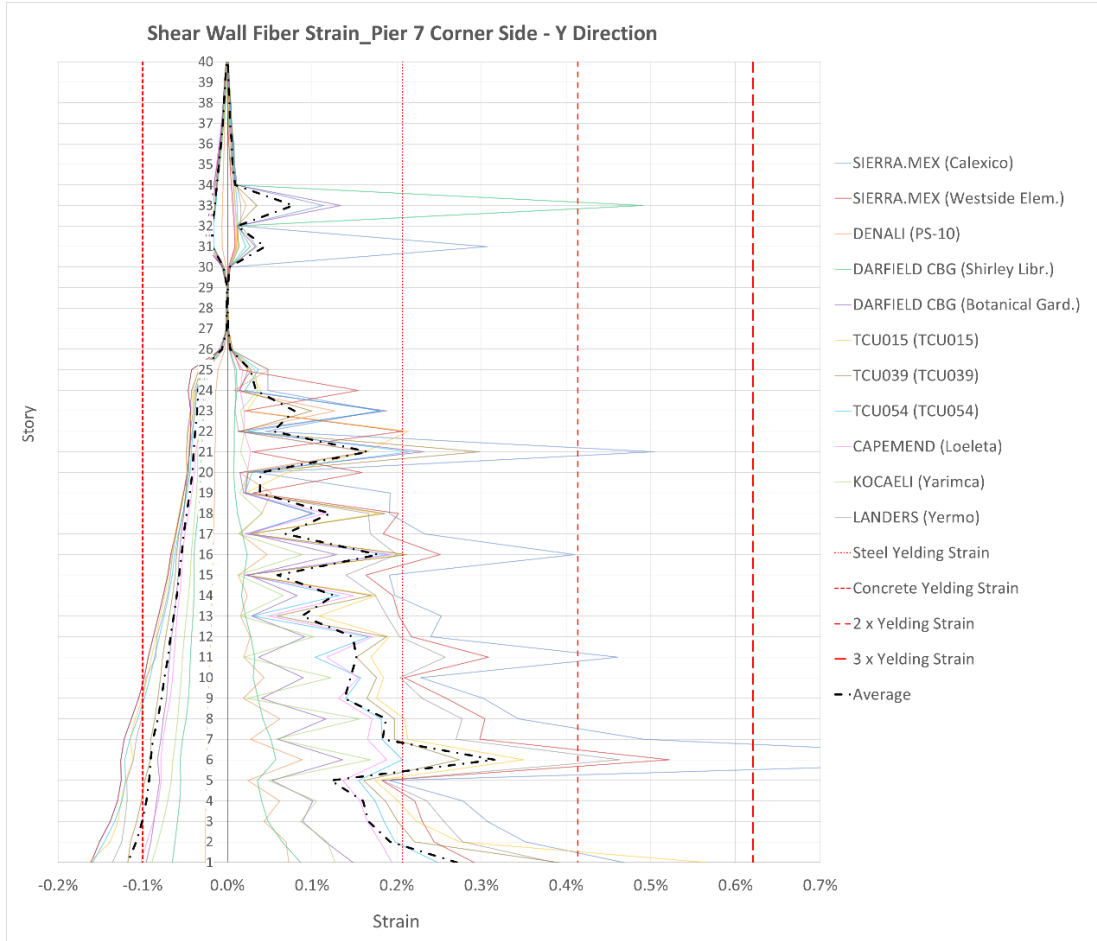


Figure 4.71 Option D_MCE (R=3) – NLRHA Y Direction Pier 7 Corner Side Fiber Strain

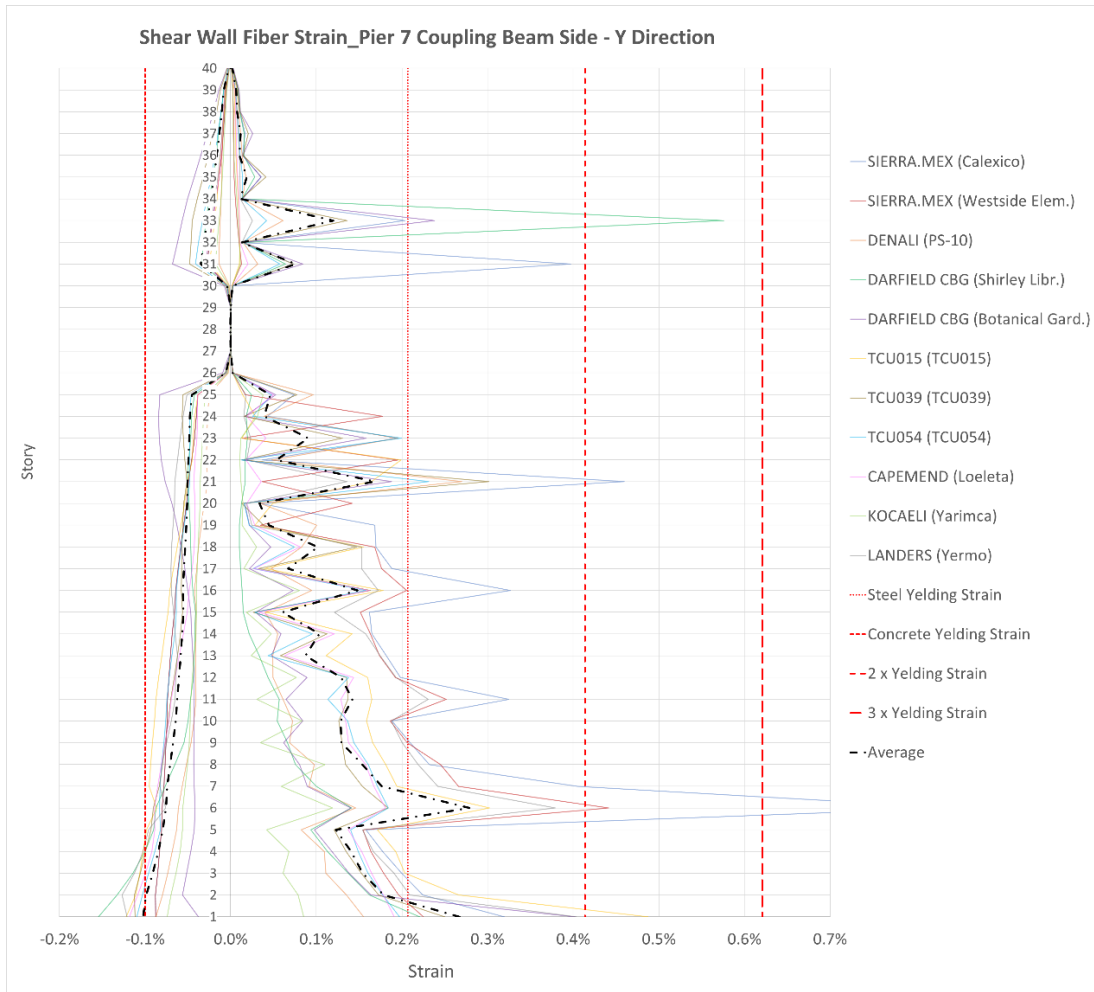


Figure 4.72 Option D_MCE (R=3) – NLRHA Y Direction Pier 7 Coupling Beam Side Fiber Strain

4.3.1.6 Option D – Flexure Demands

The NLRHA spaghetti and their corresponding Flexure Demands couples are shown below. The M-N plots are built following the same procedure proposed in Chapter 3.3.4.

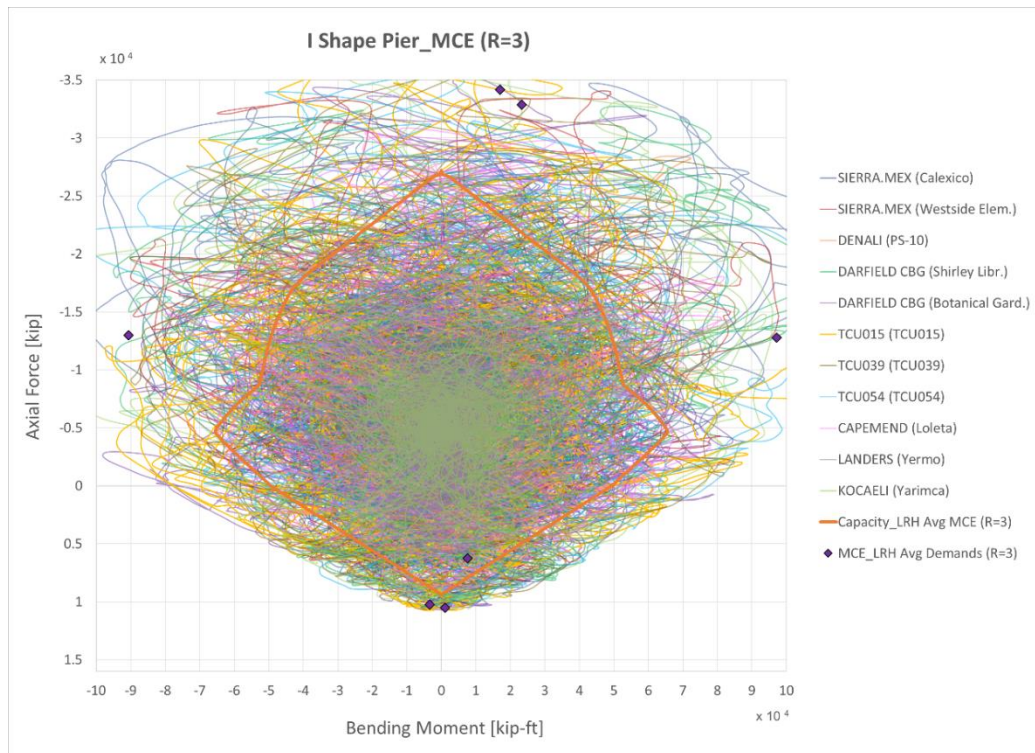


Figure 4.73 Option D_MCE (R=3) – NLRHA Stand-Alone Shear Wall Flexure Demands 1

For convenience all the spaghetti will be represented in a single orange color in order to easier be compared with the other results of Option D in the final plots, Figure 4.74.

Chapter 4

Nonlinear Verification Analysis

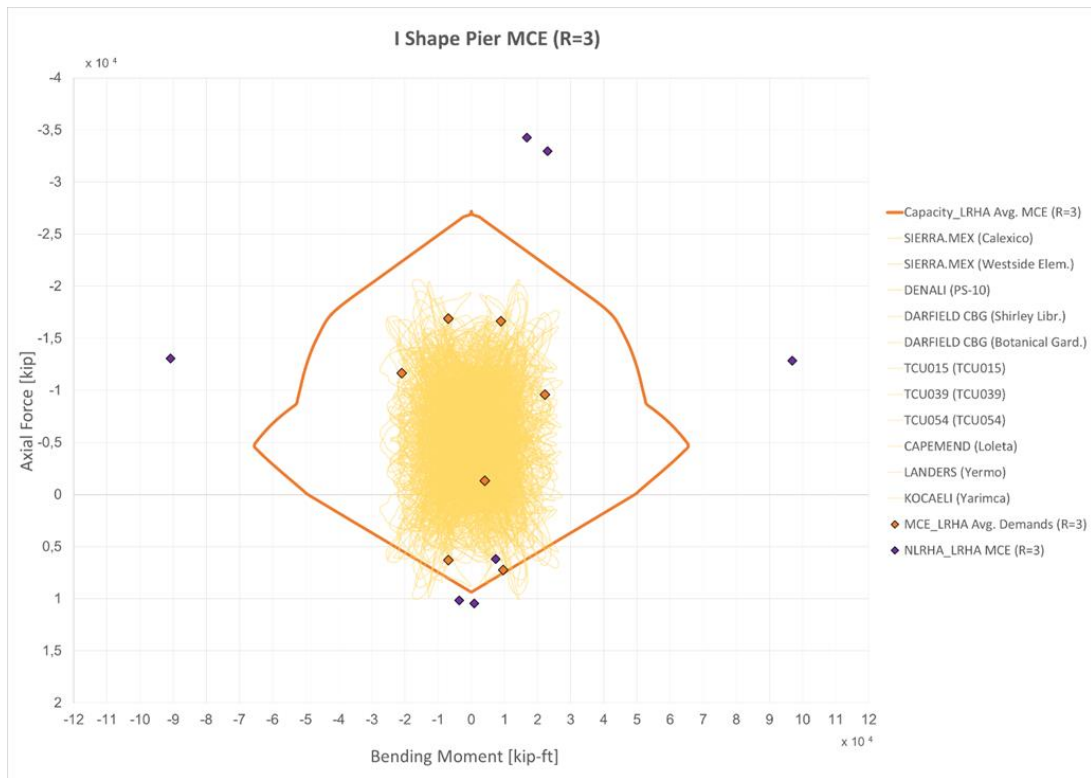


Figure 4.74 Option D_MCE (R=3) – NLRHA Stand-Alone Shear Wall Flexure Demands 2

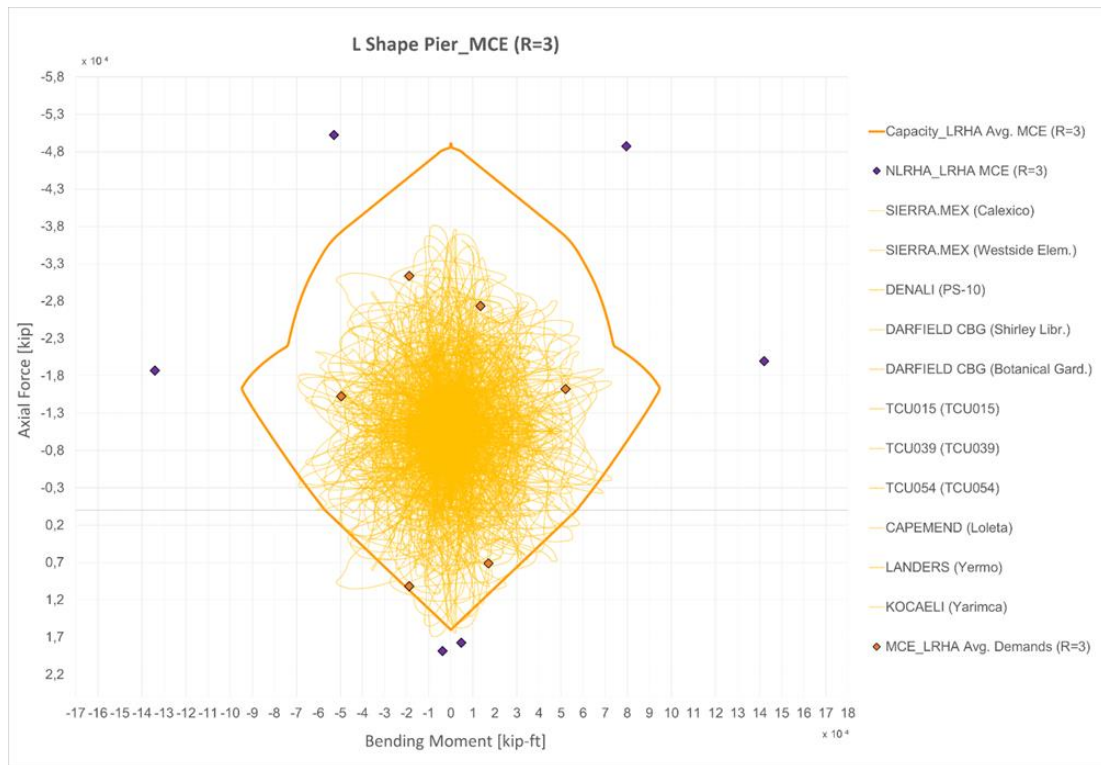


Figure 4.75 Option D_MCE (R=3) – NLRHA Compound Shear Wall Flexure Demands

CHAPTER 5

RESULTS COMPARISON

The chapter is dedicated to the comparison of all the results obtained, in order to show both which Design Procedure best predicts the Nonlinear Behavior and which one of them is able to provide the most ductility with the least amount of rebar. For this purpose, all the previous charts are summarized and analyzed together.

5.1 Prediction of Nonlinear Behavior: Story Drift

As already mentioned before, in each story the code requires that the mean of the absolute values of the maximum story drift ratios from the suite of 11 time history analysis shall not exceed 0.03. Moreover, in each story the maximum story drift ratio in any analysis shall not exceed 0.045.

5.1.1 Story Drift - X Direction

The following plots show the maximum story drift in X direction of the Nonlinear Response History Analysis compared to the relative Response Spectrum Analysis maximum story drift. It is worth noticing that for Option A_MCE (R=7.5) the RSA underestimates the maximum story drift ratio cause the NLRHA results are higher, although still below the maximum limit imposed by the code, *Figure 5.1*.

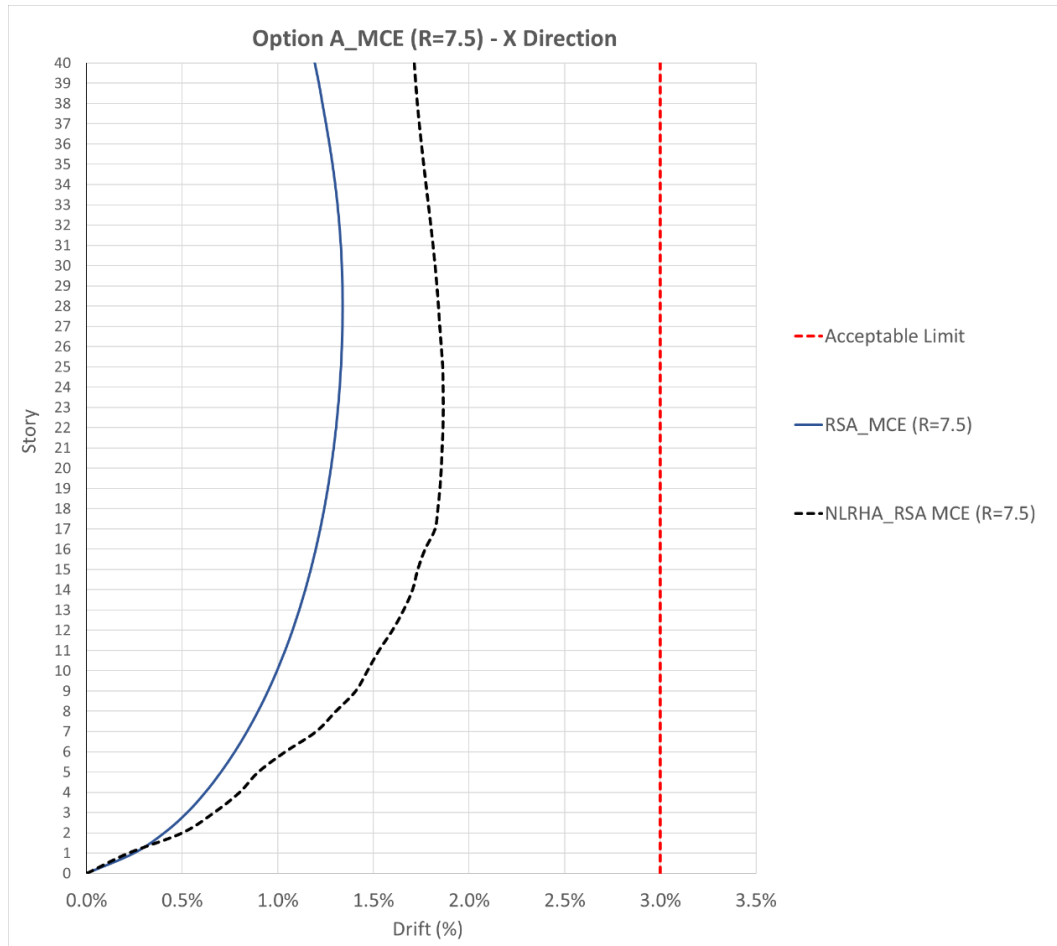


Figure 5.1 Option A_MCE (R=7.5) – X Direction Story Drift Comparison

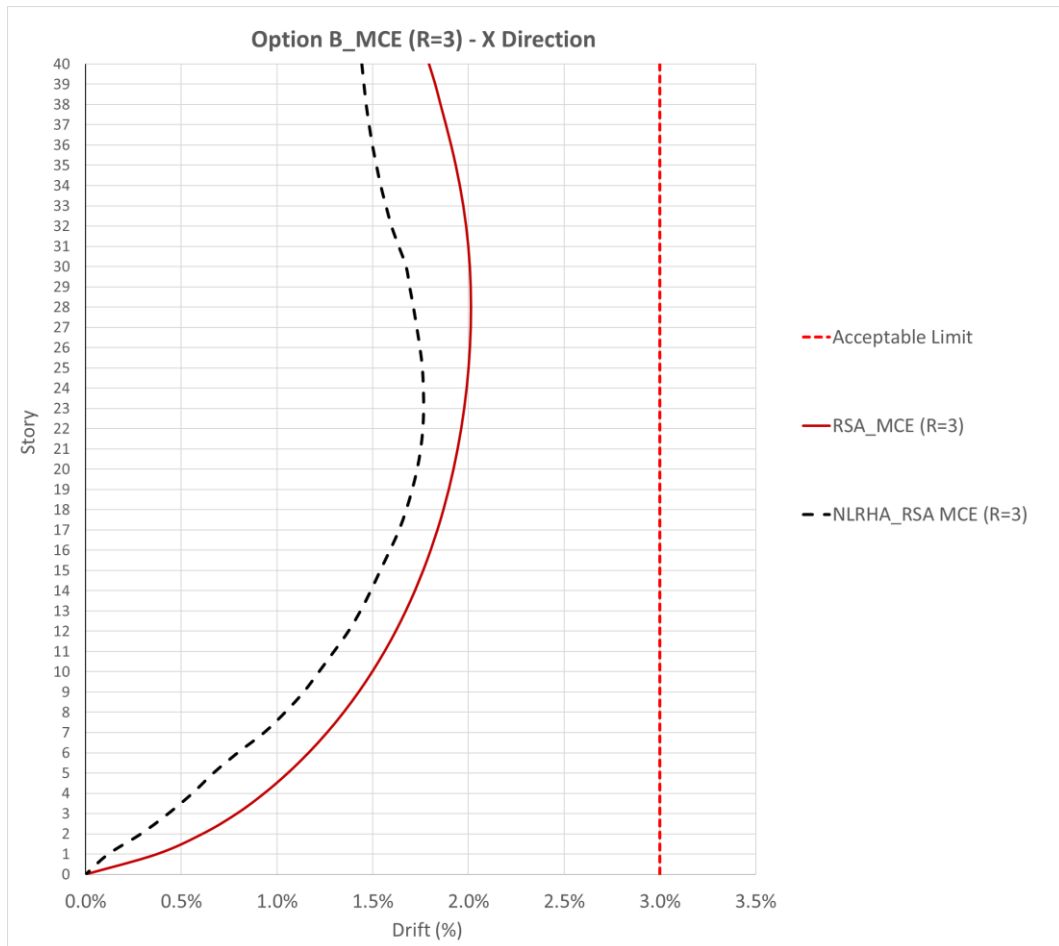


Figure 5.2 Option B_MCE (R=3) - X Direction Story Drift Comparison

Regarding the Option B_MCE (R=3) the exact opposite is noticed. The RSA overestimates the maximum story drift ratio over the NLRHA results, *Figure 5.2*.

As it is shown in *Figure 5.3*, the results of Option D_MCE (R=3) are the best of the three options. The RSA maximum story drift profile is quite similar to the NLRHA profile, presenting a good prediction of nonlinear drift.

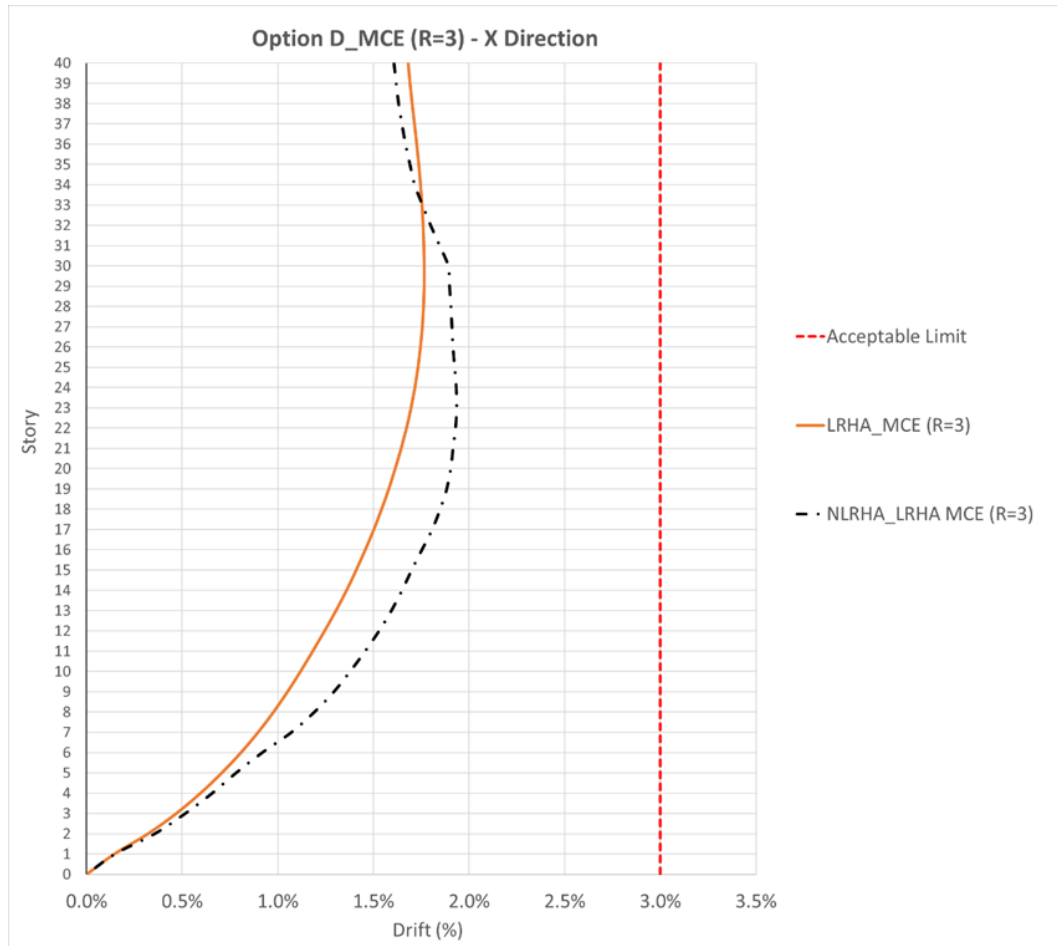


Figure 5.3 Option D_MCE (R=3) - X Direction Story Drift Comparison

5.1.2 Story Drift - Y Direction

As it is possible to see, along Y direction the above considerations are even more confirmed. The linear RSA which predicts in the best way the nonlinear behavior, shown by NLRHA, is clearly Option D_MCE (R=3): in this case, *Figure 5.6*, the RSA maximum story drift profile and the NLRHA profile are very close, even coincident up to almost story 20.

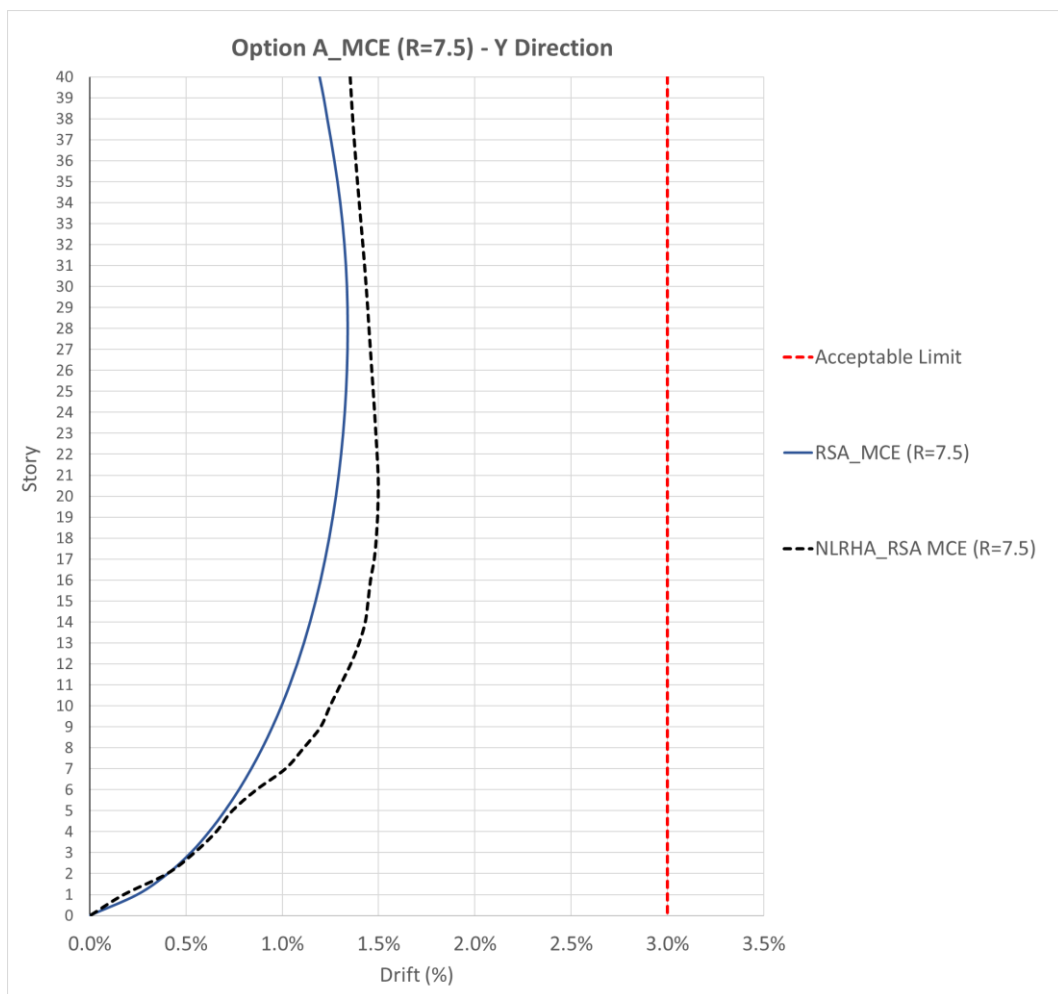


Figure 5.4 Option A_MCE (R=7.5) - Y Direction Story Drift Comparison

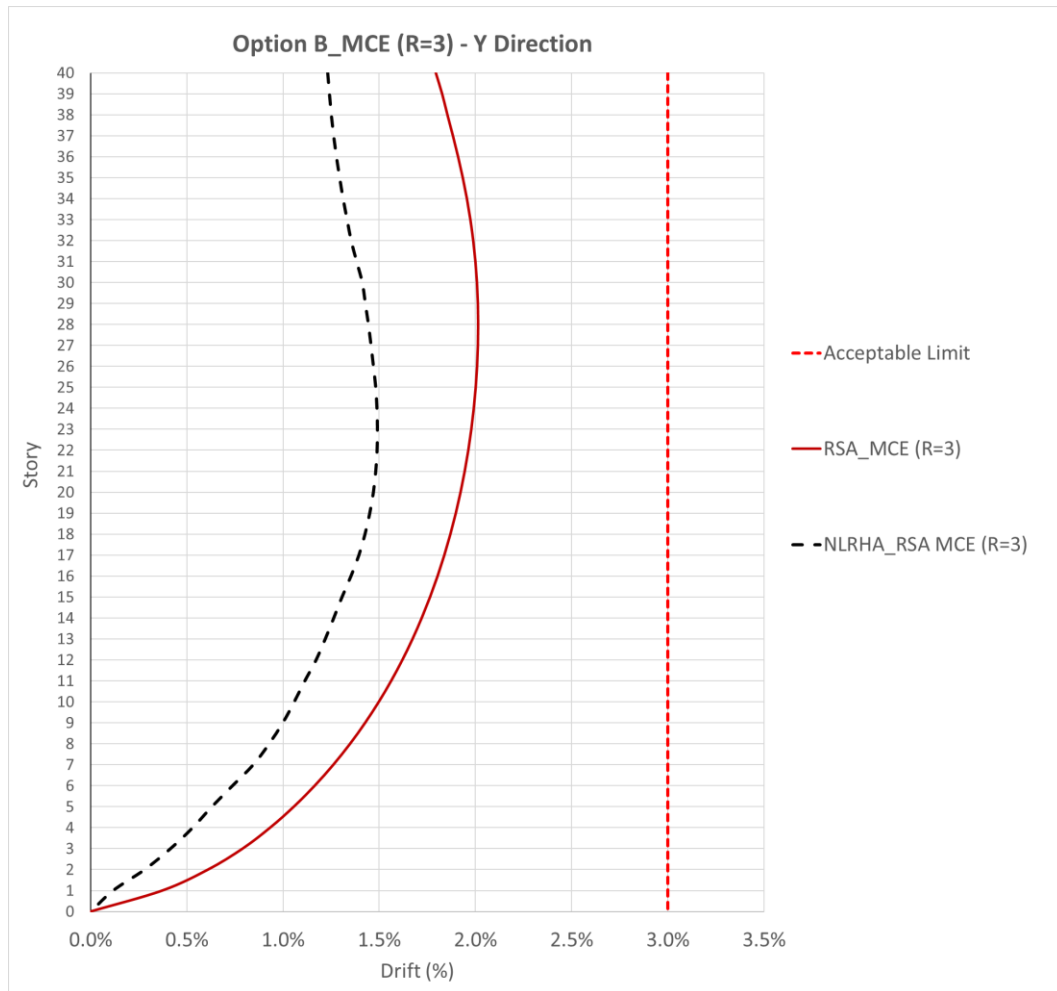


Figure 5.5 Option B_MCE (R=3) - Y Direction Story Drift Comparison

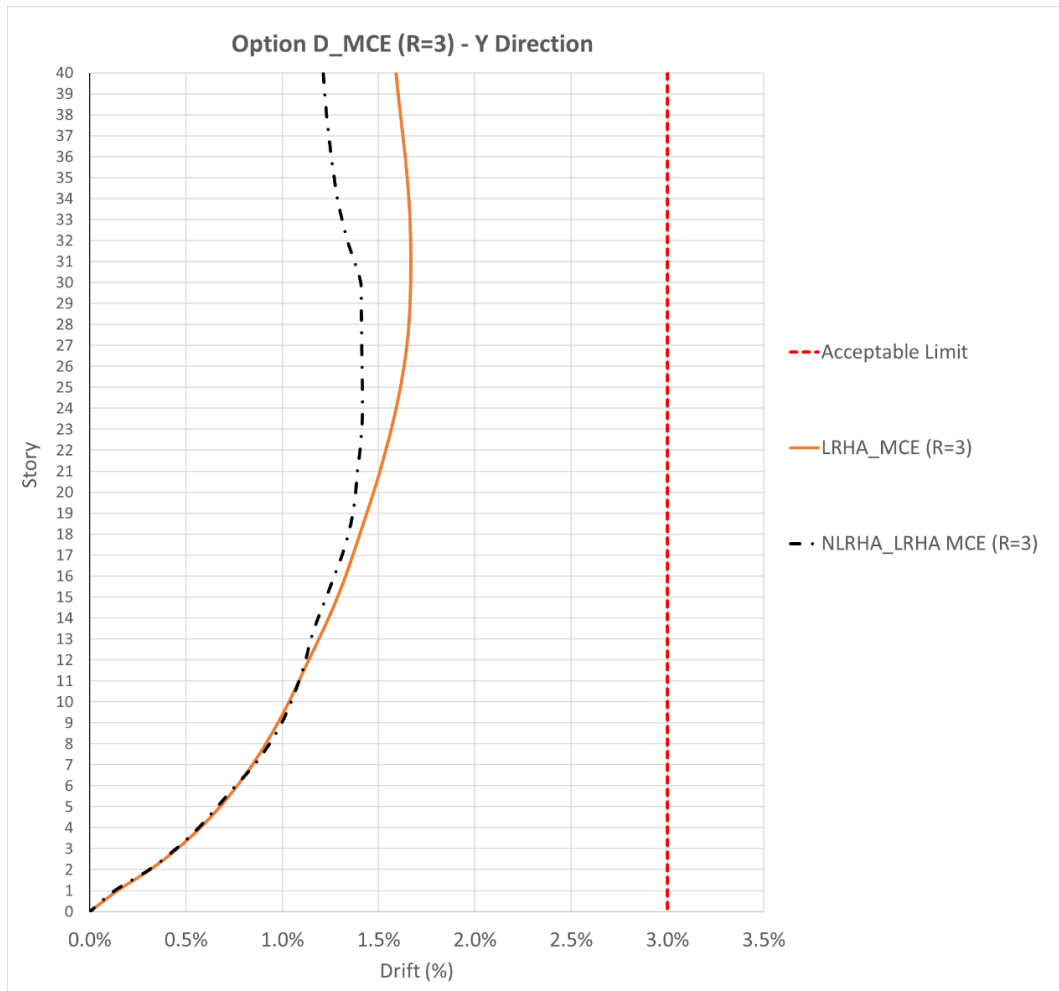


Figure 5.6 Option D_MCE (R=3) - Y Direction Story Drift Comparison

5.2 Prediction of Nonlinear Behavior: Story Shear

Below is a summary of story core shear stresses as a function of $\sqrt{f_c}c_{exp}$, considering only walls with the plane parallel to the direction of the shear forces to be resistant. ACI 18.10.4.4 requires all individual piers be less than $10\sqrt{f_c}c_{exp}$ and a group of piers sharing a common lateral force to be less than $8\sqrt{f_c}c_{exp}$. This last case is the more restricted for the prototype model referred to in the present research.

All the results show that the abovementioned limit of $8\sqrt{f_c}c_{exp}$ is never exceeded. Since further investigations are conducted with NLRHA and shown to be satisfy these criteria, it is determined to be acceptable.

5.2.1 Story Shear - X Direction

As already mentioned, along X direction the walls able to be resistant are shown in the following *Figure 5.7*:

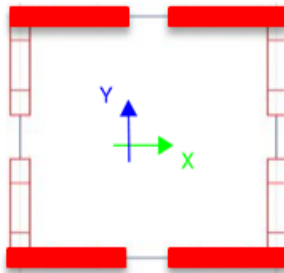


Figure 5.7 X Direction Shear Resistant Core

The plots of the compared story shear results between RSAs and the respective NLRHAs are shown below for the three studied Options.

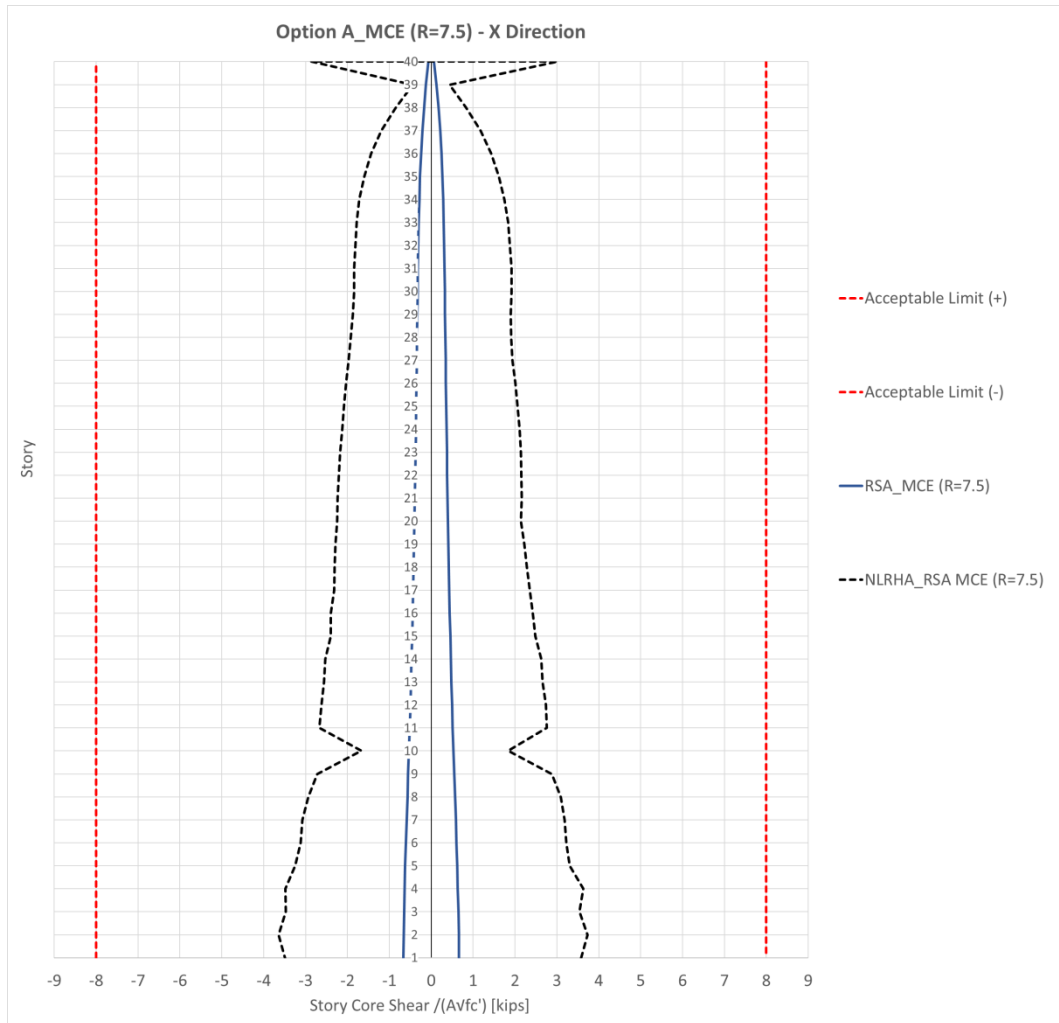


Figure 5.8 Option A_MCE (R=7.5) – X Direction Story Shear Comparison

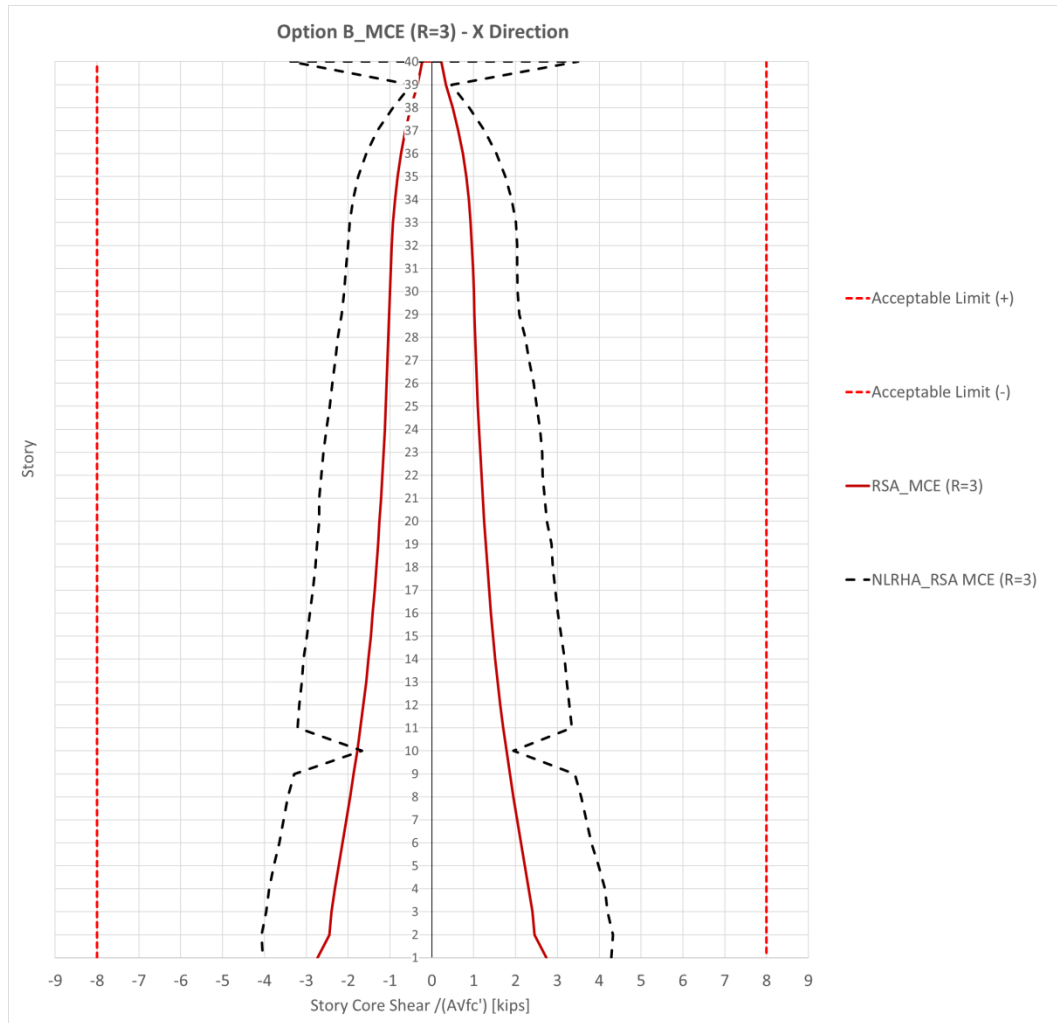


Figure 5.9 Option B_MCE (R=3) - X Direction Story Shear Comparison

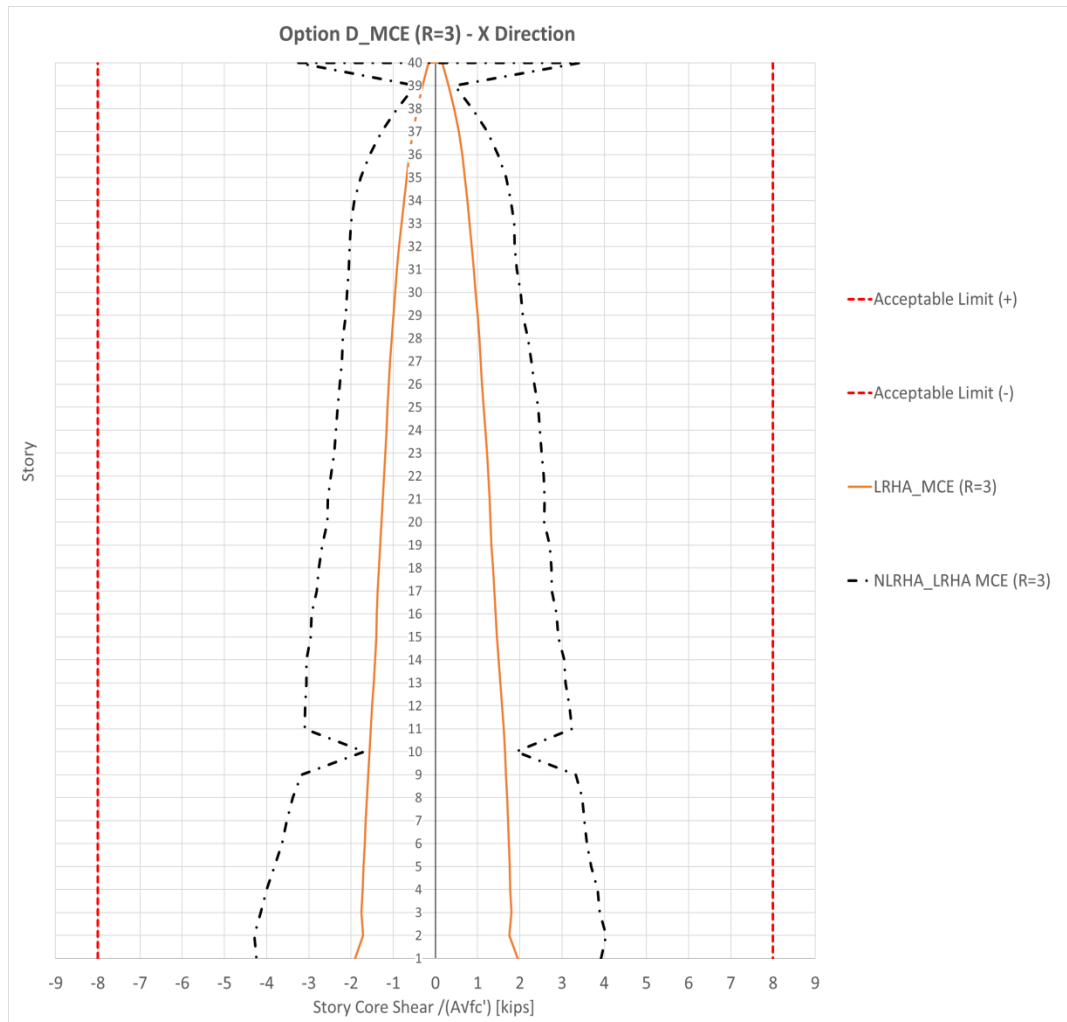


Figure 5.10 Option D_MCE (R=3) - X Direction Story Shear Comparison

As it is simple to observe, in all the three cases the nonlinear story shears are higher than the linear ones and this is a confirmation of the literature.

5.2.2 Story Shear - Y Direction

As done for the X direction, even for the Y direction the walls able to be resistant are shown in the following *Figure 5.11*:

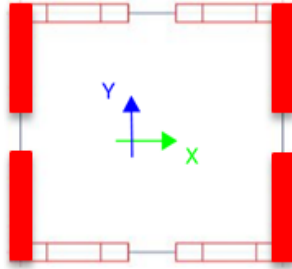


Figure 5.11 Y Direction Shear Resistant Core

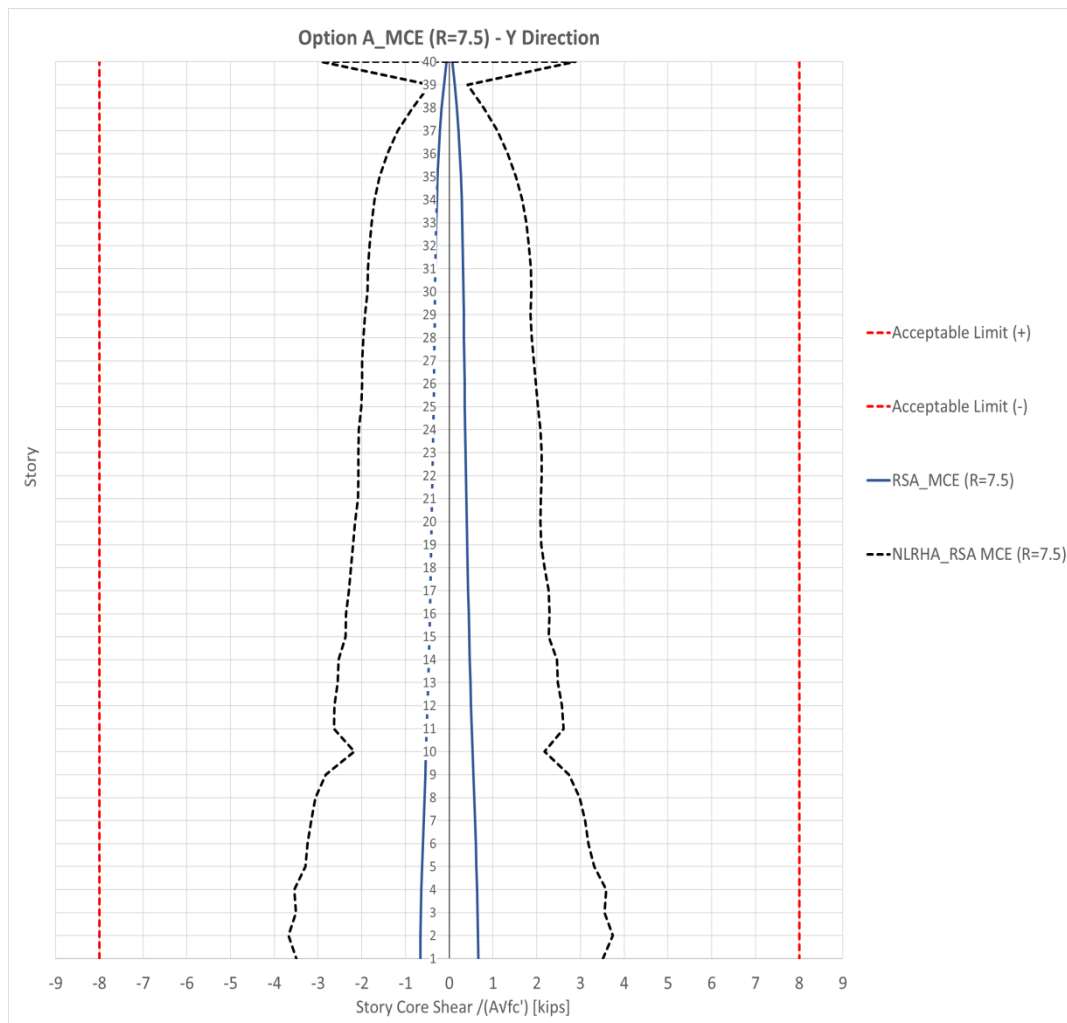


Figure 5.12 Option A_MCE (R=7.5) - Y Direction Story Shear Comparison

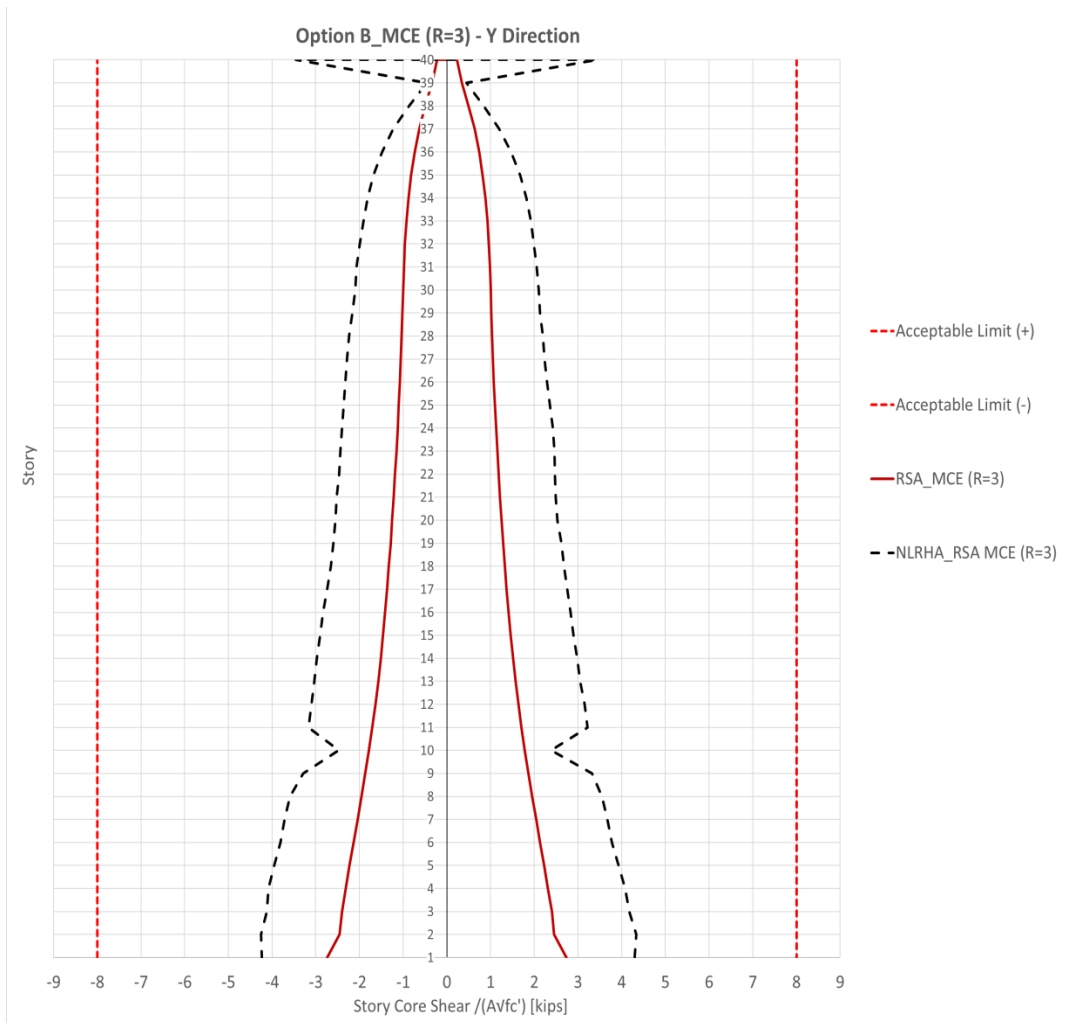


Figure 5.13 Option B_MCE (R=3) - Y Direction Story Shear Comparison

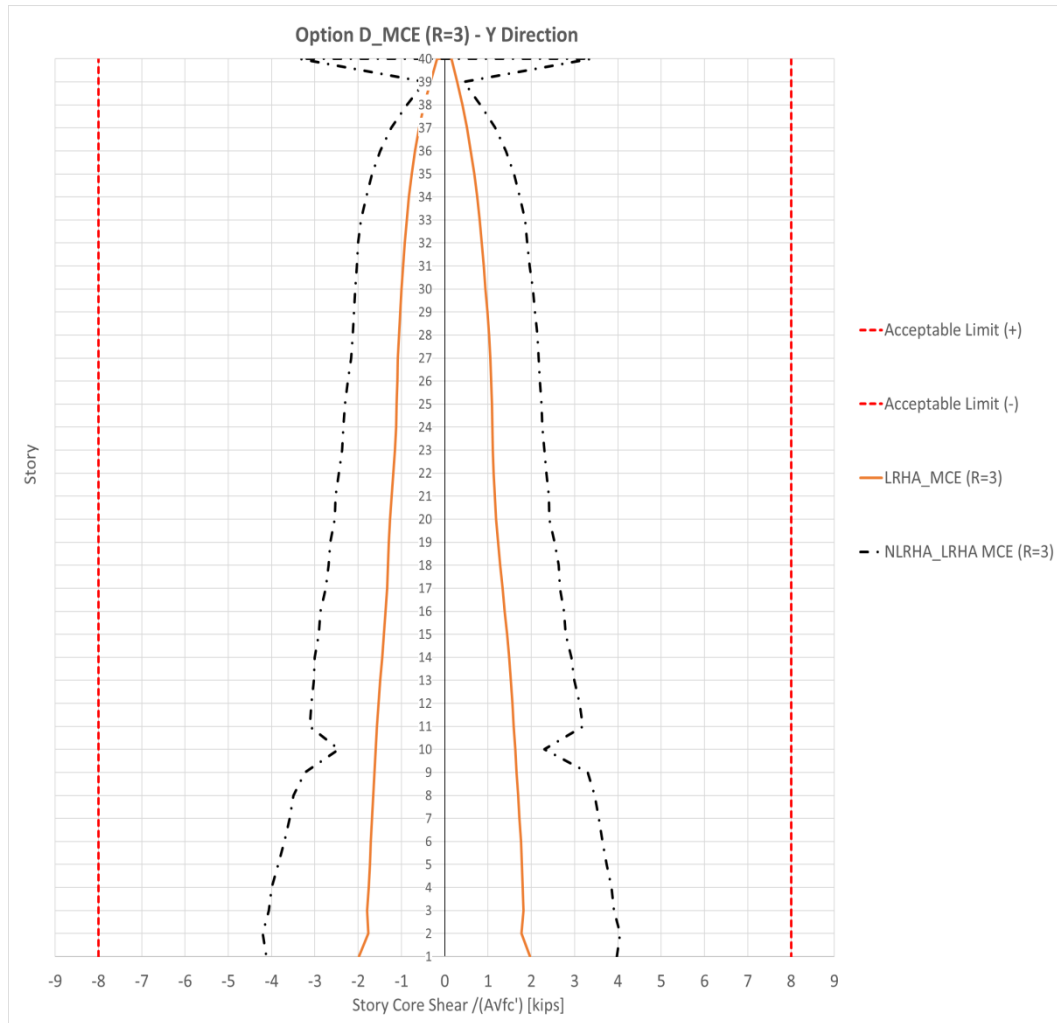


Figure 5.14 Option D_MCE (R=3) - Y Direction Story Shear Comparison

It is obvious that the same thing applies to the Y direction as to the X direction.

5.3 Coupling Beams Plastic Rotation Comparison

The plastic rotation limit is 0.05 radians for diagonally reinforced link beams and 0.04 for conventionally reinforced link beams where span to depth ratio is greater than or equal to 4.0. As already described in the chapter 4.1.2, the prototype model object of the present research has diagonally reinforced link beams.

5.3.1 Coupling Beams Plastic Rotation - X Direction

Along X direction the results of only one plastic hinge of the Link Beam 4 are shown cause the most significant. The location of the mentioned plastic hinge is shown in blue in the following *Figure 5.15*:

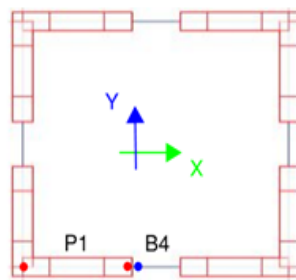


Figure 5.15 Coupling Beam 4 Plastic Hinges Position

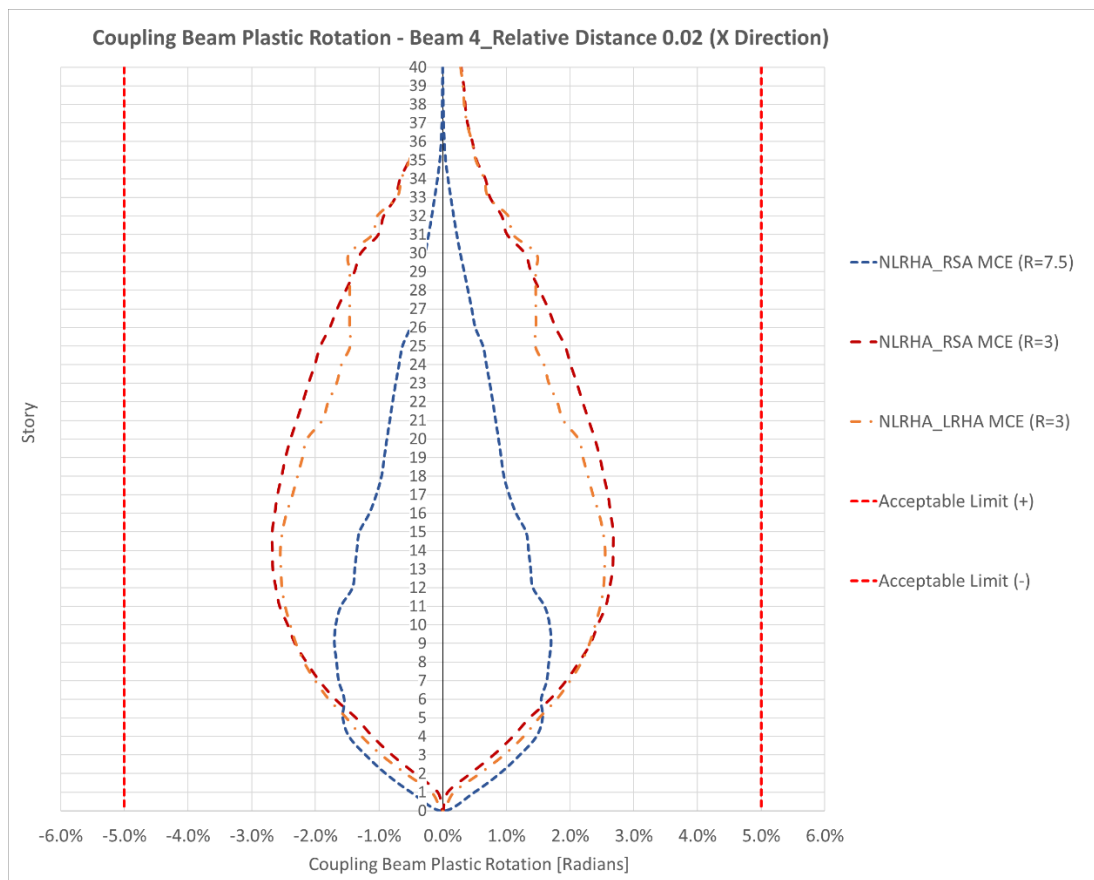


Figure 5.16 X Direction Link Beam 4 Plastic Hinge Rotation Comparison

As is possible to see, the NLRHA with a bigger R factor allows much less plastic rotation of link beams compared to the NLRHAs with a smaller R factor. Option A_MCE (R=7.5) therefore provides less energy dissipation in link beams.

5.3.2 Coupling Beams Plastic Rotation - Y Direction

Similar to the previous case, along Y direction the results of only one plastic hinge of the Link Beam 3 are shown cause the most significant. The location of the mentioned plastic hinge is shown in blue in the following *Figure 5.17*:

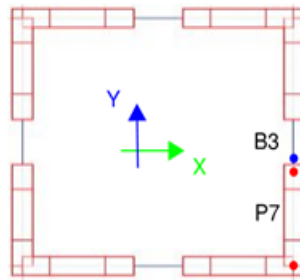


Figure 5.17 Coupling Beam 3 Plastic Hinges Position

As visibly shown in Figure 5.18, even along Y direction Option A_MCE (R=7.5) provides less ductility in link beams than Option B and Option D, which are related to a smaller R factor (R=3).

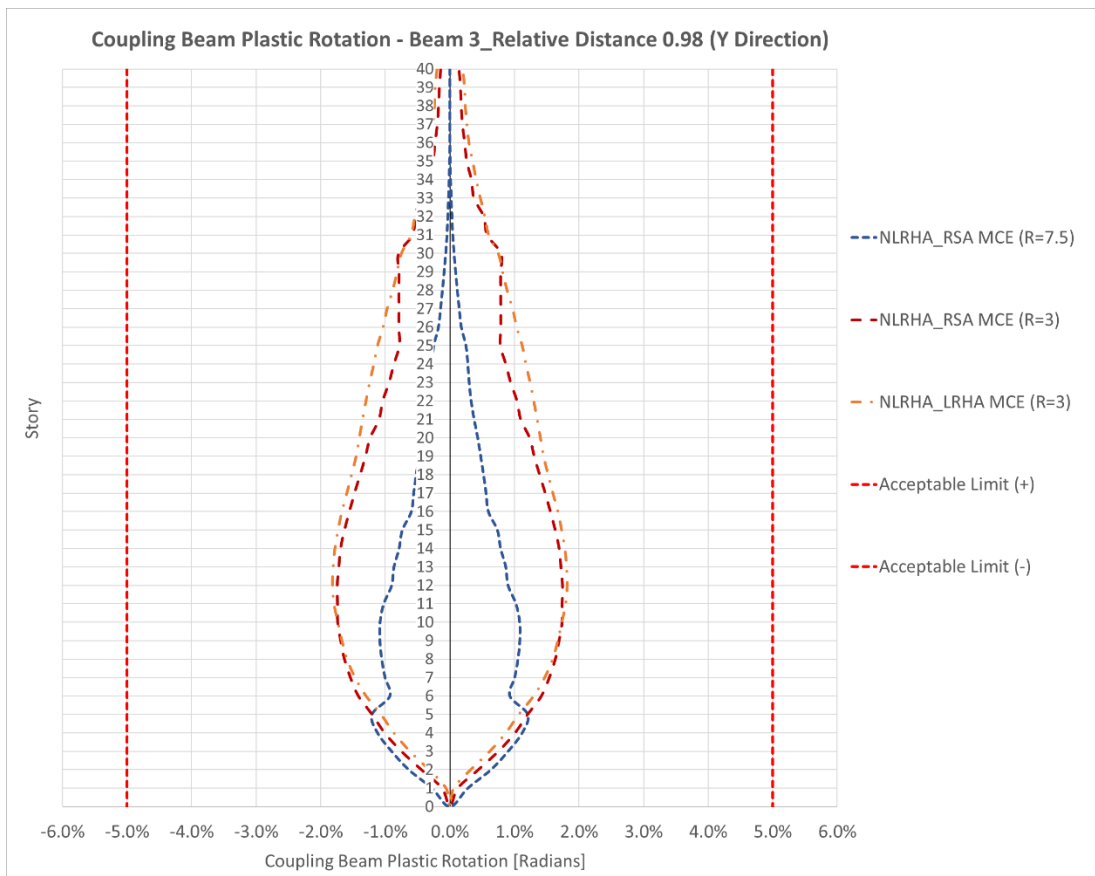


Figure 5.18 Y Direction Link Beam 3 Plastic Hinge Rotation Comparison

5.4 Shear Walls Fibers Strain Comparison

The maximum compressive strain is limited to 0.012 in confined concrete and to 0.0015 in unconfined concrete. The unconfined concrete limit is obtained by dividing the original 0.003 by a safety coefficient of 2 and further dividing it by a safety coefficient of 3 according to Jack Mohele and M. J. N. Priestley. The effective maximum compressive limit of unconfined concrete is therefore 0.0005, approximated then to 0.001. The maximum longitudinal reinforcement strain is limited to 0.05 in tension and 0.012 in compression to avoid rebar fracture and buckling respectively. Yield Strain is 0.0024 (or 0.24%) in tension.

5.4.1 Shear Walls Fibers Strain – X Direction

Along X direction the results of only two fibers are shown, particularly the two outermost edge fibers of the analyzed pier, cause the most significant. In X direction are displayed the plots of Pier 1 Boundary Zones. The location of the two mentioned fibers are shown in red in the following *Figure 5.19*:

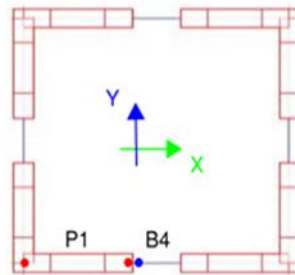


Figure 5.19 Pier 1 Fibers Position

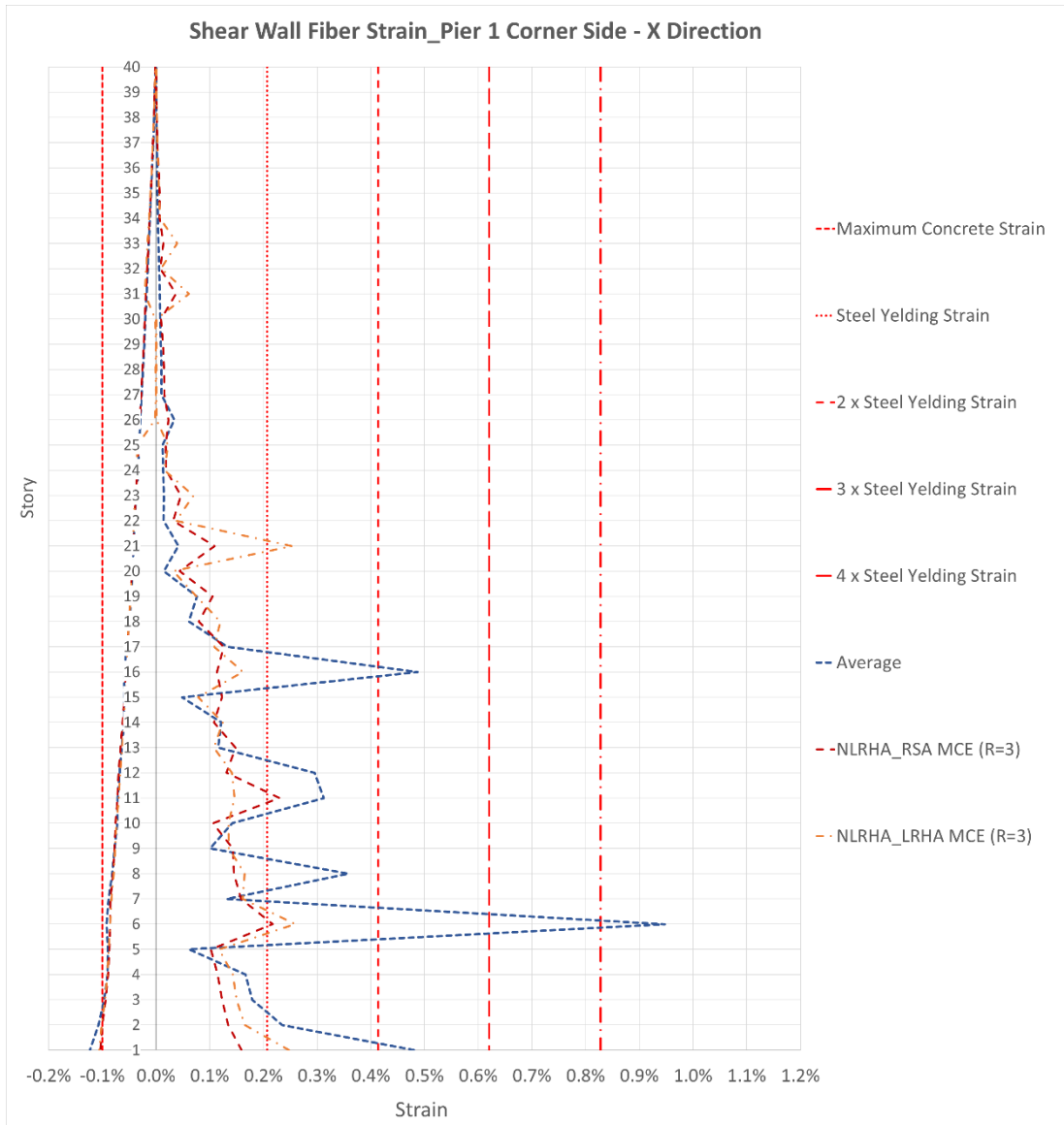


Figure 5.20 X Direction Pier 1 Corner Side Fiber Strain Comparison

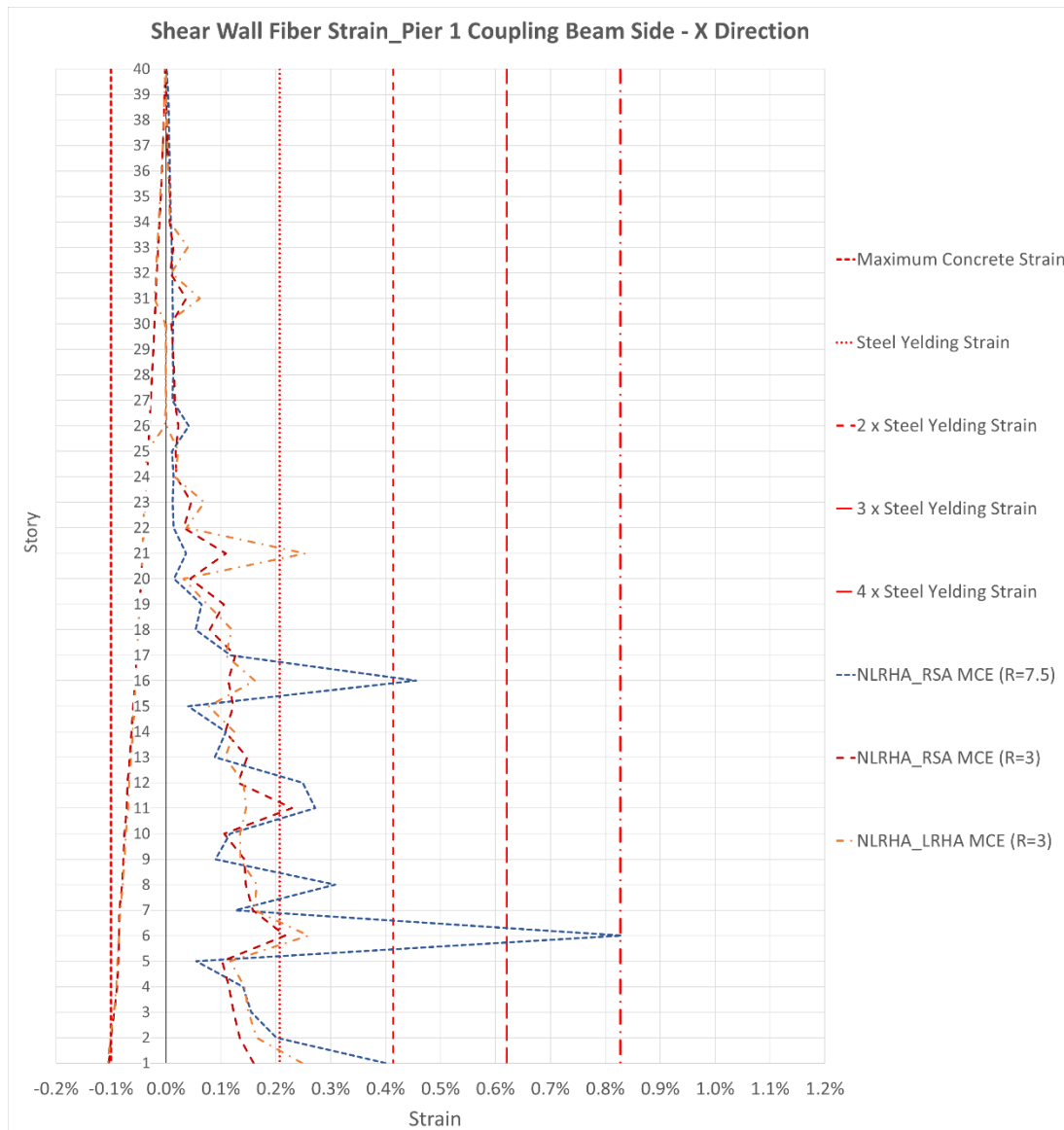


Figure 5.21 X Direction Pier 1 Coupling Beam Side Fiber Strain Comparison

As it is possible to see, there is no energy dissipation in compression and the maximum compressive strain limit of unconfined concrete is barely reached.

Regarding the tensile strains, contrary to what has been seen for the link beams plastic rotation in chapter 5.3, Option A_MCE (R=7.5) provides more ductility in shear walls than Option B and Option D, both related to an R factor equal to 3.

5.4.2 Shear Walls Fibers Strain – Y Direction

Along Y direction the results of only two fibers are shown, particularly the two outermost edge fibers of the analyzed pier, cause the most significant. In Y direction are displayed the plots of Pier 7 Boundary Zones. The location of the two mentioned fibers are shown in red in the following *Figure 5.19*:

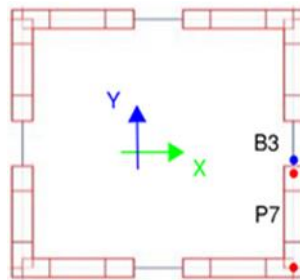


Figure 5.22 Pier 7 Fibers Position

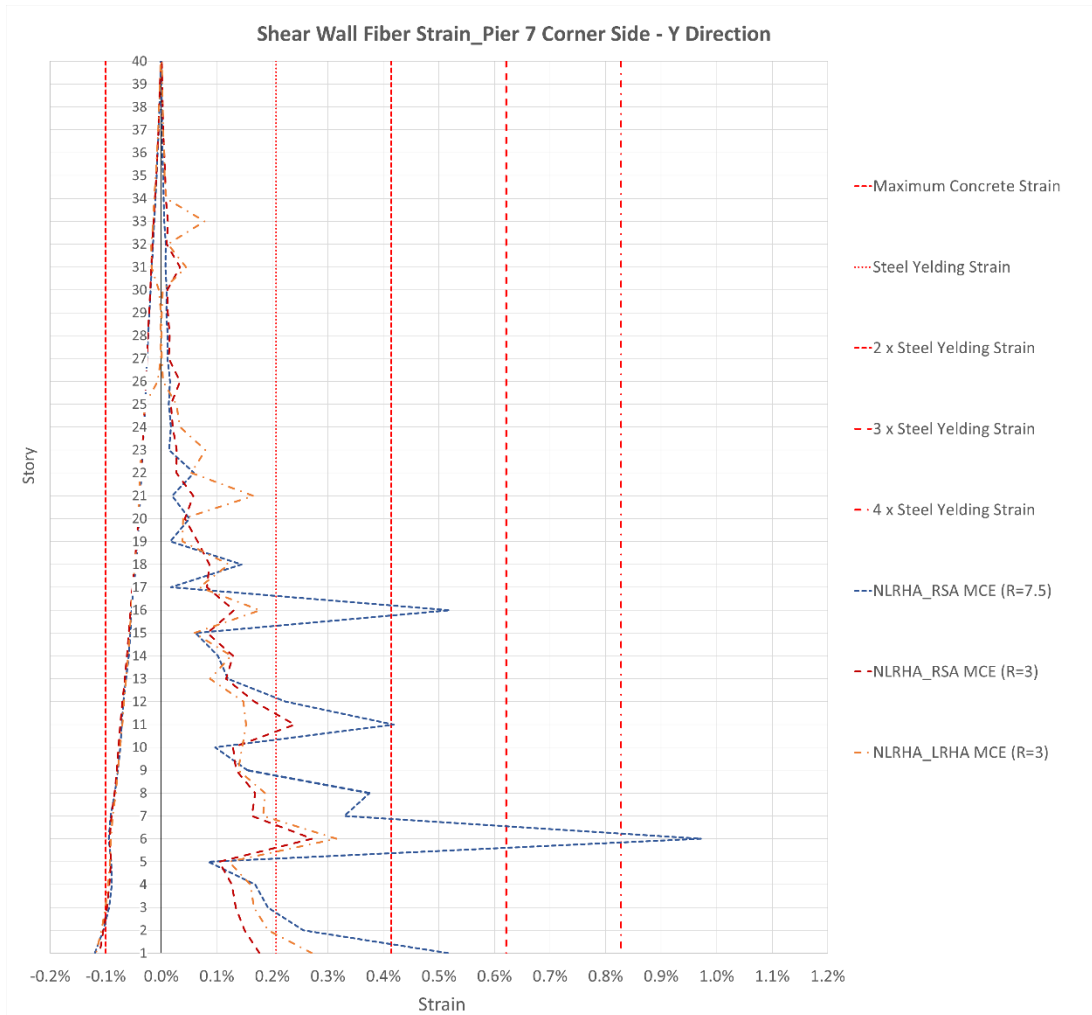


Figure 5.23 Y Direction Pier 7 Corner Side Fiber Strain Comparison

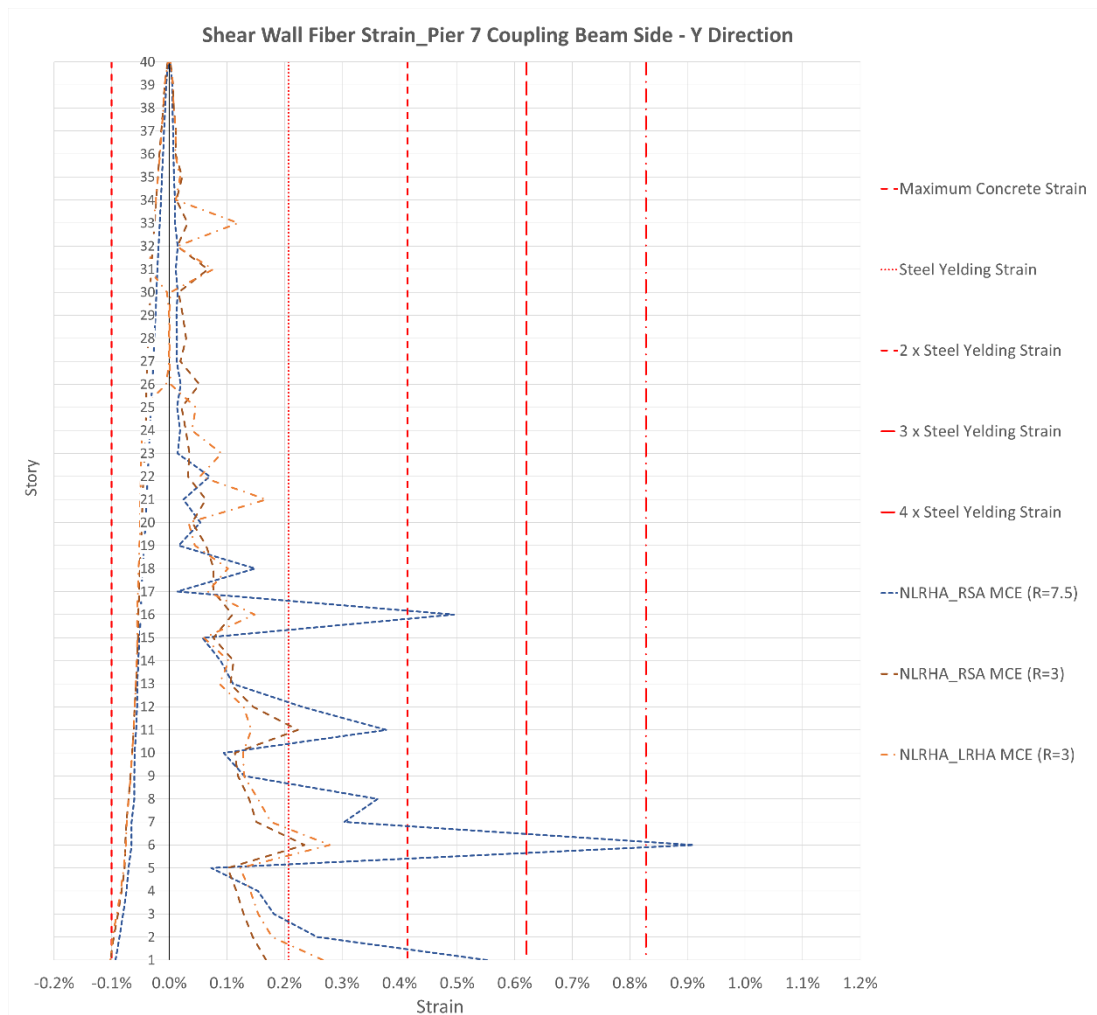


Figure 5.24 Y Direction Pier 7 Coupling Beam Fiber Strain Comparison

As visibly shown in *Figure 5.24*, even along Y direction Option A_MCE (R=7.5) provides more ductility in shear walls than Option B and Option D, which are related to a smaller R factor (R=3).

5.5 Prediction of Nonlinear Behavior: Flexure Demands

The following plots represent the analysis Flexure Demands and the N-M Capacity Curves of all the analyses previously conducted. The demands derived by RSAs are represented by dots whereas the NLRHAs demands are shown by spaghetti and by their dots obtained as explained in chapter 3.3.4.

As already explained in the previous chapters, for this research purpose the plots are all referred to the base section of the Piers, the Story 1 bottom sections, cause the most loaded of the building. Axial-Moment interaction design of all piers is conducted with the software S-Concrete which conducted ACI 318-11 chapter 21 design checks using expected material strengths.

The following plots show how it is possible to extract flexure demands in order to design shear walls providing a good dissipative behavior of tall buildings in high-seismic regions without being too conservative.

5.5.1 Stand-Alone Shear Wall (I Shape)

In the present chapter are shown all the flexure demands related to the Stand-Alone Shear Wall with a rectangular shape and not seen as compound with other walls. The Axial Force-Bending Moment couples are summarized in two plots, one related to MCE (R=7.5) designs and one related to MCE (R=3) designs.

5.5.1.1 MCE (R=7.5)

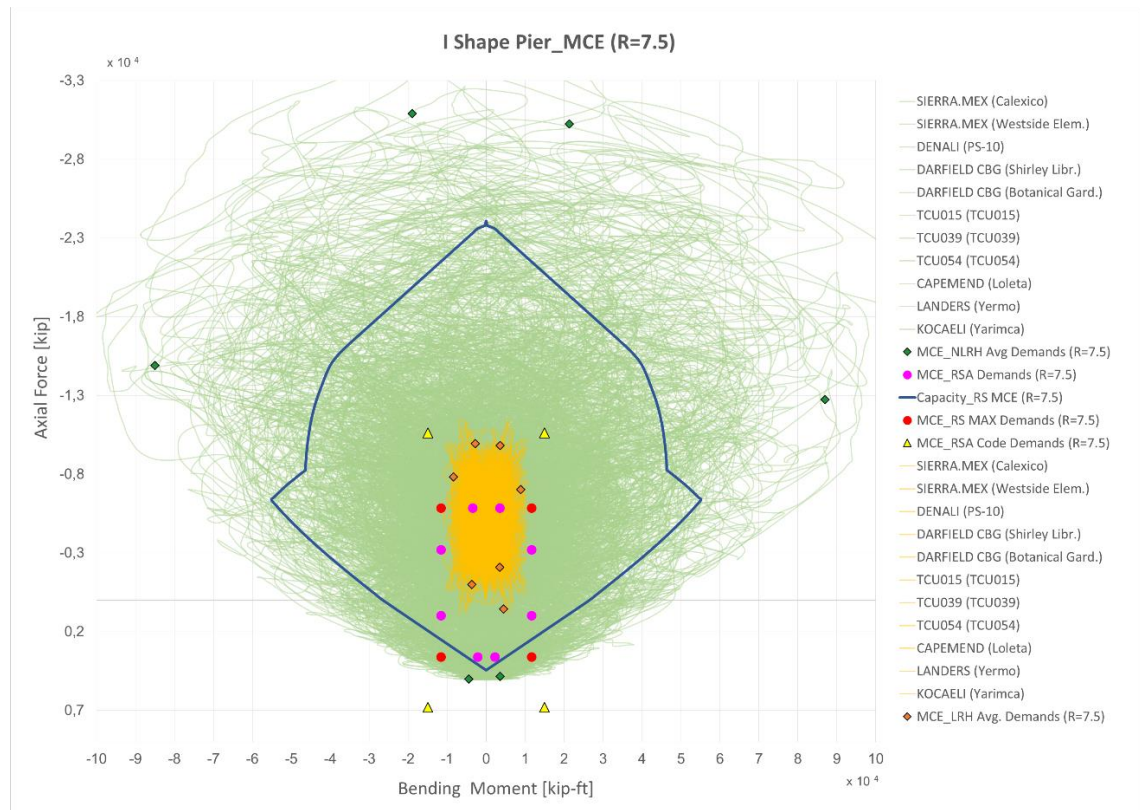


Figure 5.25 Stand-Alone Shear Wall Flexure Demands Plot - MCE (R=7.5)

In the MCE (R=7.5) plot, *Figure 5.25*, are shown:

- The Traditional Code Response Spectrum Design Methodology Flexure Demands (yellow triangles) of chapter 3.2.1;
- The Maximum Flexure Demands (red dots) of the Response Spectrum Design Methodology proposed in chapter 3.3.2;
- The Option A_MCE (R=7.5) Flexure Demands (magenta dots) of the Proposed Response Spectrum Design Methodology of chapter 3.3.2;
- The Capacity Curve (blue line) related to the Option A_MCE (R=7.5) Proposed Design determined in chapter 3.3.2;
- The Option C_MCE (R=7.5) spaghetti with their relative average Flexure Demands (orange rhombs) of the Proposed Linear Response History Design Methodology of chapter 3.3.5;

- The Nonlinear Response History Spaghetti with their relative average Flexure Demands (green rhombs) represented the Nonlinear Behavior, resulted from chapter 4.2.1.

As it is easy to notice, the Traditional Code Design (yellow triangles) is too conservative and the shear wall section turns out so over reinforced and does not provide a ductile behavior. The Maximum Flexure Demands (red dots) extracted by the proposed RSA are also too conservative even if needing less section rebar. On the other side, the Option C_MCE (R=7.5) of LRHA (orange rhombs) leads to a too weakly reinforced section and because of this not considered as a Proposed Design Methodology. The Option A_MCE (R=7.5) Flexure Demands (magenta dots) extracted with the new Design Methodology Proposed in chapter 3.2.2. gives the best solution. Based on this Design Methodology the section results less reinforced compared to the other all traditional Design Methodologies and, consequently, able to provide a good amount of ductility as the two Tension-Bending Moment couples of NLRHA Flexure Demands (green rhombs) show. In fact, looking at the positive Axial Force part of the plot, Figure 5.25, it is possible to see that the spaghetti are out of the Capacity Curve related to the Option A_MCE (R=7.5) design: this behavior means that the rebars are reaching the yielding strain and that they are acting with a nonlinear behavior able to provide energy dissipation.

5.5.1.2 MCE (R=3)

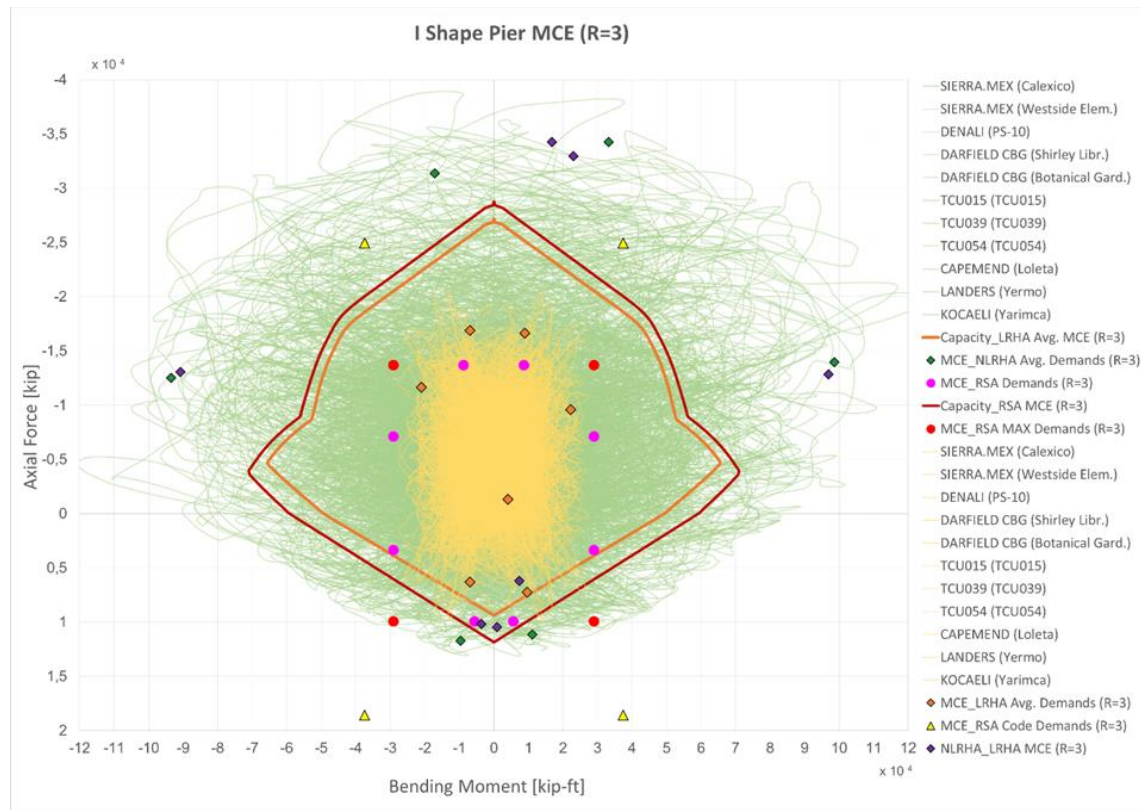


Figure 5.26 Stand-Alone Shear Wall Flexure Demands Plot - MCE (R=3)

In the MCE (R=3) plot, *Figure 5.26*, are shown:

- The Traditional Code Response Spectrum Design Methodology Flexure Demands (yellow triangles) of chapter 3.2.1;
- The Maximum Flexure Demands (red dots) of the Response Spectrum Design Methodology proposed in chapter 3.3.3;
- The Option B_MCE (R=3) Flexure Demands (magenta dots) of the Proposed Response Spectrum Design Methodology of chapter 3.3.3;
- The Capacity Curve (red line) related to the Option B_MCE (R=3) Proposed Design determined in chapter 3.3.3;
- The Option D_MCE (R=3) spaghetti with their relative average Flexure Demands (orange rhombs) of the Proposed Linear Response History Design Methodology of chapter 3.3.6;

- The Capacity Curve (orange line) related to the Option D_MCE (R=3) Proposed Design determined in chapter 3.3.6;
- The Nonlinear Response History Spaghetti with their relative average Flexure Demands (green rhombs) represented the Nonlinear Behavior, resulted from chapter 4.2.2;
- The Nonlinear Response History Spaghetti with their relative average Flexure Demands (purple rhombs) represented the Nonlinear Behavior, resulted from chapter 4.3.1.

The plot in *Figure 5.26* shows that the above considerations are also valid in this case, and even more marked. The efficiency of the Proposed Design Methodology, the Option B_MCE (R=3) in this case, compared to the other all Traditional Methodologies is even more evident if the R factor is equal to 3.

Regarding the Option D_MCE (R=3), it is possible to appreciate that if the section had been designed with these Flexure Demands it would have been even slightly less reinforced section, as already shown in the previous chapters, cause the orange relative Capacity Curve is smaller than the red one, *Figure 5.26*. Looking at the Tension-Bending Moment couples of NLRHA Flexure Demands (purple rhombs), they are also out of the abovementioned Capacity Curve due to their relative spaghetti (chapter 4.3.1), even if not so much as the Option B does.

Consequently, Option B is definitely the best Proposed Design Methodology to extract Flexure Demands to guarantee a considerable reduction in the quantity of section rebar and at the same time have a good ductility.

5.5.2 Composite Shear Wall (L Shape)

The present chapter illustrates the differences in the extraction of Flexure Demands between considering the L Shear Walls, principal purpose of this research, as separated Stand-Alone Walls or as Compound.

The Axial Force-Bending Moment couples related to L-Shape Shear Wall designs are summarized in two plots, as done in chapter 5.5.1, one related to MCE (R=7.5) and one related to MCE (R=3) designs.

5.5.2.1 MCE (R=7.5)

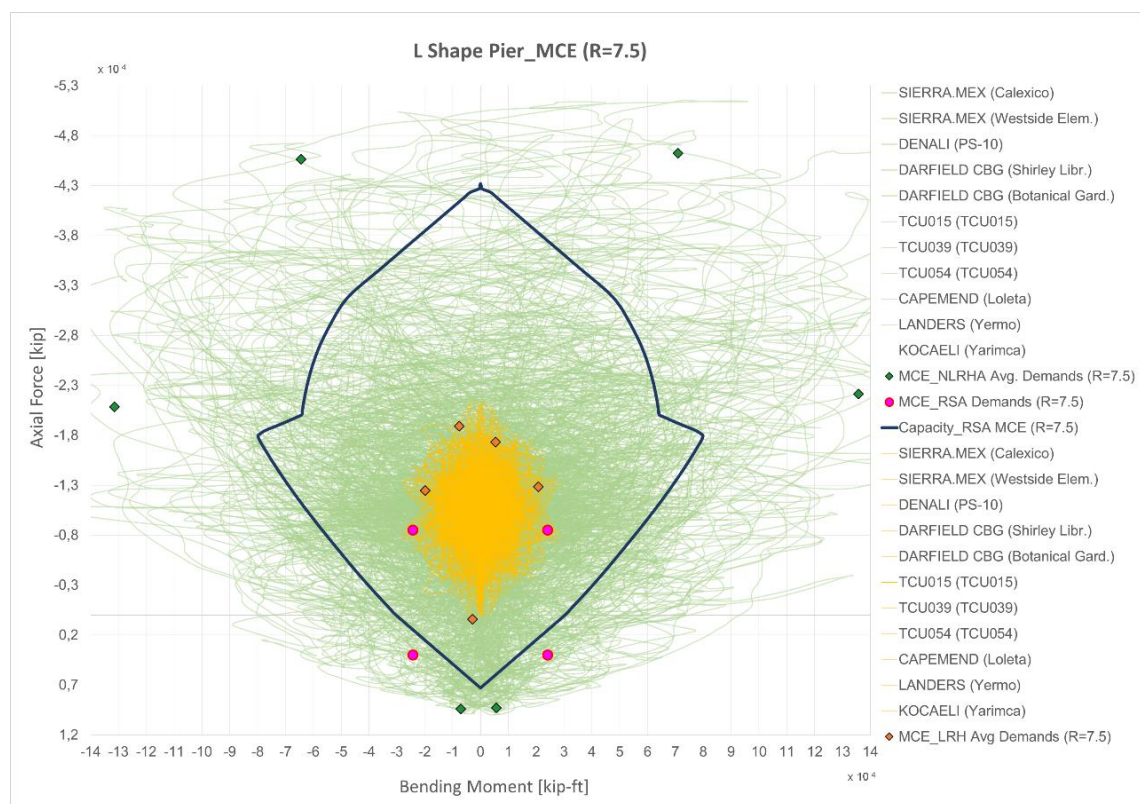


Figure 5.27 Compound Shear Wall Flexure Demands Plot - MCE (R=7.5)

In the MCE (R=7.5) plot, Figure 5.27, are shown:

- The Axial Force - Biaxial Bending Flexure Demands (magenta dots with red outline) extracted by the Traditional Response Spectrum Design Methodology performed on L-Shape Piers of chapter 3.2.2;

- The Capacity Curve (blue line) related to the Option A_MCE (R=7.5) Proposed Design Methodology, built as explained in chapter 3.3.2;
- The Option C_MCE (R=7.5) spaghetti with their relative average Flexure Demands (orange rhombs) of the Proposed Linear Response History Design Methodology of chapter 3.3.5;
- The Nonlinear Response History Spaghetti with their relative average Flexure Demands (green rhombs) represented the Nonlinear Behavior, resulted from chapter 4.2.1.

As it is possible to notice, the Proposed Design Methodology allows a less reinforced L-Shape section rather than if designed following the Traditional Axial Force - Biaxial Bending Design, as already concluded in the previous chapters. This is also proved by the position of the Axial Force - Biaxial Bending Flexure Demands (magenta dots with red outline): they are out of the Capacity Curve (blue line) related to the Option A_MCE (R=7.5) Proposed Design Methodology. It can also easily be concluded that if the L-Shape pier had been designed with the same Flexure Demands (magenta dots with red outline), it would not have provided enough ductility cause the NLRHA average Flexure Demands (green rhombs) would have been almost inside the hypothetical capacity curve.

Regarding the Option C_MCE (R=7.5) spaghetti with their relative average Flexure Demands (orange rhombs), as already shown in chapter 5.5.1, they would have led to a too weakly reinforced section and because of this not considered as a Proposed Design Methodology.

5.5.2.2 MCE (R=3)

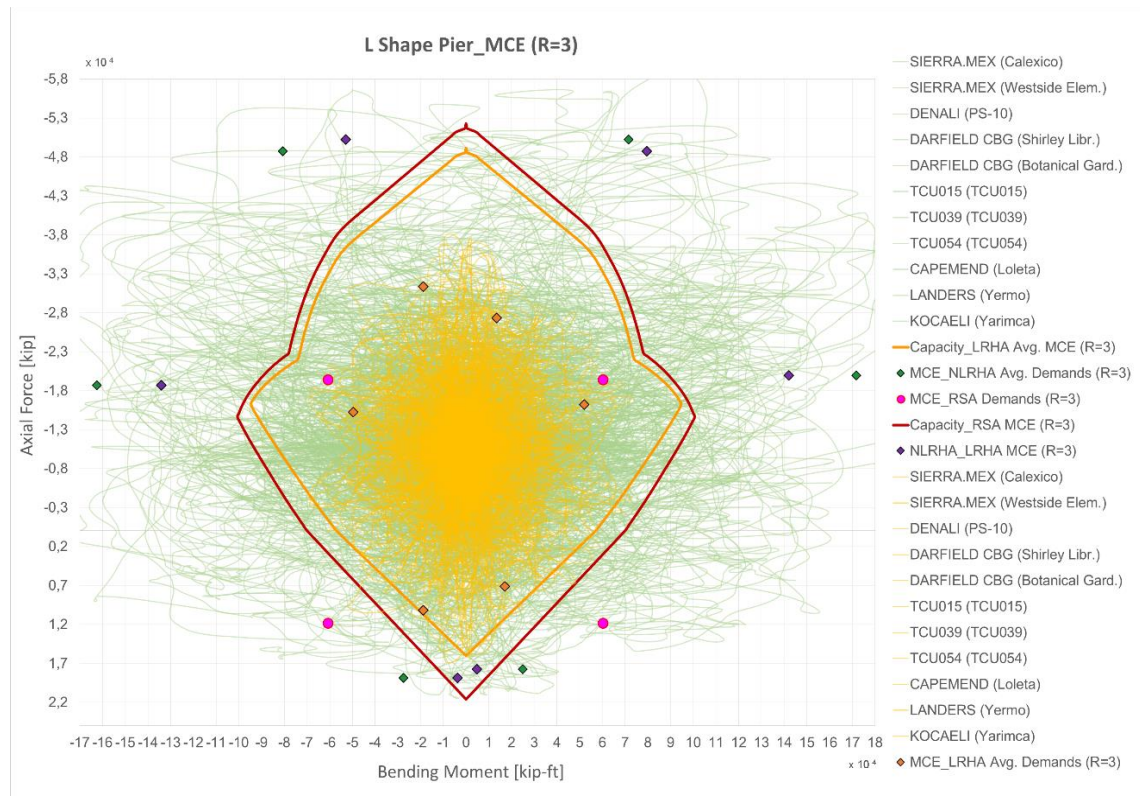


Figure 5.28 Compound Shear Wall Flexure Demands Plot - MCE (R=3)

In the MCE (R=3) plot, *Figure 5.28*, are shown:

- The Axial Force - Biaxial Bending Flexure Demands (magenta dots with red outline) extracted by the Traditional Response Spectrum Design Methodology performed on L-Shape Piers of chapter 3.2.3;
- The Capacity Curve (red line) related to the Option B_MCE (R=3) Proposed Design Methodology, built as explained in chapter 3.3.3;
- The Option D_MCE (R=3) spaghetti with their relative average Flexure Demands (orange rhombs) of the Proposed Linear Response History Design Methodology of chapter 3.3.6;
- The Capacity Curve (orange line) related to the Option D_MCE (R=3) Proposed Design determined in chapter 3.3.6;

- The Nonlinear Response History Spaghetti with their relative average Flexure Demands (green rhombs) represented the Nonlinear Behavior, resulted from chapter 4.2.2;
- The Nonlinear Response History Spaghetti with their relative average Flexure Demands (purple rhombs) represented the Nonlinear Behavior, resulted from chapter 4.3.1.

The plot in *Figure 5.28* shows that the above considerations are also valid in this case, and even more marked as in I-Shape Shear Walls situation. Again in this case, it is shown that the efficiency of the Proposed Design Methodology, the Option B_MCE (R=3) in this instance, compared to the other all Traditional Methodologies is even more evident if the R factor is equal to 3.

Regarding the Option D_MCE (R=3), it is possible to appreciate that if the section had been designed with these Flexure Demands it would have been even slightly less reinforced section, as already shown in the previous chapters, cause the orange relative Capacity Curve is smaller than the red one, *Figure 5.26*. Looking at the Tension-Bending Moment couples of NLRHA Flexure Demands (purple rhombs), they are also out of the abovementioned Capacity Curve due to their relative spaghetti (chapter 4.3.1), even if not so much as the Option B does.

In conclusion, even in L-Shape wall piers Option B is definitely the best Proposed Design Methodology to extract Flexure Demands to guarantee a considerable reduction in the quantity of section rebar and at the same time have a good energy dissipation behavior.

5.6 Total Reinforcements Amounts and Costs Comparison

The following plots show the total longitudinal section reinforcement areas in a single L-Shape Shear Wall over building height. The total reinforcement areas due to the Axial Force - Biaxial Bending Designs obtained by the Traditional Response Spectrum Design Methodologies on L-Shape Pier, explicated in chapter 3.2.2 in case of MCE (R=7.5) study and in chapter 3.2.3 for the MCE (R=3) one, are compared to the section rebar amounts obtained by the new Proposed Design Methodologies of chapter 3.3.2 and 3.3.3 respectively.

Afterwards, once known the total rebar amounts needed for the entire core, the total costs for longitudinal reinforcement of the whole building are calculated. The average rebar steel price is estimated as USD 1\$ per pound. One ton is 2000 pounds, so the average rebar steel price is 2000\$ per ton.

5.6.1 MCE (R=7.5)

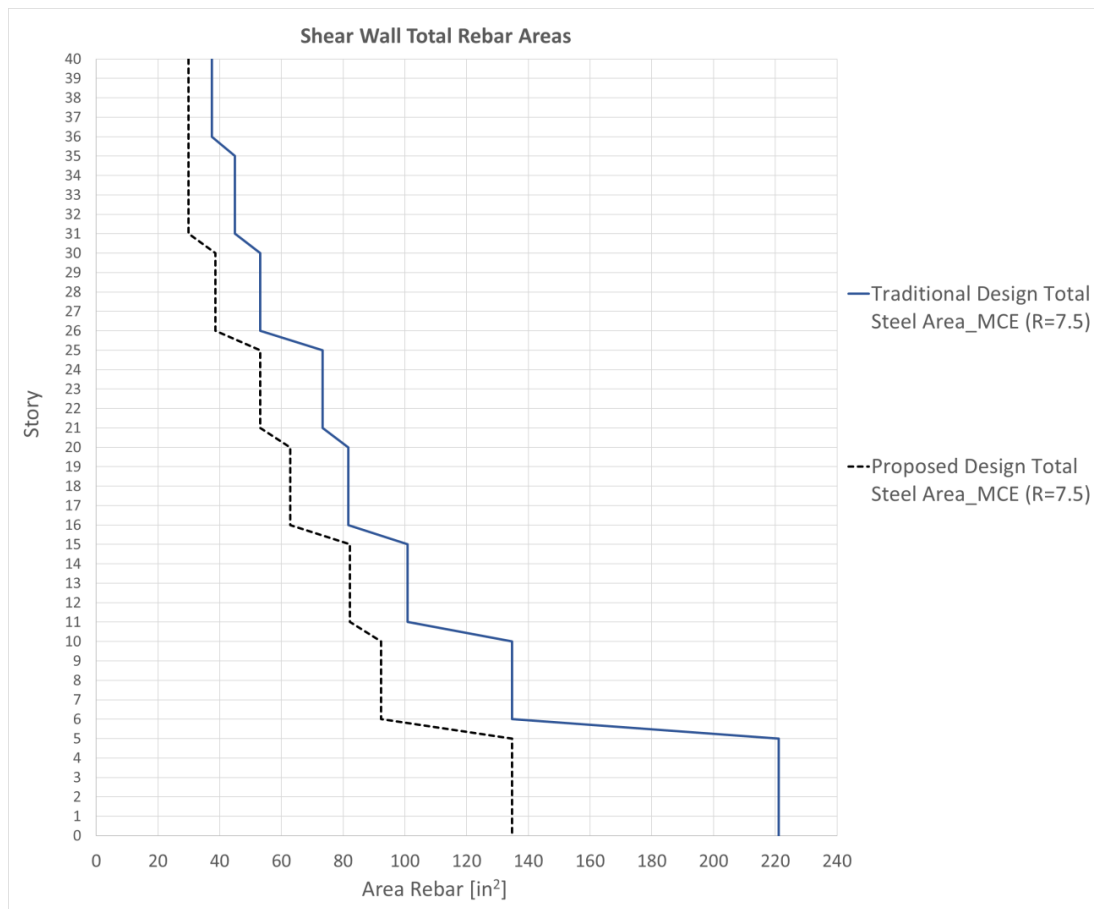


Figure 5.29 L-Shape Shear Wall Total Longitudinal Reinforcement Areas – MCE (R=7.5)

The total core longitudinal reinforcement amounts and costs in MCE (R=7.5) cases are:

- The Traditional Response Spectrum Design Methodology provides a Volume of 448'344.00 in³ of rebars, whose cost is 16'140.4 \$;
- The Proposed Design Methodology provides a Volume of 314'202.00 in³ of rebars, whose cost is 11'311.3 \$.

This Proposed Design Methodology allows to save the sum of 4'829.1 \$, almost 5'000\$.

5.6.2 MCE (R=3)

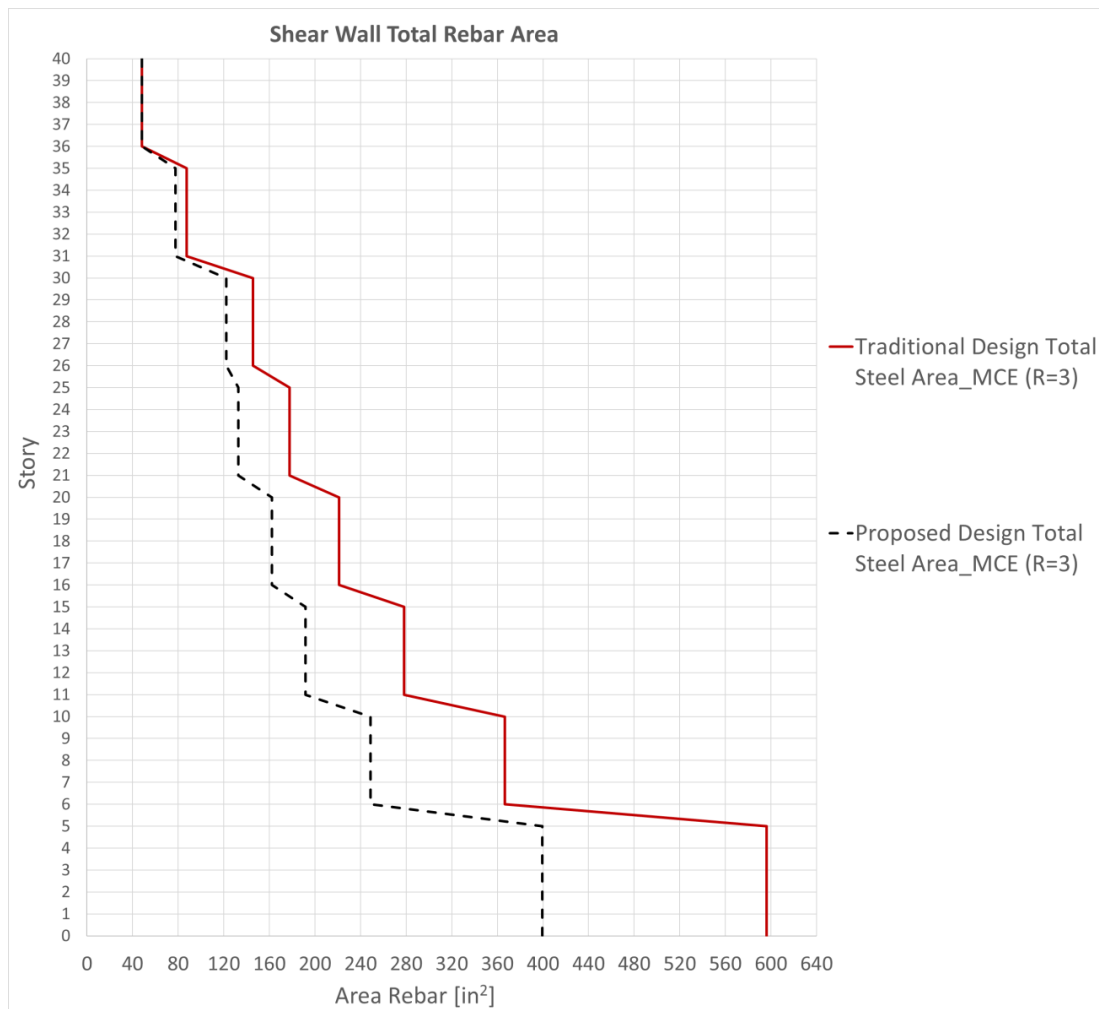


Figure 5.30 L-Shape Shear Wall Total Longitudinal Reinforcement Areas – MCE (R=3)

The total core longitudinal reinforcement amounts and costs in MCE (R=3) cases are:

- The Traditional Response Spectrum Design Methodology provides a Volume of 1'152'750.00 in³ of rebars, whose cost is 41'499\$;
- The Proposed Design Methodology provides a Volume of 829'698.00 in³ of rebars, whose cost is 29'869.1\$.

As it easy demonstrated, the Proposed Design Methodology allows to save the sum of 11'629.9 \$, almost 12'000\$.

CONCLUSIONS

The subject of this thesis was the development of a rational methodology for the design of linked compound shear walls for tall buildings in high-seismic regions. The concerned procedure has to provide guidelines to extract force demands for the design of the aforementioned reinforced concrete shear walls without being overly conservative, in order to address the lack of building codes for the design of this most used type of Lateral Force Resisting System. For this purpose, the research work presented in this thesis proposes a new design methodology which leads to an optimized rebar distribution of the section and which can accordingly also provide a better energy dissipation behavior, since it requires a smaller amount of reinforcement.

Focusing first of all on section rebar amounts, the reinforcement configurations obtained by the above mentioned Proposed Design Methodology lead to good and not overly conservative results, providing a significant amount of ductility when earthquakes occur and also a predictable nonlinear behavior.

The second key goal of this research is in fact to find a new methodology of design which accurately predicts the behavior observed in Nonlinear Response History Analysis outputs, according to the Performance Seismic Based Design procedure, while performing the best energy dissipation.

For these purposes, the results obtained are assumed to be remarkably satisfying.

The main features of the present research study can be summarized as follows:

- Story Drift: Option D_LRHA MCE (R=3) is the one of the three Proposed Design Methodologies which predicts in the best way the nonlinear

maximum Story Drift. Observing the Option A_RSA MCE (R=7.5) maximum story drift profile is possible to see that it is an underestimated prediction of nonlinear behavior compared to the relative NLRHA profile. On the other side, Option B_RSA MCE (R=3) overestimates the maximum story drift obtained by the correspondent NLRHA;

- Story Shear: In all the three studied Options the nonlinear Story Shear is bigger than the linear one. This implies a recurring underestimation of the nonlinear behavior when performing a linear analysis and this is a confirmation of the literature;
- Link Beams Plastic Rotation: The NLRHAs with the same R=3 factor, as Option B and Option D, show a similar dissipative behavior and they allow much more plastic rotation of link beams compared to the NLRHA with an higher R factor as Option A_RSA MCE (R=7.5). Option A therefore provides less energy dissipation in link beams, which might not make sense if analyzed disconnected by the shear walls fiber strain;
- Shear Walls Fiber Strain: Accordingly with link beams plastic rotation, Option B and Option D present also the same nonlinear behavior in Shear Walls Fiber Strain. Compared to the R=3 design options, Option A_RSA MCE (R=7.5) shows a much marked yielding behavior in these reinforced concrete structural elements. This means that the stressing lateral loads due to ground motions scaled by an R factor equal to 7.5 are too low and unable to lead to a good plasticization of the link beams. In order to this, the majority of the nonlinear behavior remains in the shear walls and consequently almost all the dissipative behavior of the structure is provided by the piers. A better solution is given by R=3 design options, in which the walls tensile strains barely reach the yielding limit to the advantage that the most part of the energy dissipation is provided by the link beams, which is in accordance with the conclusions above;
- Flexure Demands: The Axial Force - Bending Moment couples extracted by the Proposed Design Methodology show an inferior quantity of longitudinal rebar compared to the Traditional Design Methodologies, both in case of

MCE (R=7.5) and in case MCE (R=3). In addition, this allows to save almost the sum of 5'000\$. and almost the sum of 12'000\$ respectively.

In conclusion, the best solution to predict in the best way the nonlinear behavior is definitely Option B_RSA MCE (R=3). Flexure Demands extracted by this Response Spectrum Analysis with an R factor equal to 3 following the Proposed Design Methodology allow less reinforced I-Shape wall pier configurations and consequently lighter L-Shape pier configurations. In addition, this solution leads to saving a material amount of money.

Regarding the nonlinear behavior prediction, the Response Spectrum Analysis applied with R=3 overestimates the maximum drift guaranteeing a precautionary and safe situation. It also provides a good ductile behavior which presents more energy dissipation in link beams, allowing more plastic rotation, and less yielding in shear walls fibers. This is the most required solution because we prefer shear walls remaining more in the elastic field and have the majority of nonlinear behavior in link beams, because these are easily replaceable or repairable than shear walls.

REFERENCES

- [1] Skidmore, Owings & Merrill LLP. “*500 Folsom (Transbay Block 9) Calculation Book. Structural Seismic Design Calculations*”. San Francisco, 26 July 2017.
- [2] M. J. N. Priestley, G. M. Calvi, M. J. Kowalsky. “*Displacement-Based Seismic Design of Structure*”. IUSS PRESS, Pavia, Italy, May 2007.
- [3] R. Park, T. Paulay. “*Reinforced Concrete Structures*”. John Wiley & Sons, Inc., New York, USA, 1975.
- [4] Edward L. Wilson. “*Static & Dynamic Analysis of Structures. A Physical Approach with Emphasis on Earthquake Engineering*”. Computers and Structures, Inc., IV Ed., Berkeley, CA, USA, June 2010.
- [5] ACI 318-14. Building Code Requirements for Structural Concrete (ACI 318-14) and Commentary (ACI 318-14R). American Concrete Institute, 29 August 2014.
- [6] Jack Moehle. “*Seismic Design of Reinforced Concrete Buildings*”. McGraw-Hill Education, I Ed., 28 October 2014.
- [7] Pacific Earthquake Engineering Research Center (PEER). “*Tall building Initiative (TBI). Guidelines for Performance-Based Seismic Design of Tall Buildings*”. Version 2.01, Headquarters at the University of California, Berkeley, April 2017.
- [8] Pacific Earthquake Engineering Research Center (PEER), Applied Technology Council (ATC). “*PEER/ATC-72-1. Modeling and Acceptance Criteria for Seismic Design and Analysis of Tall Buildings*”. Headquarters at the University of California, Berkeley, October 2010.
- [9] ASCE standard ASCE/SEI 41-13. Seismic Evaluation and retrofit of Existing Buildings. American Society of Civil Engineers, 2014.

- [10] IBC 2006. Structural/Seismic Design Manual. Code Application Examples. Structural Engineers Association of California (SEAOC), Vol. I, 2006.
- [11] CBC 2016. California Building Code. California Code of Regulations, Title 24, California Building Standards Commission, USA, 2016.
- [12] IBC 2015. International Code Building. International Code Council, Inc., 30 May 2014.
- [13] ETABS CSI Manual, Integrated Building Design Software. Computers & Structures, Inc., 2016.